



UNIVERSITÀ
DEGLI STUDI
FIRENZE

DOTTORATO DI RICERCA IN
SCIENZE CLINICHE

CICLO XXXVI

COORDINATORE Prof. Lorenzo Cosmi

Automatization and remote control of the procedures necessary for monitoring the
workplace

Settore Scientifico Disciplinare MED/44

Dottorando

Dott.ssa Lucia Trevisani

Tutore

Prof. Nicola Mucci

Coordinatore

Prof. Lorenzo Cosmi

Prof. COSMI LORENZO
Matr. 998314

Abstract

Workplace surveillance is necessary to ensure a healthy working environment. This task requires ensuring compliance with safety and health standards in the work environment and monitoring factors that could potentially impact workers' health, such as sanitary facilities, canteens, and any housing the employer provides. Such monitoring ought to be conducted methodically. Specific health risks may require monitoring; thus, surveillance programmes should monitor worker exposure to such hazards. This work collects the results of the research activity on the automatization and remote control of the procedures necessary for monitoring the workplace exploited at the Occupational and Environmental Hygiene and Toxicology Laboratory of the University of Florence. The research activity hereby presented mainly focuses on sample collection and pre-treatment, every aspect linked to formaldehyde exposure and monitoring, and airborne particulate matter exposure, with particular attention on nanoparticle exposure and odour nuisances. For each one of the arguments, the outcome of both bibliographic research and experimental studies are outlined in the manuscript. Considering and possible future trends are presented based on the case studies performed during the research.

Table of Contents

1.	Introduction	1
1.1.	Research project	6
2.	Sample pre-treatment	8
2.1.	Introduction.....	8
2.2.	Solid-Phase Extraction (SPE).....	9
2.2.1.	SPE Phases.....	10
2.3.	Solid-Phase Microextraction	15
2.3.1.	Exhaustive and Non-Exhaustive techniques	16
2.3.1.1.	Non-exhaustive techniques.....	17
2.3.1.1.	Exhaustive techniques	22
2.4.	Automation.....	25
2.4.1.	Non-exhaustive techniques.....	31
2.4.2.	Exhaustive techniques	34
3.	Formaldehyde	36
3.1.	Introduction.....	36
3.2.	Generation of formaldehyde.....	37
3.2.1.	Formaldehyde gas standard generation and classification	38
3.2.1.1.	Static techniques.....	39
3.2.1.2.	Dynamic techniques	40
3.2.2.	Gaseous standard formaldehyde monitoring	42
3.3.	Risk assessment and formalin safety in pathology laboratory	43
3.3.1.	Occupational monitoring.....	44
3.3.1.1.	Personal versus area sampling	44
3.3.1.2.	Real-time, in-continuous, commercial analysers for FA air monitoring	46
3.3.1.3.	Video Exposure Monitoring (VEM) in Occupational Hygiene	48
3.3.2.	Workflow optimization.....	48
3.3.2.1.	Grossing workstation for ergonomic layout and main ventilation system	49

3.4.	Gas chromatographic determination	51
3.5.	Case studies	54
3.5.1.	First monitoring in APL.....	56
3.5.2.	Second monitoring in APL.....	61
3.5.3.	Monitoring results	74
4.	Airborne particulate matter and nanoparticles.....	79
4.1.	Introduction	79
4.2.	Case studies	83
4.2.1.	Monitoring in a 3D printing laboratory.....	84
4.2.2.	Grinding of fodder and grit in experimental stables.....	88
4.2.3.	Glassware modelling operations in a glassware room	92
4.2.4.	Additive Manufacturing Laboratory	97
4.2.4.1.	Gravimetric Method	108
4.2.4.2.	Airborne metals	111
5.	Odour nuisances	118
5.1.	Introduction	118
5.1.	Case studies	120
5.1.1.	Bituminous conglomerate production activities monitoring.....	120
5.1.2.	Odour nuisance within the municipality of Calenzano	124
5.1.3.	Odorous emissions from wastewater plant.....	129
5.2.	Emissions models	132
5.2.1.	Emissions inventory.....	132
5.2.2.	Emissions models.....	133
5.2.2.1.	Spatial disaggregation	135
5.2.2.2.	Time modulation	135
5.2.2.3.	Chemical speciation.....	136
5.2.2.4.	Deterministic models	136
5.2.2.5.	Model applications.....	138
6.	Conclusion and future trends	145

1. Introduction

The Sustainable Development Goals (SDGs), depicted in Figure 1, aim to create a more sustainable and better future for everyone while tackling global challenges such as poverty, inequality, climate change, environmental degradation, and peace and justice issues. The 17 goals are interconnected, and to ensure inclusivity and to leave no one behind, all goals must be met by 2030. [1]



Figure 1 – Sustainable Development Goals (SDGs) [1]

Goal 8, which aims to "promote sustained, inclusive and sustainable economic growth, full and productive employment and decent work for all", highlights the importance of decent work in achieving sustainable development. Decent work is critical for achieving sustainable development, and Target 8.8 aims explicitly to protect labour rights and promote a safe and decent working environment for all workers, including migrant workers, especially women migrants and those in precarious employment.

The number of non-fatal [2] and fatal [3] occupational injuries per 100,000 workers in the European Union countries in 2020 are reported in Figure 2 and in Figure 3.

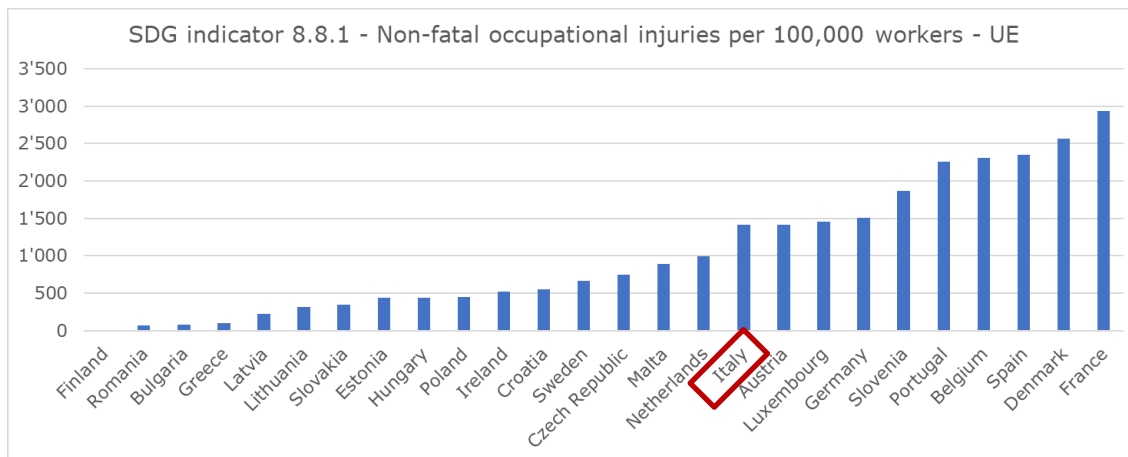


Figure 2 – Non-fatal occupational injuries per 100,000 workers in 2020 [2]

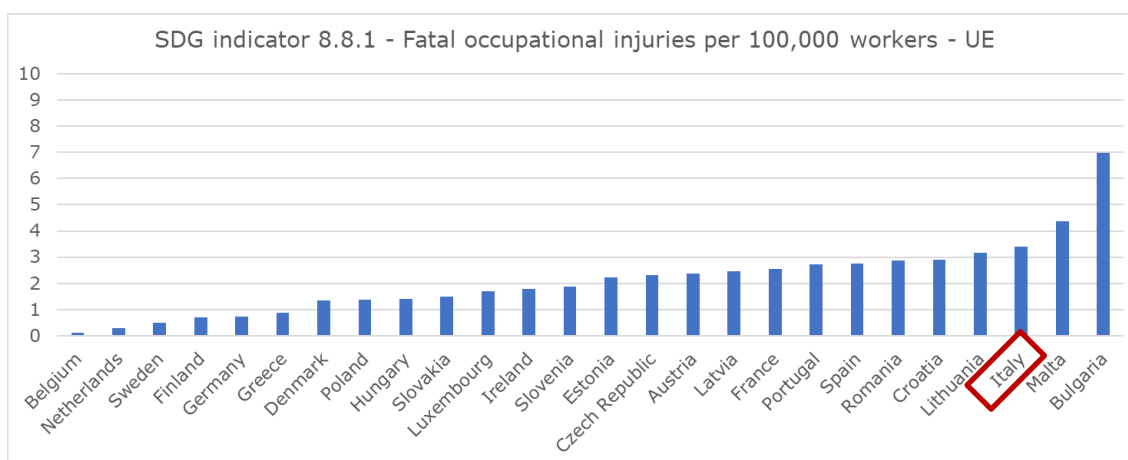


Figure 3 – Fatal occupational injuries per 100,000 workers in 2020 [3]

Occupational safety and health (OSH) is commonly described as the scientific study of identifying, acknowledging, assessing, and managing hazards that may arise in or from the workplace, which could impact the health and welfare of employees. This includes considering the potential impact on the surrounding community and the environment. The field covers a broad range of subjects and various hazards in the workplace and the environment; hence, it is intricately vast. Coordination and execution of all the "components" formulating national OSH systems, which serve as an extension of workers' and environment's safety, necessitates proficiency in several areas and disciplines. [4]

Workplace surveillance is necessary to ensure a healthy working environment. This task requires ensuring compliance with safety and health standards in the work environment and monitoring factors that could potentially impact workers' health, such as sanitary facilities, canteens, and any housing provided by the employer. Such monitoring ought to be conducted methodically. Specific health risks may require

monitoring; thus, surveillance programmes should monitor worker exposure to such hazards. The primary objectives of this monitoring are to:

- Identify existing hazards.
- Determine the level of exposure of workers to harmful agents.
- Demonstrate compliance with legal requirements.
- Assess the need for control measures.
- Ensure the effectiveness of applied control measures.

The competent authority is responsible for establishing the criteria determining the exposure level to dangerous substances or agents. It also sets levels as indicators for monitoring the working environment to implement necessary engineering control measures. The competent authority must establish limit values for worker exposure to hazardous substances and physical hazards. These exposure limits, also known as criteria for determining the level of exposure, require periodic review and updating in line with technical progress and advances in scientific knowledge. It is not feasible to continuously measure the concentration of airborne pollutants in all workplaces. Typically, a few representative air samples are taken to determine the average concentration of contaminants in the workplace. These results serve as the basis for comparison with the exposure limit value. The location and duration of the air samples should be chosen carefully to ensure representative results. Sampling should be conducted at designated areas (area sampling) or in the employee's breathing zone (personal sampling). After collection, the samples must be analysed using appropriate methods unless direct-reading instruments are used. [4] Exposure measurements serve as a proxy to assess the delivered dose to an individual. The mere presence of chemicals in the workplace or atmosphere does not assure sufficient quantities of the chemicals reaching a sensitive organ system, leading to harm. The effective dosage is contingent on multiple factors, such as the particle size of airborne dust, protective equipment (e.g., breathing apparatus and protective clothing), and other pollutants in the work surroundings. Determining the exact dose the employee receives is made more complex by multiple routes of absorption and metabolism. [5]

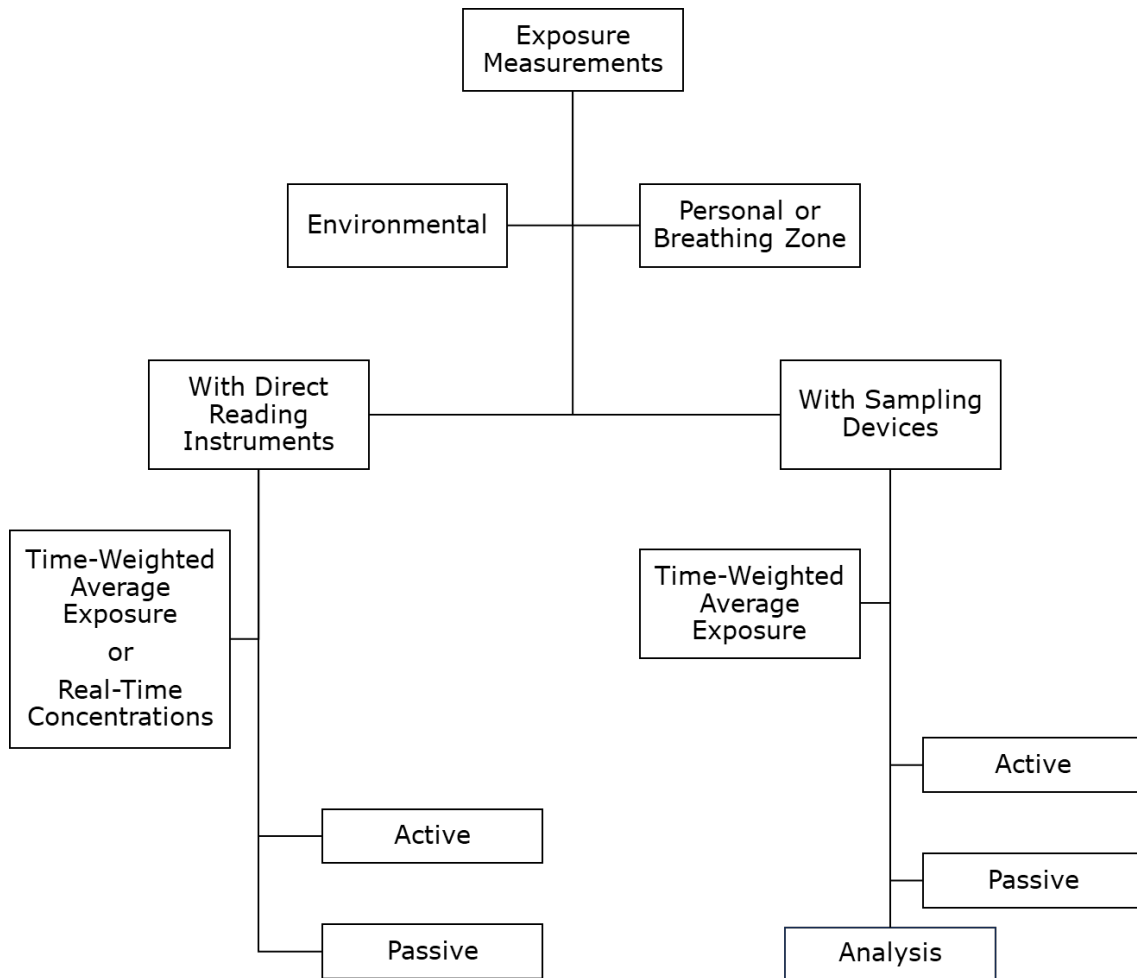


Figure 4 – Different types and devices for exposure quantification

Figure 4 presents the methods for evaluating exposure levels, employing environmental or personal monitoring near the worker's breathing zone. Measurements can also be conducted using either sampling equipment for later analysis or direct reading equipment. Sampling can be passive, with no suction source needed, or active, with air drawn in. Sampling instruments can be utilised to ascertain a time-weighted average exposure, whereas direct reading instruments can also be used to determine the concentration in real time.

Exposure levels frequently fluctuate throughout the day, week, month, or year. It is necessary to observe and document the work practices of the workers whose exposures are being measured during the monitoring period. The workplace description must incorporate personal protective equipment to accurately estimate the real exposure (the actual uptake of the chemical into the worker's body). [5] Only a few studies have specifically examined workplace location tracking and employee movement. When considering location-tracking methods, digital cameras, GPS technology, and smartphone tracking commonly come to mind. Although camera surveillance is a well-known form of surveillance, it has not been widely researched

to monitor employees in the workplace, except for specific security settings like airports and law enforcement. Workplace camera installation is regulated, with specific prohibitions in areas where employees reasonably expect privacy, including changing rooms and toilets. However, contemporary concerns involving digital cameras in the workplace pertain to questions of equity and justice in the installation, recording, analysis, and application of images. These issues reflect privacy principles, as well as concepts like social sorting. Video can be analysed as data and metadata, potentially revealing information that could be obtained from data analysis. Systems may include tracking or facial recognition capabilities or capture highly detailed images, which could disclose private information in a public space such as on a document or smartphone screen. Concerns regarding policy and management communication effectiveness relate to transparency and access. Transparency concerns camera placement, data capture, technological capabilities and storage, and sharing and usage policies. On the other hand, access concerns who has control over data collection, data storage security, and whose material may be used, as well as who has access to technology and data. It is essential to consider if cameras are placed in a way that only collects data about particular individuals or groups, how data about all groups is processed and stored equally, and whether there are different outcomes for different groups captured on camera. The relatively small number of studies on workplace camera surveillance highlights the importance of ensuring fairness and equity. The infrequent studies of workplace camera surveillance disclose that equality and fairness concerns significantly influence monitoring.

GPS or smartphone apps that can gather GPS, gyroscope, and accelerometer data enable the uncomplicated tracking of locations.

A significant proportion of research on monitoring and surveillance has centred on task monitoring. Recent meta-analyses have not covered developments since then that have centred on the potential uses of information technologies beyond performance management - specifically, regulating workers' behaviour at work through behavioural monitoring. Behavioural monitoring is predominantly applied for workplace safety and security. By utilising software, systems, algorithms, and sentiment analysis, behavioural monitoring enables the observation, quantification, and evaluation of workplace behaviour. Behavioural monitoring does not directly observe behaviour. Instead, it identifies patterns or motives in employee data from which behaviour can be inferred and predicted. [6]

Detailed activity diaries [7], GPS devices [8], or smartphone-based location tracking applications [9] could be employed to record individual human movements to obtain a suitable characterisation of the spatiotemporal mobility of individual contaminants.

The changes in workers' spatial and temporal patterns could introduce uncertainty in exposure assessment, leading to exposure evaluation errors. This, subsequently, may cause statistical analysis biases.

1.1. Research project

The research project aims to monitor the workplace remotely and automatically via sampling and analysis or direct reading instruments. This objective has several areas, such as implementing varied systems and equipment for sampling, automating the process to optimise it and minimise human error, and preparing samples to reduce errors and solvent usage. Automated sample preparation reduces worker exposure to solvents. Unattended sampling and preparation provide full process traceability, reducing time and costs. Optimal results for specific xenobiotics have been studied to optimise the results from the automation, resolution and time-consuming point of view. Direct reading instruments can facilitate continuous monitoring of the workplace when conducting workplace monitoring. These instruments possess specific characteristics, such as being wireless, portable, and battery powered. Real-time monitoring can also be achieved if the device transmits data to a cloud or is stored on a remotely accessible computer. It is necessary to amalgamate exposure information with workplace occurrences during the sampling process to attain complete monitoring and understanding of workplace and exposure data. Activity diaries or camera systems can be utilised to establish correlations between exposure measurements and work tasks.

The outcomes of both bibliographic research and experimental studies are outlined later in the manuscript. To provide further details, this thesis is organised as follows:

- Chapter 2 is about sample collection and pre-treatment, as well as the automation of these processes. It includes reviewing micro solid phase extraction techniques and commercially available technologies.
- Chapter 3 centres on formaldehyde, covering:
 - The generation of gaseous formaldehyde to calibrate and verify analysis and equipment.
 - Risk assessment.
 - Formalin safety.
 - The miniaturised extraction and on-fibre derivatisation through SPME and SPME arrow as a novel method of gas chromatographic determination.
 - Additionally, case studies are presented.

- Chapter 4 focuses on nanoparticles and metals, presenting the findings of case studies.
- Chapter 5 explores the study and evaluation of odour nuisances through an avant-garde and on-site gas chromatography system. Additionally, case studies and emissions models are presented.
- Chapter 6 summarises the conclusions and future developments of all the topics covered in the thesis.

2. Sample pre-treatment

This chapter outlines the pre-treatment and preparation of samples. It presents a range of techniques and highlights commercially available instruments with their characteristics to aid in selecting the most appropriate option based on the matrix, analytes and potential for automation and remote control.

2.1. Introduction

Sample preparation is the primary and essential step in all analytical procedures and constitutes the bottleneck of any analytical chromatographic process application. Thus, proper sample preparation is fundamental to optimise the analytical process. It must rely on a complete understanding of the available techniques, ensuring that the most suitable method meets the analysis's requirements. Understanding the operating principles of the available techniques is crucial to achieve optimal results. The aim of sample pre-treatment is to:

1. Obtain a more purified sample by eliminating non-target species in complex matrices, such as biological fluids, which isolate only a few compounds of interest.
2. Remove interferences and contamination, such as ion suppression/enhancement, in mass spectrometry applications (matrix effect) by reducing the number of substances introduced into the analytical instrument.
3. Concentrate the analytes present at trace levels in the matrix to improve sensitivity for specific analytes. A pre-concentration strategy can significantly increase the compound's concentration level, enhancing the analytical signal.

Liquid-liquid extraction (LLE) and solid-phase extraction (SPE) are the most widely recognised and extensively used comprehensive extraction techniques. They enable easy quantification and high sensitivity because all target compounds are isolated from the sample. [10, 11]

2.2. Solid-Phase Extraction (SPE)

SPE is a technique typically involving packed solid particles of chromatographic material. It consists of the interaction between the solid sorbent phase and the liquid sample solution containing the analytes. The analytes and the solid sorbent interact through various bonding types, with four main types responsible for separations: polarity, ionic/electrical charge, molecular size exclusion, and chemical reactivity. These steps can be present in SPE experiments and occur simultaneously or sequentially, depending on the chemistry involved.

The SPE separation procedure involves the following steps:

1. Conditioning of the sorbent bed.
2. Adding the sample to the SPE bed that contains the sorbent.
3. Retention of the sample in the sorbent; washing out of salts and other endogenous compounds during the wash step.
4. Elution of the retained compounds using a stronger solvent.

The sample loading or retention step involves frontal chromatography, a process in which the sample is continuously fed into the chromatographic bed. [12] Consequently, we can evaluate the concentration profile across the x -axis of the extraction phase in relation to time t by developing an expression for the dispersion of the concentration front:

$$C(x, t) = \frac{1}{2} c_s \left(1 - \operatorname{erf} \left(x - \frac{ut/(L(1+k))}{\sigma L \sqrt{2}} \right) \right) - \frac{1}{2} c_s \times \exp(2n) \times \left(1 - \operatorname{erf} \left(x - \frac{ut/(L(1+k)) + 2}{\sigma L \sqrt{2}} \right) \right) \quad \text{Eq. (1)}$$

where c_s denotes the concentration of the analyte in the sample, k represents the retention factor, which is defined as:

$$k = K_{es} \frac{V_e}{V_v} \quad \text{Eq. (2)}$$

and K_{es} is the extraction phase/sample matrix distribution constant, V_e is the volume of the extraction phase, and V_v is the void volume of the tube containing the extraction phase, σ is the root mean square dispersion of the front. Therefore, as per equation (1), the concentration of the analyte C extracted via a flow system (function of the variables time t and position x) is determined by the initial concentration of the analyte in the medium c_s , the relative position x along the extraction phase, the linear

velocity of the sample through the column u , the time t , the length of the extraction phase L , the retention factor k , the root mean square dispersion of the front σ and the theoretical plate number n . When the sorbent bed is saturated by the analytes, a breakthrough occurs. The breakthrough volume refers to the highest quantity of sample that can be loaded onto a phase without losing the target compound to a great extent. At first, the extractive sorbent phase retains the analyte quantitatively until it surpasses its retention capacity, as indicated by the sample volume. As a result, the sorbent can no longer retain the sample added to the trap, leading to equivalent inlet and outlet concentrations of the analyte. The breakthrough volume for each analyte at 1% is linked to the retention factor on the sorbent, k , the number of theoretical plates, n , and the void volume of the sample on the device V_v . The equation (3) explains the relationship.

$$V_b = (1 + k) \left(1 - \frac{2.3}{\sqrt{n}} \right) V_v \quad \text{Eq. (3)}$$

Furthermore, the extraction phase/sample matrix distribution constant is determined by the following equation:

$$n_e = \frac{K_{es} V_f V_s c_s}{K_{es} V_f + V_s} \quad \text{Eq. (4)}$$

where n_e represents the amount of analyte that reaches equilibrium extraction, c_s denotes the original concentration of the target compound in the sample, V_s indicates the sample volume, V_f represents the volume of the extraction phase and K_{es} refers to the distribution constant of the analyte between the sample matrix and the extraction phase. [13, 14, 15, 16, 17]

2.2.1. SPE Phases

SPE offers numerous benefits compared to other extraction techniques. For example, SPE sorbents are readily available and can be designed to target specific molecule types, increasing their specificity. [12] The first classification of SPE techniques is as follows:

1. Normal-phase, using a polar solid stationary phase with a non-polar sample matrix.
2. Reversed-phase, using a hydrophobic stationary phase.
3. Ion-exchange and mixed mode, more than one form of interaction between the stationary phase and the analytes is used to achieve their separation.

4. Molecularly Imprinted Polymer (MIP), the extraction of a specific analyte of interest or a class of structurally related analytes is conducted with exceptionally high selectivity, achieved through highly cross-linked polymers. [18]
5. Specialty techniques involve cartridges loaded with a precise reagent, reacting with a single type of analyte.

The following sections provide a detailed description of the various phases of SPE.

Normal-phase SPE utilises identical conditions to the first iteration of chromatography. In this process, polar analytes come into contact with the SPE's stationary phase, employing a carrier-favouring retentive interaction between them and the sorbent surface. Polar organic analytes possess functionalities that interact with the polar groups of the sorbent surface, leading to normal phase separation. Dipolar interactions between the analytes and the sorbent, including hydrogen bonding, dipole/dipole and π - π , among others, grant variable selectivity levels, permitting the segregation of substances with highly akin architectures. Polar solvents and high ionic strength aqueous solutions aid the elution of analytes from polar sorbents.

Reversed-phase SPE proves less selective in contrast with other manners of separation, such as normal-phase SPE or ion-exchange SPE. In reality, apolar sorbents encounter difficulties in distinguishing molecules with similar structures. The non-polar interactions between carbon-hydrogen bonds of functional groups present in the sorbent and analyte's carbon-hydrogen bonds are generally Van der Waals or dispersion forces. As numerous organic molecules are non-polar, the surface of non-polar sorbents can weakly bond with the analyte, resulting in the retention of most hydrophobic analytes in the sample. C18 is widely used as a sorbent in reversed-phase separations. It involves the bonding of octadecyl silane to a silica substrate. Despite its low selectivity, C18 remains the most favoured sorbent. Polar solvents increase the retention of hydrophobic analytes on C18 columns due to favourable non-polar interactions. Conversely, non-polar solvents enable elution from C18-based sorbents.

Retention in ion-exchange SPE occurs due to electrostatic interactions between oppositely charged species. Ionic functional groups on the sorbent retain analytes with an opposite charge on their molecular framework. On the other hand, mixed-mode SPE sorbents retain analytes using a combination of reversed-phase and ion-exchange interactions. Nevertheless, the retention of analytes via ion-exchange interaction is affected by:

1. pH of the solvent, sample, and sorbent. The retention interaction happens between oppositely charged entities.
2. The ionic strength of the solvent and the sample; usually, the ionic strength of the eluting solvent and the sample are typically controlled and kept as low as feasible to avoid competition for charged sites on the sorbent.
3. Equilibration of the sorbent with low selectivity counterions: the sorbent is prepared prior to analyte application to achieve optimal retention.

Two factors influence the elution of analytes from ion-exchange sorbents:

1. pH of the eluting solvent - the ionisation of the analyte or sorbent can be altered by adjusting the eluent's pH. For instance, the pH of aqueous eluents regulates the retention of protonated amine-containing analytes.
2. The ionic strength of the eluting solvent: in a similar manner to adjusting pH, the electrostatic interaction between analyte and sorbent can be diminished by employing an aqueous solution with a suitable ionic strength.
3. Elution solvent containing high selectivity counter-ions: these specific counter-ions outcompete the analyte for binding sites on the sorbent, thus inducing analyte elution.

Table 1 summarises previously provided information regarding normal-phase, reversed-phase, and ion-exchange sorbents.

AQUEOUS MATRIX (biological fluids, water, aqueous extracts of tissues, etc.)		ORGANIC MATRIX (organic extracts of tissues, hexane, dichloromethane, etc.)				
REVERSED-PHASE		ION-EXCHANGE				
Moderately polar to non-polar compound		Strong or weak cations/anions				
NON-POLAR SORBENTS		ION EXCHANGE				
POLAR SORBENTS		POLAR SORBENTS				
C18	$\begin{array}{c} \\ - Si - C_{18}H_{37} \\ \end{array}$	SCX	$\begin{array}{c} \\ - Si - C_3H_6(C_6H_6)SO_3^- \\ \end{array}$	CN	Cyanopropyl	$\begin{array}{c} \\ - Si - C_3H_6CN \\ \end{array}$
C8	$\begin{array}{c} \\ - Si - C_8H_{17} \\ \end{array}$	PRS	$\begin{array}{c} \\ - Si - C_3H_6SO_3^- \\ \end{array}$	20H	Diol	$\begin{array}{c} \\ - Si - C_3H_6OC_2H_3(OH)CH_2OH \\ \end{array}$
C2	$\begin{array}{c} \\ - Si - C_2H_5 \\ \end{array}$	CBA	$\begin{array}{c} \\ - Si - CH_2COOH^- \\ \end{array}$	SI	Silica	$\begin{array}{c} \\ - Si - OH \\ \end{array}$
CH	$\begin{array}{c} \\ - Si - C_6H_{12} \\ \end{array}$	DEA	$\begin{array}{c} \\ - Si - C_3H_6NH^+(CH_2CH_3)_2 \\ \end{array}$	NH ₂	Aminopropyl	$\begin{array}{c} \\ - Si - C_3H_6NH_2 \\ \end{array}$
PH	$\begin{array}{c} \\ - Si - C_6H_6 \\ \end{array}$	SAX	$\begin{array}{c} \\ - Si - C_3H_6N^+(CH_3)_3 \\ \end{array}$	PSA	N-propylethylenediamine	$\begin{array}{c} \\ - Si - C_3H_6NHC_2H_4NH_2 \\ \end{array}$

Table 1 - SPE phase selection [11] and sorbent structures [10]

The sensitivity and selectivity of SPE techniques have been enhanced through innovative sorbent materials. Mixed-mode stationary phases, restricted access media, immunosorbents, and Molecularly Imprinted Polymers (MIPs) have proven to be the most effective materials among those used. [13]

As previously stated, MIPs are highly cross-linked polymers engineered to extract a single analyte or a class of structurally related analytes. MIP synthesis is initiated by a template molecule designed to replicate the analyte of interest, which induces the formation of cavities or imprints that are chemically and sterically complementary to the analyte's shape. MIPs possess cavities capable of binding the target analyte via multiple interaction points (ion-exchange, reversed-phase with polymer backbone, and hydrogen bonding). Consequently, the binding sites in MIPs exhibit a robust interaction with the analyte, necessitating harsh eluting conditions but simultaneously producing purer extracts. Due to their heightened selectivity, MIPs offer a reduced background noise and matrix effect, resulting in lower detection limits. [18]

In addition to MIPs, SPE techniques can be enhanced in selectivity and sensitivity by using special techniques that chemically modify the sorbent bed to react with the sample as it passes through the cartridge. As a result, the analytes can be transformed into suitable species for analysis. For example, certain polymeric materials like polystyrene/divinyl benzene (PS/DVB) can adsorb 2,4-Dinitrophenylhydrazine (DNPH). Cartridges packed with PS/DVB-DNPH can trap aldehydes in the air, forming hydrazones on the sorbent bed. The resulting ultraviolet-responsive hydrazone derivatives are eluted and analysed by High-Performance Liquid Chromatography-Ultraviolet (HPLC-UV). This technique has been utilised to detect formaldehyde vapours in the workplace through the use of a miniaturised cartridge. [19, 20]

2.3. Solid-Phase Microextraction

In the early 1990s, Pawliszyn et al. introduced Solid-Phase Microextraction (SPME) techniques using a coated fibre. This technique was the first of its kind and has since become the most successful miniaturised sample preparation technique. [21]

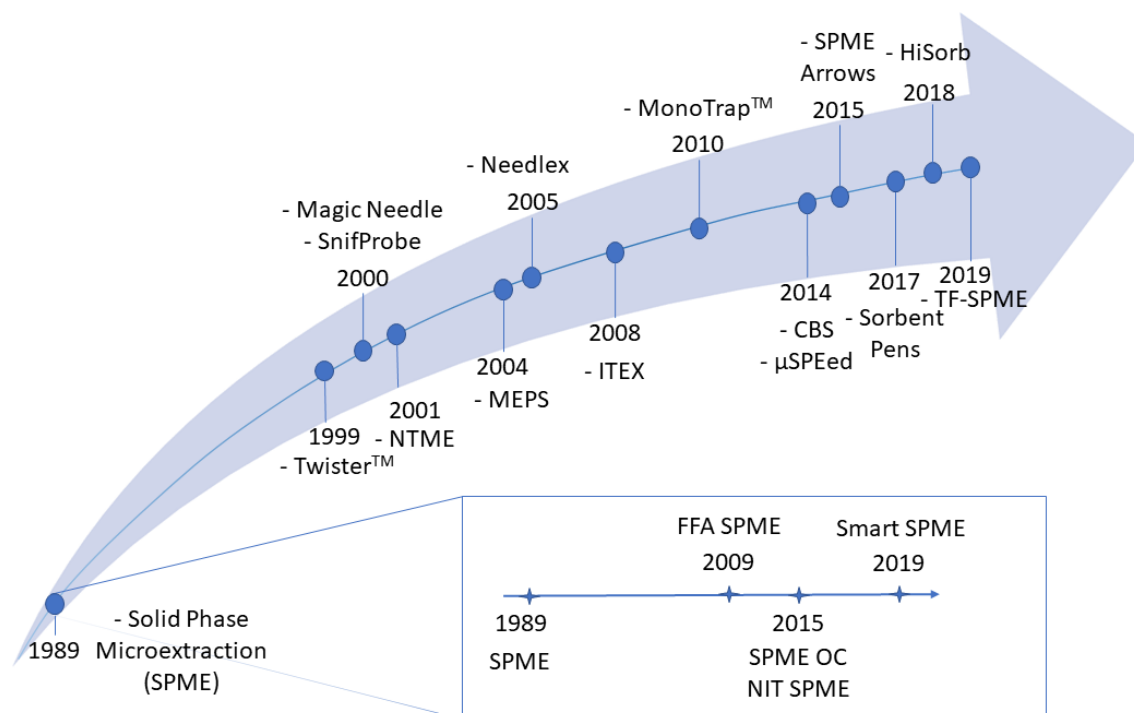


Figure 5 – Timeline of the principal solid-phase microextraction techniques developed in recent years (SPME: solid-phase microextraction; FFA: fast fit assemblies; OC: overcoated; NIT: nitinolcore; NTME: needle trap microextraction; MEPS: microextraction by packed sorbent; ITEX: in-tube extraction; CBS: coated blade spray; TF: thin film)

The timeline of primary SPME techniques developed in recent years is presented in Figure 5. Notably, over the past ten years, chromatographic systems have increasingly employed miniaturisation to automate sampling procedures, saving both time and cost, lessening environmental impact and promoting efficiency. In response to growing environmental concerns, there has been a shift towards greener technologies for sample pre-treatment, leading to the miniaturisation of pre-treatment methods. Miniaturised SPE techniques have enabled environmentally friendly sample preparation through the use of solvent-free microextraction techniques. Moreover, these compact systems offer several advantages, including reduced analysis time, small sample volumes, and effortless integration while minimising waste production. The International Union of Pure and Applied Chemistry (IUPAC) has defined Microextraction Techniques (METs) as those that use an extraction phase much smaller than the sample volume. [22] In recent years, several

published studies have highlighted the increased interest in SPE techniques due to their numerous benefits and miniaturisation, with some studies examining the use of microextraction solventless techniques for greener sample pre-treatment in green analytical chemistry. Several studies have examined the environmental benefits of combining sample preparation techniques to mitigate the drawbacks of individual methods. In addition to this, multiple reviews concentrate on liquid sample extraction techniques for liquid chromatography, affinity monolithic chromatography, and specific technologies like pipette tip micro solid-phase extraction (μ SPE), spin-column micro solid-phase extraction, thin-film solid-phase microextraction, and dispersive μ SPE. [23]

2.3.1. Exhaustive and Non-Exhaustive techniques

Generally, METs are classified into two categories: coated, like SPME fibers or in needle/in ITME methods, and tubes or needles filled with sorbent materials. [24, 25] Hereafter, fourteen commercially available solid phase METs, commonly used for chromatographic separation and mass spectrometric detection, are classified according to their geometry and their characteristics of being exhaustive or non-exhaustive, and their main features are presented.

Miniaturised methods are typically defined as non-exhaustive sample preparation techniques because they require minimal extraction phase volume relative to the amount of sample. However, some miniaturised techniques are meant and utilised as exhaustive methods. This latter category encompasses approaches such as In-Tube Micro-Extraction (ITME) or Solid-Phase Dynamic Extraction (SPDE), each with benefits and drawbacks. [26]

2.3.1.1. Non-exhaustive techniques

As mentioned, SPME is the first and most successful miniaturised sample preparation technique. It consists of a fibre enclosed in a stainless-steel needle coated with a liquid or solid sorbent phase, as shown in Figure 6.

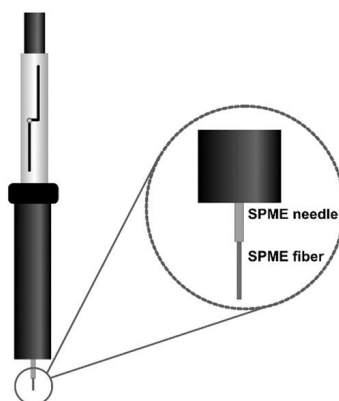


Figure 6 – Schematic of SPME holder and fiber [27]

However, the geometry of the SPME fibre leads to its fragility and instability, which are significant drawbacks. [28] StableFlex SPME fibres have been developed to overcome the fragility and instability, featuring a fused-silica core that is more flexible. Nitinol-core (NiTi) SPME fibres have also been produced, utilising a metal-alloy material with more inertness and flexibility than stainless steel. [29] Another issue associated with SPME fibre is related to SPME immersion. Direct immersion in complex matrices can result in macromolecules adhering to the adsorptive coating, decreasing the longevity of the fibre; overcoated SPME (OC) has been proposed to address this problem. [30] Another development led to the SPME Arrow, which possesses a bigger diameter SPME probe with a more robust construction, ensuring longer life, higher sample throughput and better sensitivity than traditional SPME fibres. Additionally, they have a more significant phase volume, enhancing the extraction of target analytes. Figure 7 displays the sorbent fibres of the SPME Arrows centrally placed in a stainless-steel cylinder with an inner rod and an external sheath to shield against mechanical harm and to reduce the loss of analytes. [11]

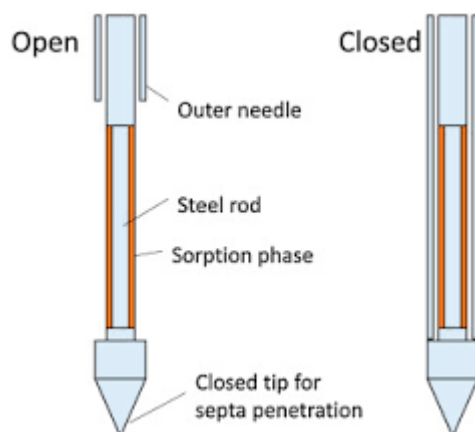


Figure 7 – The Arrow SPME system with sorbent exposed (left) and with sorbent covered by a steel tube (right) [31]

Hi-Sorbs comprise a thin inert rod wrapped with a short sleeve of polydimethylsiloxane (PDMS) used as a sorbent phase, as shown in Figure 8.

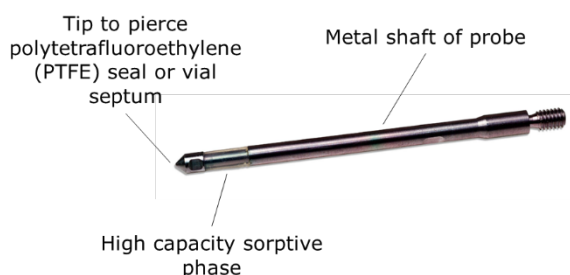


Figure 8 – Hi-Sorb

By having a relatively larger volume of PDMS sorbent than conventional SPME and fixed to a more robust metal probe, Hi-Sorb can achieve high sensitivity and robustness to matrix interferences.

As a substitute for fibre SPME, which cannot withstand aggressive LC solvents, the modern in-tube (IT) SPME has been developed, featuring an open tubular fused-silica capillary column.

Stir Bar Sorptive Extraction (SBSE) is a long-established technique, first proposed in 1999 and patented three years later. It involves a magnetic stir bar enclosed in a glass shell and coated with a sorbent layer. SBSE is a highly effective method of preconcentrating a wide range of compounds from aqueous samples. It is widely acknowledged as an excellent enrichment device. [32] The PDMS sorbent produces appropriate blanks, and the coated stir bars remain undamaged after 100 extractions. The amount of applied PDMS coating exceeds that of SPME, resulting in the ability to achieve extremely low detection limits.



Figure 9 – Stir Bar Sorptive Extraction [33]

Currently, Twister is a commercially available form of solid-phase microextraction (SPME), which uses various phases to achieve complete extraction and improved recovery of analytes. SBSE has been coupled with Ice Concentration Linked with Extractive Stirrer (ICECLES) to combine the advantages of SBSE and freeze distillation. This has resulted in a method that simultaneously preconcentrates and separates target compounds from matrix interferences. Furthermore, ultra-trace detection of a wide range of compounds can be achieved without using organic solvents when utilising thermal desorption (TD) or only a small amount of organic solvent during back extraction.

A new kind of sampler has been proposed with the MonoTrap Monolithic Material Sorptive Extraction. The design comprises a hybrid surface of porous silica monolith, providing a larger surface area. In addition, the hybrid surface contains activated carbon, graphite carbon, PDMS and has C18 functional groups, resulting in a substantial adsorption capacity. Figure 10 illustrates that MonoTrap ensures two distinct chemical processes for adsorption. Silica gel, which is more suitable for adsorbing non-polar analytes, and silica modified with activated carbon, which enhances the adsorption area to assist in retaining more polar compounds. In summary, MonoTrap offers effective adsorption solutions for different analytes. Both types of monolithic material have been functionalised with C18 groups and are available in rod and disk geometries.



Figure 10 – MonoTrap silica modified with activated carbon (left) and silica gel (right)

The sorbent phase facilitates prompt extraction through adsorption; complete desorption of target compounds requires only a small amount of solvent, eliminates preconditioning, and renders the MonoTrap reusable multiple times post-flushing.

Additionally, it permits sampling in diluted liquids and volatile chemicals before solvent or thermal desorption.

The coated blade spray (CBS) represents one of the latest non-exhaustive METs and is a sword-shaped stainless-steel sheet coated in an ultra-thin adsorbent phase. Figure 11 demonstrates this design, which enables speedy extraction from complex media. The CBS additionally facilitates Electrospray ionisation (ESI) and links with Liquid Chromatography (LC) systems via wetting the coated region with minimal solvent and applying high potential to the non-coated area. [34]



Figure 11 – Coated Blade Spray

The open bed-SPE offers various benefits, including reducing matrix effects and ionisation suppression, robustness, and versatility when dealing with various shapes, viscosities, and stiffness matrices. Furthermore, as previously anticipated, it can readily interface with analytical instrumentation, such as LC-Mass Spectrometry (MS) or directly with MS interfaces.

Thin Film-SPME (TF-SPME) is another newly developed technique in which a carbon mesh sheet is saturated with a sorbent phase, allowing for its use in both headspace and immersion extractions.



Figure 12 – TF-SPME with a stir bar in the vial

Liquid samples are frequently extracted via immersion of the TF-SPME device with a stir bar to agitate the liquid, as illustrated in Figure 12. By contrast, an agitator extracts solid samples in headspace mode. The available TF-SPME phases employ PDMS loaded with either carboxen (CAR), divinylbenzene (DVB), or Hydrophile-Lipophile Balance (HLB) particles. The TF-SPME's geometry improves the sampling rate through its slim extraction phase and expansive surface areas, resulting in a

high surface-area-to-volume ratio. The sampling rate permits a reduction in the time required to reach equilibrium while also increasing the capacity of the extraction device. [35] As previously stated, and as shown in Figure 12, for the simplification of liquid extraction, TF-SPME can generally be immersed in the sample and combined with SBSE and solvent back extraction to achieve improvements in the sensitivity and recovery of volatile compounds. [36] The two samplers can be desorbed simultaneously in a single TD tube. This setup has consistently produced the strongest responses for various volatile compounds with varying polarities. [37] Furthermore, the planar structure of the TF-SPME enables it to conform to on-site environmental sampling, as well as the direct sampling of sample surfaces or skins.

Various approaches have been taken to create a tool with sorbent coating assembled into either a needle or a glass shell to attain greater capacity, speedier extraction, and stability. This is intended to overcome SPME's primary shortcomings, including surface area flexibility, film thickness, and external coating's robustness and durability. The Needle Trap MicroExtraction (NTME), proposed by Pawliszyn's team, captures particles from the air and functions as a particle trap rather than for Volatile Organic Compounds (VOCs). The method is commercially available with different sorbents such as PDMS-DVB, Carboxen, Carbopack X, Tenax TA and polymer-based beads are used to sample organic compounds from different media. Combining various sorbents into a single needle trap could improve the extraction performance. The NTME may also be tailored to include nanoporous silica sorbent, widening the range of potential applications for this method. [38, 39]

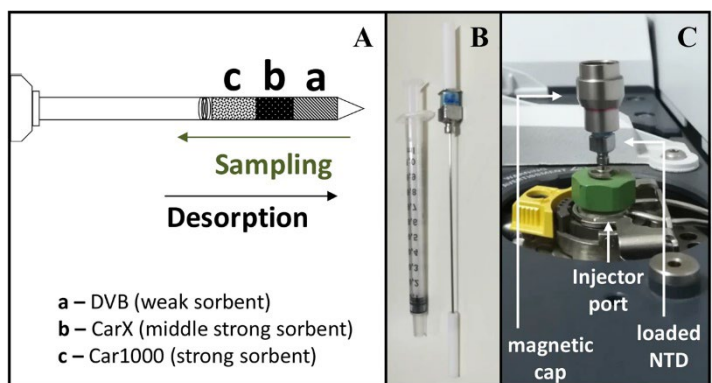


Figure 13 – Example of a possible configuration of the NTME proposed by Porto-Figueira et al. with A. schematic representation of the triple bed, B. the experimental layout used, and C. the NTME loading the extracted volatiles in the GC-MS [40]

2.3.1.1. Exhaustive techniques

Numerous exhaustive devices have been developed based on NTME and IT extraction, one of which is the NeedlEx[®], an air sampling device with an aspirating pump or manual gas-tight syringe for the analysis of alcohols, organic solvents, amines and fatty acids. [41] The NeedlEx[®] can be used for sample desorption directly by the GC injector without additional equipment. The device can be used roughly 25 to 30 times by conditioning it in the GC injection ports for 3 minutes after each analysis.



Figure 14 - NeedlEx[®]

The ITEX was developed as an In Tube MicroExtraction Technique for dynamic headspace analysis (HS), combined with thermal desorption and GC determination. [42]

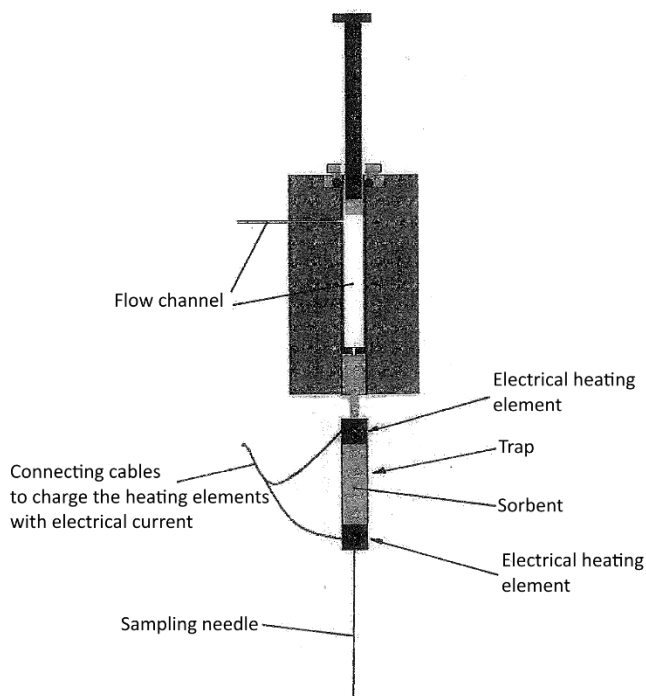


Figure 15 - ITEX, headspace extraction device [43]

The ITEX is a robust headspace enrichment technique that is easy to use and, thanks to the sorbent trap, capable of achieving sensitivity at part per trillion (ppt). The ITEX

employs a gas-tight syringe with a micro trap containing adsorbent material inside the syringe needle to concentrate the target compounds from the sample's headspace. The trap can be filled with different materials, such as Tenax, Carbopack, Carbosieve, and Molecular sieve. The ability to perform numerous syringe strokes from the headspace results in scalable sensitivity levels, rendering this method adaptable for both high and low-concentration samples. Following enrichment, the device is thermally desorbed directly into the GC injector, releasing the compounds into the inlet and conveying the sample in a highly concentrated stream to maintain column efficiency.

The Sorbent pens are compatible with the GC system and utilise the Vacuum-Assisted Sorbent Extraction technique (VASE). This allows for combining advantages from SBSE and vacuum HS-SPME, while also coupling characteristics of SPME and classical adsorbent traps. They generally contain more extraction material than SBSE (approximately 10 times) and SPME (approximately 500 times). There are two versions of the Sorbent Pen available depending on the monitoring type: headspace, which serves as a diffusive device for long-term environmental monitoring, and active, which is utilised for air sampling lasting from 5 minutes to 8 hours. The Sorbent Pen versions can be easily desorbed directly onto the head of a GC column, significantly reducing losses related to TD traps, such as additional traps to focus the analytes and lengthy transfer lines. [44]



Figure 16 – Sorbent Pen

Sorbent pens are highly durable and facilitate sampling in both field and laboratory settings, actively or passively. [45] They are versatile enough to meet various applications, including extracting organic compounds from multiple media such as wastewater, breath, and beverages. One of the most significant attributes of this apparatus is the ability to operate under a vacuum: this facet enables an enhanced

extraction efficiency of SPME, Dynamic Headspace, and other techniques that perform under atmospheric pressure, which limits diffusion rates. [46]

Microextraction by packed sorbent (MEPS) integrates extraction, pre-concentration, and clean-up into a single solution with a novel design. This miniaturised SPE device comprises a standard syringe modified to accommodate approximately 2 mg of the extraction sorbent (BIN) packed as a plug between the needle and barrel. The BIN has a mean particle size of 45 μm and can be packed with any absorption material, like silica-based or new MIPs and Restricted Access Material (RAM).



Figure 17 – MEPS

The μSPEed device is a MET system integrated into a single cartridge unit, eliminating the requirement for any supplementary fittings or tubing. It features a one-way valve that permits sample collection via syringe and eludes transit through the sorbent bed through the plunger pull. Small particles can be utilised to increase the surface area, leading to more effective separation and an overall improvement in extraction efficiency. [47] Additionally, μSPEed cartridges can be reused depending on the matrix and procedural conditions.

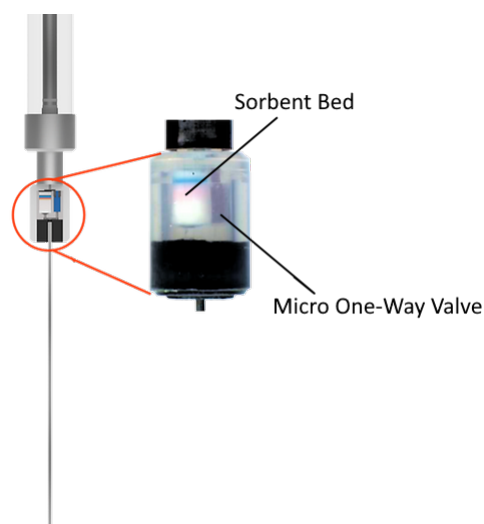


Figure 18 – μSPEed

2.4. Automation

Automated and unattended sample processing has the capability to improve laboratory efficiency, decrease costs, deliver more accurate results than manual instruments, streamline work productivity and data precision, and guarantee suitability for routine analysis. [48] MET devices are particularly well suited for automating sample preparation. Automation simplifies time-intensive sample preparation procedures and enhances analysis accuracy. Numerous commercially available automated sampling systems have been designed to handle the extraction/desorption process using various microextraction supports online or offline. The automation may focus on a specific operation or cover the entire process, and it could handle one or multiple samples simultaneously. The process of automation can follow four main configurations: sequential (which involves one sample being processed through all the steps one by one), batch-based (in which each unit of the process is performed for all the samples prior to moving to the next unit), concurrent sequential (for greater efficiency, whereby more than one sample is in the chain of operations), and parallel batch-based (which involves the running of batches of samples simultaneously). The last two constitute the primary aim of new, automated sample preparation units, as they enable the most significant productivity and time-based advantages during the analysis phase. New methods, e.g., combining selective sorbents, METs, advanced control systems, and platforms, could offer thorough and timely data on the compounds of concern. Recent advancements in high-throughput robotic microextraction systems have significantly increased the precision and throughput of analytical sessions while reducing their duration and expenses. Furthermore, downsizing the extraction devices in conjunction with the latest portable, highly sensitive analysers and customised direct injection ports may unlock novel prospects in various domains, particularly in occupations and forensics.

Along with various offline modes, the SPE technique offers the advantage of combining extraction with analysis. Online SPE facilitates partial or complete automation of the analytical process, leading to decreased analysis time, reduced analyte loss, improved analytical precision, and increased sensitivity. As a result, its combination with LC allows for fast and dependable methods, often permitting the reduction of sample volumes whilst maintaining high sensitivity levels. Column switching is typically the preferred technique for coupling online SPE with LC. For this purpose, a small pre-column, typically 2-15 mm long and 1-4.6 mm inner diameter, is used as the SPE column and connected to a conventional LC analytical column

through a switching valve. The potential arrangements for column switching comprise differing quantities of precolumns, switching valves, and pumps.

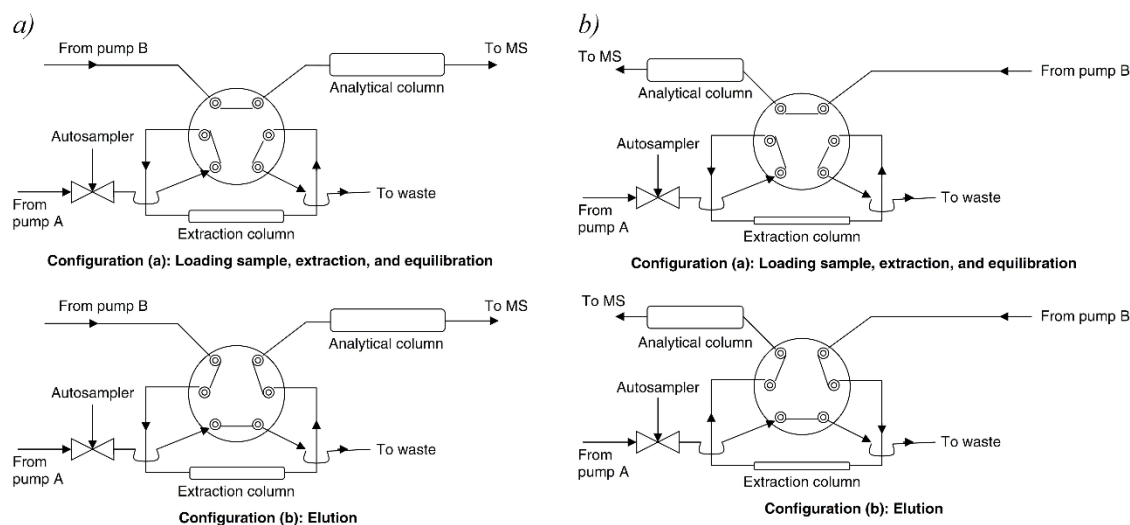


Figure 19 – Representation of online extraction system with a) direct-flushing column switching and b) back-flushing column switching

Figure 19 illustrates a straightforward column switching setup. When the valve is in "Configuration (a)", the sample is inserted into the SPE column that has been conditioned with appropriate solvents. Meanwhile, the analytical column is equilibrated with the chromatographic mobile phase. Once the interfering compounds have been eluted, the valve is shifted to "Configuration (b)". The analytes are eluted from the SPE column in either direct-flushing mode (a) or back-flushing mode (b). The compounds are then transferred to the analytical column for separation and subsequent detection. During separation, the valve is switched to its initial position ("Configuration (a)") and the SPE column is rinsed to prepare it for the next sample injection without any carryover effects. Although the process and online SPE-LC method are similar, the sorbents used in online SPE differ. The sorbents used in conventional SPE include the same materials employed in analytical columns. Chemically functionalised silica, ion-exchange, mixed-mode, and specialist materials, as outlined in section 2.2.1, show limited selectivity in SPE. These materials can also concentrate other matrix constituents alongside or in competition with the target analytes, resulting in alterations to the extraction process, separation, and detection. However, more selective sorbents exist: specialty monolithic, RAM, MIP and immunoaffinity extraction (IAE) sorbents are just a few examples. Monolithic materials, also referred to as continuous beds or phases, are composed of a single piece of silica rod or organic polymer with flow-through pores. These pores vary in size, with smaller pores providing larger surface area for effective separation capacity and larger ones minimising flow resistance. Monolithic materials are a solution for

issues commonly found in conventional particulate materials, such as large void volumes between packed particles and slow mass transfer. RAMs designed for bioanalysis have been found to be effective in removing macromolecules by size exclusion. Their pore size and hydrophilic shielding prevent larger molecules from entering the inner region of the sorbent while still allowing small molecule analytes to access the internal region, where retention occurs. Only small molecules can permeate the pores and interact with a RAM stationary phase, while larger molecules are excluded and washed away. RAM pre-columns are employed in bioanalysis to eliminate proteins and process environmental samples such as water or sediment. MIPs offer several advantages, including high specificity, physical-chemical stability, ease of preparation, and the potential to target a wide range of molecules. Silica-based materials that bind with antibodies create the so-called IAE sorbents, which exhibit high selectivity towards specific classes of target compounds. When the antibodies are immobilised onto a pressure-resistant support, the resulting material can fit into an extraction column and effectively extract a particular analyte from complex matrices, offering high selectivity and sensitivity. [49] IAE sorbents developed for proteins or viruses demonstrate greater selectivity than those designed for small molecules. Antibody cross-reactivity has been utilised and improved in IAE sorbents, capable of separating structurally similar analytes. The IAE-based approach can selectively determine specific groups of natural pollutants in groundwater and surface water. Two other types of online μ SPE, not yet commercially available but actively studied, are worth mentioning - in-tube SPME and magnetic beads. In-tube SPME is an SPME variant that utilises a GC capillary column section. This extraction system can be connected to a commercial HPLC autosampler. The preparation of magnetic beads uses the same process for obtaining magnetic particles. The preparation of magnetic beads uses the same process for obtaining magnetic particles. The beads are then linked to various molecules, allowing for broad applicability.

Robotic autosamplers can be classified today as Cartesian, cylindrical, polar and anthropomorphic. These configurations allow for three degrees of freedom and can be readily linked with analytical instruments for online or offline preanalytical phases. The transfer between automated segments, such as autosamplers and GC or LC-MS analysers, may occur online, without human intervention, or offline, with human involvement. The cartesian online systems can be readily integrated into LC and GC systems with customised accessories for sample clean-up, extraction, and injection, allowing for fully automated analytic sessions. These devices can accommodate various analytical methods and operate without the need for operators, streamlining method development, enhancing routine analysis throughput, and producing precise

results. The offline robotic autosamplers necessitate operator intervention to complete the analytical process, for example, transferring the prepared samples to the instrument for analysis, decapping them, or injecting them. An offline autosampler can autonomously prepare numerous samples without human intervention, undertaking diverse operations, including dispensing or weighing them. However, operator intervention is still mandatory to continue with the analysis. The automated device change enables round-the-clock operation without the need for an operator, even for complex multi-step processes, resulting in heightened laboratory productivity.

Additionally, automating repetitive or potentially hazardous manual tasks promotes optimal process safety since all processes require less human intervention. This is attributed to the shift towards a robotic system. Table 2 summarises the automated autosamplers for sample preparation, including online and offline options, key features, compatible METs, and tools.

COMPANY	INSTRUMENT	SYSTEM	MET	GC	LC	BARCODE READER	WASH STATION	WEIGHT SCALE	EVAPORATION STATION	CENTRIFUGE	AGITATOR	DILUTOR	SOLVENT MODULE	VORTEX MIXER	CHEMOMETRICS	TOOL	
ON-LINE	CTC Analytics AG	PAL RTC, RSL and LSI	SPME, SPME Arrows, MEPS, SPDE, ITEX, Monotrap	✓	✓	✓	✓			✓	✓	✓	✓	✓	✓	Grabber D885 - Liner exchange-MFX – Baker-RTC	
			SPME, SBSE, SPME ARROWS, TF-SPME	✓	✓	✓	✓	✓	✓	✓	✓	✓	✓	✓	✓	✓	TDu tray - liner exchange – MFX – Microwave – SPE-ICECLES
	EST Analytical	FLEX 2	SPME, μ SPeEd	✓		✓	✓	✓	✓	✓		✓	✓	✓			MFX
			SPME	✓	✓	✓	✓	✓	✓	✓							
	Konik Group	Robokrom	SPME	✓	✓							✓	✓	✓			
			SPME	✓	✓								✓	✓	✓		
	Moduvision Tech.	Primariz	SPME, HiSorb, TF-SPME	✓	✓	✓	✓					✓	✓	✓		✓	ATC-Wash/dry station for Hisorb- TD, focusing trap
			SPME, NTME	✓	✓	✓	✓	✓	✓	✓			✓	✓	✓		Concept 96-SPME
	PAS Tech.	CONCEPT	Cartesian three axes					✓									
	Entech Inst.	Sample Preparation Rail	Cartesian three axes	SorbentPen	✓												Sorbent Pen Spiking Portal
Cartesian two axes			MEPS	✓	✓	✓	✓	✓				✓		✓			
HTA	HT4000A	Cartesian three axes		✓	✓	✓	✓	✓									
OFF-LINE	Thermo Fisher Scientific	Thermo Scientific F5	Revolute	✓	✓	✓	✓	✓									
			Cartesian three axes		✓	✓	✓	✓									Sonic bath
	Sirius Automation	Multi-Tasker Series	Revolute		✓	✓	✓	✓									
			Cartesian three axes		✓	✓	✓	✓	✓								
	Chromtech Anal. Instr.	Chrombot	Revolute		✓	✓	✓	✓									
			Cartesian three axes		✓	✓	✓	✓	✓								
EPREP PTY LTD	EPREP Sample Preparation workstation	Cartesian three axes	μ SPeEd	✓	✓	✓	✓										
Axel Senrau with Mettler-Toledo	CHRONECT Quanto	Revolute		✓	✓	✓	✓	✓								Combinable with PAL series	

Table 2 – Automated autosampler for sample preparation (online or offline) and their main characteristics and tools

In the area of offline sample preparation systems that allow the use of modern METs, anthropomorphic robotic devices have gained prominence in recent years. [48] Due to highly advanced research, these tools have been integrated into analytical applications. Robotic arms can execute both transportation and active manipulation tasks to achieve operations resembling those of humans. This enables the use of manual laboratory devices and equipment. [50] These novel robotic devices can perform various tasks, incorporating all essential movements required for the latest METs through the flexibility attained from the revolute joints (refer to Figure 20).

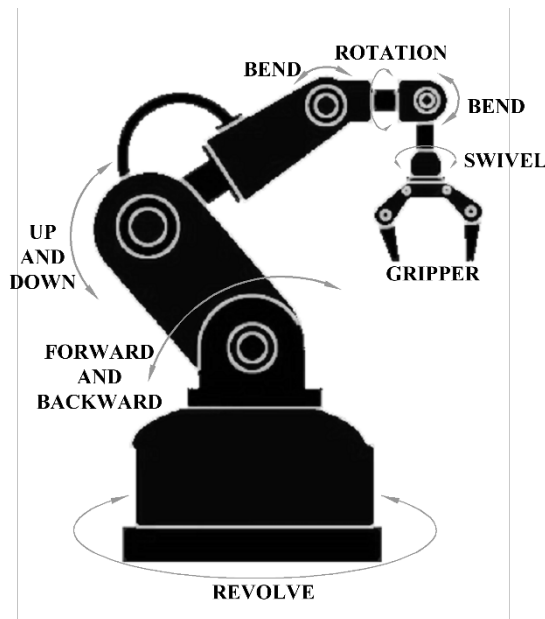


Figure 20 – Example of the robotic arm with revolute joints

Automating a laboratory can be a significant investment; however, it is typically justified by the reduced labour costs and the ability to handle a large volume of samples. To support this, compatible software devices for automation systems have been developed and released for clinical and research applications. Chemometric and predictive software tools have been proposed to optimise the workflow and develop sample preparation methods. They enable the prediction of chromatograms while considering variable experimental settings, fast peak identification, easy-to-use deconvolution and quantitation. This software leads to cost and analysis reduction needed for achieving optimal instrumental conditions aligned with analytical needs.

Hereafter the detailed information regarding the automation of the non-exhaustive and exhaustive METs introduced in paragraph 2.3.1 are presented.

2.4.1. Non-exhaustive techniques

The Fast Fit Fiber Assembly (FFA-SPME) has been proposed to automate the SPME-based process fully. This system allows the exchange of SPME fibers to be carried out automatically through a dedicated autosampler. [31] In addition, to improve data consistency and traceability, the Custodion system was proposed. The SPME syringe contains a memory chip that records both the syringe's internal diameter (I.D.) and other metadata associated with the sample. [32] The Custodion system can commence injection and analysis automatically, negating the requirement for the user to initiate an "analysis start" button. This function allows for fully automated analytical sessions with a high-throughput rate. Seamless sample preparation is then facilitated by Smart SPME fiber assemblies, which combine Smart technology with SPME instruments. Each device comprises an SPME fiber within a holder and a coded chip specifying the fibre chemistry type, dimensions, lot number, stroke-count, injection and conditioning durations, usage, and expiry dates. The compatibility of SPME and related tools on contemporary autosamplers enables the creation of a more efficient analytical method with completely automated sample preparation. This leads to increased productivity, traceability and a reduction in personnel-related exposure. In fact, miniaturisation and automation are pivotal in developing methods that align with Green Analytical Chemistry (GAC), and SPME has demonstrated itself as one of the most widely used and adaptable techniques. [33, 34] A fully automated multimode platform has been devised for reliable automation of sampling, pre-concentration, and solid-phase METs usage, including SPME, SPME trap, HiSorb and thermal desorption. It facilitates automated sampling of liquids, solids, vapours, and GC injection, increasing productivity. Its SPME-trap is compatible with both conventional SPME and Arrow. Furthermore, extracting multiple samples from either a single vial or replicating vials onto the trap before desorption is permissible, resulting in amplified analyte responses and an increased yield of identified compounds. [36] Moreover, this autosampler presents a customised injection port for thermal desorption of Hi-Sorb, allowing the management of this device in full automation.

Full automated analytical session with Twister can be achieved thanks to a Multi-Purpose Sampler, which can use a dedicated thermal desorption unit or system for Gas Chromatography analysis. Compounds that are involatile, polar or thermally labile can be extracted with a proper solvent, thanks to Twister Back Extraction (TBE) prior to determination by Liquid Chromatography. [49] Also, ICECLES can be wholly automated, coupling autosampler systems with specific thermal units.

MonoTrap in GC analysis can be fully automated with a multimode inlet and an autosampler tool for liner change and desorption. The process uses a specially designed glass tube for thermal desorption, which facilitates the insertion, storage, and automatic desorption of the sampled MonoTrap.

CBS is currently under development and could potentially be equipped with a new injection port for MS instruments to eliminate chromatographic separation and enable direct analysis. An example of such a port is the Open Port Sampling Interface (OPSI), developed by Van Berkel and Kertesz, which enables direct assays from sample preparation tips and SPME fibers. This technology can be applied to various screening applications, including drug research, food safety, environmental analysis and forensics. [51]

Automated extraction for GC analysis from TF-SPME can be carried out via the Multi-Purpose Sampler or the Centri. However, once the TF-SPME has been loaded with the target analyte, the sample must be transferred manually into a liner or metal desorption tube for GC analysis by thermal desorption. The Bruschi configuration offers high-throughput processing of aqueous samples for LC analysis. The system is composed of 96 TF-SPME devices set in a 96-well plate, which extracts the samples. The extracted samples are moved to another 96-well plate containing an extraction solvent to desorb the devices before LC injection. It is a highly efficient system. This sample preparation can be achieved using a workstation operated manually or robotic, which automates all preconditioning, extraction, washing, and desorption steps. [52]

In Figure 21, technical details of the non-exhaustive devices, covering the design characteristics, extraction phase, GC injection port, and automation, are summarised.









EXTRACTION DEVICE	NAME Producer	DESIGN CHARACTERISTICS	EXTRACTION PHASE			GC INJECTION PORT	AUTOMATION
			AREA [mm ²]	VOLUME [μL]	SORBENT		
	SPME <i>Supelco-Restek- Pas Tech.</i>	Conventional 100 μm × 10 mm coating – 0.7 mm o.d.	40	0.9	PDMS-PA- CAR/PDMS-PEG- DVB/CAR/PDMS- PDMS/DVB	Conventional (liner 0.75 mm i.d.)	On-line Off-line
	SPME-Arrow <i>Restek Corp.</i>	1.1-1.5 needle o.d.	44 to 62.8	3.8 to 11.8	PDMS-PA-Carbon WR/PDMS- PDMS/DVB- DVB/Carbon WR- PDMS	Conventional (liner 2.0 mm i.d.)	On-line Off-line
	Hi-Sorb <i>Markes Int.</i>	Standard (8 cm) or Short (4 cm) length	65	65	PDMS-PDMS/DVB- PDMS/CWR- DVB/CWR/PDMS	HiSorb extraction module	On-line Off-line
	Twister <i>Gerstel GmbH</i>	10 -20 mm length	-	63 to 126	PDMS-PDMS/EG	TDU or TDS	On-line Off-line
	Monotrap <i>GL Science Inc</i>	2.9-10 mm diameter	45 to 160	-	AC/C18-C18- GRAPHITE/C18- GRAPHITE/PDMS	Optic-4	On-line Off-line
	TF-SPME <i>Gerstel GmbH</i>	40 × 4.85 × 0.04 mm	198	200	PDMS-PDMS/DVB- PDMS/CAR- PDMS/HLB	TDU	On-line Off-line
	CBS <i>Restek Corp.</i>	42 mm length	30	-	PAN/HLB	OPSI	On-line
	NTME <i>Pas Tech.</i>	gauge 22 or 23 length of 50 – 80 mm	3.0	-	Tenax- PDMS-DVB- Carbopack-Carboxen- Carboxistev	Conventional (liner split/splitless)	On-line Off-line

Figure 21 – Non-exhaustive METs and their main features
 PDMS: polydimethylsiloxane; PA: polyacrylate; CAR: carboxen; PEG: polyethylene glycol;
 DVB: divinylbenzene; Carbon WR or CWR: carbon wide range; AC: activated carbon; HLB:
 hydrophilic-lipophilic balanced; PAN: polyacrylonitrile; TDU: thermal desorption unit; TDS:
 thermal desorption system; OPSI: open port sampling interface

2.4.2. Exhaustive techniques

The desorption and subsequent conditioning of the sampling device in the GC injection port can be fully automated using three-axis autosamplers with NeedlEx. These autosamplers also allow for automation with ITEX. Furthermore, specific three-axis autosamplers, which include a range of support tools for optimising workflow, consent to the switch from ITEX to a conventional syringe without human intervention.

Sorbent Pens are capable of performing offline sample enrichment from a GC system, enabling the simultaneous extraction of multiple samples. They can also be effortlessly applied to complete automation with a dedicated unit or a specific sample preparation rail, which permits the analysis of up to 120 pre-extracted devices using four removable 30-position racks. [44]

MEPS can be conducted manually or using fully automated online systems coupled with autosamplers compatible with GC analysis or LC-elution. [53] A digital analytical syringe is an automated device that is specifically designed for MEPS. It is capable of performing high-precision liquid handling processes in full automation. [54] More traditional autosamplers, capable of handling MEPS, comprise three axes and a two-axis autosampler that can automatically carry out all MEPS sample preparation and injection procedures.

The μ SPEed cartridges are controlled by either an analytical and portable syringe or a dedicated digital syringe driver. The latter is capable of handling greater back pressure than the former. This feature is particularly advantageous when working with complex media like biological fluids, which can frequently cause blockages. Furthermore, a sample preparation workstation facilitates the offline automation of μ SPEed cartridges. This makes it possible to establish sequential procedures and prepare samples away from analytical instruments. Samples can be transferred directly to a wide range of autosampler racks and subsequently to the analytical instrument, such as a chromatographic analyser, simplifying sample procedures. [55]

In Figure 22, technical details of the exhaustive devices, covering the design characteristics, extraction phase, GC injection port, and automation, are summarised.






EXTRACTION DEVICE	NAME Producer	DESIGN CHARACTERISTICS	EXTRACTION PHASE			GC INJECTION PORT	AUTOMATION
			AREA [mm ²]	VOLUME [μL]	SORBENT		
	Needlex Shinwa Chem Ind. LTD	i.d. 0.5 mm-o.d.0.7 mm- length 85 mm	3.0	-	Tenax- PDMS-DVB- Carbopack-Carboxen	Conventional (liner split/splitless)	On-line Off-line
	ITEX CTC Anal. AG	ITEX Syringe 1300μl	3.0	-	Tenax-Carbopack- Carboxteve-Carboxen	Conventional (liner split/splitless)	On-line
	Sorbent Pen Entech Inst.	6.1 mm o.d- Length 88.9 mm	-	10	Tenax-Tenax/Carbopack- PDMS/Tenax- PDMS/Tenax/Carbopack- Carboxen-Carbopack- PDMS/Tenax- Tenax/Carbopack	SPDU-5800	On-line Off-line
	MEPS SGE Anal. Sci.	syringe 100-250 μL removable needle	< 1.0	-	C18-C2-Silica-C8- C8/SCX-SAX	Conventional (liner split/splitless)	On-line Off-line
	μSPEd ePREP	length <1 cm, 3 μm sorbent particle size	<1.0	-	C18-WAX-PFAS- PS/DVB-Silica- PS/DVB/Phenyl- SAX_PS/DVB- SCX_PS/DVB-CxyI	Conventional (liner split/splitless)	On-line

Figure 22 – Exhaustive METs and their main features
i.d.: internal diameter; *o.d.*: outer diameter; PDMS: polydimethylsiloxane; DVB: divinylbenzene; AC: activated carbon; PEG: polyethylene glycol; PS: polystyrene; SCX: strong cation exchange; WAX: weak anion exchange; SPDU: sorbent pen desorption unit

3. Formaldehyde

This chapter presents various themes regarding formaldehyde. It will cover how formaldehyde can be generated to check measurement systems, monitor and limit formaldehyde exposure in pathology laboratories, and determine formaldehyde in GC analysis.

3.1. Introduction

Formaldehyde (FA) is a ubiquitous environmental chemical and is among the most significant of the 188 Hazardous Air Pollutants (HAPs) designated by the US Environmental Protection Agency (EPA). It spontaneously forms as a biogenic compound, being a metabolic intermediate in most living systems. It is emitted into the atmosphere during the physiological activities of some plants, and marine environments are also natural sources of FA. The prevalence of this xenobiotic is mainly attributable to its status as one of the most extensively manufactured chemicals on the global stage. It serves as a primary chemical feedstock in myriad industrial processes, while FA-based resins constitute the bulk of all FA applications. Notably, it serves as a broad-spectrum biocide and is used for disinfection purposes and in preserving biological tissues. In addition to its use as a raw material for many chemicals, pure FA is also required. However, because of its tendency to polymerize, it is unavailable commercially. Instead, it is supplied as formalin, a solution of 37% (w/w) FA in water. It is stabilized with 10% (w/w) methanol to prevent the polymerisation process. Therefore, despite its toxic nature, FA holds economic importance and sees wide usage. Consequently, individuals are environmentally and/or occupationally exposed to FA.

Several countries have adopted international standards stipulating reference ranges for the levels of FA found in indoor and outdoor environments, as well as in items such as cosmetics, textiles, toys, food, and drink. Indoor environments contain various sources of FA, which may be temporary (e.g., cooking, combustion), intermittent (e.g., indoor chemistry, air cleaners) or permanent (e.g., wood-based products, building products). [56, 57]

Due to its omnipresence and natural diffuse emission sources, chronic exposure to FA poses a significant risk to human health. It is strongly associated with cancer, making it the most significant chronic effect of FA exposure. Additionally, FA may result in adverse effects on the central nervous system, sensitization, contact

dermatitis, irritant effects on the mucosal surface of the eyes and the upper airways, as well as bronchial asthma. [58]

Acute exposure to FA by inhalation causes local irritation to mucous membranes, including the eyes, nose and upper respiratory tract, along with coughing, wheezing, chest pains, and bronchitis as additional acute effects. [58]

Given its extensive usage, toxicity and volatility, measuring exposure to FA is a subject of significant interest to ensure the protection of human health. Therefore, there is a pressing need for improvements in the detection limits of many analytical methods.

3.2. Generation of formaldehyde

The generation of FA standards in test atmospheres is essential for developing and testing analytical methods, evaluating and calibrating air monitors, analytical instruments, personal sampling devices and toxicological effects studies. Implementing an analytical technique or instrument substantially depends on the necessary calibration to confirm its accuracy and precision. The need to accurately measure low levels of FA has increased the demand for standardised gaseous mixtures to be prepared for calibration purposes with well-known and controllable concentrations. Recent years have complicated the calibration process by developing highly sensitive instruments. Consequently, new validated methods have been proposed to determine low levels of airborne FA, characterised by real-time and continuous reading. Among these, chemisorption substrates and solid-phase microextraction methods are of great relevance. [20, 59] It is not always feasible to have the derivative available commercially for the latter method to be used as a standard reference material to inject the solution, making the preparation of an accurate, reproducible, and controllable standard atmosphere generation crucial. The system must produce multi-component atmospheres, achieving FA concentrations at the ppb level while ensuring the traceability of primary state variables such as mass, volume, temperature, and pressure. Additionally, it's necessary to have a broad dynamic concentration range. During operation, the multi-component atmosphere generated, which contains FA, must maintain stable concentration, short stabilization times, and precise humidity and temperature control. Furthermore, conducting a simultaneous sample of a sufficient number of sensors under identical environmental conditions to verify the accuracy and precision of novel measurement methods necessitates using an exposure chamber.

3.2.1. Formaldehyde gas standard generation and classification

It is of utmost importance to comprehend the various gas standard generation techniques characteristics, and differences in order to determine the most appropriate procedure for testing an air monitoring device or analytical method. Gas standard generation techniques are typically grouped into static and dynamic categories.

Pure standard FA can be prepared in several ways, such as thermal depolymerization of 1,3,5-trioxane or paraformaldehyde (PFA) and a formalin solution. The formalin solution is obtained by dissolving PFA in hot water (at 100°C) with 0.1 sodium hydroxide through evaporation or a heated airstream. When PFA is in an aqueous solution, it reacts quickly to produce formaldehyde, methylene glycol, and polymethylene glycol in the absence of a polymerization inhibitor such as methanol. The significant disadvantages of this method are the significant amounts of water, methanol and methoxymethanol or dimethoxymethane produced in the gas mixture. [60, 61]

Sections 3.2.1.1 and 3.2.1.2 report the classification of systems into static and dynamic generation systems, as depicted in Figure 23. The static group comprises methanol catalytic oxidation, vaporization using hot-injection and vacuum, nebulization and FA evaporation. In contrast, permeation tube and diffusion tube systems are assigned to the dynamic group. However, the differentiation between these two categories is not always distinct: certain static systems, such as evaporation, could be used as dynamic generation techniques with the use of upgrades and specific tooling.

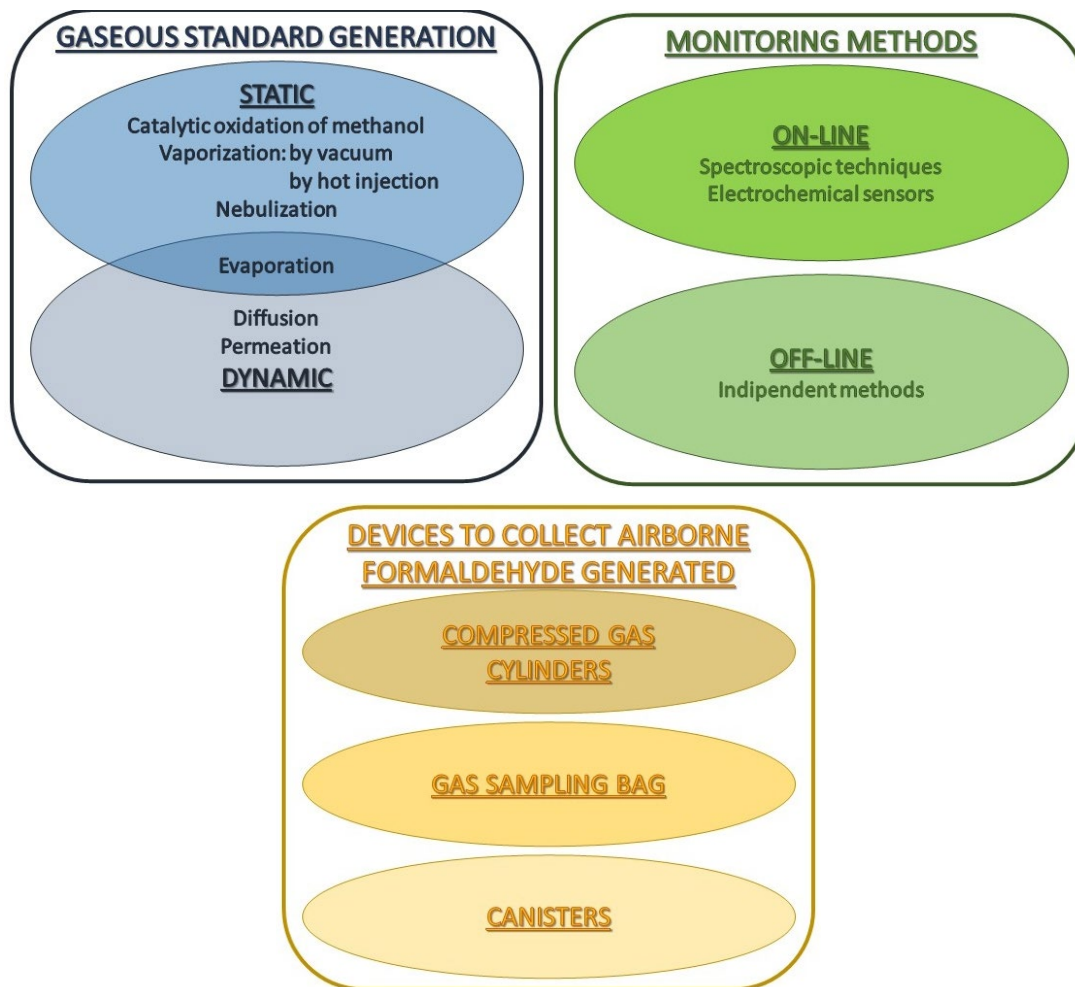


Figure 23 – Graphical representation of the generation systems, the monitoring methods and the sampling devices for formaldehyde gaseous standard

3.2.1.1. Static techniques

Preparing standard FA by a static technique consists of adding a known volume of pure gaseous aldehyde to a known volume of gaseous diluent, such as nitrogen or purified air, in a closed vessel. The resulting homogeneous mixture is then stored under controlled conditions until required.

Among the advantages of static methods, it is important to note that they are easy to set up and inexpensive. Nevertheless, they also have disadvantages, notably that they may be impacted by analyte losses owing to absorption on the internal surface of the container. Furthermore, limited volumes can be produced due to potential leakages, and maintaining constant pressure in a closed system is often difficult. Small amounts of a component introduced into a dilution gas can affect a method's overall precision and accuracy. Due to this, preparing standard FA at very low concentrations using static methods is not viable.

To enhance static techniques, new systems have been developed. For instance, there are proposals for new systems to vaporise chemicals. Hot injector systems have been designed to replace the conventional GC injector port. Additionally, introducing a three-axis robotic autosampler permits the automation of injection and the collection of FA standards in bag analysis. Automation in gas chromatography (GC) systems can be accomplished through the use of a bagtray mounted on the autosampler, which can handle the necessary analytical repetitions for a validation study. [62]

Regarding the evaporation of FA solution, new instruments have been introduced. These include an accessory that directly introduces headspace vapours from various sample containers and a device designed for loading sorbent tubes with gas or liquid-phase standards using a precision syringe in an unheated injector.

3.2.1.2. Dynamic techniques

Dynamic techniques involve introducing a consistently generated pure gaseous FA at a known generation rate into a diluent flowing system. Due to the high reactivity of FA, it must be stabilized in an aqueous solution or in a solid state, such as in 1,3,5-trioxane or polyformaldehyde (PFA). These two compounds are FA trimer and polymeric forms, respectively, as shown in Figure 24. PFA is a polydisperse polymer with a molecular composition ranging from 8 to 100 monomers per unit.

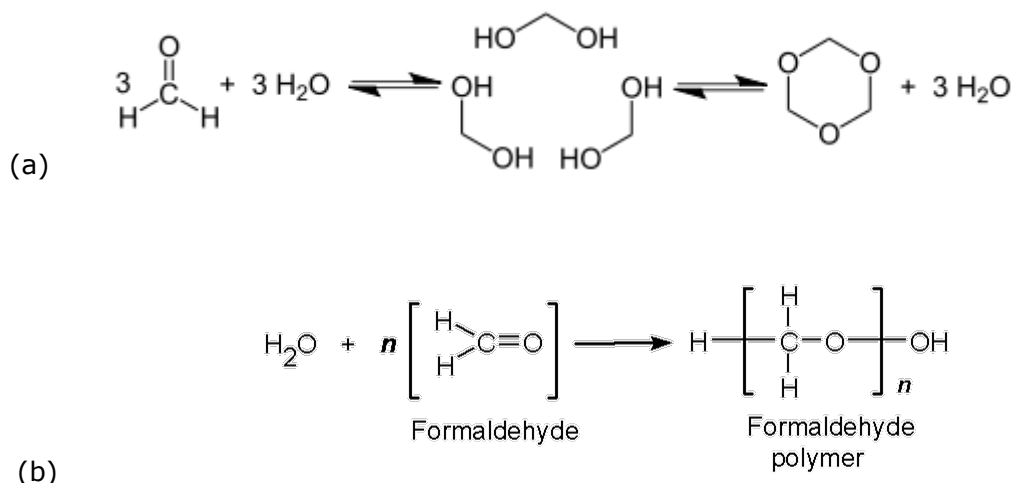


Figure 24 – (a) Generation of 1,3,5-trioxane by the acid-catalysed cyclic trimerization of FA in concentrated aqueous solution, and (b) formation of FA polymers

Although dynamic techniques are often more complex and require relatively more expensive equipment compared to static techniques, they offer numerous advantages. It is worth noting that, as standards are continuously generated, any loss of analytes due to absorption onto the internal walls of the system is negligible. Additionally, significant quantities of gas standards can be produced, and concentrations can be adjusted to create a wide dynamic range. The key features

that render this technology appropriate for calibrating and assessing analytical instruments or sampling devices are its ability to adjust the range of concentrations, volume, and flow rate of the generated standards.

The standard method for generating gaseous FA dynamically is by depolymerizing PFA or polyoxymethylene (POM) within a permeation tube. Consequently, a gas stream composed solely of monomeric FA and without water is produced. It should be noted that the sublimation of POM releases 10% trioxane and water, which is bound within the polymeric molecular framework at a level of approximately 4%. National Metrology Institutes (NMI) employed a POM permeation tube to produce reference standards of FA diluted in nitrogen: the amount of FA can be estimated from the loss of mass of the permeation tube, but its determination could be affected by the loss of polymer or water. [63]

PFA is commercially available at approximately 95% purity, with the remaining 5% consisting mostly of water in both bonding and non-bonding forms, which varies depending on the degree of polymerization. The presence of water could lead to a loss of analyte mass in the permeation tube and the POM. To evaluate the effectiveness of the generation system, one should consider comparing the theoretical FA permeation rate with the experimental findings.

The use of permeation tube technology poses fewer challenges for its wide-scale implementation when compared to other generation systems. However, documented drawbacks exist with this technology, including issues with the motor-driven syringe pump, the nebulizer system, and the conversion of methanol into FA. Each of these disadvantages is discussed below.

The motorised syringe pump system is impacted by the formation of FA oligomers on the needle tip when using concentrated formalin (up to 3%). Additionally, water condensate can accumulate inside the hot injector after 8 hours of vapourisation, and time constraints due to the syringe volume can also affect the system's performance. Furthermore, the system exhibits poor repeatability (e.g., within 8.4% Relative Standard Deviation (RSD)).

Additional testing is required to optimise the nebulisers' geometry and ensure adequate robustness.

The conversion of methanol using catalytic methods is not yet available for commercial use and is primarily aimed towards research-specific or semi-quantitative applications.

Numerous permeation generation systems are now available, characterised by a wide variety of permeation tubes with high accuracy and precision, even at the lowest concentrations. Moreover, the permeation system is the preferred method for producing FA standards in compressed gas cylinders, which, using a gas dilution of a gaseous standard, can be considered a true dynamic generation system.

The technique for generating standard FA gas using permeation tubes has been found to be the most effortless and cost-effective system. It is a robust method that provides stable concentrations of standard FA over time. It is worth noting that the standard air generation system needs to be validated using independent methods, which vary depending on the air-generating techniques. When developing a reliable system for producing gaseous standards, it is therefore essential to incorporate the necessary verification support equipment based on performance requirements, cost and practicality.

3.2.2. Gaseous standard formaldehyde monitoring

Many systems have integrated detectors, typically electrochemical or spectroscopic sensors, to validate the performance of gaseous FA standard generators. The selection of the preferred detection system should depend on the ultimate aim of the produced FA standard. Electrochemical detectors are more affordable and user-friendly and can be integrated into generation systems. However, they are less precise and sensitive than spectroscopic detectors and often require significant amounts of time to recover between successive runs. Spectroscopic detectors, on the other hand, exhibit greater sensitivity and specificity. Nonetheless, their integration into the generation system might prove to be complex, often necessitating external connection and introducing a possible leakage source within the system. Despite their limitations, spectroscopic detectors, especially those utilising cavity ring-down spectroscopy and middle-infrared laser absorption (with a detection limit ranging between 0.001 and 0.100 ppm), are preferred for verifying FA gaseous standards due to their high sensitivity and sampling frequency. This validation aids in the refinement of studies or calibrations for high-sensitivity direct reading instruments.

In cases where the adoption of these direct reading instruments may result in inadequate, an independent method must be used. Typically, the FA gaseous standards produced are evaluated through comparison with the DNPH derivatization method. [64] This well-established method is considered the reference method for determining the derivatised FA concentrated on a solid sorbent, to the extent that this procedure based on the certified FA-DNPH-hydrazone standard is used in most Proficiency Testing (PT) programs. While the determination of non-derivatized FA

without pre-concentration steps may be achieved with a GC system that has a specific detector, the use of external standardization by injecting known concentrations of FA Certified Reference Material (CRM) and then directly injecting gaseous FA makes the GC system with a specific detector highly attractive for potential innovation. [64]

GC, which identifies specific compounds by their retention time, is also used in manufacturers' calibrated direct-reading instruments to verify atmospheres produced in laboratories.

3.3. Risk assessment and formalin safety in pathology laboratory

As outlined in section 3.1, acute health effects associated with exposure to FA primarily involve a sensation of smell and irritation of the nose, nasal cavity, pharynx, larynx, and eyes. [65] Additionally, FA has sensitising properties, which can trigger an allergic skin reaction. Alongside these short-term health effects, concern has been raised regarding the long-term effects, including an elevated risk of developing cancer. [66] Studies have confirmed that FA is genotoxic and causes the formation of DNA adducts. Additionally, exposure-response relationships for FA have been found to be nonlinear, and relevant genetic polymorphisms have yet to be identified. [65]

Whilst most workers exposed to airborne FA work in chemical and plastic factories, the healthcare sector records the highest mean levels of airborne FA exposure. [20] Typically, three common scenarios are examined where FA is being used: operating theatres where small biopsies are soaked in closed-circuit 4% FA containers, anatomic pathology laboratories (APLs) where biopsies are registered, and APLs where biopsies are cut. [20] In the latter scenario, high levels of airborne formaldehyde have been found in APLs where correct and safe practices were not adopted, or adequate structural measures for formalin emissions were lacking. [19, 67]

It is necessary to anticipate, recognize, evaluate and control workplace conditions to prevent workers' exposure. In APL, one crucial consideration is the ideal layout of spaces. In detail, the dissection area requires suitable lighting, proper ventilation, washable and non-absorbent surfaces, and laboratory personnel must wear appropriate protective clothing, and gloves and other equipment (e.g., photography, tissue macerators, disposal containers) are necessary to minimize exposure risk. The dissection room should be comfortable for pathologists and technicians to work freely without disruption while adhering to the aforementioned safety measures.

Subsequently, the analysis will focus on monitoring and minimising FA occupational exposure. An ergonomic and practical design for grossing pathology operations will be suggested, and how the adoption of safe practices, supported by real-time, continuous FA monitoring, limits worker exposure will be highlighted.

3.3.1. Occupational monitoring

If a workplace's risk assessment indicates a need for monitoring to assess the quantitative or qualitative extent of pollutants in or around the workplace, periodic or continuous workplace air monitoring is mandatory. The primary purposes of air monitoring are to ensure compliance with legislation, determine exposure levels, and demonstrate the effectiveness of control measures. Therefore, monitoring must be included in a pre-planned strategy based on risk assessment. The selection of an air monitoring strategy should take into account the most cost-effective and practical approach.

3.3.1.1. Personal versus area sampling

Area monitoring is advisable for detecting harmful chemical sources and testing protective equipment's effectiveness. However, it is comparatively less informative than personal exposure monitoring and is implemented in fewer cases. Personal exposure monitoring allows for continuous monitoring of workers' breathing areas, simplifying the tracking of worker movements and job variety. Risk evaluation and management can be conducted flexibly, depending on the risk and situation, to determine the necessity to monitor, the required monitoring method, and the time interval before re-monitoring. The procedure and concept of area sampling vary significantly.

The correlation between the data obtained through personal exposure monitoring and area monitoring (personal versus area sampling) was investigated, and it was found that personal monitoring generally gives higher concentrations than area sampling. This occurrence may be attributed to personal exposure monitoring involving sampling air that contains relatively higher concentrations of chemicals due to the movement of workers. UNI EN 689:2019 advocates using personal sampling devices in the worker's breathing zone. Meanwhile, UNI EN 1540:2022 and ISO 18158:2016 define the breathing zone as a hemisphere in front of the face, with a radius of approximately 30 cm. The hemisphere is centred on an imaginary line extending from ear to ear and is connected to the top of the head and the larynx by an imaginary plane, as shown in Figure 25.

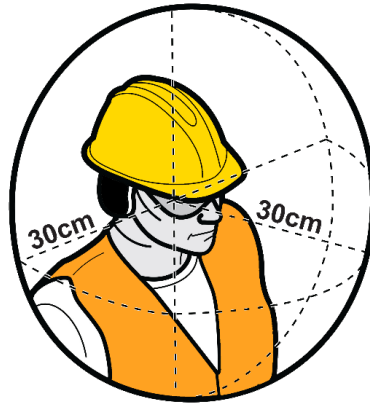


Figure 25 – Breathing zone

However, previous studies have demonstrated comparable median concentrations of FA for personal and area exposures, indicating their comparability with an approximate ratio of 1.0. This was observed particularly when work processing did not require continuous movement around the work area. [67, 68, 69] Based on this correlation, the proposed solution is an innovative ergonomic chair. It is equipped with a piezoresistive pressure sensor that detects the operator's presence, a barcode reader for personal identification, and a headrest fitted with remotely managed instruments that continually monitor the breathing zone. The chair is situated in front of the workstation, which is set up for use with fume cupboards. This innovative apparatus combines the in-built continuous monitoring devices with the benefits of an ergonomically designed workstation. [70]



Figure 26 – Sampling strategy proposed by Dugheri et al. [70] with personal sampling conducted by two NEMO XT on the headrest, DNPH-coated cartridge with a pump and area sampling performed by a Gasera

3.3.1.2. Real-time, in-continuous, commercial analysers for FA air monitoring

An instantaneous measurement method is a simplified measurement of the airborne concentration of target substances in situ, characterised by the ability to obtain results quickly. Comparisons conducted in experimental and field settings implied that the performances of direct-reading instruments are on par with the reference methods, rendering them seamlessly integrable into an occupational hygiene plan to prevent significant acute and chronic toxicity. [20, 67, 71, 72] Moreover, the growing interest in more environmentally friendly monitoring has led to an increase in the development of real-time, in-continuous smart detectors compared to the traditional indirect sampling method.

The handheld electrochemical sensor lacks specificity because of the high cross-sensitivities. Nevertheless, an active filter can be employed to remove interferences or a filter impregnated with DNPH can be used to reduce the influence of other Volatile Organic Compounds (VOCs) and solve this issue.

The accuracy of measurements is ensured by a selection of real-time analysers, some of which can be considered as confirmatory level monitoring instruments: infrared, photometric, differential optical absorption spectroscopy, cavity ring-down spectroscopy, fluorimetric, mass spectrometric techniques and GC separation coupled with a methanisation oven and a flame ionisation detector show measurement uncertainties comparable to those of the official methods. [20]

The sampling frequency and duration should allow for monitoring airborne FA concentrations up to approximately one-tenth of the occupational exposure limit. However, there are notable variations among different guidelines related to FA exposure in occupational settings, not only in terms of the concentration values, as demonstrated in Figure 27, but also in terms of which limit to evaluate. [67, 73] As a result, the modern approach to managing FA emissions in such settings is to adhere to the As Low As Reasonably Achievable (ALARA) principle, with the objective of staying as close as possible to the ubiquitous value, given its carcinogenic properties. In this context, it is crucial to consider the relationship between indoor and outdoor pollutants. While previous literature reported higher levels of indoor FA concentrations compared to outdoor ones, it is worth noting that outdoor FA concentrations, particularly in polluted urban areas, can now reach levels equivalent to those found indoors. [56] In healthcare settings with low FA levels, outdoor sources of airborne FA pollution may pose a potential threat to indoor air quality. Therefore, obtaining an accurate reading of the background pollution is crucial. [74]

In this new context, novel direct-reading FA monitoring devices have been proposed to facilitate real-time sampling with enhanced sensitivity, enabling the detection of even minimal fluctuations in FA concentration (up to 0.001 ppm), which is below the ubiquitous value that commonly occurs. Furthermore, remote control integration can further simplify and improve monitoring operations.

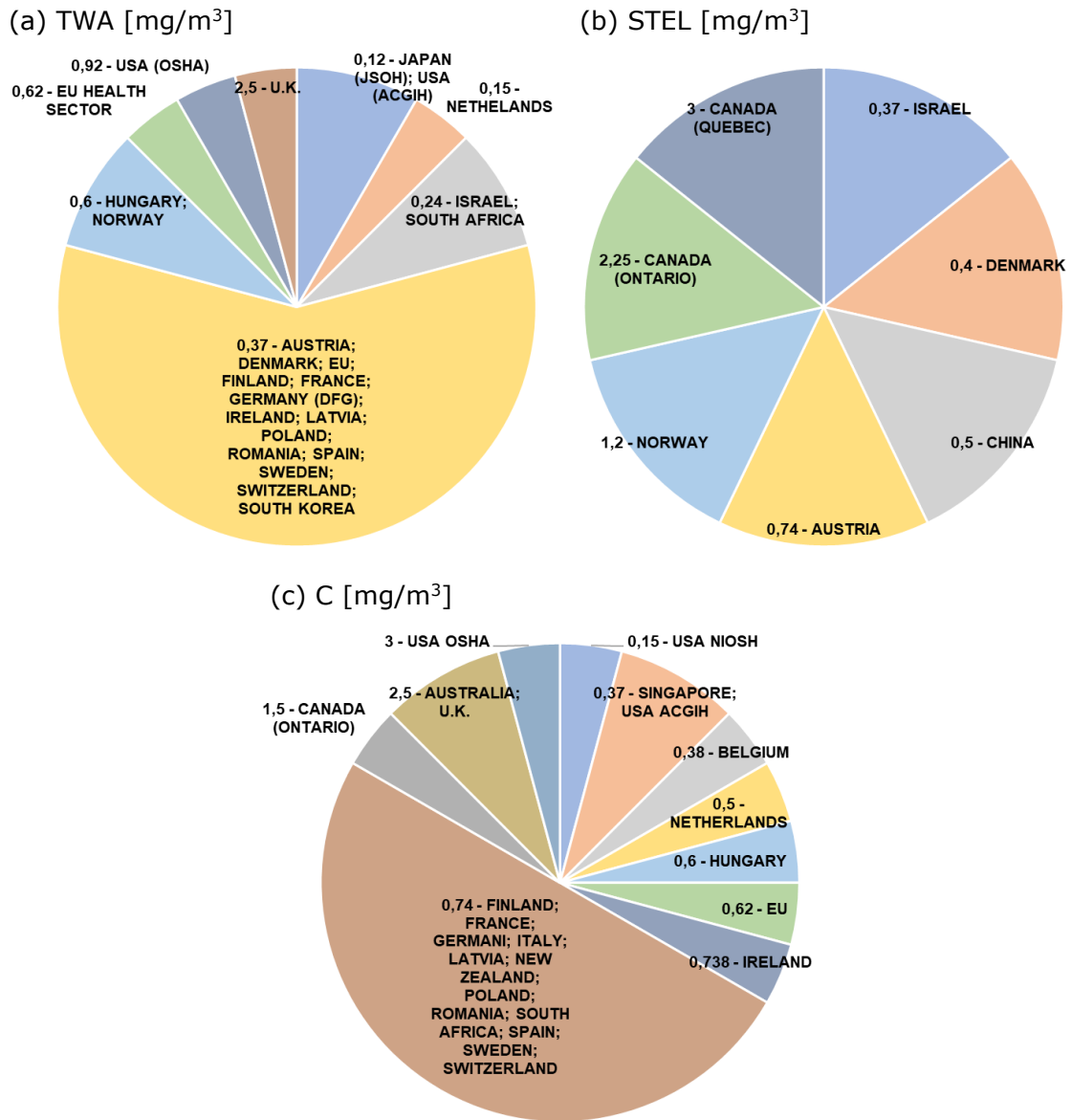


Figure 27 – Graphical representation of the heterogeneity of occupational exposure limits [mg/m³] for FA, (a) Time Weighted Average (TWA), (b) Short-Time Exposure Limit (STEL), (c) Ceiling Limit Value

3.3.1.3. Video Exposure Monitoring (VEM) in Occupational Hygiene

Conventional monitoring strategies, whether by direct or indirect reading methods, present issues as the work activity that leads to high exposure cannot be identified. The worker's activity during the surveys might not be discernible. The spatiotemporal mobility of individual contaminants in air sampling has been characterised by utilising detailed activity diaries [7], GPS devices [75], or smartphone-based location tracking applications [9] to record individual human movements. [76] It should be noted, however, that the detailed activity diaries may not be comprehensive or contain ambiguities that may inhibit the identification of risky work tasks. Moreover, simultaneous monitoring of two or more workers can complicate identifying high-risk activities. Video Exposure Monitoring (VEM) records work activities on video while direct-reading devices perform person/area monitoring. The VEM requires the merging and synchronising of video and exposure data for joint analysis, enabling accurate identification and noticing of excessive exposure levels. Therefore, the VEM enables a precise understanding of the link between an activity or event and exposure and permits prompt intervention and prevention of recurring hazardous conditions.

3.3.2. Workflow optimization

New, reliable methods of airborne FA monitoring and implementing safe practices in APLs are critical issues of increasing interest. [64, 77] It is imperative to implement optimisation measures to ensure safe handling and use of formalin in APL workflows. Enhanced work practices, from an occupational hygiene perspective, make a substantial impact on air quality. To comply with safety regulations, adopting best practices and employing engineering air handling systems is necessary. Process and system redesign may also be beneficial. Furthermore, adopting ergonomic design, including body-friendly adjustments and streamlined workflows, contributes to these best practices. Therefore, adopting ergonomic workstations is a technical solution for reducing FA emissions from the APL grossing room. The effectiveness of the new ergonomic workstation needs to be investigated, and it may be linked to potential customization options involving digital imaging and dictaphone recording systems, the latest generation of cassette printer, and safety devices for the collection and neutralization of any remaining formalin waste during biopsy slicing. Additionally, implementing such technologies may facilitate the standardization of Anatomy Pathology (AP) procedures and workflow.

3.3.2.1. Grossing workstation for ergonomic layout and main ventilation system

The fume-hood cupboards have recently undergone some improvements to increase their flexibility and incorporate optional tools to enable multitasking. It is crucial to emphasize that fume-hood cupboards should possess qualities, including ease of access to standard workflow operating features, maintenance of ergonomic postures, and safer formalin management. The latest generation of grossing rooms features ergonomic workstations that differ from conventional fume-hood cupboards. They are equipped with a laminar and/or back downdraft ventilation system and a working surface without front glass, which allows for wider freedom of movement and better ergonomic posture. One of the significant advancements pursued and introduced lately in the progress of contemporary grossing workstations is high-performance, budget-friendly digital optical consoles that can capture top-quality images of tissue specimens.

Modern workstations have become increasingly flexible and efficient, featuring various new capabilities such as modular architecture, connectivity through middleware with the APL's information system, a Digital Pathology System (DPS) that records complete images of processed specimens, and Voice Recognition Technology (VRT) - with a dictaphone.

These modern workstations aim to simplify the slicing of biopsies by pathologists. They come equipped with an open work surface, nozzles for continuous washing with water, and personalized ergonomic adjustments. Customization options allow for a reduction in workflow actions required outside of the workstation's area, which could significantly lower FA emissions. Furthermore, using special pads to adsorb and neutralise FA on the slicing plane and a patented FA neutraliser capable of converting excess formalin into harmless polymers has the potential to reduce the emission of harmful fumes.

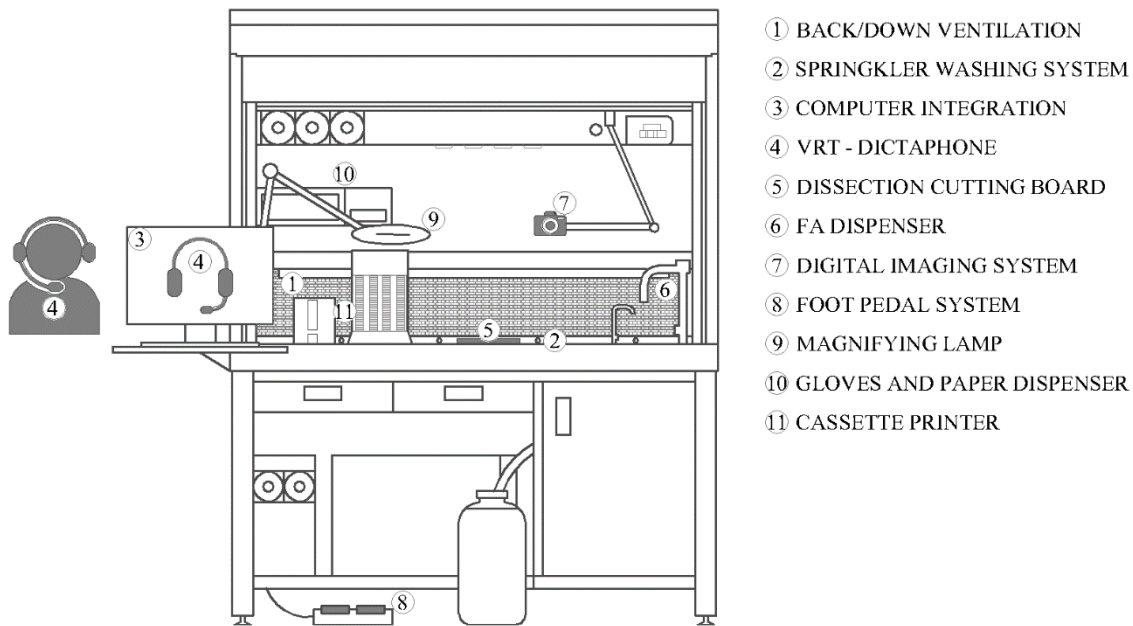


Figure 28 – Schematic representation of new ergonomic grossing workstation and possible customization solutions

Figure 28 depicts a schematic representation of the new ergonomic grossing workstation with many different customisation options.

Another essential factor in reducing FA exposure and safeguarding the operators' health in grossing rooms is the general ventilation system. The engineering controls that are required are a computer-based control system, the Building Management System (BMS), which must be installed to control and monitor the building's mechanical and electrical equipment, such as the heating, ventilation and air conditioning (HVAC) system, and to interface with the workplace exhaust system. This centralised system would enable rapid identification and repair of technical faults.

3.4. Gas chromatographic determination

Multiple methods exist for analysing airborne FA concentration, with validated techniques for quantifying gaseous FA concentration being based on active or passive sampling. The first method employs 2,4-dinitrophenylhydrazine (DNPH) as a derivatizing compound on a filter or cartridge [78], which will subsequently be analysed via LC or GC [79] through chemical extraction. The second method utilizes O-(2,3,4,5,6-pentafluorobenzyl) hydroxylamine (PFBHA) as a reagent on the solid sorbent, such as SPME fiber and thermal desorption in the injection port of GC. The corresponding reactions are illustrated in Figure 29.

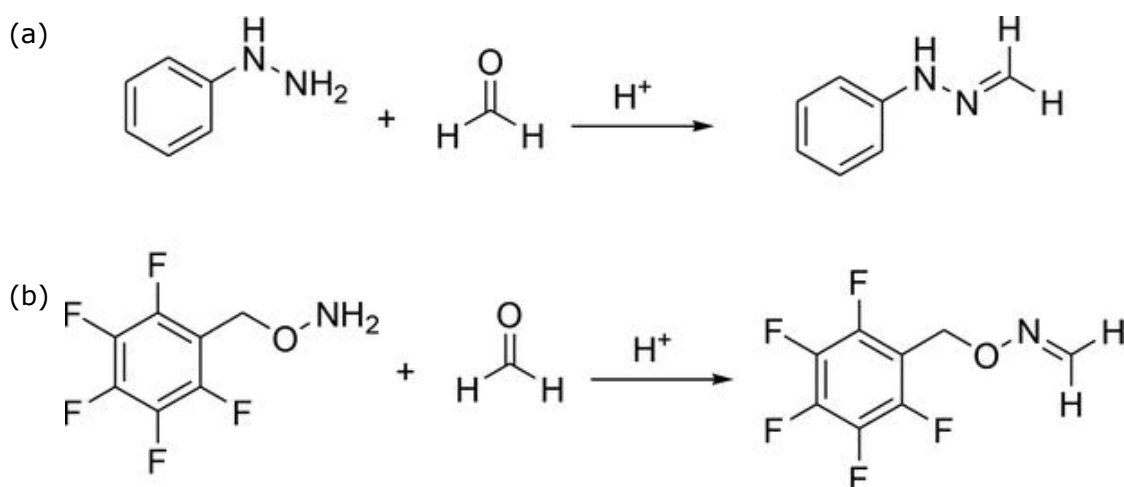


Figure 29 – Chemical reaction of (a) DNPH and FA and of (b) PFBHA and FA

An automated method for the rapid analysis of FA has been developed and assessed for its high efficiency and greenness through on-fibre derivatisation with PFBHA. A comparison between SPME and SPME Arrow, introduced in section 2.3.1.1, was made, highlighting the benefits and drawbacks of both approaches.

Both techniques, SPME and SPME Arrow using PFBHA for on-fibre derivatisation, are valuable approaches for the determination of FA. Various factors affect the extraction-derivatization, which have been studied and optimised. The method yielded satisfactory outcomes in regard to linearity, precision, accuracy, and sensitivity. Standard solutions were used to test and develop the SPME and SPME Arrow techniques, which allowed assessing their usefulness.

The PFBHA loading levels on both SPME and SPME Arrow were assessed by exposing the devices in a vial's headspace, using a 50 mg/mL PFBHA solution for 1, 2, 4, 8, and 16 minutes. Figure 30 depicts the findings: PFBHA loading on the device increased until minute 4 for all methods, then remained constant for SPME, whilst SPME Arrow showed a slight growth for prolonged periods. Additionally, the increased

surface area of the adsorbent phase allows a double mass of PFBHA to be loaded on SPME Arrow compared to SPME, which proportionally enhances the level of FA-oxime. This characteristic makes SPME Arrow more suitable for higher concentrations of FA and/or in the presence of interferences.

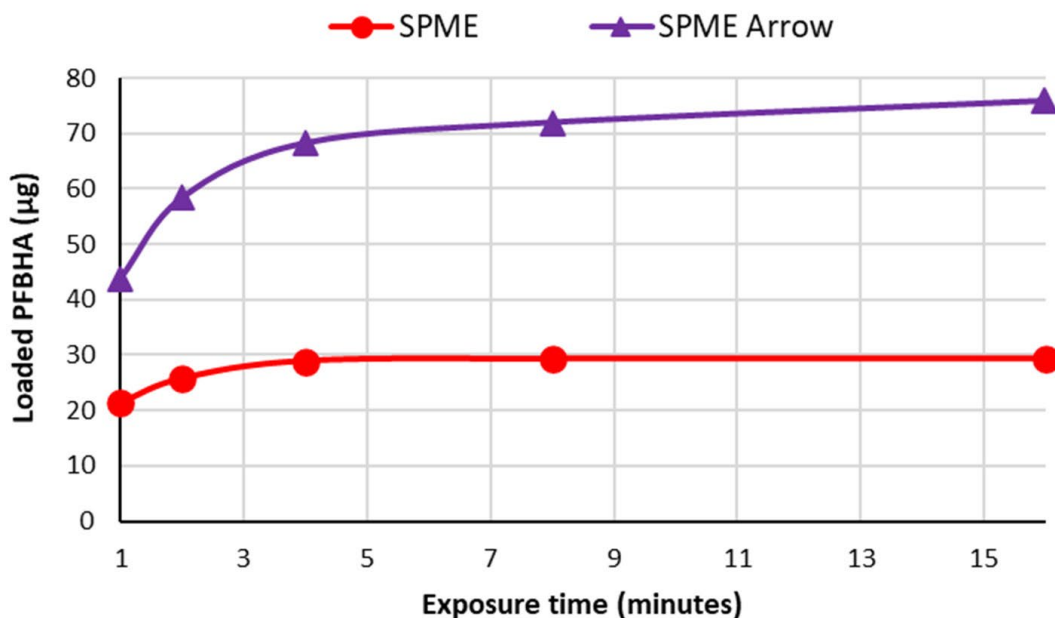


Figure 30 – PFBHA loading comparison between SPME and SPME Arrow fiber as a function of exposure time

SPME Arrow has greater mechanical stability than SPME fiber, which results in a lengthier equipment lifetime, higher sample throughput and better sensitivity. However, the septum of the vial quickly deteriorates after 8-10 injections with SPME Arrow, and this device has a higher cost and the need for specific injectors and liners, which is why SPME is more versatile.

A numerical score ranging from 1 to 10 (1-3 for standard, 4-7 for moderate, and 8-10 for outstanding) was assigned to six parameters used to evaluate the two devices: compatibility, sensitivity, mechanical stability, loading capacity, cost per injection (cost of a single injection considering 100 injections), and throughput. The results are presented in Figure 31.

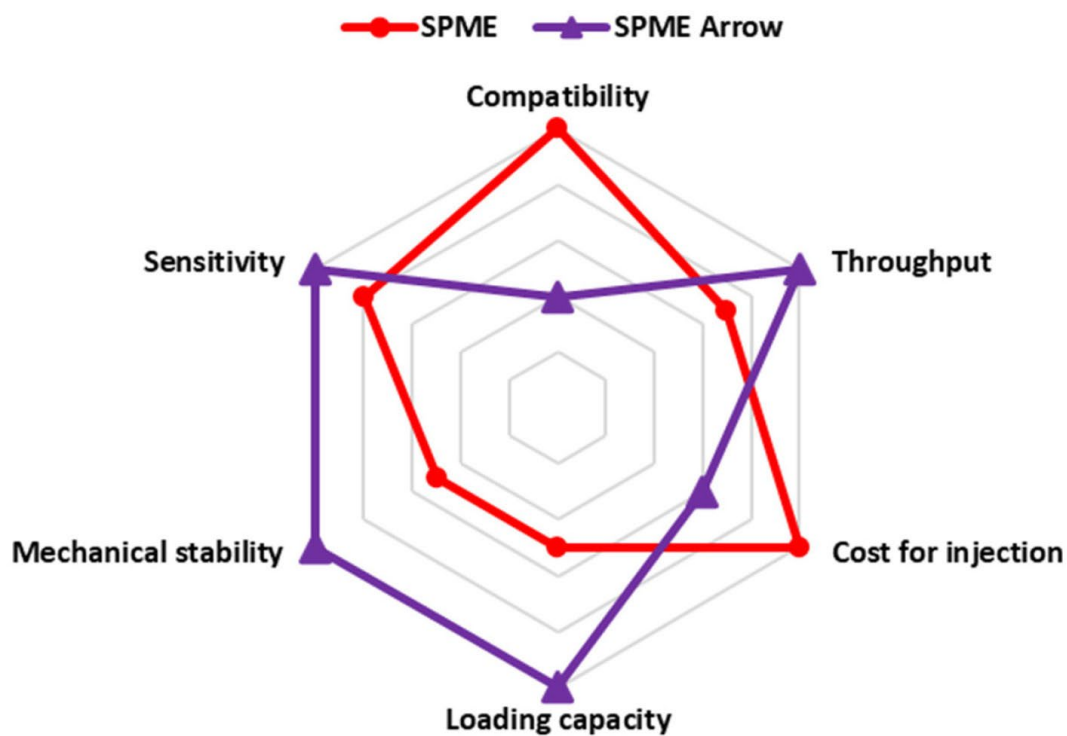


Figure 31 – Radar chart of comparison between SPME and SPME Arrow

As the main differences between the two devices are about compatibility and loading capacity, SPME is recommended up to concentrations to whom the loading capacity is sufficient to extend the range of concentrations which can be determined and to enhance the applicability of the method in different contexts, SPME Arrow is better.

3.5. Case studies

We carried out two separate monitoring studies in anatomical pathology laboratories. The instruments employed comprised:

- The Nemo XT, a passive sampler utilising a nanoporous formaldehyde sensor, operates through a sol-gel process and is based on colour variation. Readings are taken every two hours using an optical reader. The data collected with the Nemo XT can be monitored through a computer or smartphone app.

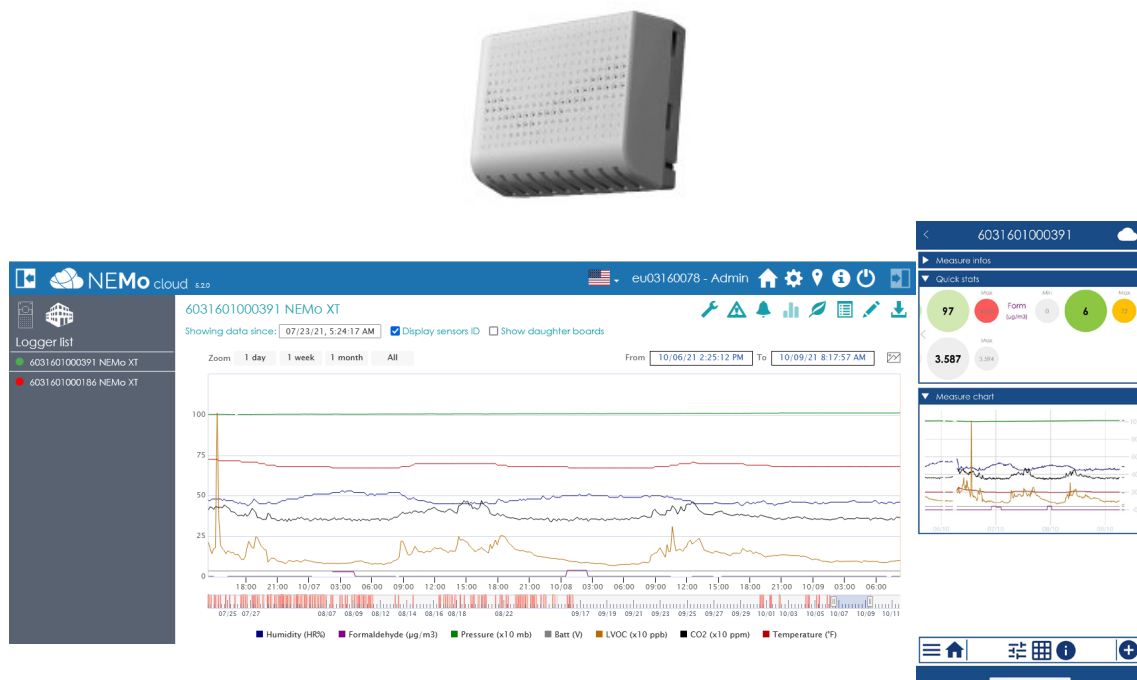


Figure 32 – The Nemo XT (above) and the screens from the computer (left) and the smartphone (right)

- The six-position GasCheck Basic automatic collector box is equipped with a GSM module. This device enables formaldehyde sequential sampling with dinitrophenylhydrazine (DNPH) cartridges; the flow rate is adjustable from 0.2 to 2.0 L/min. It is programmable (flow rate, the start and end time of each cartridge's sampling, and the time between two sequential samples) and can be activated through SMS.



Figure 33 – GasCheck Basic automatic collector box equipped with a GSM module (left) and the detail of the interior of the GasCheck with six DNPH cartridges (right)

Moreover, during the first monitoring, we utilised:

- GASERA ONE FORMALDEHYDE, a photoacoustic gas analyser that can be controlled remotely. It employs a combination of ultra-sensitive cantilever-enhanced photoacoustic detection technology and a quantum cascade laser source, which operates at a Mid-IR fundamental spectral absorption line of FA. This combination enables the device to reach a sensitivity level of less than one part per billion, allowing for reliable measurements of ambient background levels of FA. Additionally, it offers a high level of stability and only requires re-calibration every several months to several years.



Figure 34 – Gasera One Formaldehyde

Whilst during the second one:

- ProCeas FORMALDEHYDE, a pre-calibrated infrared laser spectrometer designed to measure formaldehyde concentrations in ambient air. This instrument utilizes OFCEAS IR laser technology (WO 03031949) to detect formaldehyde with high specificity, accuracy, selectivity, and stability. The analyser features an easy-to-install low-pressure sampling system and

operates continuously, 24 hours a day, seven days a week. It has a Windows-based operating system and can be remotely managed through TeamViewer. If connected to the internet, operating this system remotely and accessing the collected data in real time is possible.

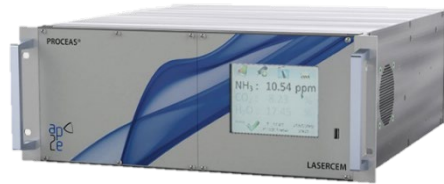


Figure 35 – ProCeaS Formaldehyde

The forthcoming section will present the results and compare the monitoring methods used.

3.5.1. First monitoring in APL

A comparison is made between the results obtained with the Nemo XT (top graph from Figure 36 to Figure 43) and the Gasera One Formaldehyde (bottom graph from Figure 36 to Figure 43). The green lines represent the shift's start and end, and the concentrations are expressed in mg/m^3 .

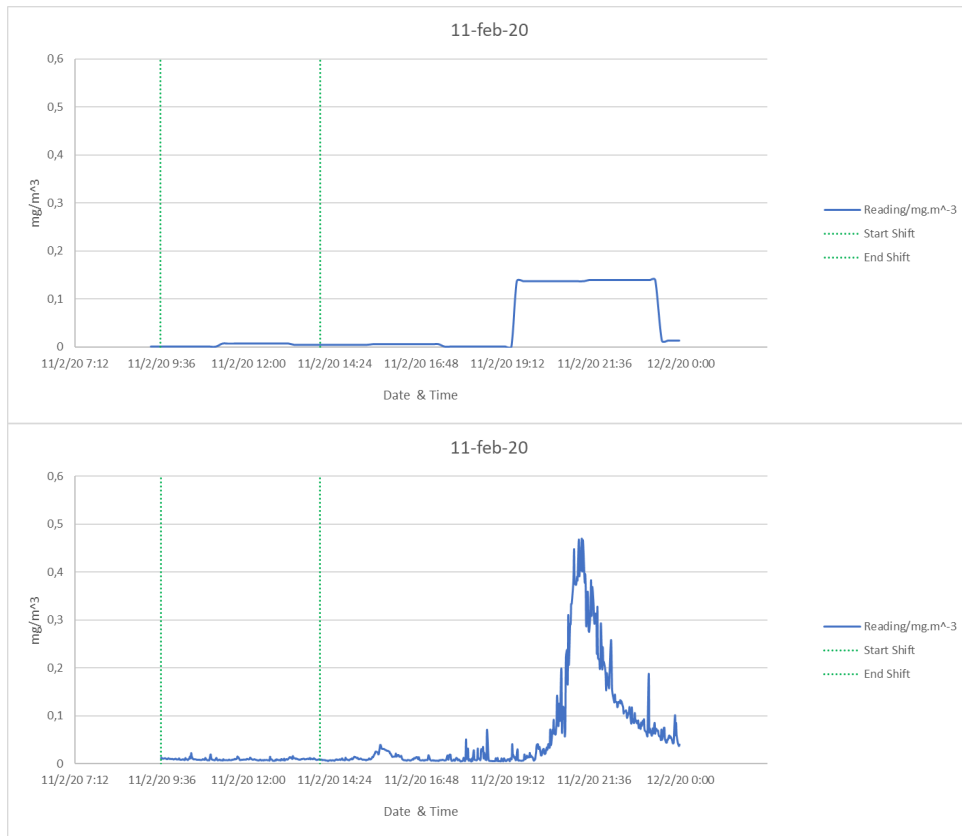


Figure 36 – Anatomical parts reduction room: Concentration values [mg/m³] measured on 11 February 2020

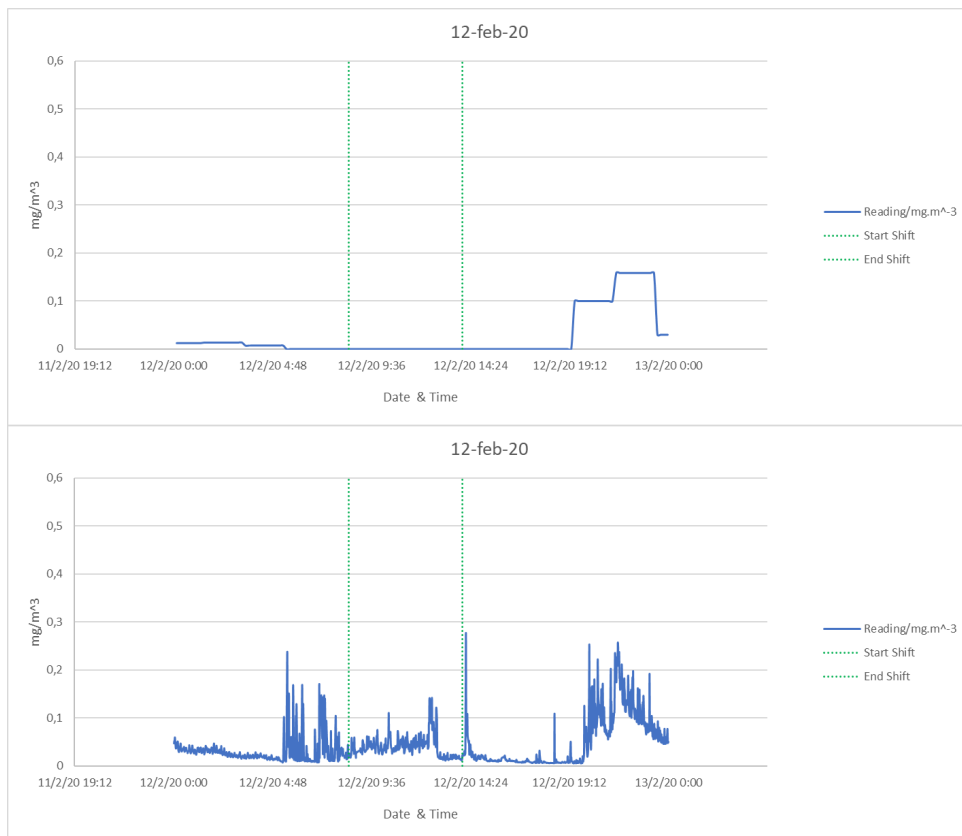


Figure 37 – Anatomical parts reduction room: Concentration values [mg/m³] measured on 12 February 2020

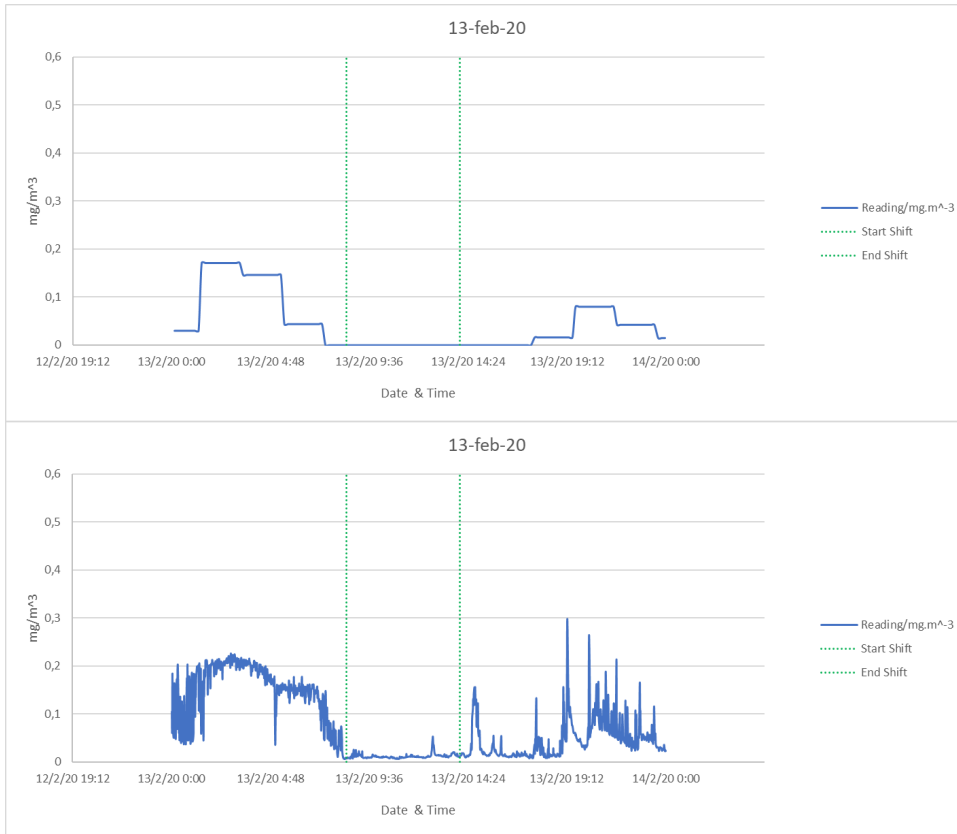


Figure 38 – Anatomical parts reduction room: Concentration values [mg/m³] measured on 13 February 2020

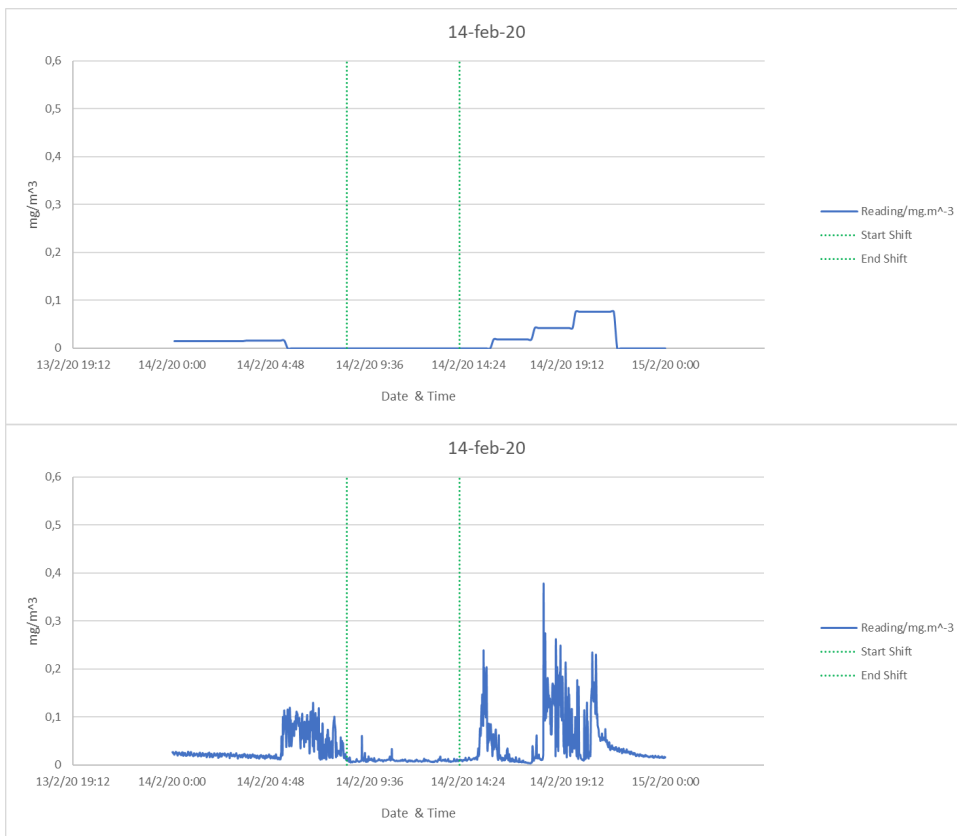


Figure 39 – Anatomical parts reduction room: Concentration values [mg/m³] measured on 14 February 2020

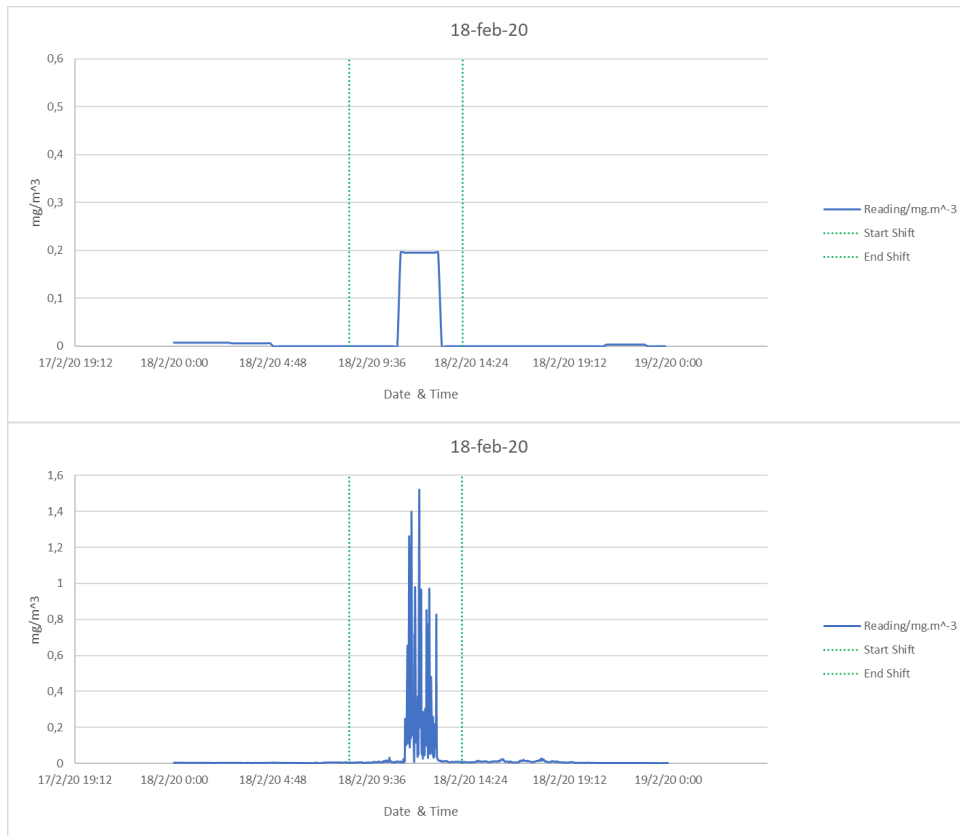


Figure 40 – Reception room: Concentration values [mg/m³] measured on 18 February 2020
Please Note that in the under graph, the y-axis is from 0 to 1.6 mg/m³

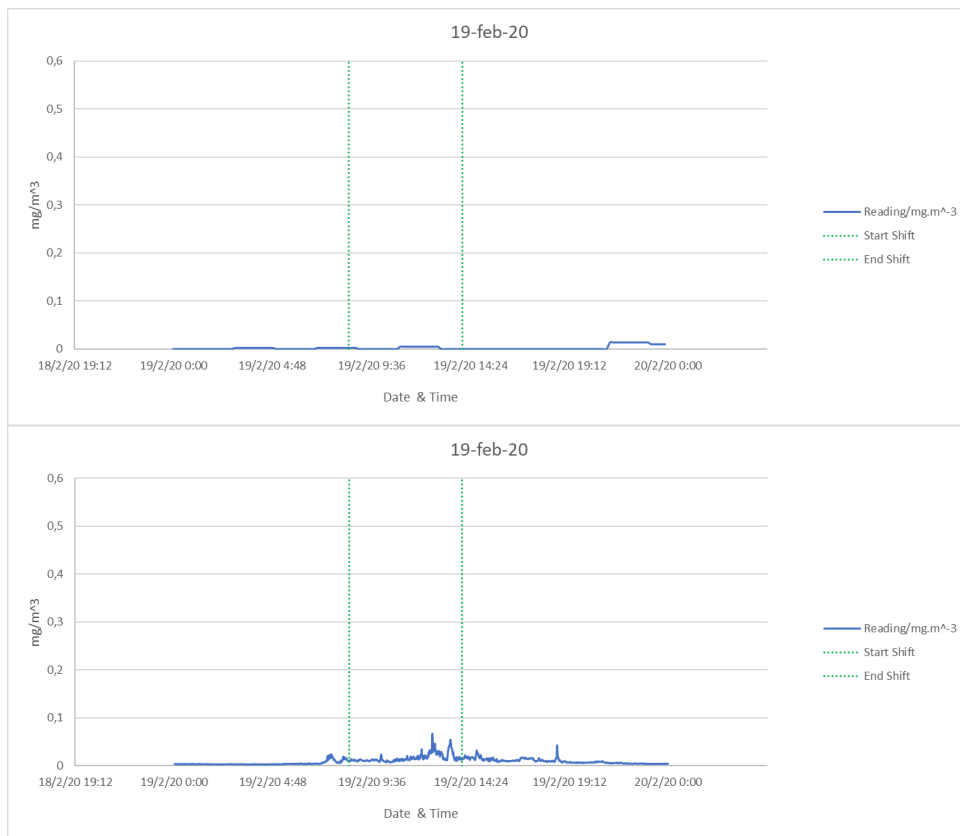


Figure 41 – Reception room: Concentration values [mg/m³] measured on 19 February 2020

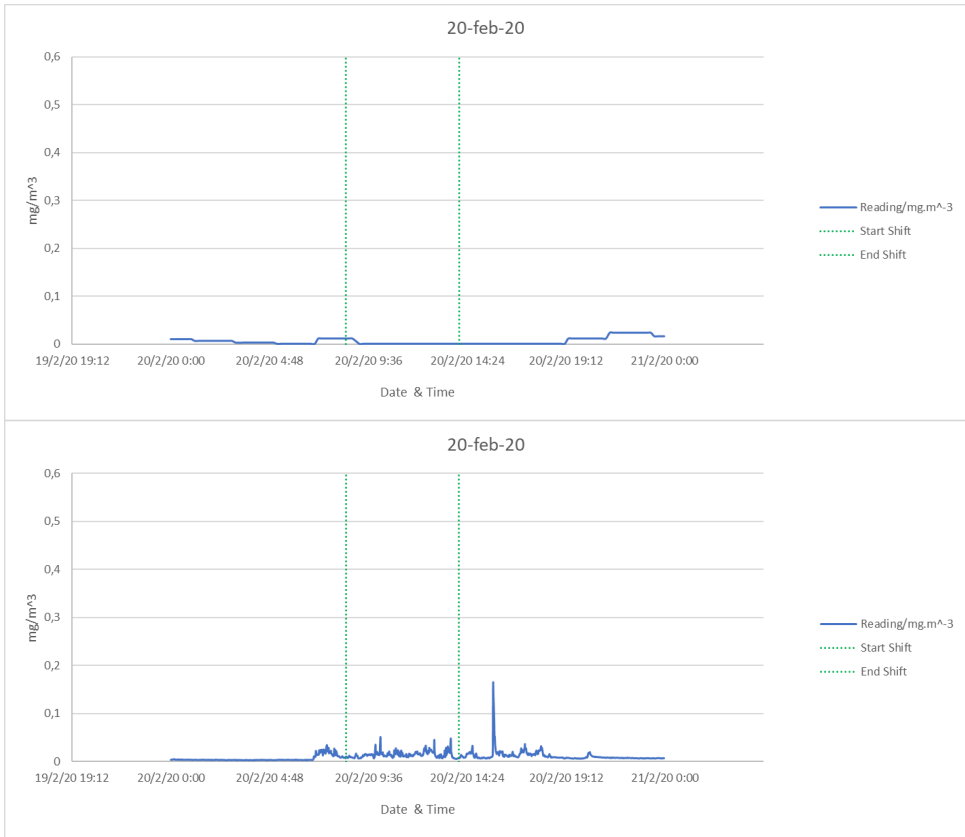


Figure 42 – Reception room: Concentration values [mg/m³] measured on 20 February 2020

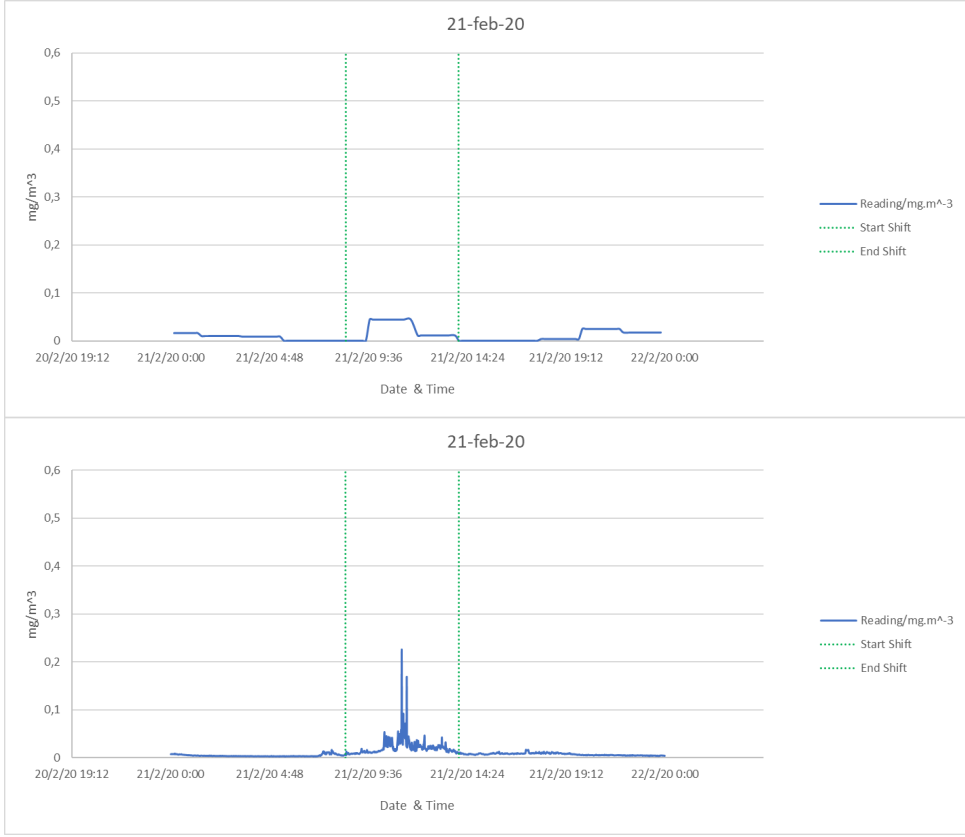


Figure 43 – Reception room: Concentration values [mg/m³] measured on 21 February 2020

3.5.2. Second monitoring in APL

A comparison is made between the results obtained with the Nemo XT (top graph from Figure 44 to Figure 67) and the ProCeas (bottom graph from Figure 44 to Figure 67). The green lines represent the shift's start and end, and the concentrations are expressed in mg/m^3 .

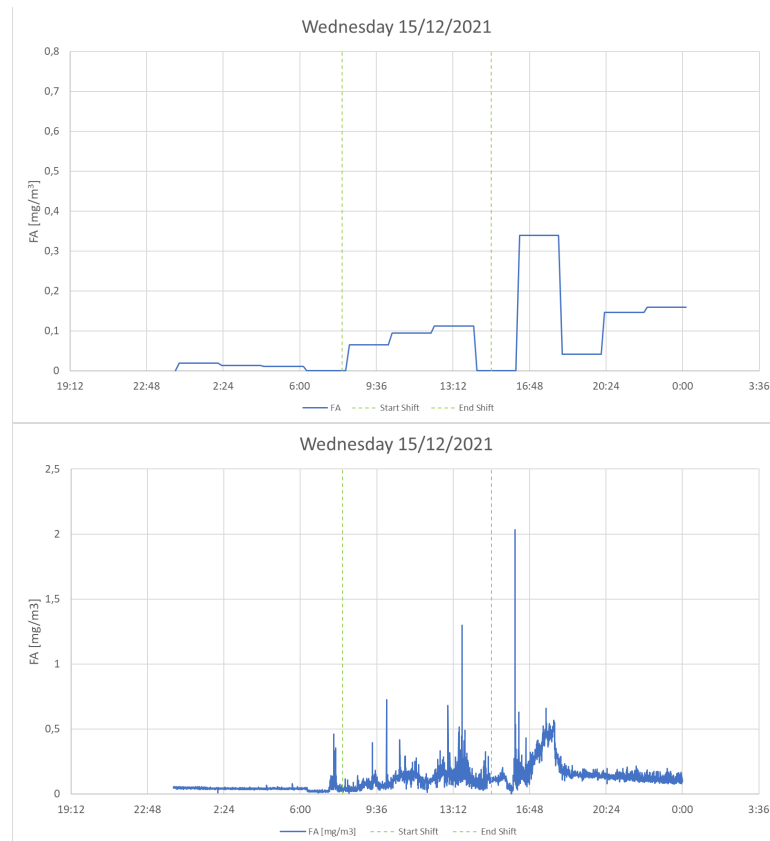


Figure 44 –Concentration values [mg/m^3] measured on 15 December 2021

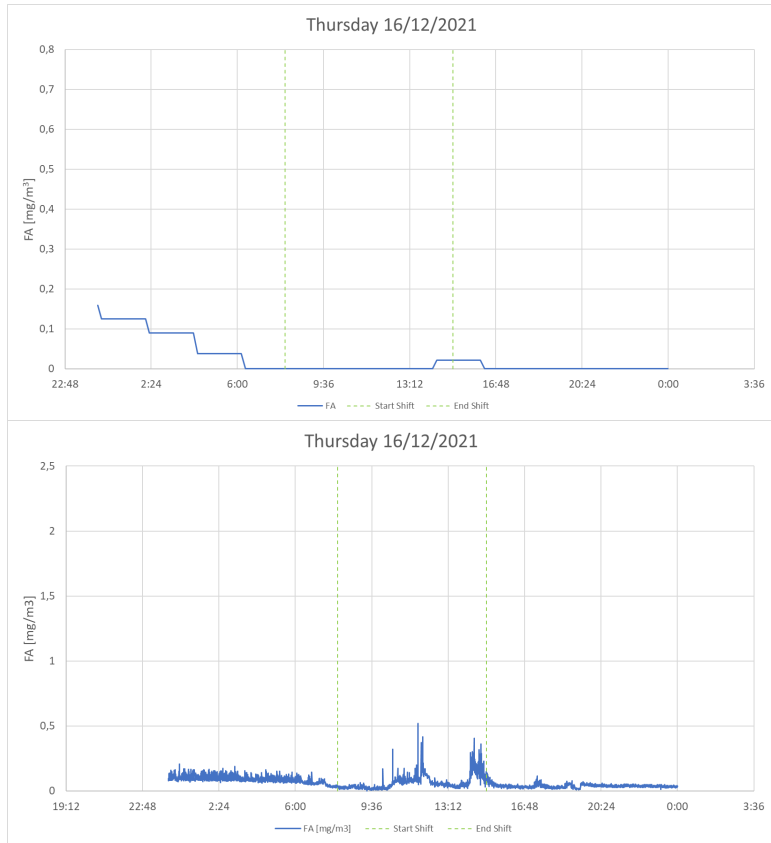


Figure 45 –Concentration values [mg/m³] measured on 16 December 2021

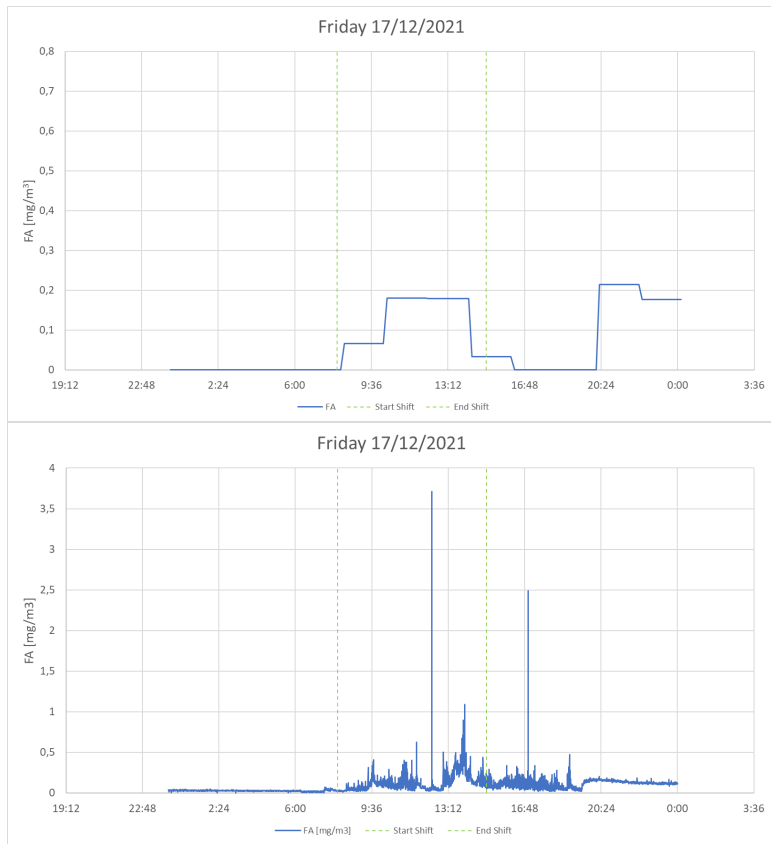


Figure 46 –Concentration values [mg/m³] measured on 17 December 2021.
Please Note that in the under graph, the y-axis is from 0 to 4 mg/m³

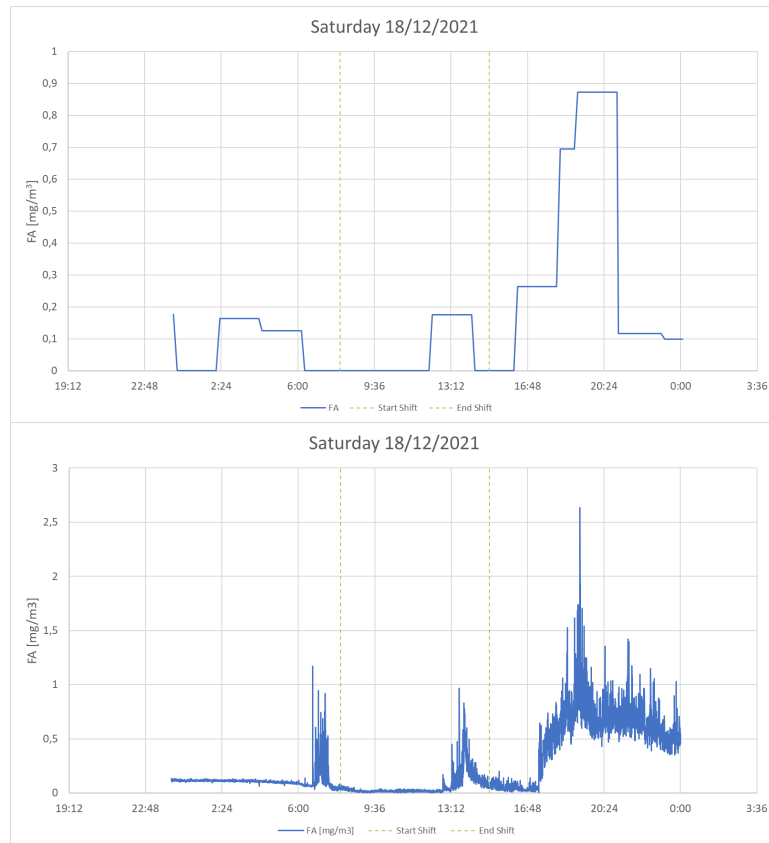


Figure 47 –Concentration values [mg/m³] measured on 18 December 2021. Please Note that in the under graph, the y-axis is from 0 to 3 mg/m³

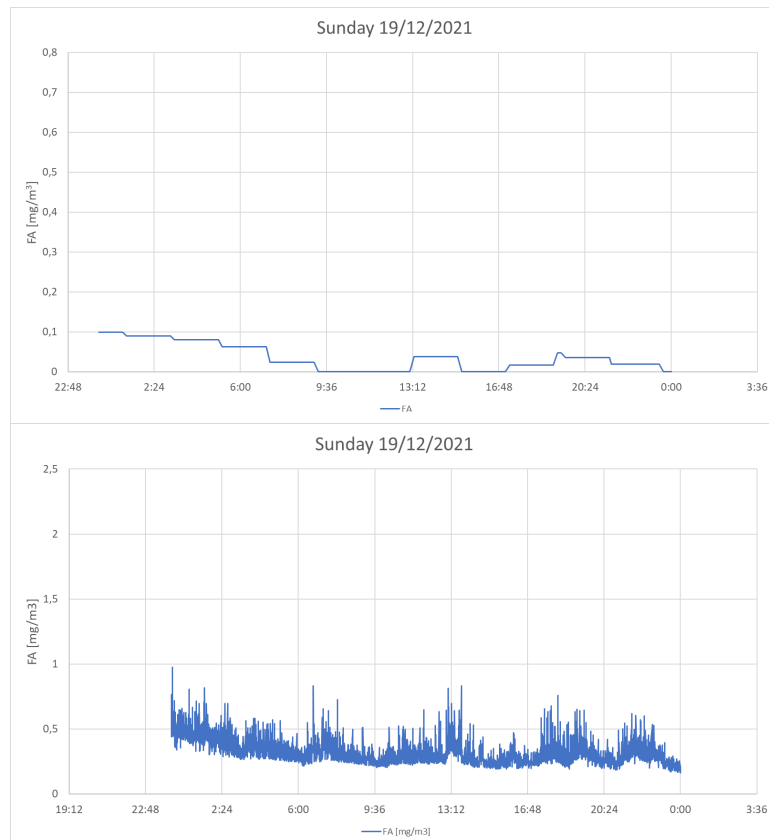


Figure 48 –Concentration values [mg/m³] measured on 19 December 2021

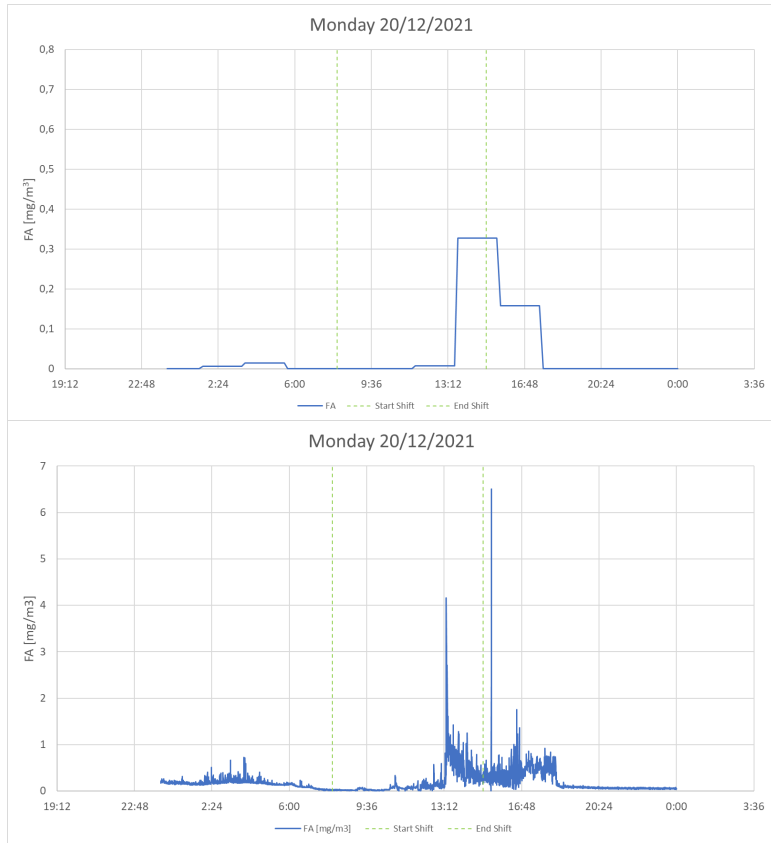


Figure 49 –Concentration values [mg/m³] measured on 20 December 2021.
Please Note that in the under graph, the y-axis is from 0 to 7 mg/m³

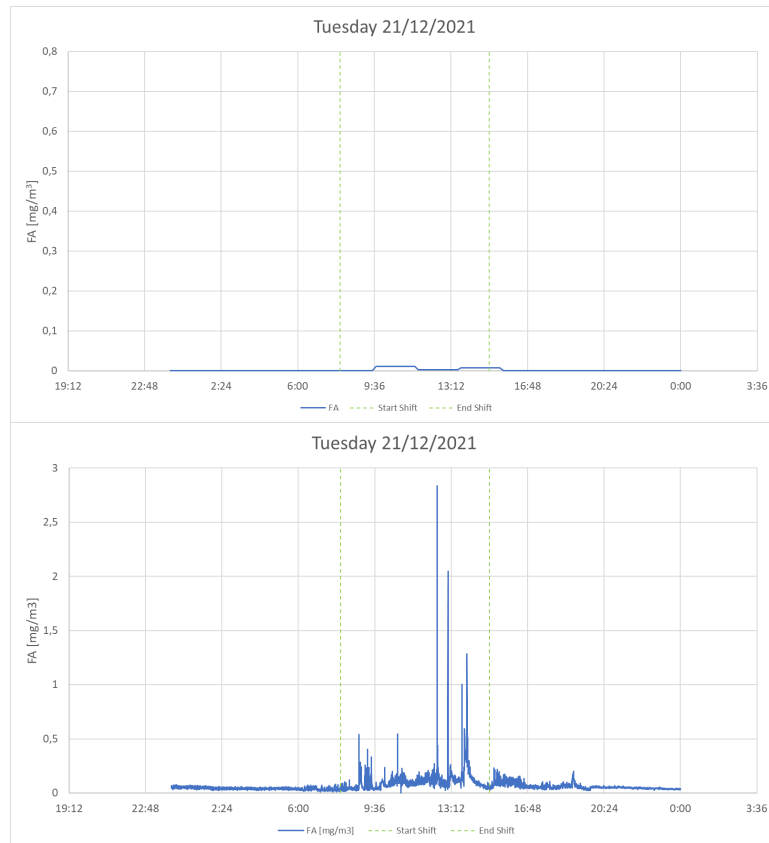


Figure 50 –Concentration values [mg/m³] measured on 21 December 2021. Please Note that in the under graph, the y-axis is from 0 to 3 mg/m³

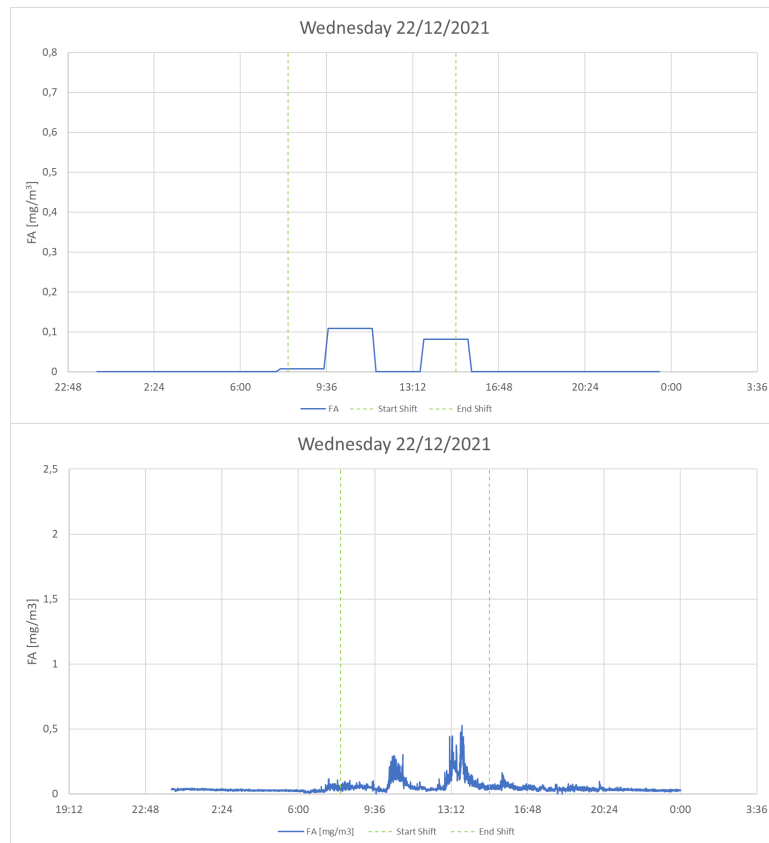


Figure 51 –Concentration values [mg/m³] measured on 22 December 2021

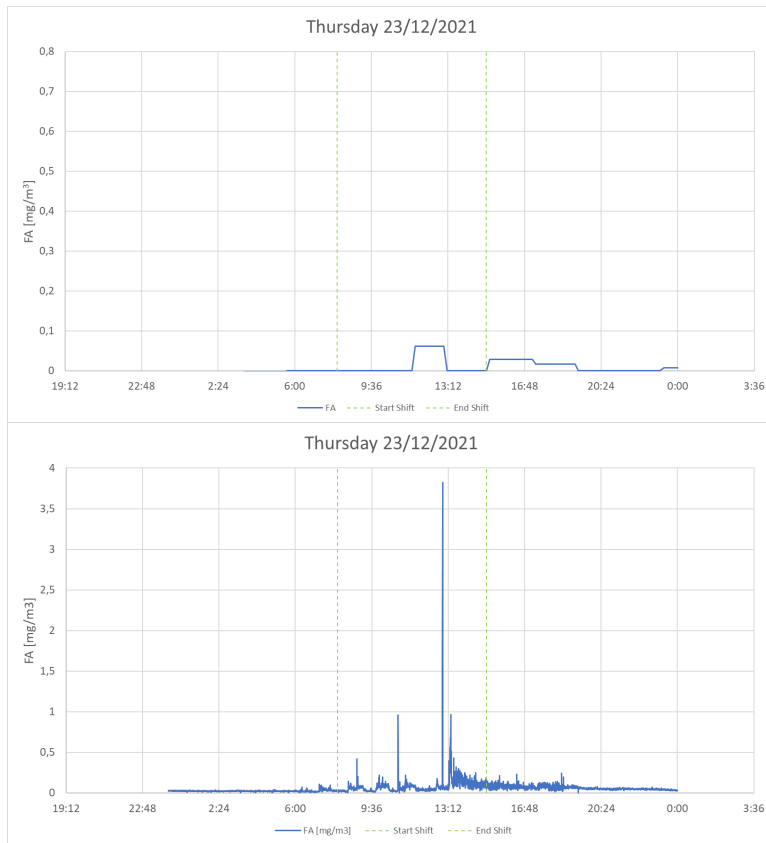


Figure 52 –Concentration values [mg/m³] measured on 23 December 2021. Please Note that in the under graph, the y-axis is from 0 to 4 mg/m³

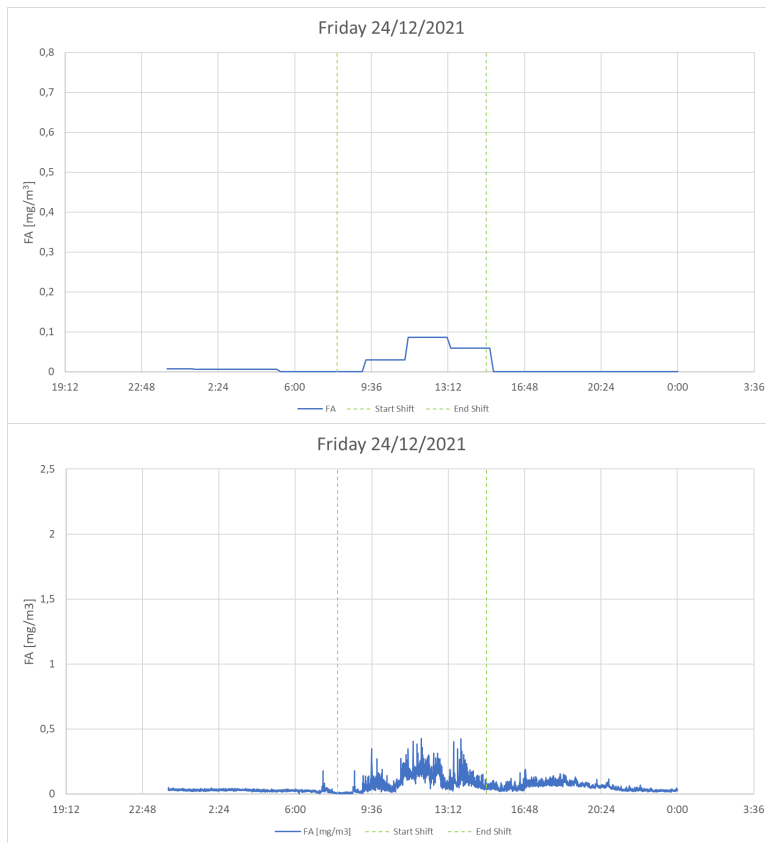


Figure 53 –Concentration values [mg/m³] measured on 24 December 2021

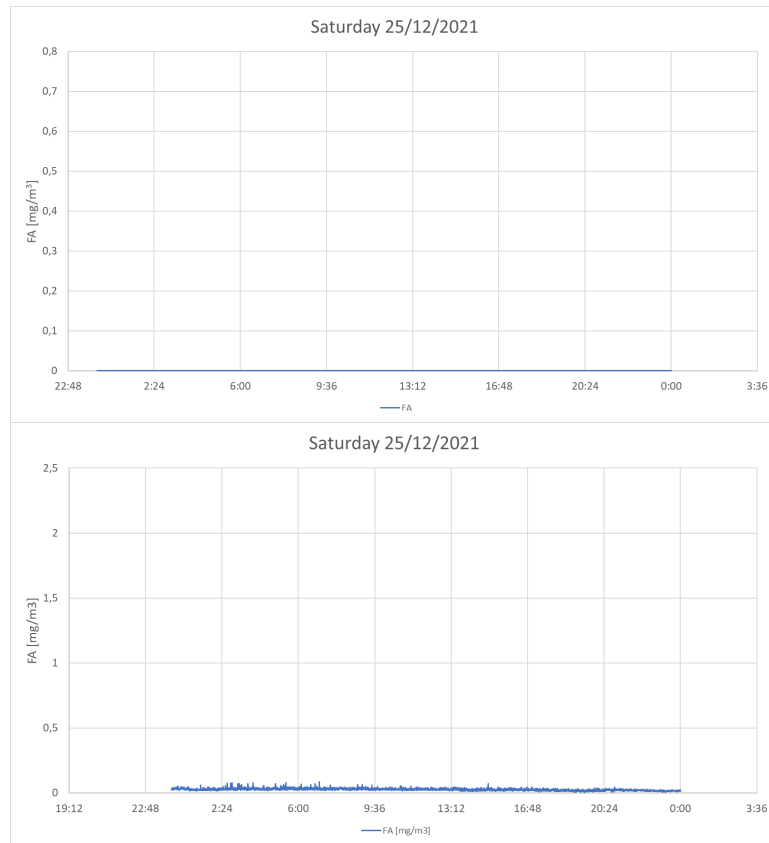


Figure 54 –Concentration values [mg/m³] measured on 25 December 2021

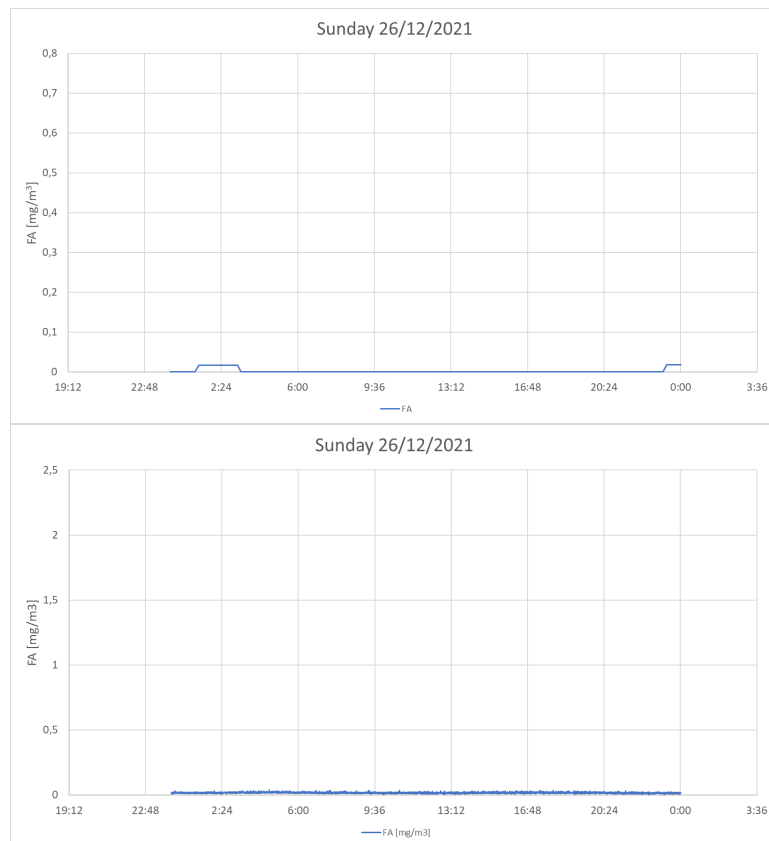


Figure 55 –Concentration values [mg/m³] measured on 26 December 2021

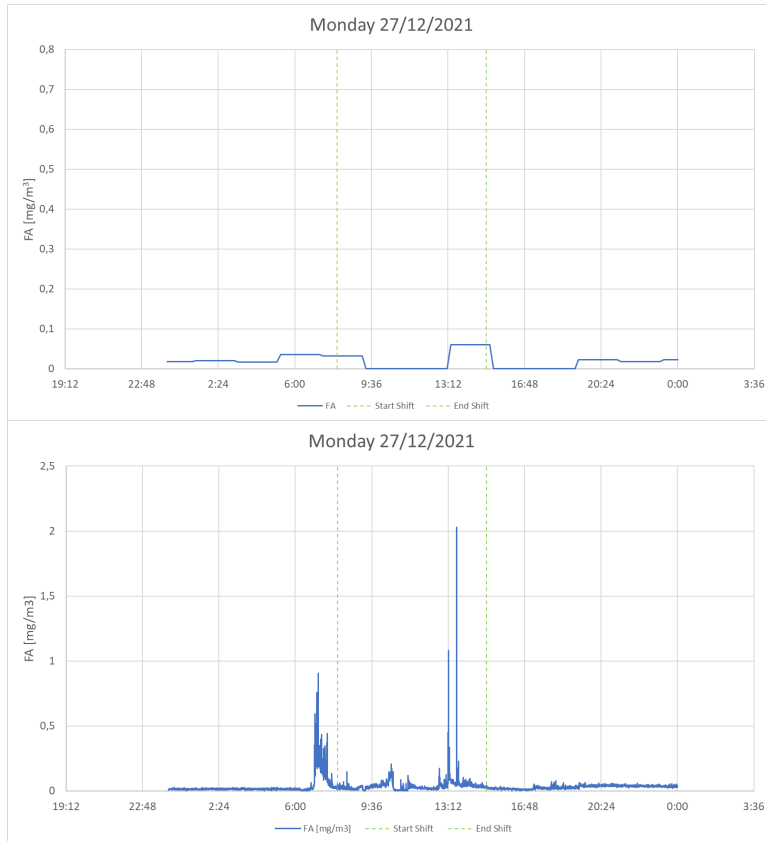


Figure 56 –Concentration values [mg/m³] measured on 27 December 2021

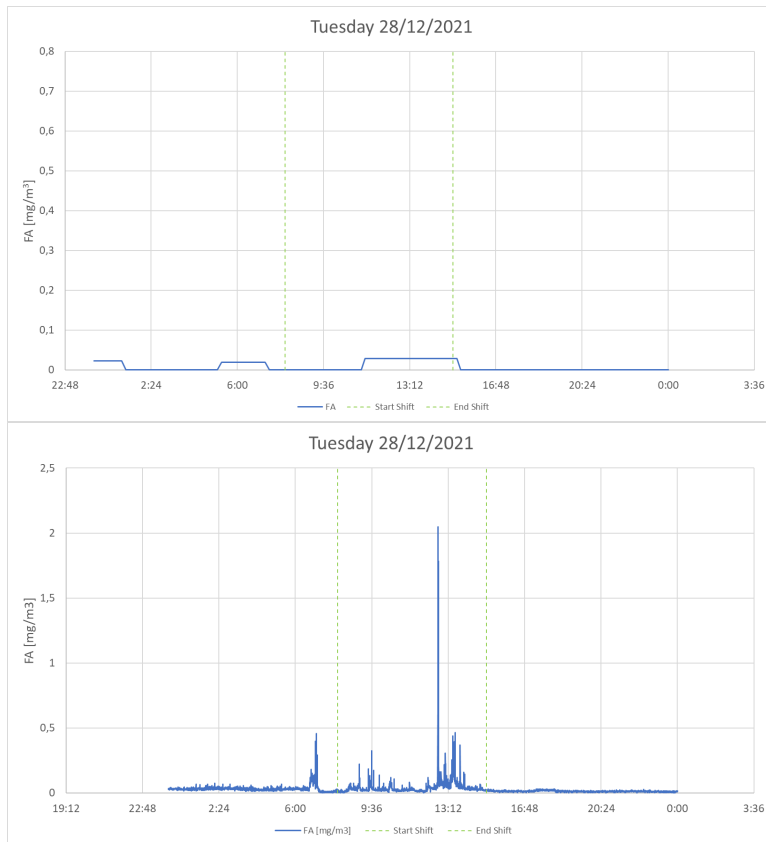


Figure 57 –Concentration values [mg/m³] measured on 28 December 2021

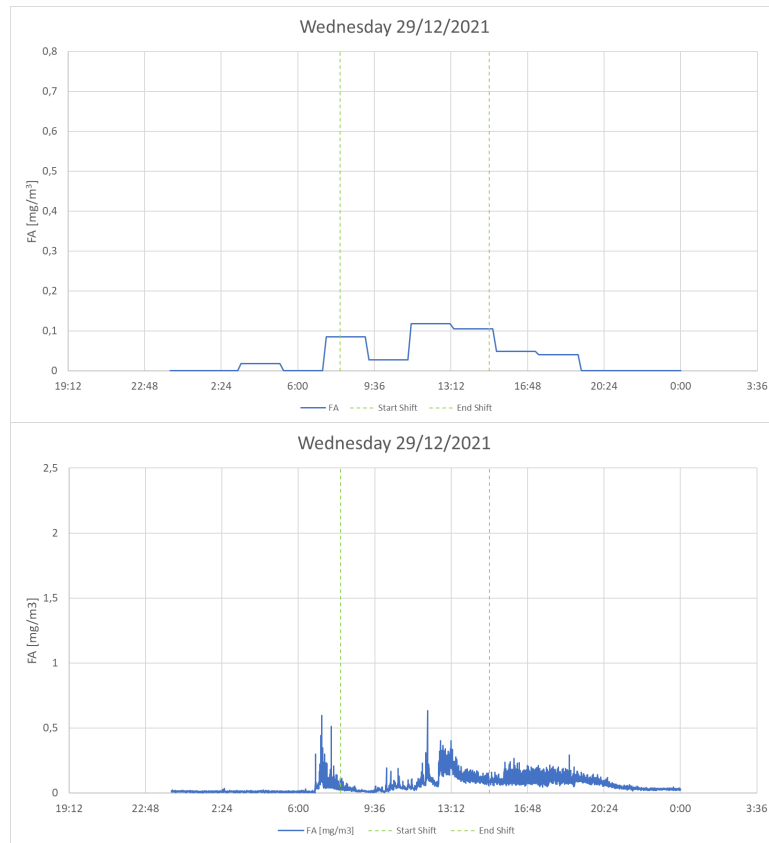


Figure 58 –Concentration values [mg/m³] measured on 29 December 2021

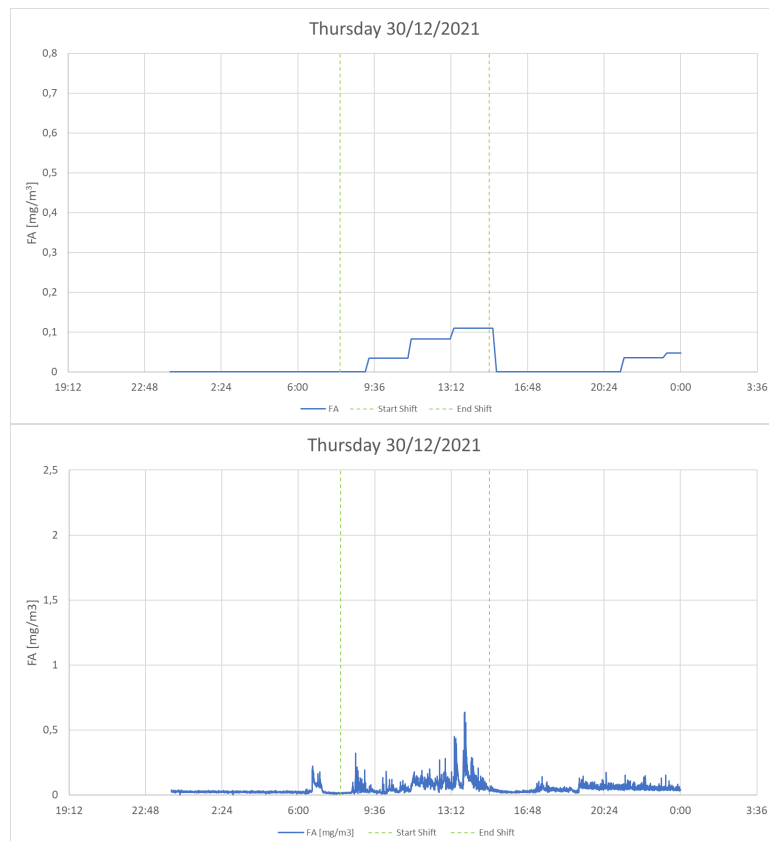


Figure 59 –Concentration values [mg/m³] measured on 30 December 2021

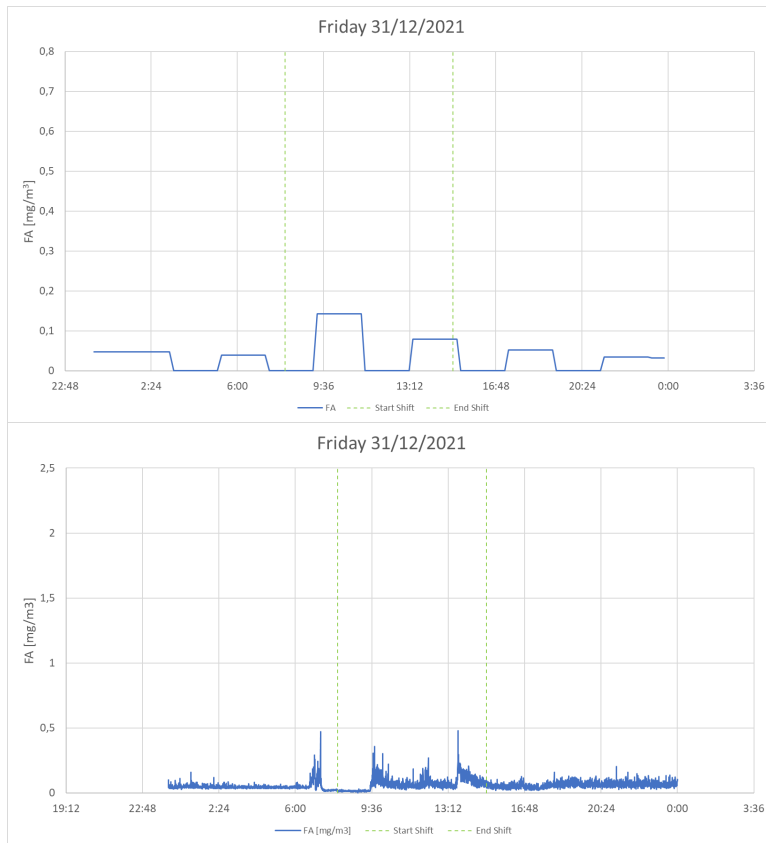


Figure 60 –Concentration values [mg/m³] measured on 31 December 2021

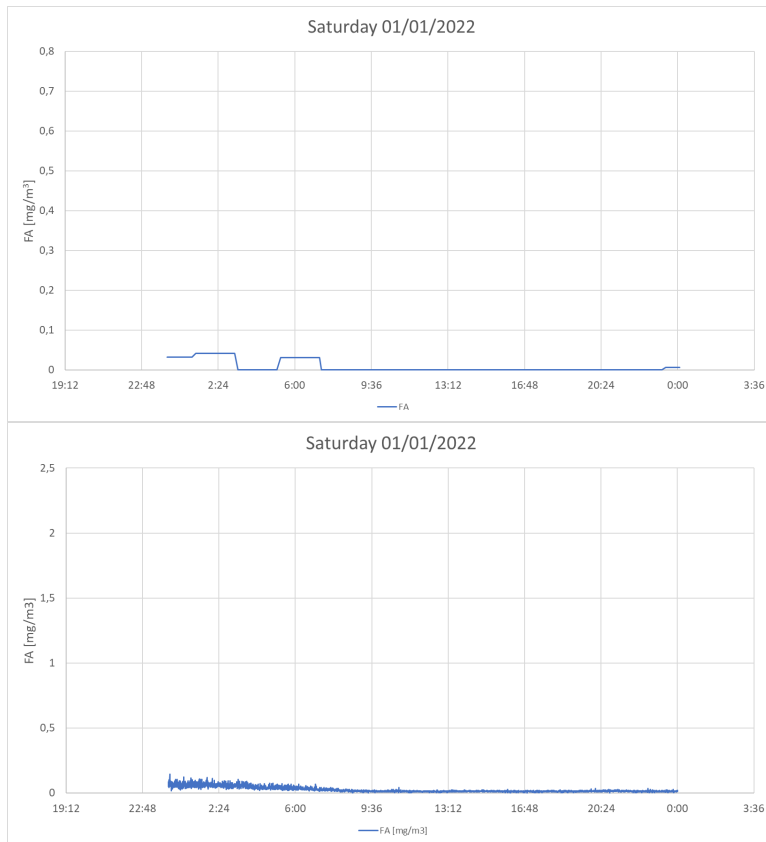


Figure 61 –Concentration values [mg/m³] measured on 01 January 2022

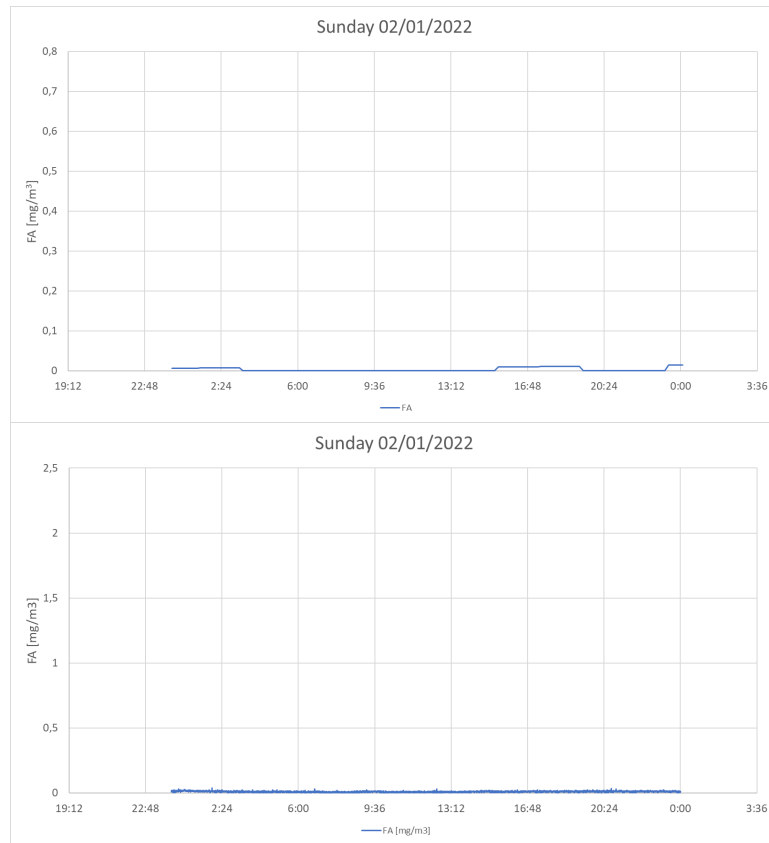


Figure 62 –Concentration values [mg/m³] measured on 02 January 2022

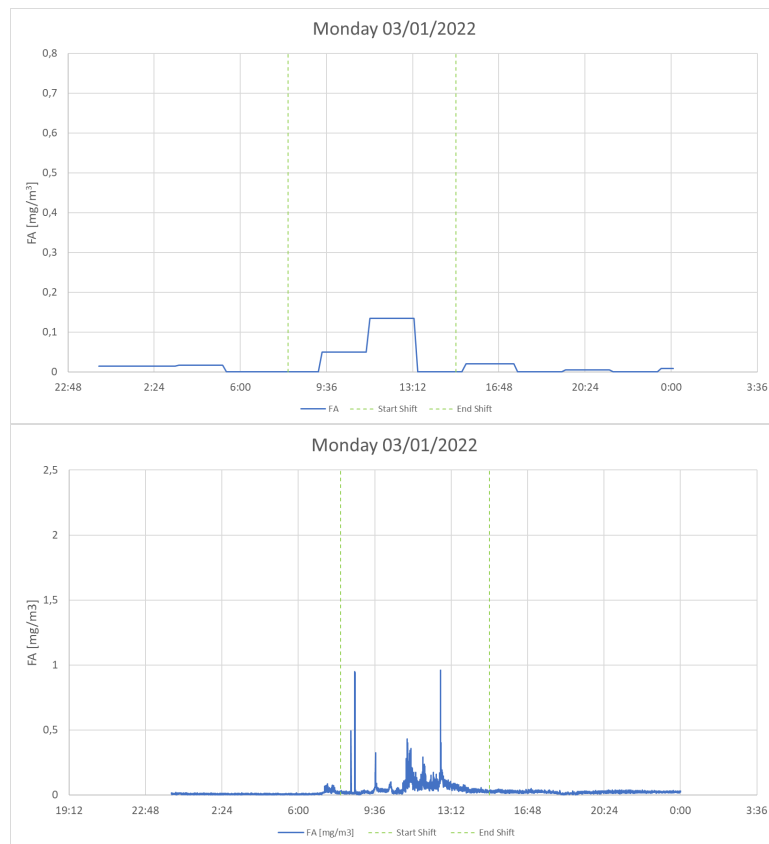


Figure 63 –Concentration values [mg/m³] measured on 03 January 2022

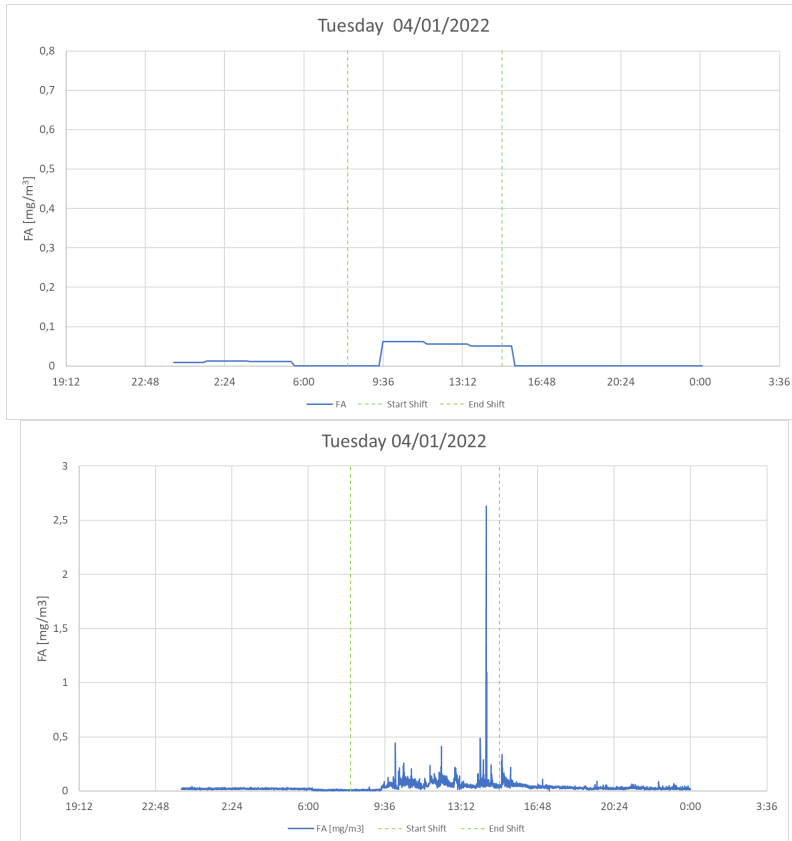


Figure 64 –Concentration values [mg/m³] measured on 04 January 2022.
Please Note that in the under graph, the y-axis is from 0 to 3 mg/m³

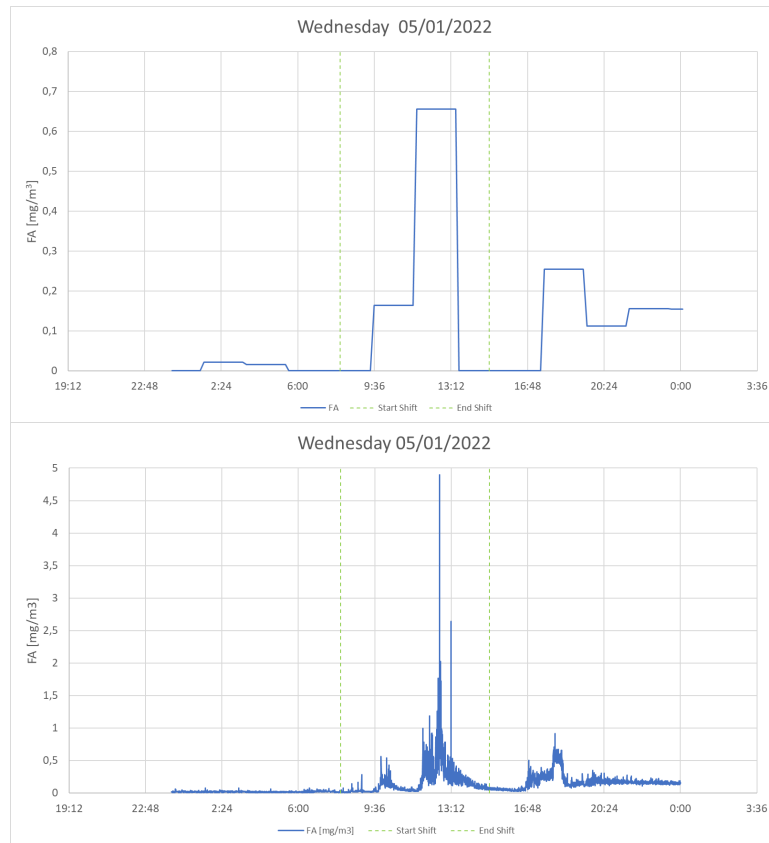


Figure 65 –Concentration values [mg/m³] measured on 05 January 2022. Please Note that in the under graph, the y-axis is from 0 to 5 mg/m³

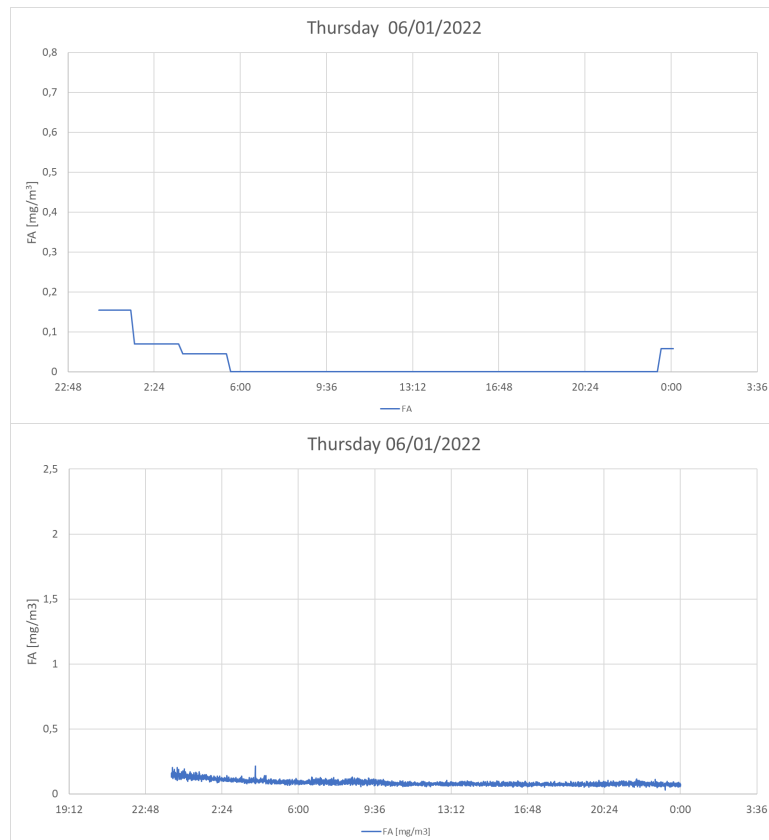


Figure 66 –Concentration values [mg/m³] measured on 06 January 2022

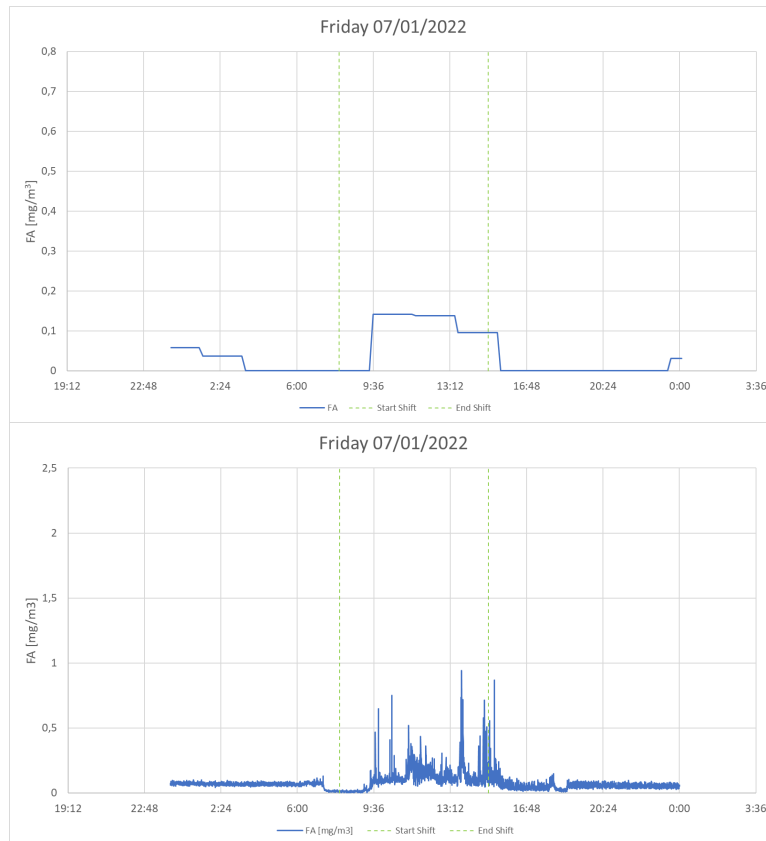


Figure 67 –Concentration values [mg/m³] measured on 07 January 2022

3.5.3. Monitoring results

The first monitoring, some results presented in section 3.5.1, was only to check compliance with exposure limits. The limit taken as a reference was 120 µg/m³, the Time Weighted Average (TWA) limit proposed by the American Conference of Governmental Industrial Hygienists (ACGIH).

In addition to the continuous monitoring with Nemo XT and Gasera One Formaldehyde, DNPH cartridges were used for sampling during working hours to assess physicians' and nurses' exposure, as shown in Figure 26, for personal monitoring. The monitoring results are shown in Figure 68 and Figure 69: the first is the statistical evaluation with nine samples taken in the breathing zone of the physicians working in the APL, and the second is a preliminary evaluation based on five samples taken in the breathing zone of the nurses. Both evaluations are based on the UNI EN 689:2019 standard.

Descrizione dei dati: APL - Physician

OEL
120,00

Dati dei campioni
3 ≤ n ≤ 50

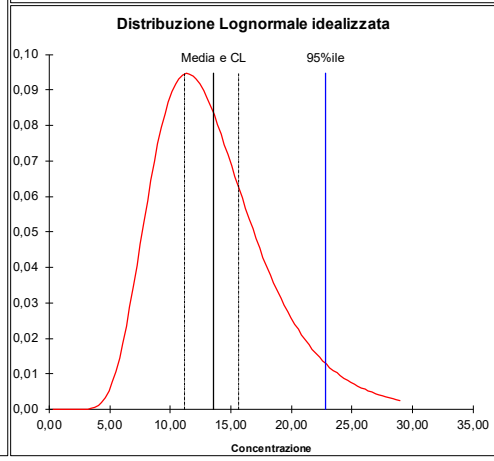
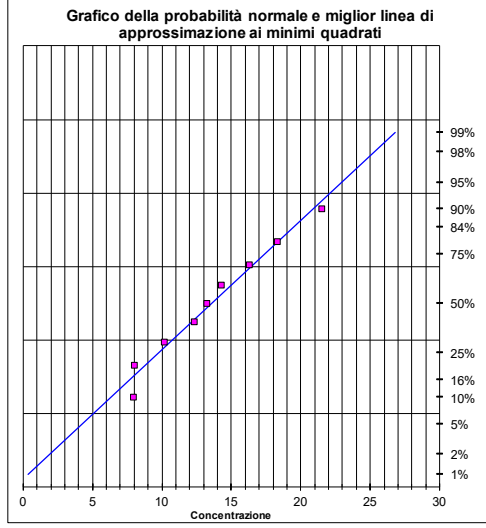
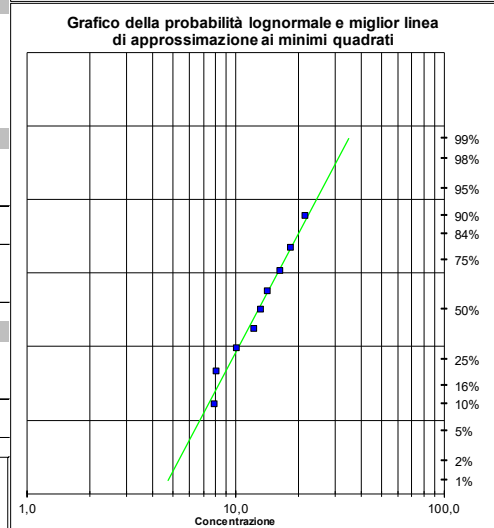
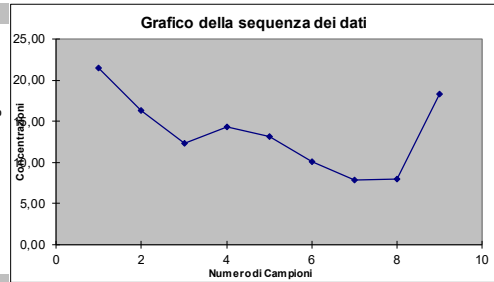
21,50
16,30
12,30
14,30
13,20
10,15
7,92
8,04
18,30

STATISTICHE DESCRITTIVE	
Numero di campioni (n)	9
Valore massimo (max)	21,500
Valore minimo (min)	7,920
Range	13,580
% superiore all'OEL	0,000%
Media	13,557
Mediana	13,200
Deviazione standard	4,599
Media dei dati trasformati logaritmicamente (ln)	2,554
Deviazione standard dei dati trasformati logaritmicamente	0,348
Media geometrica	12,861
Deviazione standard geometrica	1,417

TEST SULL'ADEGUATEZZA DELLA DISTRIBUZIONE	
Test W dei dati trasformati logaritmicamente	0,955
Lognormale (a=0,05)?	SI
Test W dei dati	0,958
Normale (a=0,05)?	SI

STATISTICHE PARAMETRICHE LOGNORMALI	
Stima della media aritmetica - MVUE	13,569
LCL _{1,95%} - Metodo Esatto di Land	11,186
UCL _{1,95%} - Metodo Esatto di Land	15,601
95esimo Percentile	22,807
UTL _{0,5%,95%}	36,96
Percentuale al di sopra dell'OEL (%>OEL)	0%
LCL _{1,95%} >OEL	<0,1
UCL _{1,95%} >OEL	<0,1

STATISTICHE PARAMETRICHE NORMALI	
Media	13,557
LCL _{1,95%} - t	10,706
UCL _{1,95%} - t	16,407
95esimo Percentile - Z	21,122
UTL _{0,5%,95%}	27,496
Percentuale al di sopra dell'OEL (%>OEL)	0,000



Distribuzione Normale		Applicabile
UR	23,15	
n	9,00	
UT	2,035	
COMPLIANCE		

Distribuzione Log-Normale		Applicabile
UR	6,41	
n	9,00	
UT	2,035	
COMPLIANCE		

Figure 68 – Exposure assessment based on UNI EN 689:2019 (statistical evaluation)

Descrizione dei Dati	Valori di concentrazione [$\mu\text{g}/\text{m}^3$]	Indice di esposizione (I)
APL - Nurse	8,45	0,07
APL - Nurse	21,40	0,18
APL - Nurse	9,30	0,08
APL - Nurse	9,60	0,08
APL - Nurse	8,90	0,07
	Compliance	UNI EN 689:2019 Valutazione preliminare
	Non applicabile	UNI EN 689:2019 Valutazione statistica

Figure 69 – Exposure assessment based on UNI EN 689:2019 (preliminary evaluation)

From the continuous monitoring of the days from 11th to 13th February 2020 in the anatomical parts reduction room (from Figure 36 to Figure 38), an increase in the FA levels can be observed after the work shift: this was caused by the switching off of the fume-hood cupboards because the work surfaces weren't well cleaned and traces of PFA were present. The peak on 18 February 2020 in the reception room (Figure 40) was caused by pre-loaded containers that weren't well sealed and were contaminated with formalin.

Regarding the second monitoring, some considerations have also been made to compare the different monitoring techniques.

Table 3 compares the results obtained with the GasCheck sequential sampler with the DNPH cartridges and the mean value recorded with the Nemo XT.

Table 3 – Concentration values obtained through the sequential sampler GasCheck compared to the mean concentration registered with the Nemo in the same period

ID	Data	Flow [L/min]	Starting Time	Ending Time	Formaldehyde GasCheck [$\mu\text{g}/\text{m}^3$]	Nemo mean value [$\mu\text{g}/\text{m}^3$]
F0_GC	16/10/2021	0.2	08:00	15:00	65.6	74.094
F1_GC	17/10/2021	0.2	08:00	15:00	8.6	0
F2_GC	18/10/2021	0.2	08:00	15:00	52.6	58.957
F3_GC	19/10/2021	0.2	08:00	15:00	48.5	42.475
F4_GC	20/10/2021	0.2	08:00	15:00	5.6	5.639
F5_GC	21/10/2021	0.2	08:00	15:00	7.9	5.732
F0_GC	22/10/2021	0.2	08:00	15:00	48.9	36.150
F1_GC	23/10/2021	0.2	08:00	15:00	69.5	54.639
F2_GC	24/10/2021	0.2	08:00	15:00	12.6	0
F3_GC	25/10/2021	0.2	08:00	15:00	44.6	39.544
F4_GC	26/10/2021	0.2	08:00	15:00	30.6	12.804
F5_GC	27/10/2021	0.2	08:00	15:00	31.6	24.705
F0_GC	02/11/2021	0.2	08:00	15:00	34.6	26.583

Table 3 – cnt.

ID	Data	Flow [L/min]	Starting Time	Ending Time	Formaldehyde GasCheck [µg/m ³]	Nemo mean value [µg/m ³]
F1_GC	03/11/2021	0.2	08:00	15:00	30.6	23.618
F2_GC	04/11/2021	0.2	08:00	15:00	12.2	6.909
F3_GC	05/11/2021	0.2	08:00	15:00	21.6	11.535
F4_GC	06/11/2021	0.2	08:00	15:00	65.5	55.986
F5_GC	07/11/2021	0.2	08:00	15:00	9.6	0

A comparison between the results obtained with Nemo XT and ProCeas is also proposed here: an analysis of the total number of days and the number of working days monitored was carried out.

Table 4 – Total days monitored analysis

	Nemo XT	ProCeas
Total days monitored	96 (100%)	79 (100%)
Average 8h > 370 µg/m ³	1 (1.04%)	0 (0%)
Max > 740 µg/m ³	3 (3.13%)	43 (54.43%)
Average 24h > Average 8h	32 (33.33%)	17 (21.52%)

Table 5 – Working days monitored analysis

	Nemo XT	ProCeas
Working days monitored	78 (100%)	65 (100%)
Average 8h > 370 µg/m ³	1 (1.28%)	0 (0%)
Max > 740 µg/m ³	3 (3.85%)	42 (64.62%)
Average 24h > Average 8h	18 (23.08%)	7 (10.77%)

The second monitoring also highlighted some concerns about the working environment and procedures. An assessment based on detailed diaries of the workflow was made, and the high levels of FA found can be linked to the following:

- Sample reduction activities from large anatomical pieces.
- Barrier height in the fume hood greater than 25 cm.
- Presence of formalin-impregnated gauze in biological collection containers outside the safety area of the fume hood.
- Use of formalin-contaminated gloves outside the hood suction area.
- Cutting activities performed near the up-and-down barrier of the fume hood.

- Presence of paraformaldehyde on work surfaces and in fume hood drainage traps.

4. Airborne particulate matter and nanoparticles

This chapter examines the exposure to airborne particulate matter, with a primary focus on nanoparticles. Several case studies will be presented, applying a monitoring device which has been tested in various occupational environments.

4.1. Introduction

Atmospheric aerosols comprise an intricate combination of minute and larger particles, which may be released directly into the atmosphere or derived from gas-particle conversion processes. Particle size is considered the most crucial among the parameters used to characterise their behaviour and origins. Chemical composition, removal, and the time these particles remain in the atmosphere correlate with particle size. Typically, ambient atmospheric particles range in diameter from 0.01 to 100 μm .

- Coarse particles, typically accounting for most of the mass of PM10 (particulate matter), are those between 2.5 and 10 μm .
- Fine particles are those between 0.1 and 2.5 μm .
- Ultrafine particles (UF) or nanoparticles (NPs), depending on their source, are particles between 0.1 and 0.01 μm .

Fine and ultrafine particles collectively form PM2.5, which includes all particles with a diameter smaller than 2.5 μm .

The human respiratory tract can be divided into three main regions based on size, structure, and function: the head, the tracheobronchial region (also known as the conducting airway), and the gas exchange region (also known as the parenchymal, alveolar, or pulmonary region). Size-selective sampling is intended to help discern the amount of aerosol expected to be available for deposition in a region. Most sampling conventions have been defined in terms of particle penetration into respiratory regions rather than deposition or expected particle dose. The specific definitions used, adopted by the European Committee for Standardization (CEN), are:

- The inhalable fraction is the mass fraction of total airborne particles inhaled through the nose and mouth.
- The thoracic fraction is the mass fraction of inhaled particles that penetrate beyond the larynx.

- The respirable fraction is the mass fraction of inhaled particles penetrating the non-ciliated airways.

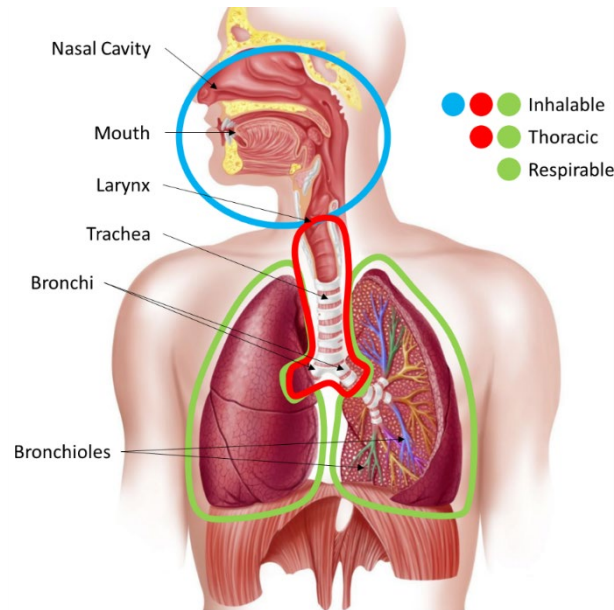


Figure 70 – Airborne particulate matter deposition in the human respiratory tract

The above definitions are expressed in terms of the mass fraction. Compared with total airborne particles, the particle sizes with a 50% penetration for the thoracic and respirable fractions are 10 μm and 4 μm , respectively (particle sizes refer to aerodynamic diameter), as shown in Figure 71.

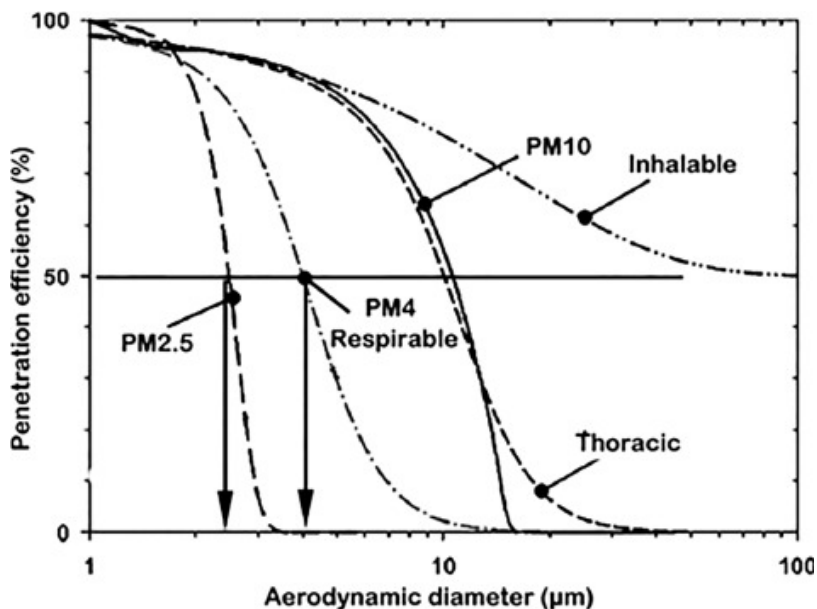


Figure 71 – Penetration curves for workplace concentration limits (inhalable, thoracic, respirable dust) and for environmental (PM10, PM2.5 dust limits) [80]

These criteria were developed specifically for workplace atmospheres. Because particles must generally settle to exert biological effects, these conventions, based

on regional exposure (i.e., particles that penetrate a region of the respiratory tract), are conservative in that they overestimate the amount of inhaled material that settles and is therefore available to induce an effect. [81]

Airborne particles, known as PNORs or PNOCs (Particulates Not Otherwise Regulated/Classified), have the following characteristics:

- Insoluble or poorly soluble in water or lung fluids.
- Have low toxicity, i.e. they are not cytotoxic, genotoxic or otherwise chemically reactive with lung tissue.

There are no occupational exposure limits for these dusts. However, although biologically inactive and incapable of causing significant organic disease, it is now recognised that inert dust, whether mineral or inorganic, may have adverse effects upon inhalation exposure. For this reason, the American Conference of Governmental Industrial Hygienists (ACGIH) recommends that air concentrations in workplaces be kept below 3 mg/m³ for the respirable fraction and 10 mg/m³ for the inhalable fraction until a specific weighted exposure limit is established. [82]

A more suitable metric for measuring ultrafine particles is the deposited surface concentration in the lung (LDSA). LDSA combines the idea that toxic compounds are found primarily on the surface of particles with the efficiency of particle deposition in the alveolar area of the human respiratory system. It was introduced to describe the harmfulness of particulate pollutants in inhaled air. [83]

The health impacts of airborne particulate matter rely mostly on their concentration and the nature of their components. As a matter of fact, they penetrate to different depths within the respiratory system according to their diameter. Additionally, organic and inorganic chemicals present at the particles' surface also influence the type and severity of the health effects. Soluble substances can be absorbed by the body and deposited, causing local disturbances. High levels of PM₁₀ and PM_{2.5}, even if limited to one or two days, have been linked to more severe effects such as discomfort (symptoms) and changes in respiratory function (bronchitis, asthma). Sustained exposure over time to even low levels of PM₁₀ and PM_{2.5} is linked to heightened respiratory ailments, including coughs, phlegm, asthma, decreased lung capacity, reduced respiratory function, chronic bronchitis, and adverse effects on the cardiovascular system. Exposure to smaller particulate matter (PM_{2.5}) is associated with higher mortality from respiratory diseases and an increased risk of respiratory tract cancer. Cancer has also been associated with the presence of carcinogens absorbed onto particle surfaces (like polycyclic aromatic hydrocarbons - PAHs in the

case of soot), which, through PM_{2.5}, can penetrate the most profound areas of the lungs.

As per the American Society for Testing and Materials, NPs are particles that measure between 1-100 nm in size. NPs may vary in size, origin, form (e.g., spherical, tubular, filamentous, or irregular), and chemical nature and may exist in a dispersed state or fused, aggregated, or agglomerated form. Depending on their origin, nanoparticles can be classified as natural or anthropogenic. Natural nanoparticles are essential components of our ecosystem, originating from nanofossils, volcanoes, chemical combustion processes, microbial agents, and water sediment components. On the other hand, anthropogenic nanoparticles are man-made and subdivided into engineered and incidental nanoparticles. Health risks vary, depending on the composition of the nanomaterial. Nanomaterials generally exhibit comparable health effects to larger particles of corresponding materials. Like other substances, nanomaterials can be absorbed, distributed, and metabolized upon entry into the body. Nanomaterials have been detected in various systems, including the lungs, liver, kidneys, heart, reproductive organs, brain, spleen, skeleton, soft tissues, and fetuses. Although some mechanisms of the associated health risks have been identified, complete comprehension is yet to be attained. Certain nanomaterials may lead to lung injuries, such as acute or chronic inflammatory reactions, the risk of which seems to increase as the particle size decreases. These injuries may include tissue damage, oxidative stress, chronic toxicity, cytotoxicity, fibrosis, and tumour formation. Additionally, certain nanomaterials may have an effect on the cardiovascular system. Because of their small size, nanomaterials are capable of penetrating the body in ways that larger particles cannot.

Metals and metal oxides have been demonstrated to permeate the olfactory bulb through the olfactory nerve, whilst carbon nanotubes have been observed to cross the placenta and enter the fetus. The potential safety hazards of some nanopowder materials are exacerbated by their high flammability, explosiveness and catalytic properties. In particular, metal nanopowders, including microscale powders, exhibit increased sensitivity to ignition the finer their particles, thereby increasing the likelihood of violent explosions. The self-ignition temperature decreases as the particles become finer. Nanomaterials have a tendency to form loosely connected aggregates, known as agglomerates. Although agglomeration results in an increase in size, it does not have a significant impact on the total surface area. The surface area is believed to be linked to health effects, at least for certain types of nanoparticles.

4.2. Case studies

The standard UNI EN 16966:2019 "Workplace exposure - Measurement of exposure by inhalation of Nano-Objects and their Aggregates and Agglomerates (NOAA) - Metrics to be used such as number concentration, surface area concentration and mass concentration" outlines the metrics to be employed when measuring inhalation exposure to NOAA. It details various techniques for measuring a particular atmospheric concentration metric for NOAA and addresses potential issues and limitations that will need to be taken into account in the future when adopting occupational exposure limits and determining compliance with them. The metrics to be considered include particle number ($\#/cm^3$), particle surface area ($\mu m^2/cm^3$), as well as mass ($\mu g/m^3$) or volume ($\mu m^3/m^3$).

The Mini Wide Range Aerosol Spectrometer (MiniWRAS) (Figure 72) is an instrument that merges an optical particle counter with an ion-mobility spectrometer. Particles pass through an optical beam produced by a laser diode source in the optical counter. The system measures size distributions between 250 nm and 32 μm in 31 size channels by utilizing a photodiode to detect perpendicular scattered light and a wide-field reflector, which results in a lower detection limit and reduced effect size associated with refractive index. The electrical sensor comprises an unipolar electric diffusion loader, a time-multiplexed electrode and a Faraday cup electrometer. Particles are drawn from the aerosol stream using the electric diffusion loader; the charged aerosol, dependent on the electrical voltage, charge and particle diameter, then strikes the multiplexed electrode. The Faraday cup electrometer measures only particles with the correct electrical mobility (between 10 nm and 250 nm). The MiniWRAS particle counter provides particle analysis in 41 size channels from 10 nm to 32 μm , with a volumetric flow rate of 1.2 L/min. The mass distribution can be calculated assuming spherical particles and converted into PM fractions. Thus, the MiniWRAS enables the acquisition of data on the mass concentration patterns of inhalable, thoracic, and respirable fractions, as well as the total concentration and the concentration of PM₁, PM_{2.5}, and PM₁₀. Additionally, it details particles' size distribution based on their numerosity or mass. Accordingly, it provides all relevant information with reference to the metrics outlined in the UNI EN 16966:2019 standard, clarifying them by size subdivision. Furthermore, this device can be managed remotely without the need for electricity for a duration of up to 12 hours. To summarise, the MiniWRAS is the most comprehensive and appropriate tool for continuously evaluating nanoparticle exposure.



Figure 72 – Mini Wide-Range Aerosol Spectrometer (MiniWRAS)

All the monitoring hereafter presented (sections from 4.2.1 to 4.2.4) has been carried out through the MiniWRAS.

4.2.1. Monitoring in a 3D printing laboratory

Airborne dust was monitored during 3D printing of drone accessory components using different thermoplastic materials and printer models. Two printers had an insulated print chamber, while the third had a partially insulated and sealed chamber. The materials used were Acrylonitrile Butadiene Styrene (ABS) and Acrylonitrile Styrene Acrylate (ASA).

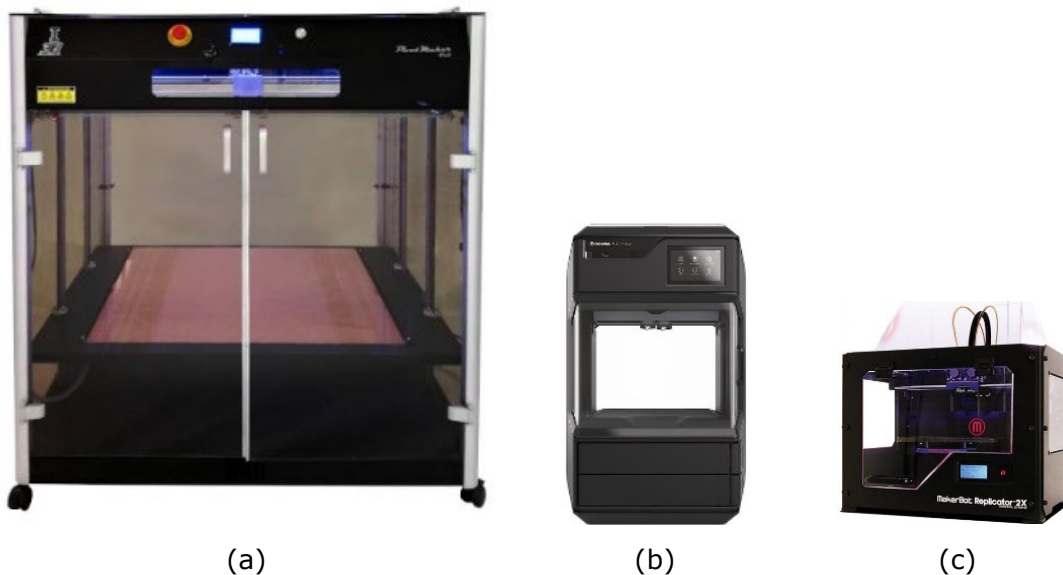


Figure 73 – Printers with an insulated print chamber using ABS (a) and (b), and printer with partially insulated and sealed chamber using ASA (c)

The operations were monitored for a total of 6 hours. Printer (a) was utilized in a printing operation lasting approximately 48 hours, with the start and initial hours of the process being monitored. Printers (b) and (c) were involved in shorter printing tasks that were monitored as a whole.

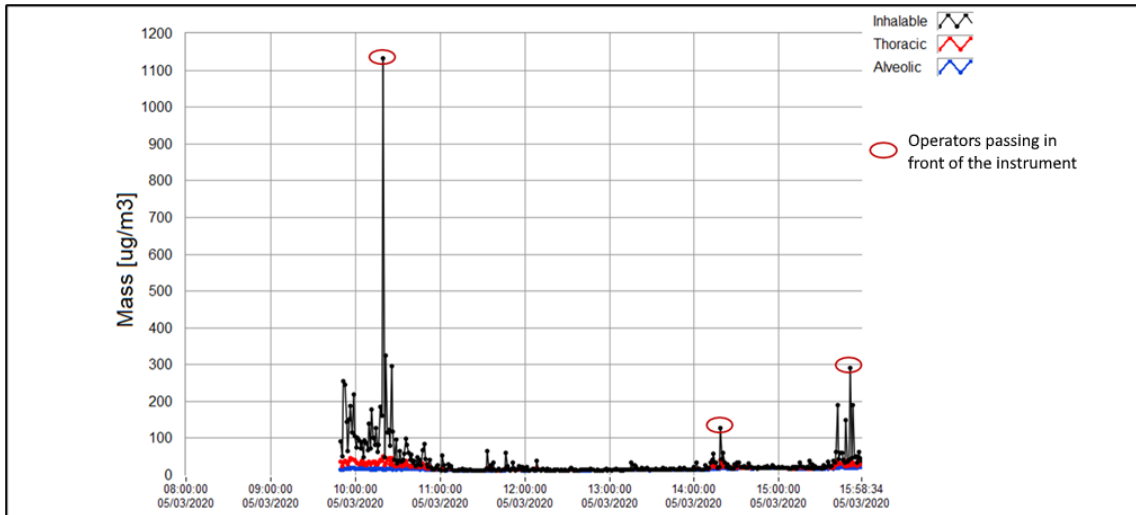


Figure 74 – Trends over time of concentrations of inhalable, thoracic, and respirable fractions

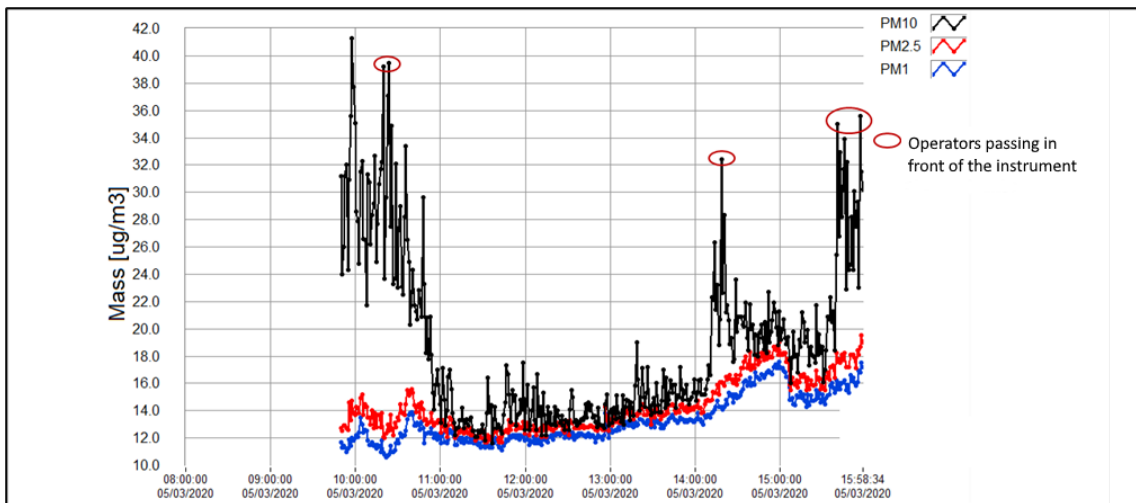


Figure 75 – Trends over time of concentrations of PM10, PM2.5, and PM1

As explained in the above section, the UNI EN 16966:2019 standard offers various metrics for measuring exposure to airborne nanoparticles. These include:

- The number ($\#/cm^3$).
- The surface area ($\mu m^2/cm^3$).
- The mass ($\mu g/m^3$), or volume ($\mu m^3/m^3$).

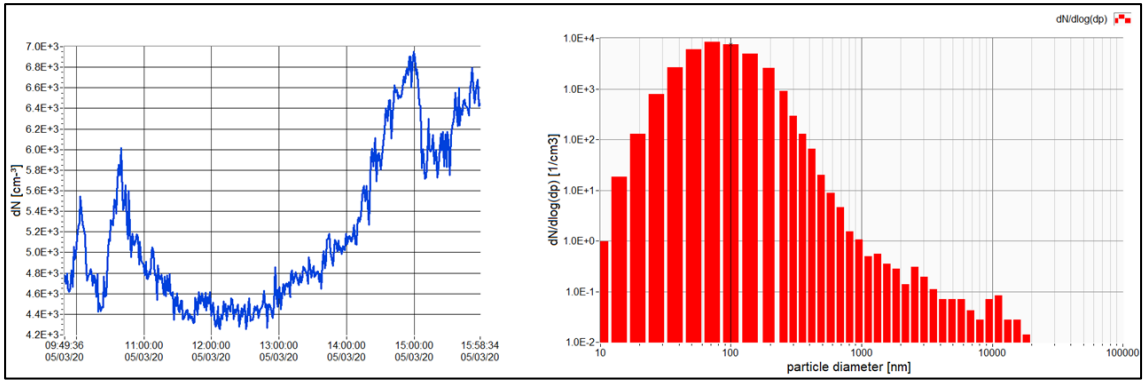


Figure 76 – Time trend of numerical concentration and particle size distribution

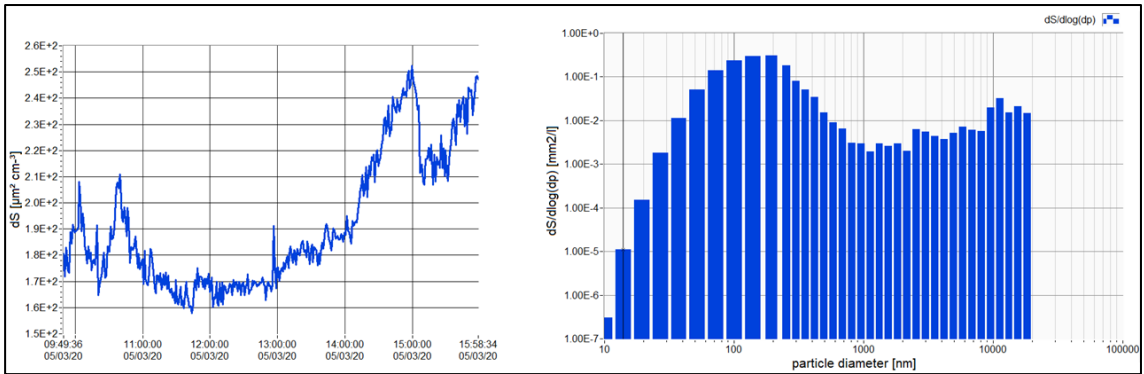


Figure 77 – Time trend of surface area concentration and particle size distribution

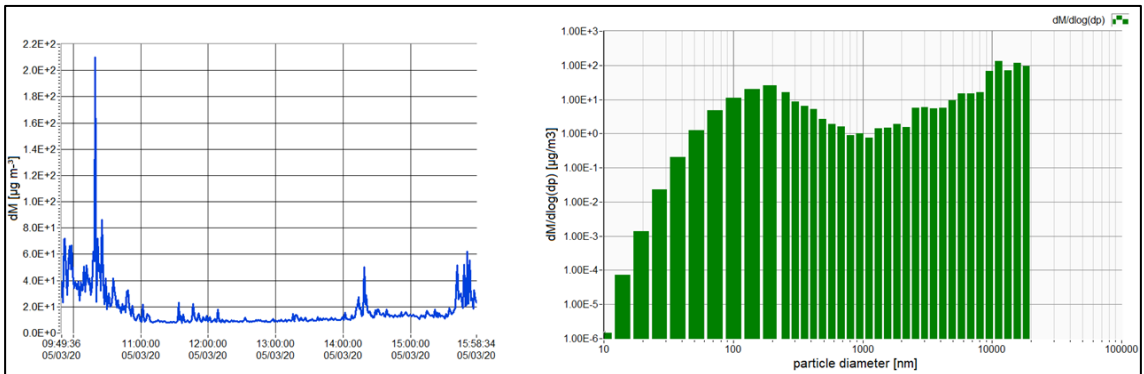


Figure 78 – Time trend of concentration and particle size distribution

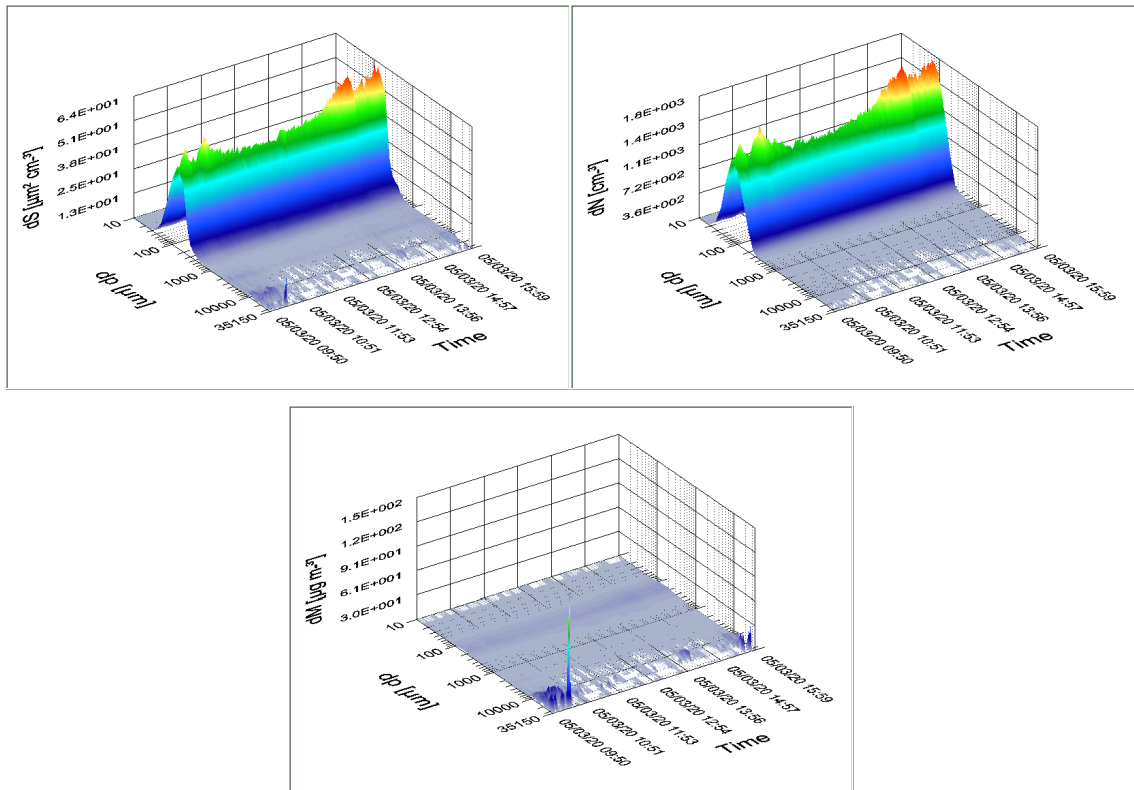


Figure 79 – Three-dimensional depiction of diverse concentrations in relation to particle size and time

Based on the surveys conducted, there is no evidence of significance concerning airborne particles measuring in either micrometers or nanometers. As shown in Figure 74, the concentrations of inhalable and respirable (reported as alveolic in the figure) fractions are below 1.2 mg/m^3 throughout monitoring, thus below the limit values introduced in Section 4.1. Moreover, in Figure 75, it can be observed that PM10 concentrations are below 0.042 mg/m^3 , and PM2.5 and PM1 concentrations are below 0.02 mg/m^3 for the entire duration of the monitoring.

4.2.2. Grinding of fodder and grit in experimental stables

Fodder and grit grinding stages using a laboratory mill equipped with horizontal blades placed inside a hood were monitored for airborne particulate emissions. The mill is used to prepare about ten samples per day, with a cleaning step between each session to prevent contamination. This cleaning process is carried out by employing a compressor; however, a vacuum cleaner test has been conducted. The hood remains active during all loading, grinding, unloading and cleaning stages.

Several operations were performed during sampling, as shown in Table 6.

Table 6 – Operations performed during the monitoring and time schedule of each one

	TIME SCHEDULE	OPERATION
1)	10:25	Grinding of fodder and grit
2)	10:40	Cleaning with the compressor
3)	10:42	Grinding of grit
4)	10:45	Cleaning test with the vacuum cleaner
5)	10:49	Shutting down of the hood



Figure 80 – Phase 1) Grinding of fodder and grit



Figure 81 – Phase 2) Cleaning with the compressor



Figure 82 – Phase 4) Cleaning test with the vacuum cleaner

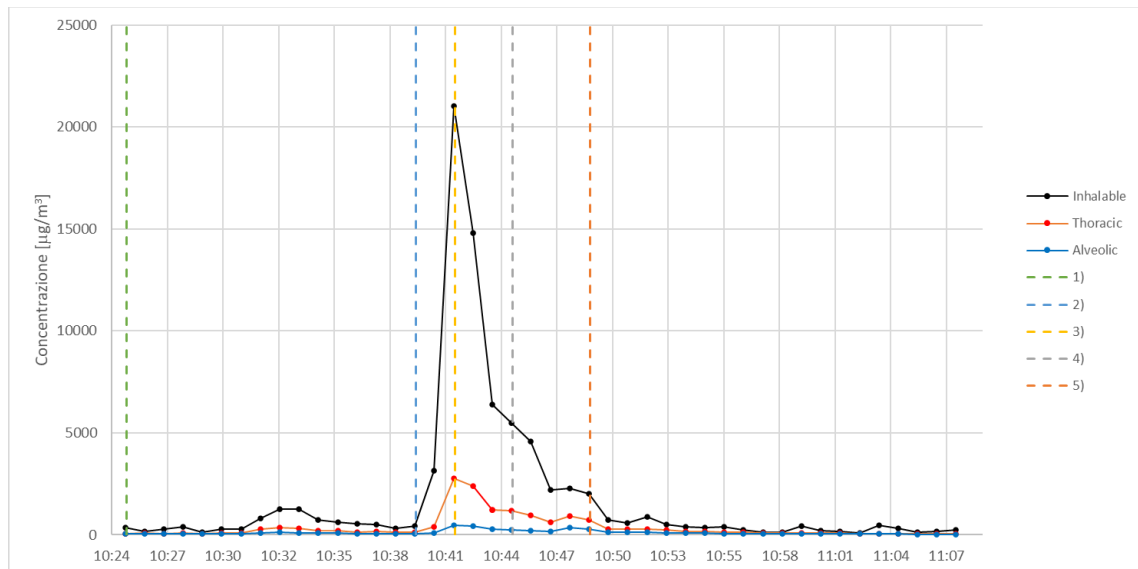


Figure 83 – Trends over time of concentrations of inhalable, thoracic, and respirable fractions

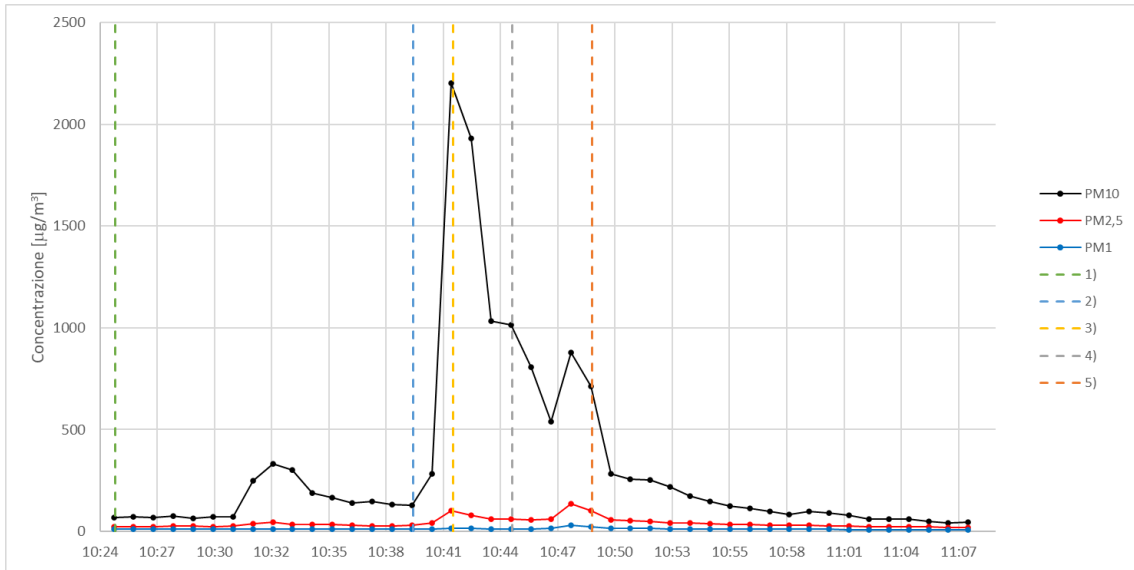


Figure 84 – Trends over time of concentration of PM10, PM2.5, and PM1

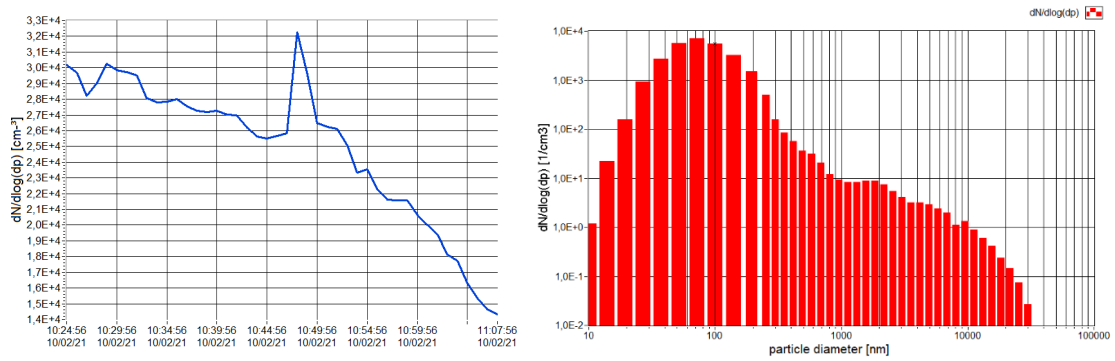


Figure 85 – Time trend of numerical concentration and particle size distribution

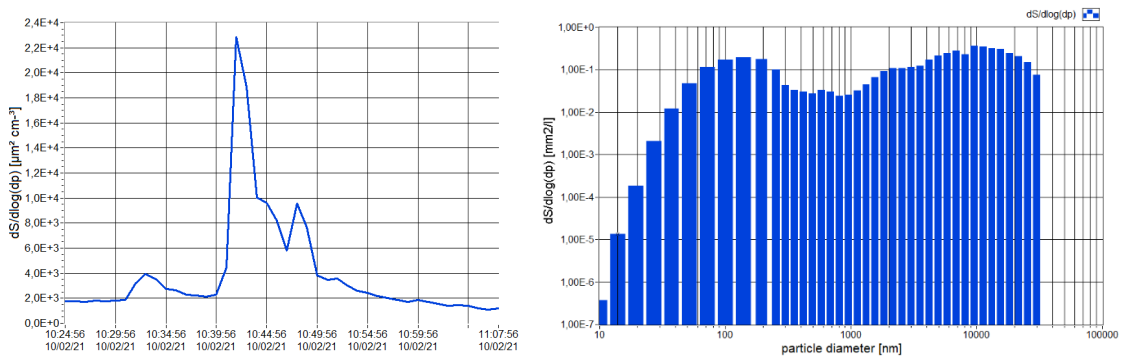


Figure 86 – Time trend of surface area concentration and particle size distribution

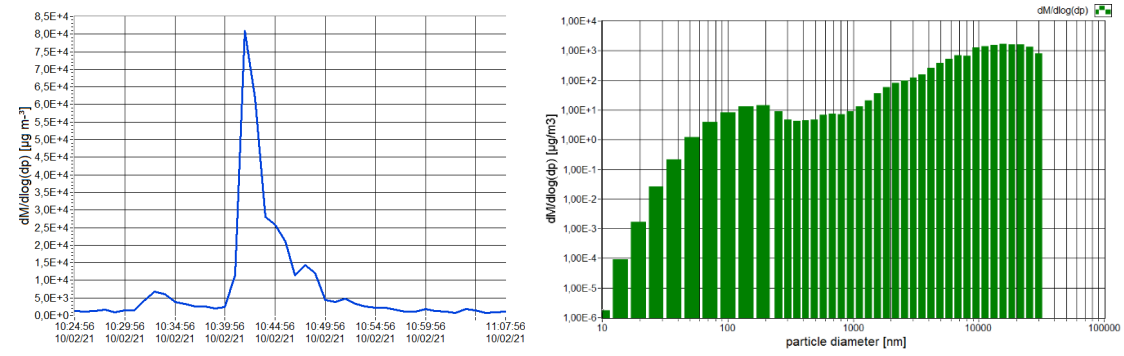


Figure 87 – Time trend of concentration and particle size distribution

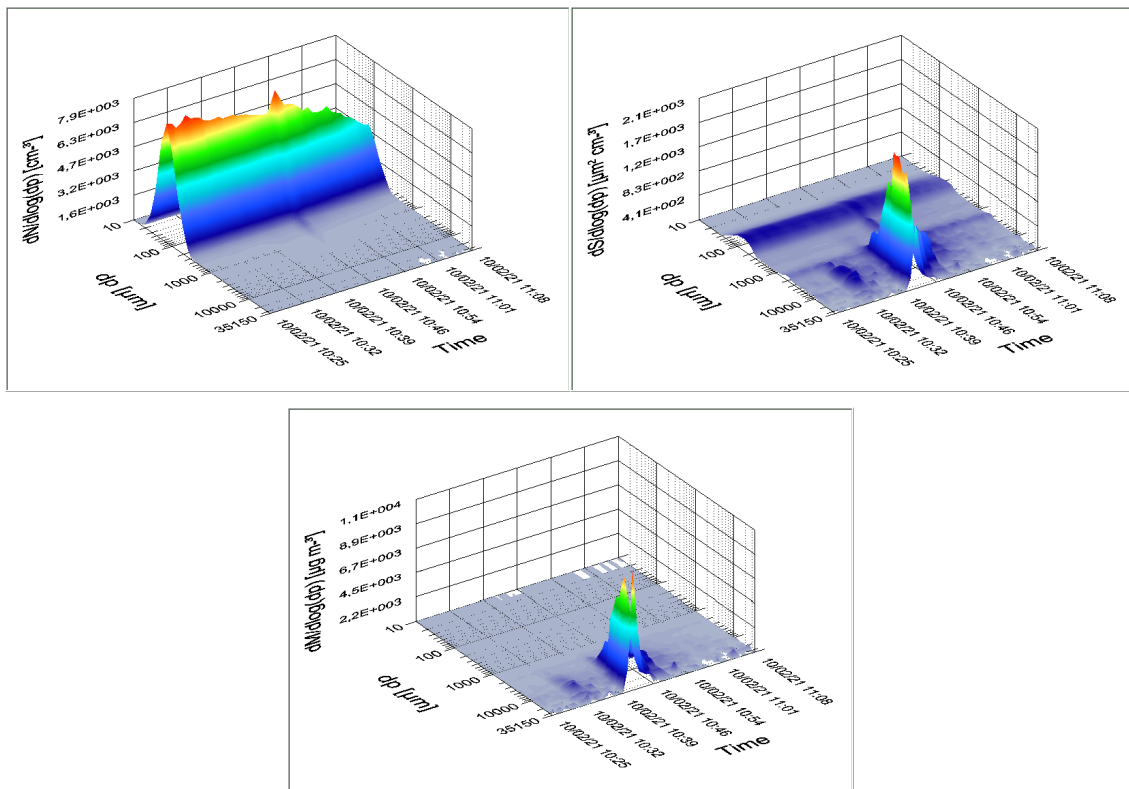


Figure 88 – Three-dimensional depiction of diverse concentrations in relation to particle size and time

The findings demonstrate no significant risk associated with the release of airborne particles, including both micrometer and nanometer-sized particles. As can be seen in Figure 83, the proposed limit value of 10 mg/m³ for the respirable fraction is only exceeded after the compressor cleaning phase. In fact, as shown in Figure 84, this operation causes the resuspension of particles and, therefore, the highest exposure levels; to reduce this criticality, a vacuum cleaning system is strongly recommended, given its availability. Excluding the mill cleaning step by the compressor, the concentrations of the respirable fraction are always under 10 mg/m³, and the thoracic and inhalable fractions (shown as alveolic in the figure) are always below 2.5 mg/m³. Figure 84 shows how the different phases affect the PM10 concentration trend, while

PM2.5 and PM1 concentrations are always below 0.1 mg/m³ and are only affected by changes due to cleaning, whether by compressor or vacuum.

4.2.3. Glassware modelling operations in a glassware room

The monitored operations included the ignition of the glass forming flame, the subsequent manual shaping of the molten object and finally the extinction of the flame in a glassware room. Methane, air, and oxygen are used to fuel the welding and tempering operations.



Figure 89 – Monitored activities

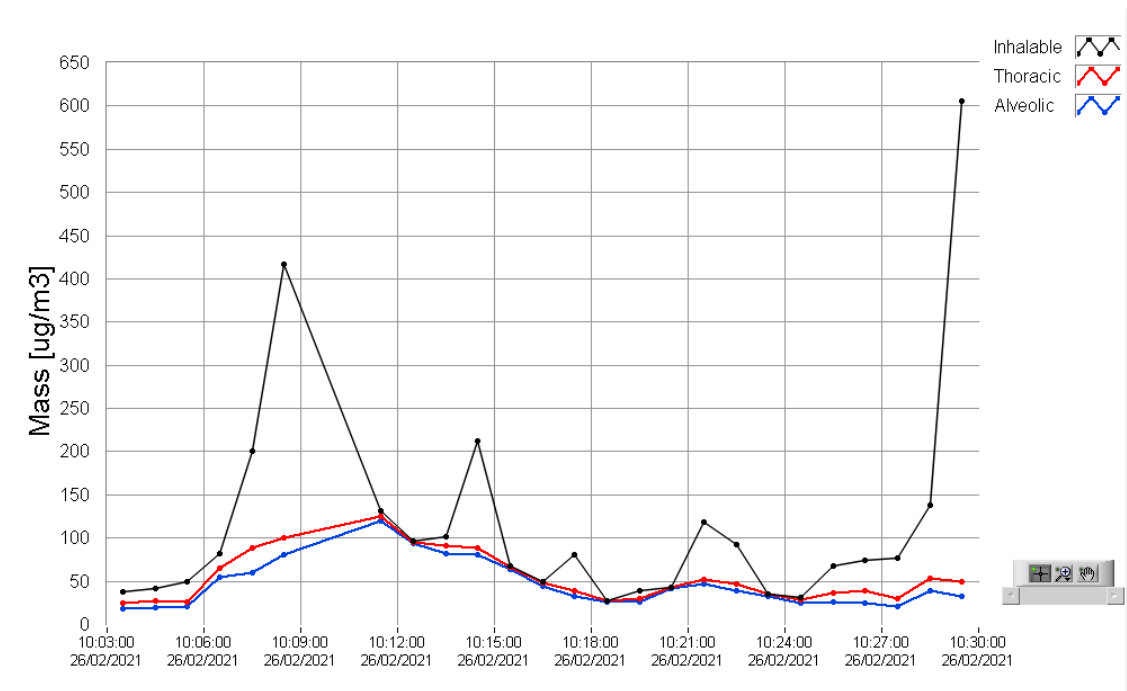


Figure 90 – Trends over time of concentrations of inhalable, thoracic, and respirable fractions

The graph in Figure 90 illustrates the time trend of the inhalable, thoracic, and respirable fractions of airborne particles released during the monitored operations. The flame was ignited at 10:05 a.m. and extinguished at 10:14 a.m. Throughout the different work phases, the highest peak value for the inhalable fraction was approximately 420 $\mu\text{g}/\text{m}^3$. The thoracic and respirable fractions experienced a slight increase during the work phases but did not reach a peak. The peak inhalable fraction observed at 10:30 a.m. resulted from personnel passing in front of the instrumentation sensor and the door opening to the outside.

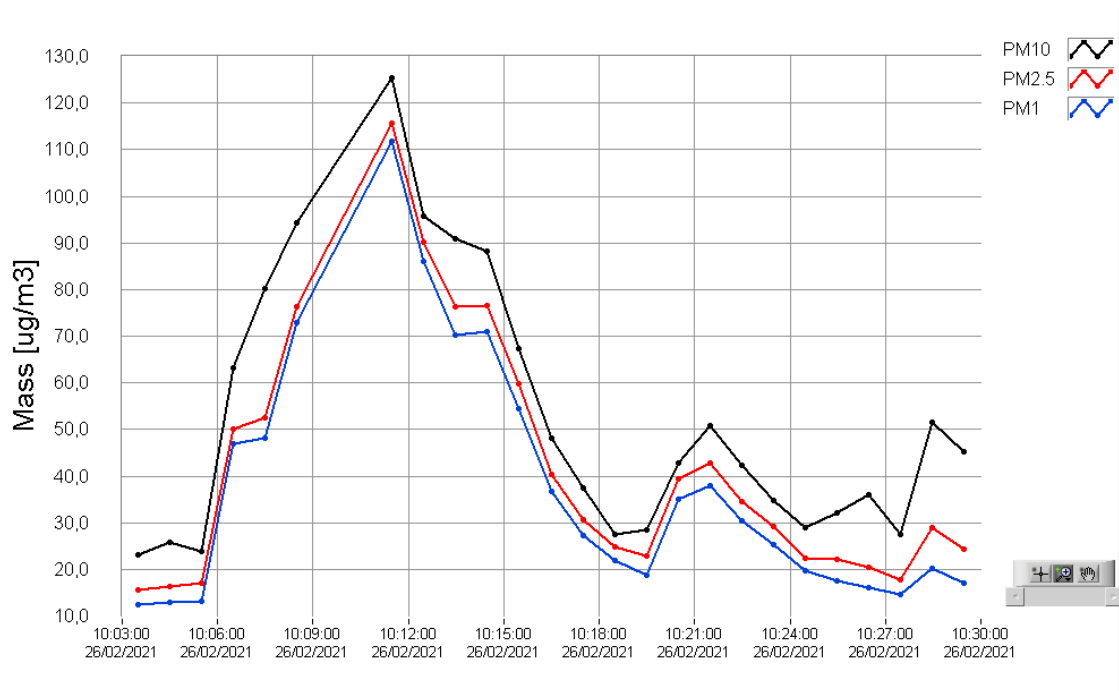


Figure 91 – Trends over time of concentration of PM10, PM2.5, and PM1

The above graph illustrates the time trends of the PM10, PM2.5, and PM1 fractions. Each of these fractions demonstrates a maximum peak of 127 $\mu\text{g}/\text{m}^3$ for PM10, 115 $\mu\text{g}/\text{m}^3$ for PM2.5, and 111 $\mu\text{g}/\text{m}^3$ for PM1 at approximately 10:11 a.m. This results in a minor increase in all particulate fractions, which shortly return to background concentrations.

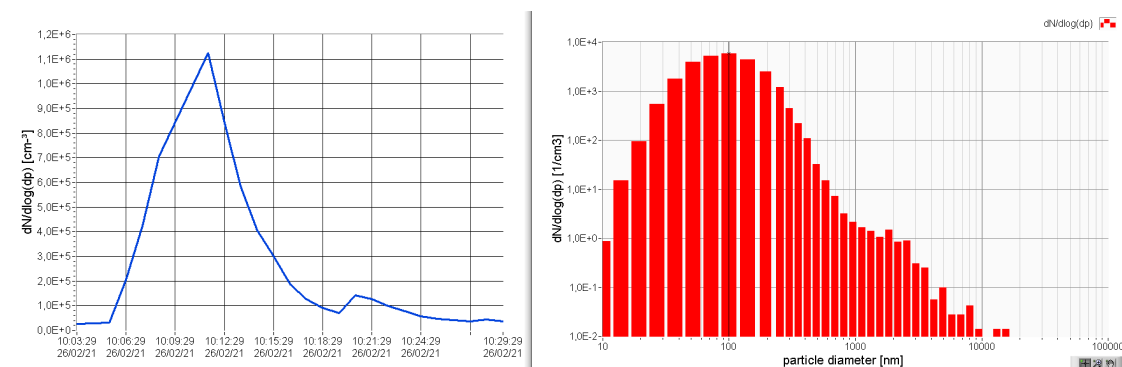


Figure 92 – Time trend of numerical concentration and particle size distribution

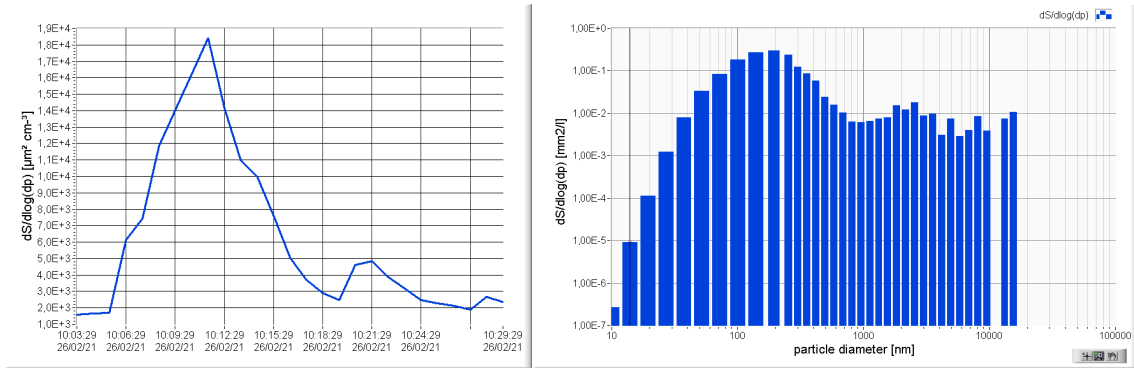


Figure 93 – Time trend of surface area concentration and particle size distribution

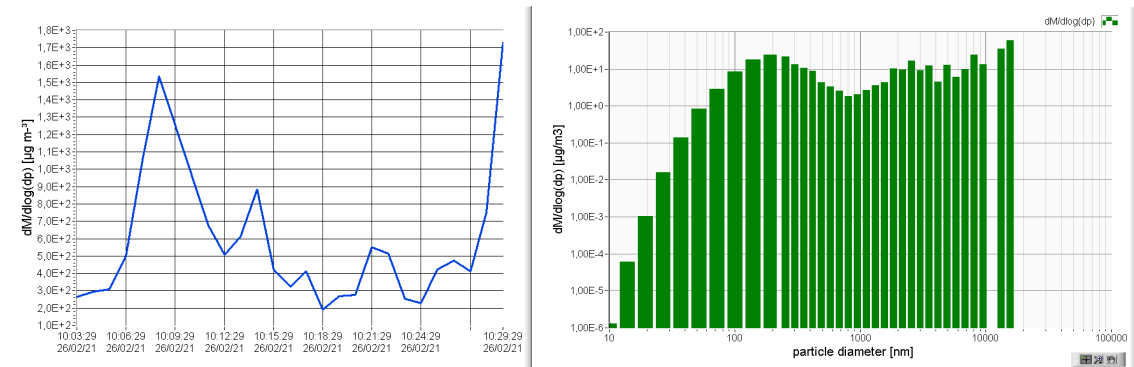


Figure 94 – Time trend of concentration and particle size distribution

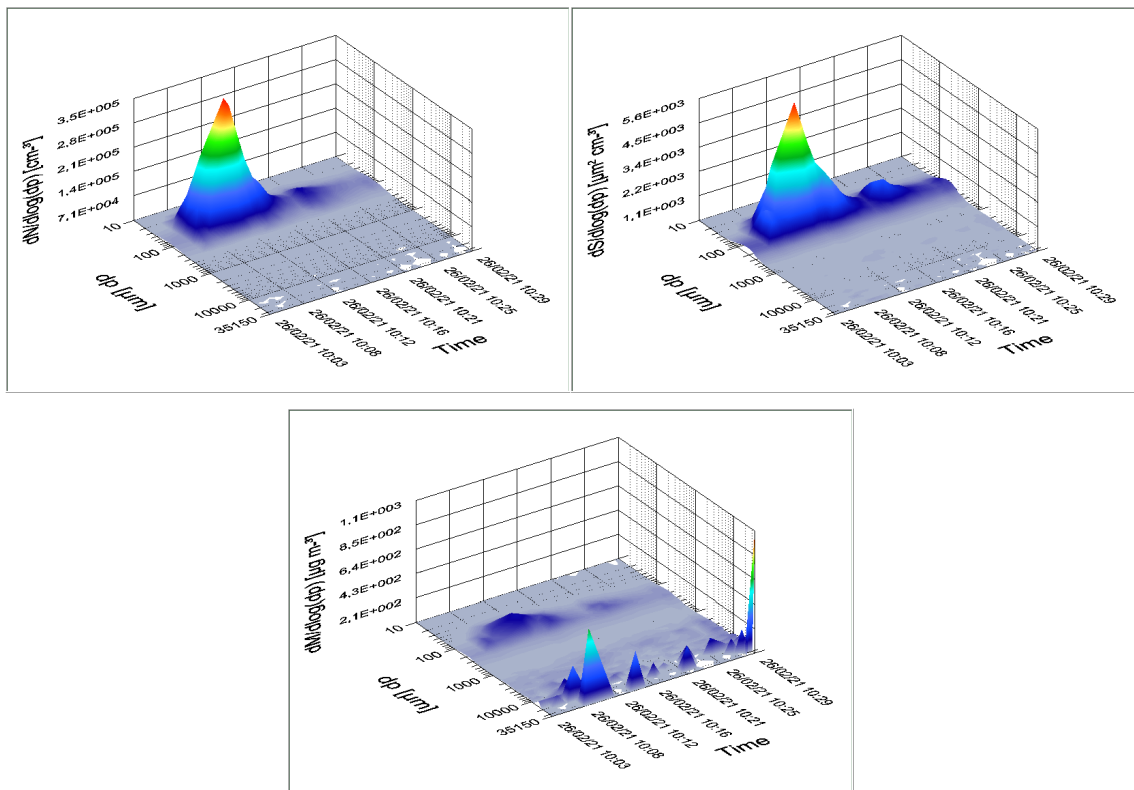


Figure 95 – Three-dimensional depiction of diverse concentrations in relation to particle size and time

Based on the metrics outlined in the UNI EN 16966:2019 standard for measuring airborne nanoparticle exposure, the highest concentration occurs between 10:08 and 10:11 a.m., aligning respirable and particulate matter results. When normalised for particle size, particles measuring approximately 100 nm or slightly larger contribute the most to the number and surface area of particles. The primary contribution for particle mass normalized to particle size seems to be from particles with nominal diameters exceeding 10 μm . As observed in Figure 90, the spike in mass concentration normalized to particle size observed at 10:30 a.m. is due to the movement of personnel in front of the sensor that led to the opening of the door to the outside. The trends highlighted in Figure 92, Figure 93 and Figure 94 are represented in three dimensions in Figure 95.

The findings demonstrate no significant risk associated with the release of airborne particles, including both micrometer and nanometer-sized particles. In fact, the inhalable fraction is always below 0.65 mg/m^3 , and the thoracic and respirable fractions (shown as alveolic in the figure) are always lower than 0.15 mg/m^3 , as shown in Figure 90. In Figure 91, the trends for PM₁₀, PM_{2.5} and PM₁ are similar throughout the monitoring, and their concentrations are always lower than 0.13 mg/m^3 .

4.2.4. Additive Manufacturing Laboratory

Airborne particulate matter was monitored in an Additive Manufacturing (AM) laboratory, a laboratory where three-dimensional objects are constructed by successive layering of materials. Specifically, the monitored laboratory has seven powder bed casting machines and uses metal powders (20-60 μm size) containing high levels of cobalt, chromium, and nickel.

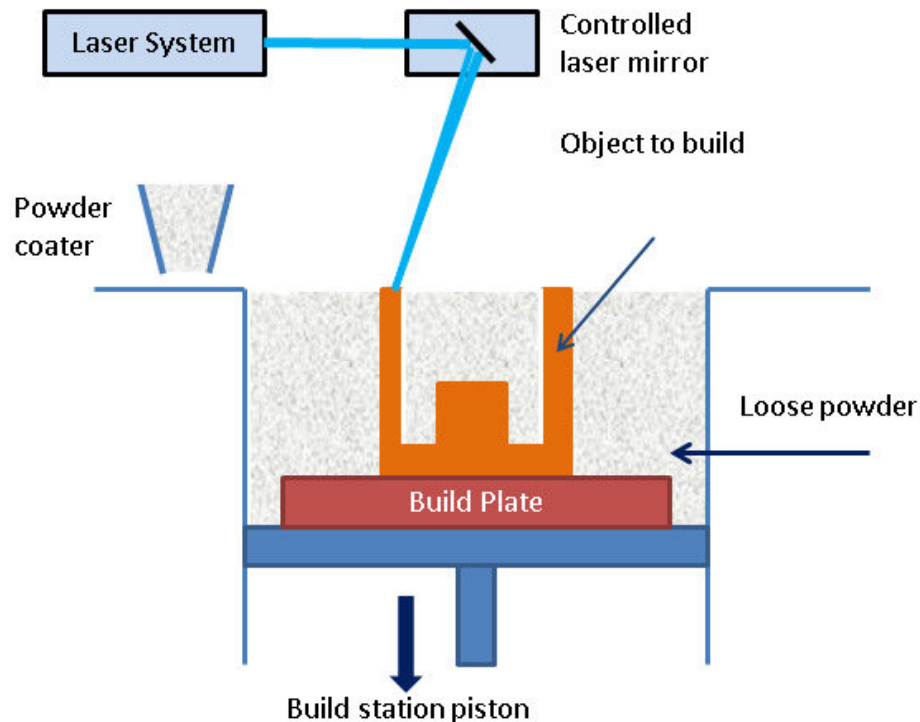


Figure 96 – Schematic representation of the powder bed fusion process [84]

Monitoring was carried out on three different days.

The Total Particle Number Concentrations (TPNC) were measured using MiniWRAS before the beginning of the work shift to determine the background level (BCK) and during each task considered; the temporal progression of the TPNC can be used to evaluate the risk related to individual activities that the printer operator carries out. The results are shown in Table 7, Table 8 and Table 9, and the trends of inhalable, thoracic and respirable fractions, total particles, and lung-deposited surface area are shown in Figure 97, Figure 99, and Figure 101 on the three monitoring days.

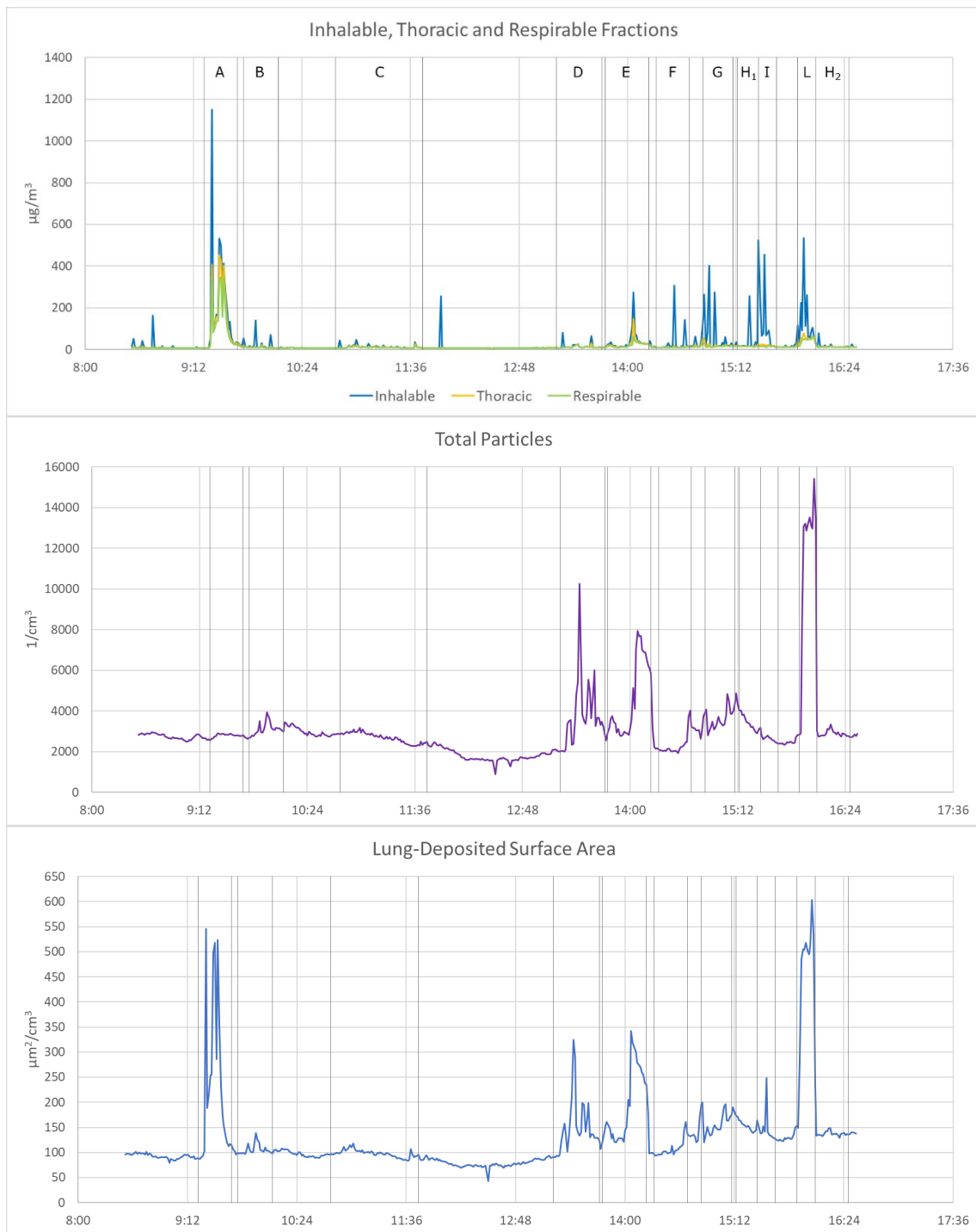


Figure 97 – Inhalable, Thoracic and Respirable Fractions, Total Particles, and Lung-Deposited Surface Area on the first monitoring day

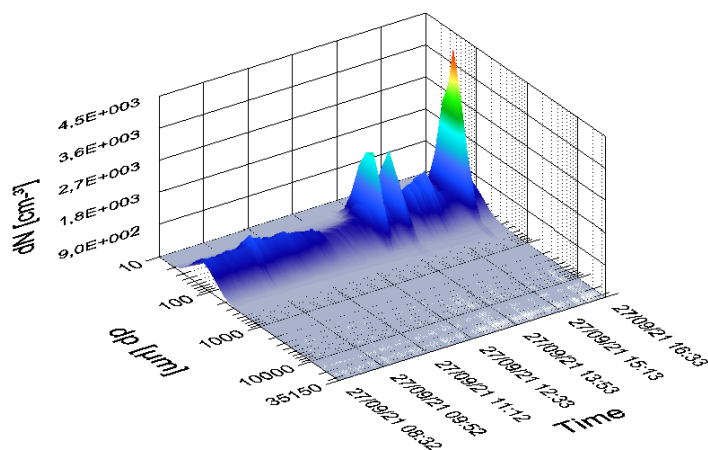


Figure 98 – 3D distribution of the number of total particles on the first monitoring day

Table 7 – Nanoparticle emissions on the first monitoring day and the relative ratio with the background value

Operation	OEL [N°/cm ³]	Reference Value Indoor [N°/cm ³]	Background [N°/cm ³]	TPNC [N°/cm ³]	Higher Particle Class	TPNC/BCK ratio
MW-A	20,000 [85]	1,000-10,000 [86]	1,604	2,797.9	52-139 nm	1.7
MW-B				3,115.2	52-139 nm	2.0
MW-C				2,689.4	52-139 nm	1.7
MW-D				3,855.9	52-139 nm	2.4
MW-E				4,610.8	52-139 nm	2.9
MW-F				2,329.6	52-139 nm	1.5
MW-G				3,639.8	52-139 nm	2.3
MW-H1				3,406.9	52-139 nm	2.1
MW-H2				2,896.9	52-139 nm	1.6
MW-I				2,618.7	52-139 nm	1.8
MW-L				10,571.9	52-139 nm	6.6

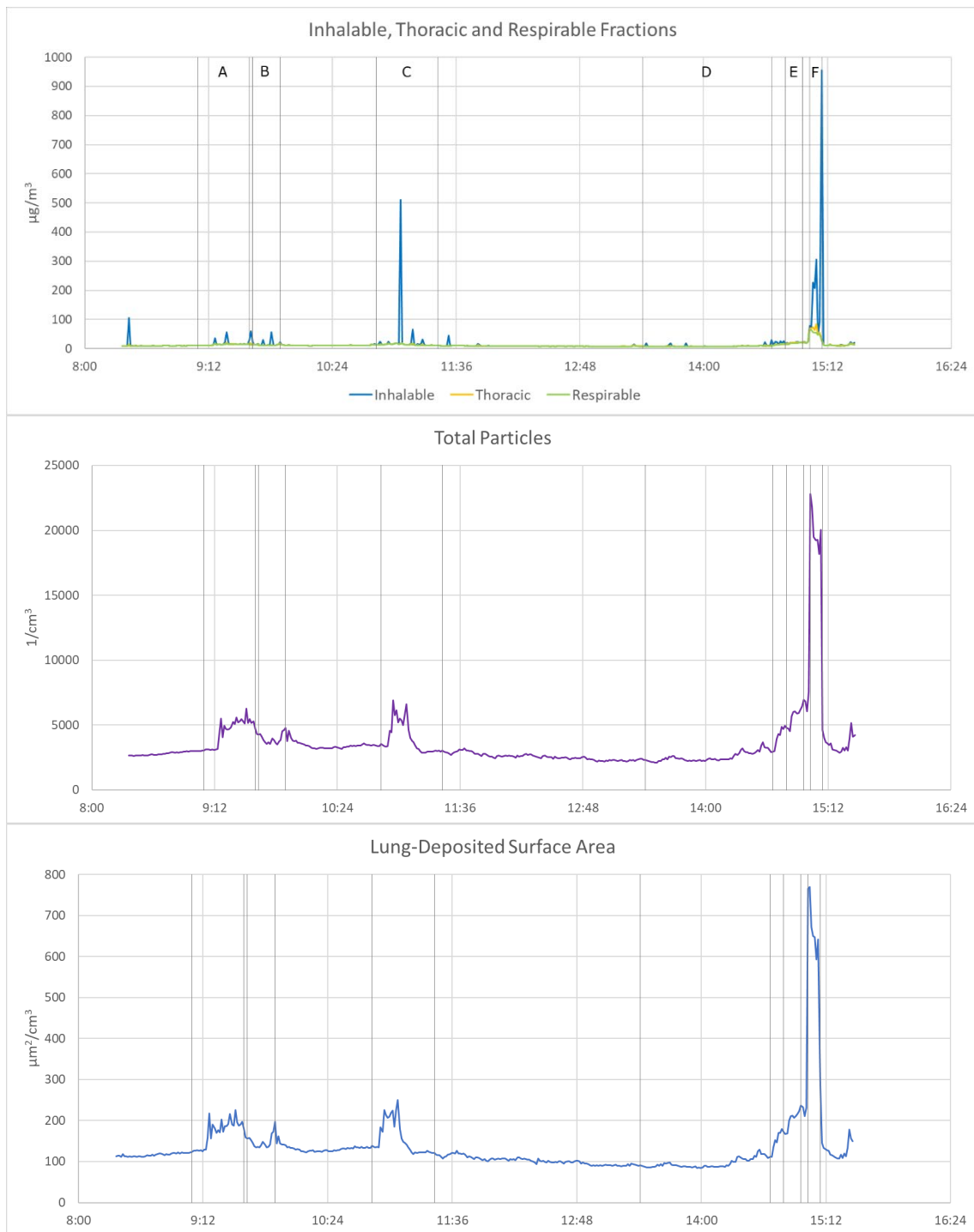


Figure 99 – Inhalable, Thoracic and Respirable Fractions, Total Particles, and Lung-Deposited Surface Area on the second monitoring day

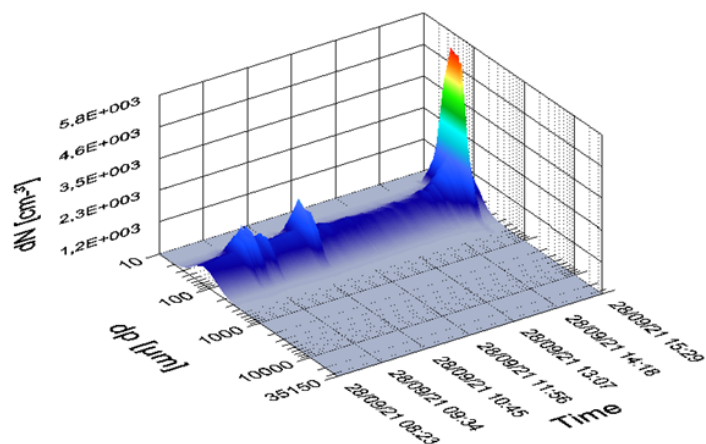


Figure 100 – 3D distribution of the number of total particles on the second monitoring day

Table 8 – Nanoparticle emissions on the second monitoring day and the relative ratio with the background value

Operation	OEL [N°/cm ³]	Reference Value Indoor [N°/cm ³]	Background [N°/cm ³]	TPNC [N°/cm ³]	Higher Particle Class	TPNC/BCK ratio
MW-A	20,000 [85]	1,000-10,000 [86]	1,604	4,520.2	52-139nm	2.8
MW-B				3,964.7	52-139nm	2.5
MW-C				3,941.1	52-139nm	2.5
MW-D				2,542.8	52-139nm	1.6
MW-E				5,748.0	52-139nm	3.6
MW-F				18,192.0	52-139nm	11.3

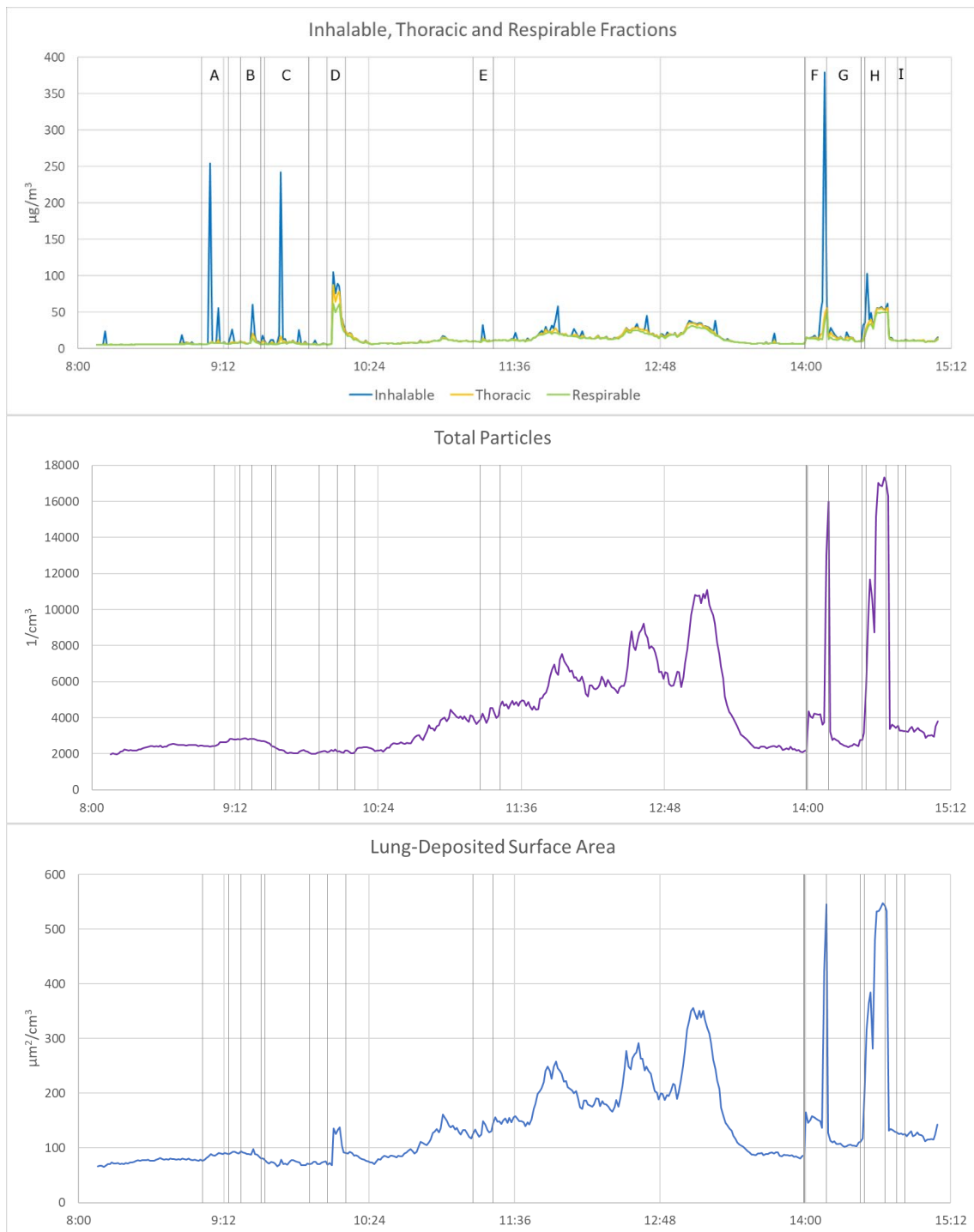


Figure 101 – Inhalable, Thoracic and Respirable Fractions, Total Particles, and Lung-Deposited Surface Area on the third monitoring day

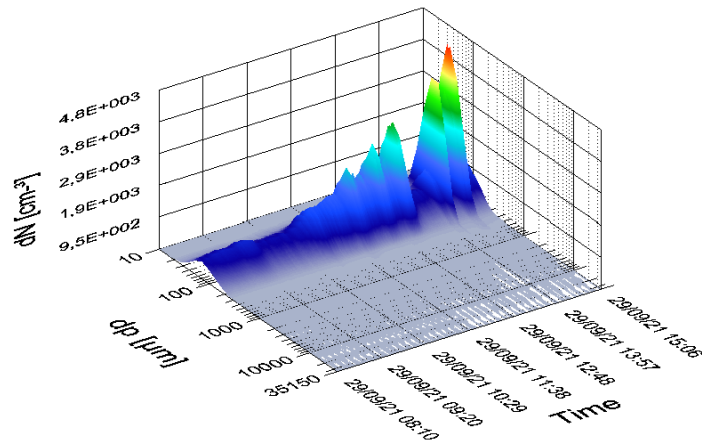


Figure 102 – 3D distribution of the number of total particles on the third monitoring day

Table 9 – Nanoparticle emissions on the third monitoring day and the relative ratio with the background value

Operation	OEL [N°/cm ³]	Reference Value Indoor [N°/cm ³]	Background [N°/cm ³]	TPNC [N°/cm ³]	Higher Particle Class	TPNC/BCK ratio
MW-A	20,000 [85]	1,000-10,000 [86]	1,604	2,681.5	52-139nm	1.7
MW-B				2,690.7	52-139nm	1.7
MW-C				2,110.6	52-139nm	1.3
MW-D				2,107.4	52-139nm	1.3
MW-E				4,182.1	52-139nm	2.6
MW-F				5,655.1	52-139nm	3.5
MW-G				3,363.8	52-139nm	2.1
MW-H				13,324.9	52-139nm	8.3
MW-I				3,324.4	52-139nm	2.1

Exposure assessment to nanoscale dust does not have well-defined exposure limits for this airborne particle fraction. For this reason, the approach proposed by ISO/TS 12901-2:2014 was used for the exposure assessment of the operators engaged in the various Metal Additive operations. Thus, in addition to adopting the limit value recommended by IFA and BSI for total airborne particles (TPNC) of 20,000 N°/cm³ [85], the background value of total particles (BCK) is used as a reference and related to the number of total particles detected in each monitored operation (TPNC/BCK). From this two-pronged approach, monitoring results from the three days of sampling show that in no operation is the recommended limit of 20,000 N°/cm³ exceeded and that only some post-processing operations have a TPNC/BCK ratio from 3.5 (MW-F, third monitoring day) to 11.3 (MW-F, second monitoring day). These operations, however, are performed with a Tyvek suit and an electroventilated respirator;

consequently, operator exposure is minimized using PPE. In addition, it is noteworthy that the reference background value, obtained by monitoring with machinery switched off, is very low, in line with the TPNC concentration values found in the literature in offices and domestic dwellings (1,000-10,000 n/cm³). [86]

We monitored in detail the following operations:

- The refilling of the machine tank with powder either with the manual open (O1) or closed (O2) system.
- The removal and cleaning of the final product and the recovery of unused powder (within the operating area of the machine) either with a specific external vacuum cleaner (O3) or by manually dragging the powder into the perforated grid around the build plate (O4).
- The sieving of the recovered powder (O5).
- The dedusting of the final product with compressed air in the reserved post-process area (O6).

The total particle number concentrations (TPNC) were measured using MiniWRAS before the beginning of the work shift to determine the background level (BCK) and during each hazardous task considered; the temporal progression of the TPNC can be used to evaluate the risk related to individual activities that the printer operator carries out. The results are shown in Table 10, and the trends of the TPNC for the monitored operations over time are shown in Figure 103 – Figure 108. In addition, the more relevant size classes of the particles on the TPNC are reported for each task.

Table 10 – Nanoparticle emissions during the monitored operations in additive manufacturing and the relative ratio with the background value

Operation	OEL [N°/cm ³]	Reference Value Indoor [N°/cm ³]	Background [N°/cm ³]	TPNC [N°/cm ³]	Higher Particle Class	TPNC/BCK ratio
O1	20,000 [85]	1,000-10,000 [86]	1,604	2,797,9	52-139nm	1.7
O2				2,110.6	52-139nm	1.3
O3				3,855.9	52-139nm	2.4
O4				2,689.4	52-139nm	1.7
O5				4,610.8	52-139nm	2.9
O6				10,571.9	52-139nm	6.6

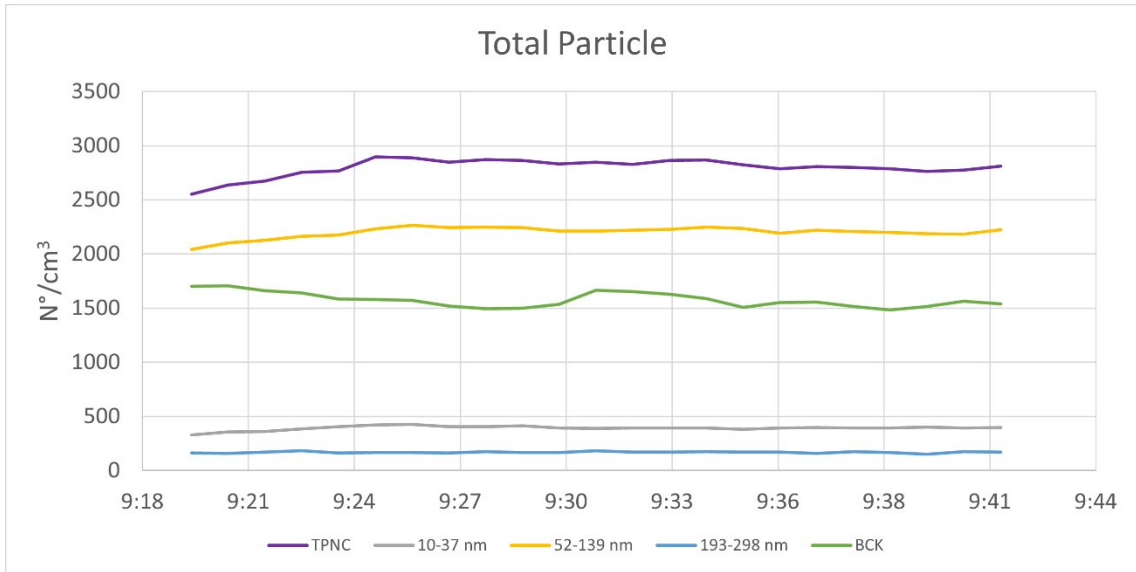


Figure 103 – TPNC trends and the main particle size classes for O1-manual loading of the metal powder

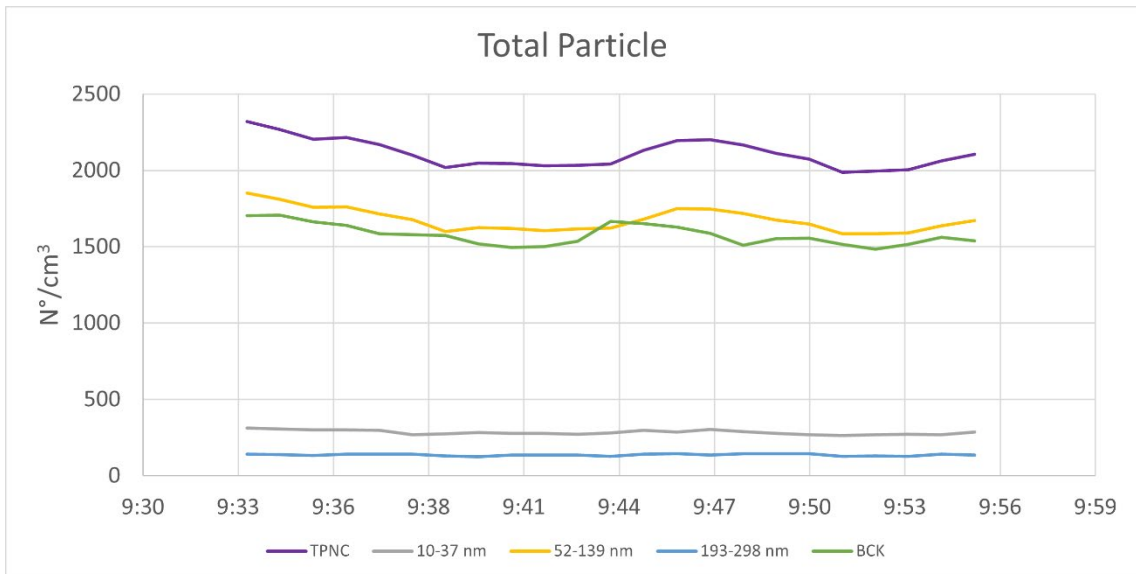


Figure 104 – TPNC trends and the main particle size classes for O2-loading of the metal powder with a closed system

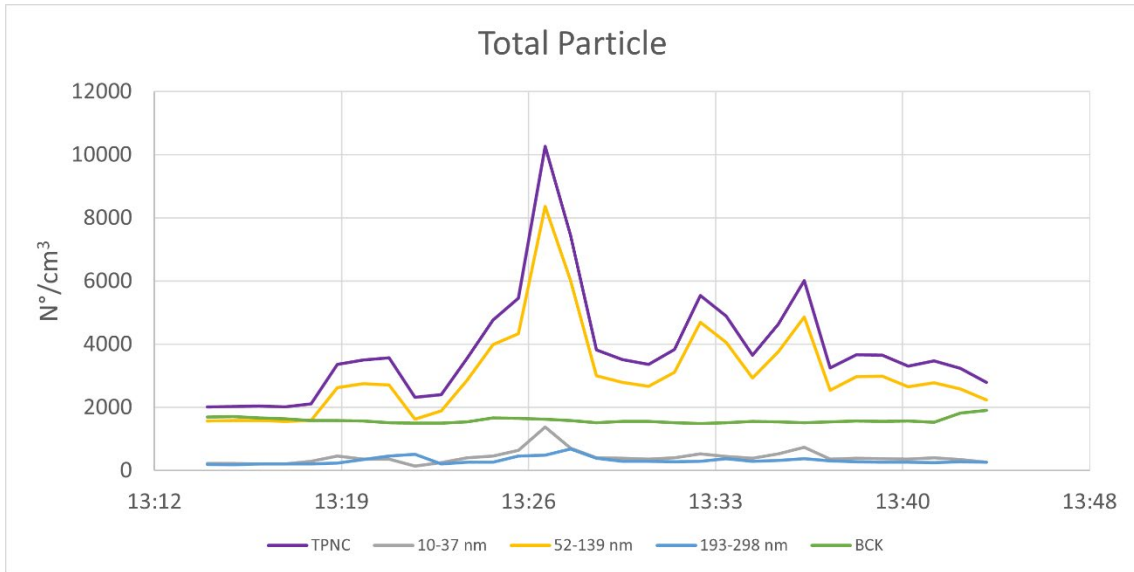


Figure 105 – TPNC trends and the main particle size classes for O3-removing and cleaning of the final product and the recovering of unused powder with an external specific vacuum cleaner

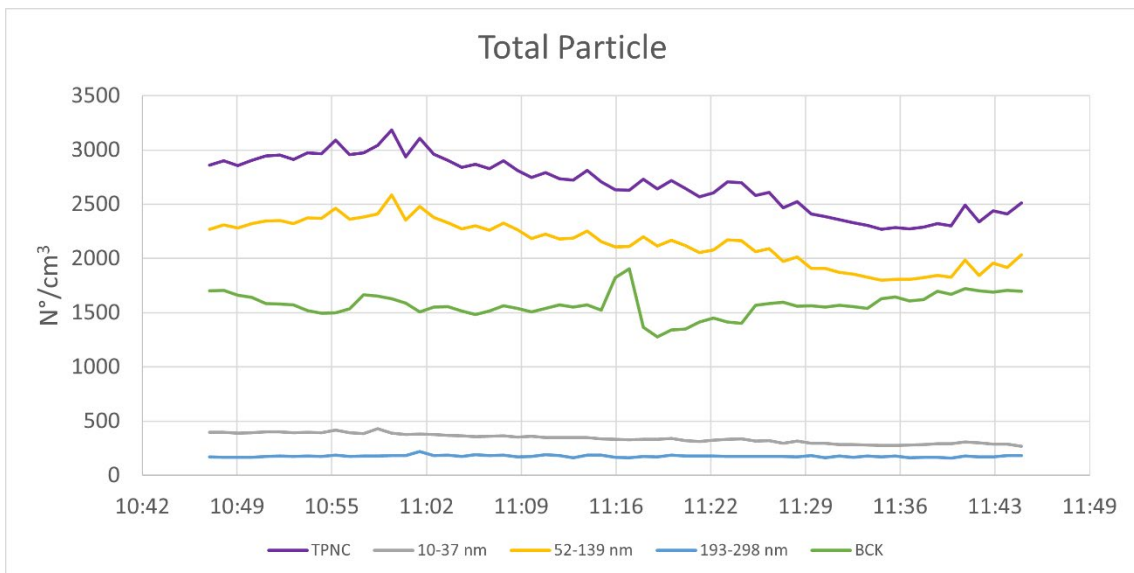


Figure 106 – TPNC trends and the main particle size classes for O4-removing and cleaning the final product and recovering unused powder by manually dragging the powder into the perforated grill around the building plate

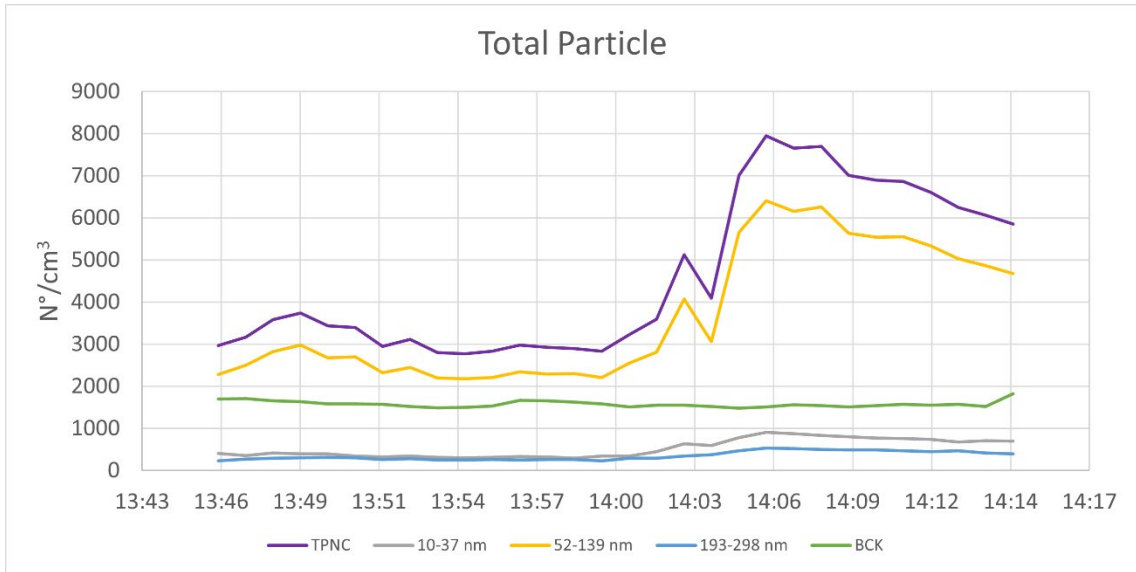


Figure 107 – TPNC trends and the main particle size classes for O5-sifting of recovered powder

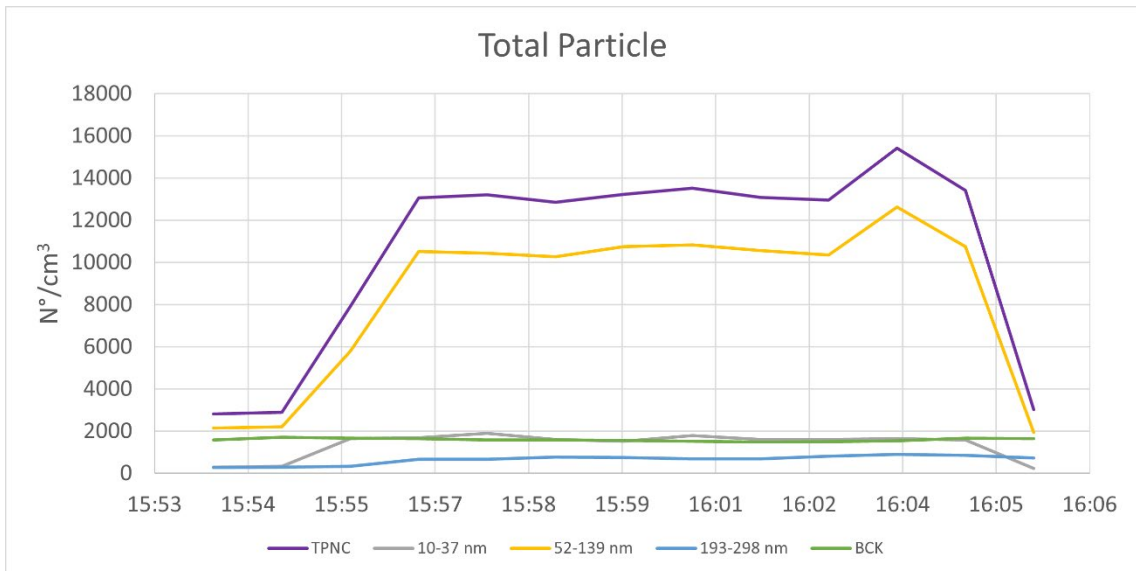


Figure 108 – TPNC trends and the main particle size classes for O6-depowdering of the final product with compressed air in the post-process restricted area

4.2.4.1. Gravimetric Method

The gravimetric method was also used to assess exposure to airborne dust's inhalable and respirable fractions. Specifically, filters placed inside a Gillian IPS IOM sampler (Figure 109 (a)) with a flow rate of 2,000 mL/min were used for the inhalable fraction and a Higgins Dewell cyclone (Figure 109 (b)) with a flow rate of 2,200 mL/min for the respirable fraction; the analysis was performed using a Sartorius Mechatronics MSE 6.6s microbalance with a resolution of 1.0 µg, following the provisions of Legislative Decree 25/2002, which refers to standard UNI EN 481:1994 for the definition of particle size fractions for the measurement of airborne particles.

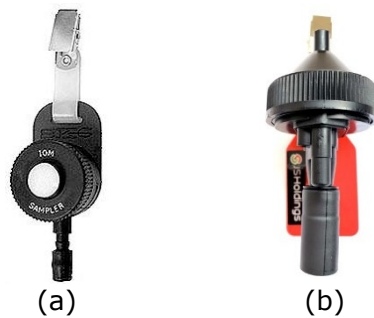


Figure 109 – IOM (a) and Higgins (b) personal sampling factors

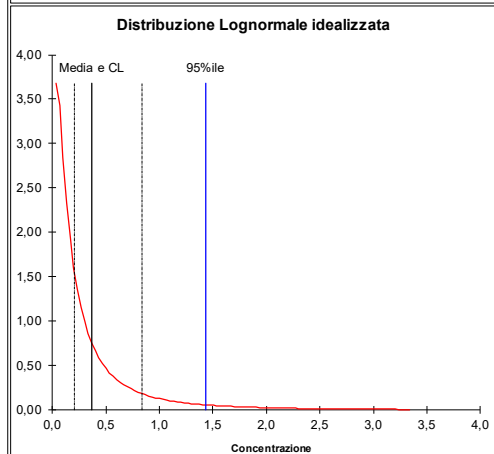
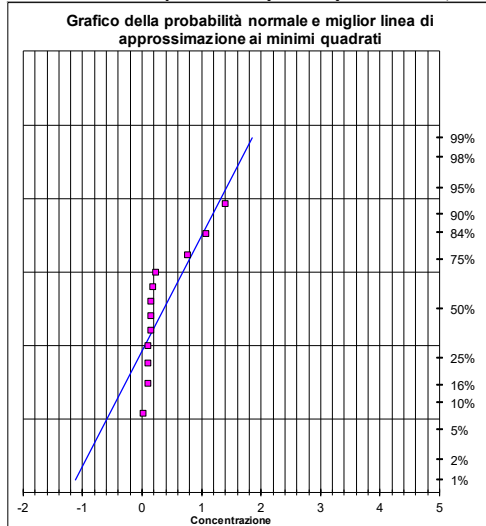
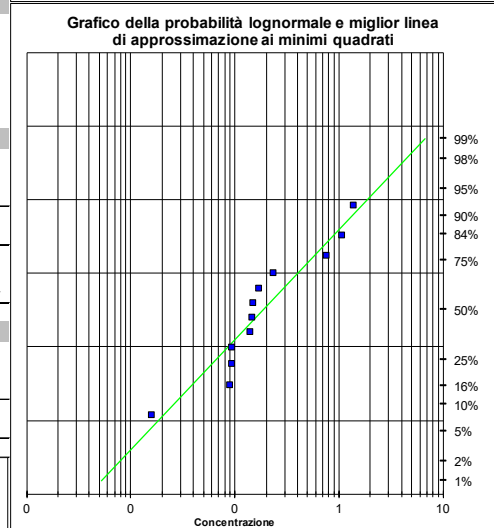
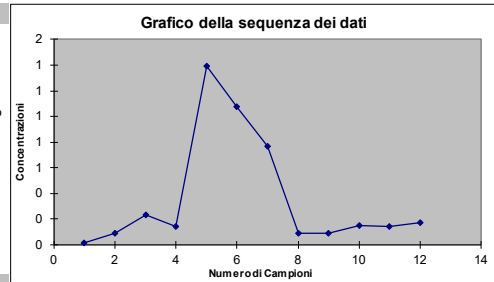
The exposure to the inhalable and respirable fractions of four operators was assessed on each of the three monitoring days. The gravimetric method results are shown in Table 11.

Table 11 – Results of airborne particulate sampling (inhalable and respirable fractions) using the gravimetric method

Operator	Day	Duration [min]	Volume IOM [L]	Inhalable Fraction [mg/m ³]	Volume Higgins [L]	Respirable Fraction [mg/m ³]
1	1	355	710	0.016	781	0.015
2		351	702	0.090	772	0.020
3		393	786	0.233	865	0.015
4		297	594	0.145	653	0.028
1	2	355	710	1.390	781	0.068
2		351	702	1.072	772	0.356
3		393	786	0.764	865	0.044
4		297	594	0.093	653	0.963
1	3	355	710	0.093	781	0.050
2		351	702	0.151	772	0.065
3		393	786	0.140	865	0.053
4		297	594	0.171	653	0.068

Descrizione dei dati: Metal Additive-Frazione Inalabile

STATISTICHE DESCRITTIVE	
OEL	12
Numero di campioni (n)	1,390
Valore massimo (max)	0,016
Valore minimo (min)	1,374
Range	0,000%
% superiore all'OEL	0,363
Media	0,148
Mediana	0,453
Deviazione standard	-1,681
Media dei dati trasformati logaritmicamente (ln)	1,238
Deviazione standard dei dati trasformati logaritmicamente	0,186
Media geometrica	3,450
Deviazione standard geometrica	
TEST SULL'ADEGUATEZZA DELLA DISTRIBUZIONE	
Test W dei dati trasformati logaritmicamente	0,915
Lognormale (a=0,05)?	SI
Test W dei dati	0,706
Normale (a=0,05)?	NO
STATISTICHE PARAMETRICHE LOGNORMALI	
Stima della media aritmetica - MVUE	0,364
LCL _{1,95%} - Metodo Esatto di Land	0,207
UCL _{1,95%} - Metodo Esatto di Land	0,839
95esimo Percentile	1,428
UTL _{0,5%,95%}	5,52
Percentuale al di sopra dell'OEL (%>OEL)	6%
LCL _{1,95%} >OEL	<0,1
UCL _{1,95%} >OEL	#####
STATISTICHE PARAMETRICHE NORMALI	
Media	0,363
LCL _{1,95%} - t	0,129
UCL _{1,95%} - t	0,598
95esimo Percentile - Z	1,108
UTL _{0,5%,95%}	1,602
Percentuale al di sopra dell'OEL (%>OEL)	0,000



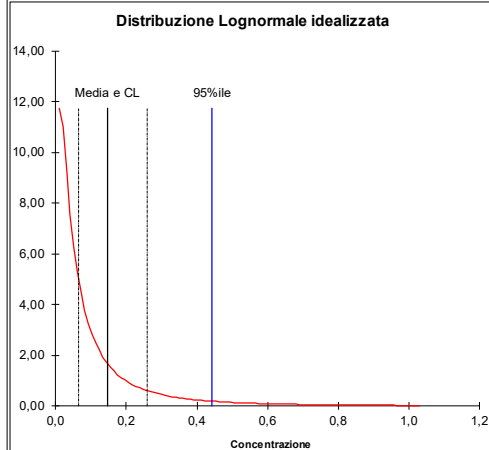
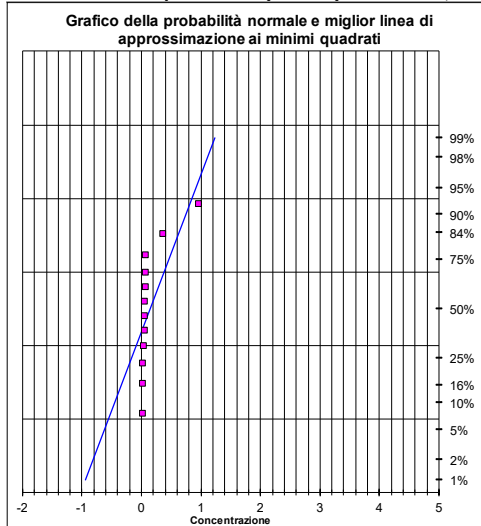
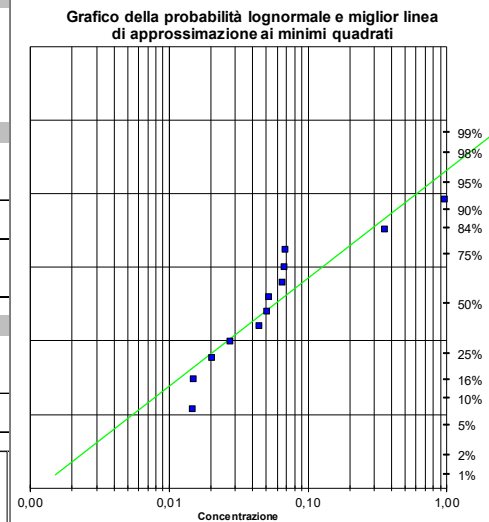
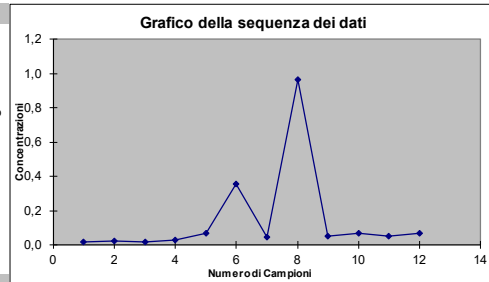
Distribuzione Normale		Non Applicabile
UR	21.29	
n	12	
UT	1.961	
NON APPLICABILE		

Distribuzione Log-Normale		Applicabile
UR	3.22	
n	12	
UT	1.961	
COMPLIANCE		

Figure 110 – Inhalable fraction exposure assessment based on UNI EN 689:2019 (statistical evaluation)

Descrizione dei dati: Metal Additive-Frazione Respirabile

STATISTICHE DESCRITTIVE	
OEL	3
Numero di campioni (n)	12
Valore massimo (max)	0,963
Valore minimo (min)	0,015
Range	0,949
% superiore all'OEL	0,000%
Media	0,145
Mediana	0,051
Deviazione standard	0,274
Media dei dati trasformati logaritmicamente (ln)	-2,845
Deviazione standard dei dati trasformati logaritmicamente	1,233
Media geometrica	0,058
Deviazione standard geometrica	3,432
TEST SULL'ADEGUATEZZA DELLA DISTRIBUZIONE	
Test W dei dati trasformati logaritmicamente	0,867
Lognormale (a=0,05)?	NO
Test W dei dati	0,517
Normale (a=0,05)?	NO
STATISTICHE PARAMETRICHE LOGNORMALI	
Stima della media aritmetica - MVUE	
LCL _{1,95%} - Metodo Esatto di Land	0,064
UCL _{1,95%} - Metodo Esatto di Land	0,258
95esimo Percentile	0,442
UTL _{95%,95%}	1,70
Percentuale al di sopra dell'OEL (%>OEL)	
LCL _{1,95%} %>OEL	<0,1
UCL _{1,95%} %>OEL	####
STATISTICHE PARAMETRICHE NORMALI	
Media	
LCL _{1,95%} - t	0,004
UCL _{1,95%} - t	0,287
95esimo Percentile - Z	0,595
UTL _{95%,95%}	0,894
Percentuale al di sopra dell'OEL (%>OEL)	
	0,000



Distribuzione Normale		Non Applicabile
UR	10.43	
n	12	
UT	1.961	
NON APPLICABILE		

Distribuzione Log-Normale		Applicabile
UR	3.2	
n	12	
UT	1.961	
COMPLIANCE		

Figure 111 – Respirable fraction exposure assessment based on UNI EN 689:2019 (statistical evaluation)

4.2.4.2. Airborne metals

Exposure to airborne metal dusts was assessed by extracting metals from filters sampled with the IOM and Higgins impactors using a solution of hydrochloric acid and nitric acid 50: 50 and analysed by mass spectrometry with an inductive plasma source ICP-MS following NIOSH Method 7300 'Elements by ICP 7300-Nitric/Perchloric Acid Ashing', OSHA ID-125G 'Metal and Metalloid Particulates In Workplace Atmospheres (ICP analysis)' and subsequent updates. The Threshold Limit Values (TLVs) considered for the monitored metals are as follows: cobalt and organic compounds TLV-TWA=0.02 mg/m³ (ACGIH 2021); chromium metal TLV-TWA=0.5 mg/m³ (ACGIH 2021 - Legislative Decree 81/2008); manganese element and inorganic compounds TLV-TWA=0.1 mg/m³ (ACGIH 2021); nickel and insoluble inorganic compounds TLV-TWA=0.2 mg/m³ (ACGIH 2021). Table 12 shows the concentrations of metals found on the filters of the IOM and Higgins impactors of the four operators involved in MA operations on the monitoring days.

Table 12 – Results of metal analyses of samples collected by the IOM and Higgins impactors

Operator	Day	Cr [µg/m ³]	Co [µg/m ³]	Mn [µg/m ³]	Ni [µg/m ³]
1	1	5.703	0.096	0.022	9.945
2		0.971	0.252	0.016	1.619
3		0.950	0.980	0.002	1.298
4		1.878	1.586	0.031	5.263
1	2	4.489	0.083	0.021	7.893
2		2.360	1.980	0.022	6.343
3		0.961	0.911	0.005	1.338
4		1.771	1.559	0.022	5.256
1	3	0.457	0.118	0.015	0.787
2		1.597	1.802	0.018	5.023
3		0.429	0.054	0.007	0.711
4		0.533	0.288	0.012	1.107

The graphs below (Figure 112 - Figure 115) show the concentration of each metal monitored and how it compares to the limit.

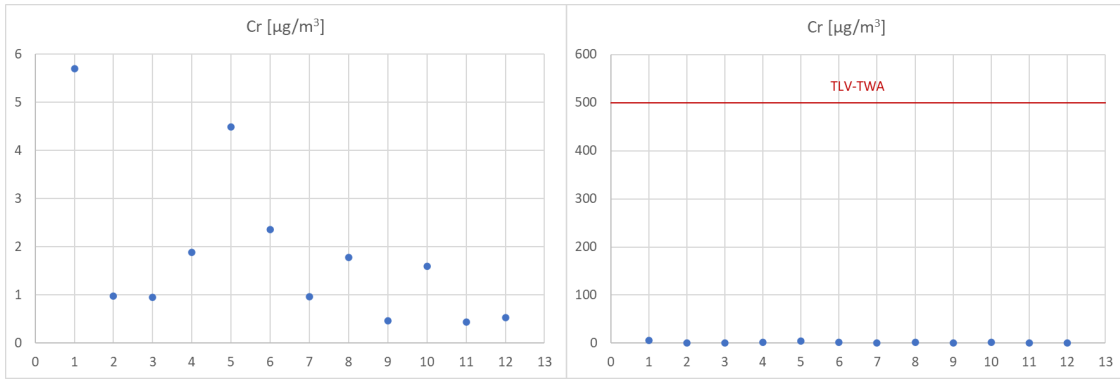


Figure 112 – Trend of measured Cr concentrations (left) and comparison of measured concentrations with TLV-TWA (right)

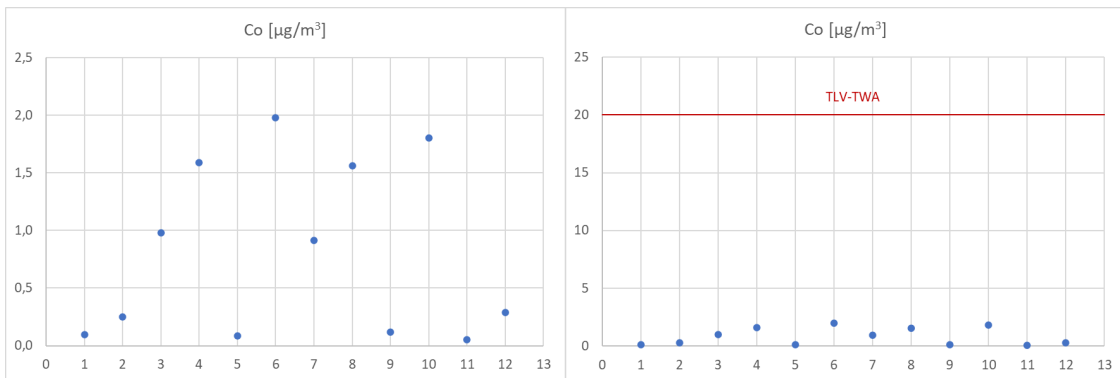


Figure 113 – Trend of measured Co concentrations (left) and comparison of measured concentrations with TLV-TWA (right)

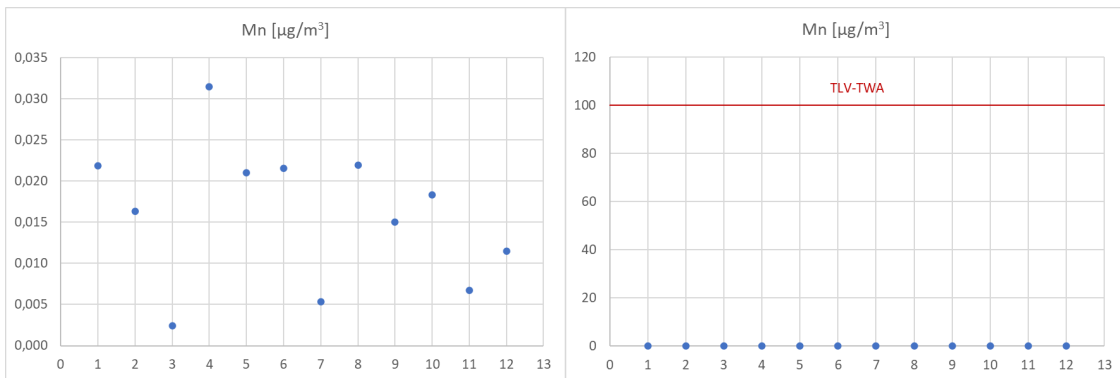


Figure 114 – Trend of measured Mn concentrations (left) and comparison of measured concentrations with TLV-TWA (right)

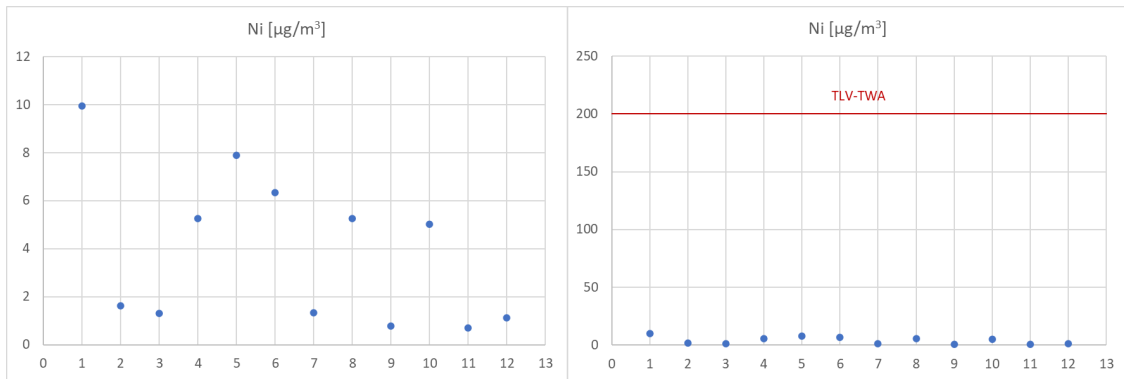


Figure 115 – Trend of measured Ni concentrations (left) and comparison of measured concentrations with TLV-TWA (right)

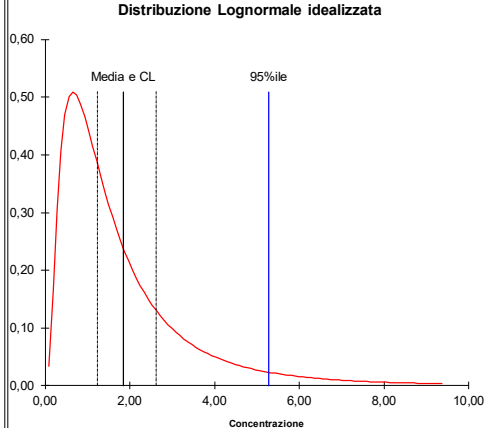
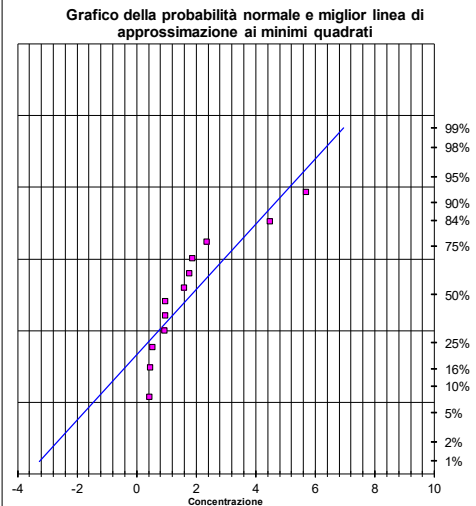
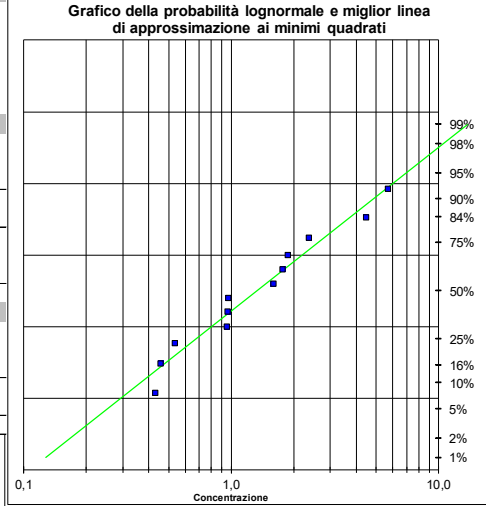
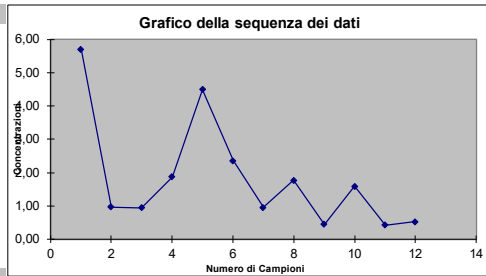
Figure 116 – Figure 119 show the results of the metal exposure assessments sampled and analysed using the statistical methodology prescribed by UNI EN 689:2019. As can be seen from the trends in the measured concentrations and the results of the statistical evaluations, there is no exceedance of the limit value or non-compliance for any of the samples or any of the metals.

Descrizione dei dati: Metal Additive - Cr

OEL	STATISTICHE DESCRITTIVE
500	Numero di campioni (n) 12
	Valore massimo (max) 5,703
	Valore minimo (min) 0,429
	Range 5,274
	% superiore all'OEL 0,000%
	Media 1,842
	Mediana 1,284
	Deviazione standard 1,657
	Media dei dati trasformati logaritmicamente (ln) 0,283
	Deviazione standard dei dati trasformati logaritmicamente (l) 0,839
	Media geometrica 1,327
	Deviazione standard geometrica 2,313
	TEST SULL'ADEGUATEZZA DELLA DISTRIBUZIONE
	Test W dei dati trasformati logaritmicamente 0,946
	Lognormale (a=0,05)? SI
	Test W dei dati 0,794
	Normale (a=0,05)? NO
	STATISTICHE PARAMETRICHE LOGNORMALI
	Stima della media aritmetica - MVUE 1,818
	LCL _{1,95%} - Metodo Esatto di Land 1,240
	UCL _{1,95%} - Metodo Esatto di Land 2,622
	95esimo Percentile 5,271
	UTL _{95%,95%} 13,16
	Percentuale al di sopra dell'OEL (%>OEL) 0%
	LCL _{1,95%} %>OEL <0,1
	UCL _{1,95%} %>OEL <0,1
	STATISTICHE PARAMETRICHE NORMALI
	Media 1,842
	LCL _{1,95%} - t 0,983
	UCL _{1,95%} - t 2,701
	95esimo Percentile - Z 4,568
	UTL _{95%,95%} 6,375
	Percentuale al di sopra dell'OEL (%>OEL) 0,000

Dati dei campioni
3 ≤ n ≤ 50

5,70
0,97
0,95
1,88
4,49
2,36
0,96
1,77
0,46
1,60
0,43
0,53



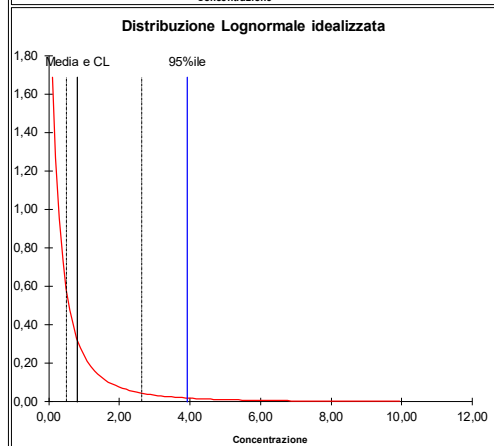
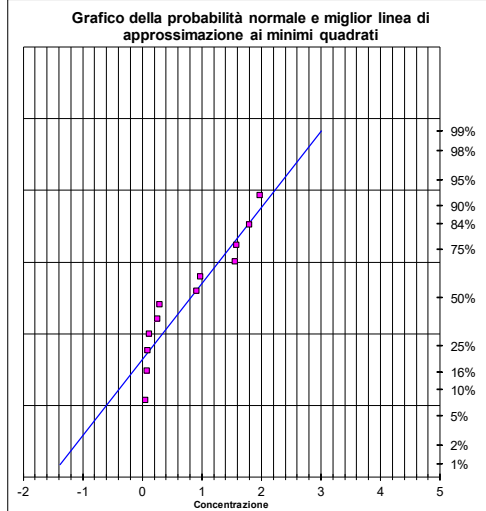
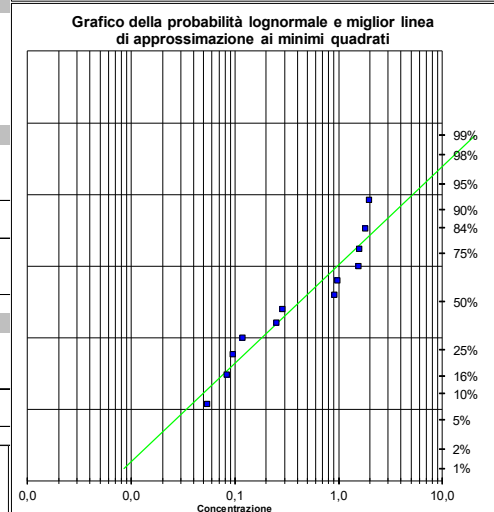
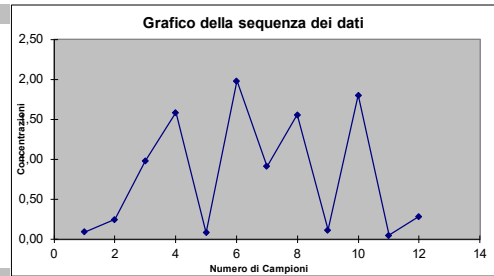
Distribuzione Normale	Non Applicabile
UR	300,63
n	12,00
UT	1,961
Non Applicabile	

Distribuzione Log-Normale	Applicabile
UR	7,07
n	12,00
UT	1,961
COMPLIANCE	

Figure 116 – Chromium exposure assessment based on UNI EN 689:2019 (statistical evaluation)

Descrizione dei dati: Metal Additive - Co

STATISTICHE DESCRITTIVE	
OEL	20
Dati dei campioni 3 ≤ n ≤ 50	0,10
	0,25
	0,98
	1,59
	0,08
	1,98
	0,91
	1,56
	0,12
	1,80
	0,05
	0,29
Numero di campioni (n)	12
Valore massimo (max)	1,980
Valore minimo (min)	0,054
Range	1,926
% superiore all'OEL	0,000%
Media	0,809
Mediana	0,599
Deviazione standard	0,752
Media dei dati trasformati logaritmicamente (ln)	-0,870
Deviazione standard dei dati trasformati logaritmicamente (l)	1,359
Media geometrica	0,419
Deviazione standard geometrica	3,894
TEST SULL'ADEGUATEZZA DELLA DISTRIBUZIONE	
Test W dei dati trasformati logaritmicamente	0,876
Lognormale (a=0,05)?	SI
Test W dei dati	0,842
Normale (a=0,05)?	NO
STATISTICHE PARAMETRICHE LOGNORMALI	
Stima della media aritmetica - MVUE	0,931
LCL _{1,95%} - Metodo Esatto di Land	0,502
UCL _{1,95%} - Metodo Esatto di Land	2,637
95esimo Percentile	3,920
UTL _{95%,95%}	17,28
Percentuale al di sopra dell'OEL (%>OEL)	22%
LCL _{1,95%} %>OEL	<0,1
UCL _{1,95%} %>OEL	>99,9
STATISTICHE PARAMETRICHE NORMALI	
Media	0,809
LCL _{1,95%} - t	0,419
UCL _{1,95%} - t	1,199
95esimo Percentile - Z	2,047
UTL _{95%,95%}	2,868
Percentuale al di sopra dell'OEL (%>OEL)	0,000

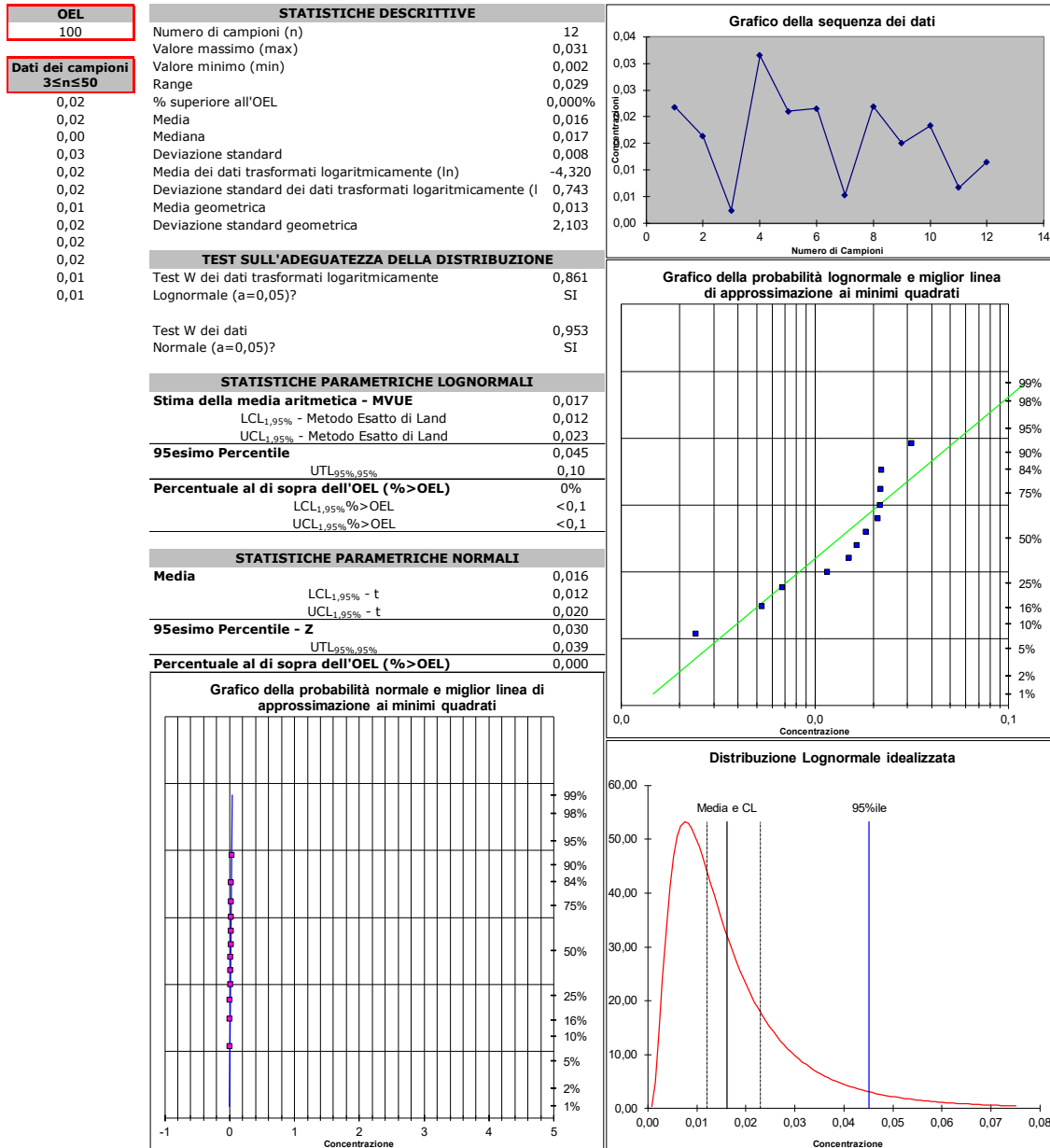


Distribuzione Normale		Non Applicabile
UR	25,51	
n	12,00	
UT	1,961	
Non Applicabile		

Distribuzione Log-Normale		Applicabile
UR	2,84	
n	12,00	
UT	1,961	
COMPLIANCE		

Figure 117 – Cobalt exposure assessment based on UNI EN 689:2019 (statistical evaluation)

Descrizione dei dati: Metal Additive - Mn



Distribuzione Normale		Applicabile
UR	11903,21	
n	12,00	
UT	1,961	
COMPLIANCE		

Distribuzione Log-Normale		Applicabile
UR	12,01	
n	12,00	
UT	1,961	
COMPLIANCE		

Figure 118 – Manganese exposure assessment based on UNI EN 689:2019 (statistical evaluation)

Descrizione dei dati: Metal Additive - Ni

OEL
200

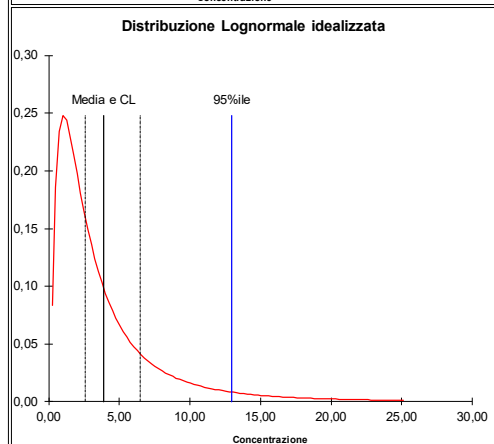
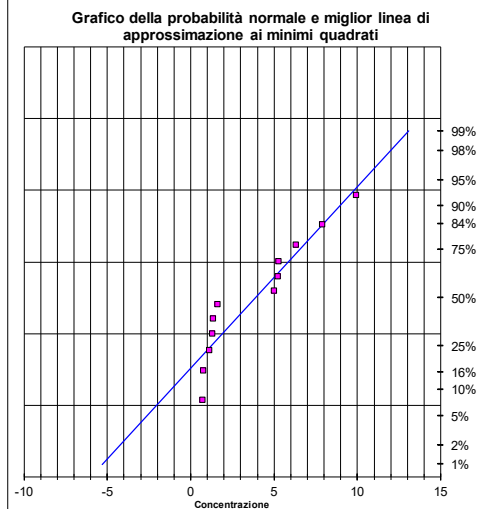
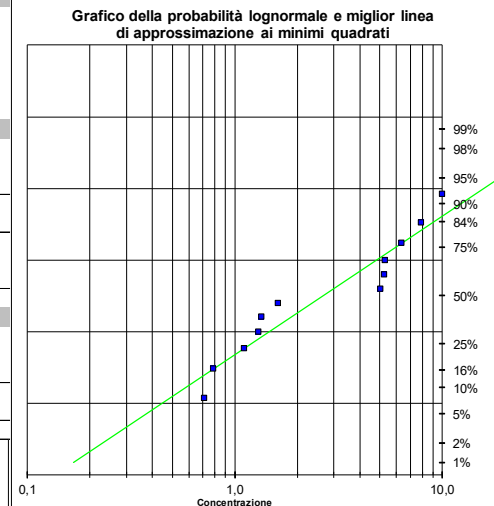
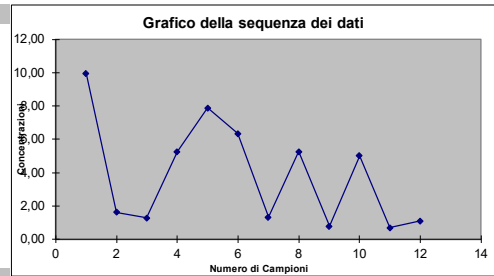
Dati dei campioni
3 ≤ n ≤ 50

STATISTICHE DESCRITTIVE	
Numero di campioni (n)	12
Valore massimo (max)	9,945
Valore minimo (min)	0,711
Range	9,235
% superiore all'OEL	0,000%
Media	3,882
Mediana	3,321
Deviazione standard	3,157
Media dei dati trasformati logaritmicamente (ln)	0,975
Deviazione standard dei dati trasformati logaritmicamente (l)	0,965
Media geometrica	2,651
Deviazione standard geometrica	2,624

TEST SULL'ADEGUATEZZA DELLA DISTRIBUZIONE	
Test W dei dati trasformati logaritmicamente	0,881
Lognormale (a=0,05)?	SI
Test W dei dati	0,866
Normale (a=0,05)?	SI

STATISTICHE PARAMETRICHE LOGNORMALI	
Stima della media aritmetica - MVUE	
LCL _{1,95%} - Metodo Esatto di Land	4,009
UCL _{1,95%} - Metodo Esatto di Land	2,585
UCL _{1,95%} - Metodo Esatto di Land	6,494
95esimo Percentile	
UTL _{95%,95%}	12,960
UTL _{95%,95%}	37,13
Percentuale al di sopra dell'OEL (%>OEL)	
0%	0%
LCL _{1,95%} %>OEL	<0,1
UCL _{1,95%} %>OEL	###

STATISTICHE PARAMETRICHE NORMALI	
Media	
Media	3,882
LCL _{1,95%} - t	2,245
UCL _{1,95%} - t	5,518
95esimo Percentile - Z	
95esimo Percentile - Z	9,075
UTL _{95%,95%}	12,519
Percentuale al di sopra dell'OEL (%>OEL)	
Percentuale al di sopra dell'OEL (%>OEL)	0,000



Distribuzione Normale		Applicabile
UR	62,13	
n	12,00	
UT	1,961	
COMPLIANCE		

Distribuzione Log-Normale		Applicabile
UR	4,48	
n	12,00	
UT	1,961	
COMPLIANCE		

Figure 119 – Manganese exposure assessment based on UNI EN 689:2019 (statistical evaluation)

5. Odour nuisances

In this chapter, odour nuisances are introduced and analysed in detailed within two case studies and a section dedicated to emissions modelling.

5.1. Introduction

Anthropogenic emissions of odours can severely restrict the use of the territory. Therefore, the attempt to link atmospheric emissions not only to concentration limits but also to odour impact limits stems from the need to ensure that activities with significant osmogenic flows do not affect the usability of the territory.

Sewage treatment plants or bituminous mixing plants (BMP) are common sources of odours. Characterising odour impacts from these plants is challenging due to the plant configuration. Some phases of production processes involve large and open areas, and transient emissions are frequent and common. In addition, odours can be released from different areas of the plant, resulting in a complex localisation of emission sources, which is reflected in a difficult assessment and measurement of odours.

In terms of BMPs, odours at these sites are mainly from the bitumen loading area/process, where high-temperature bitumen is pumped from a tanker truck to the plant reservoir, and the bitumen mix release area, where the final product (at a temperature of 170-190°C) is released into a truck. Under normal operating conditions, emissions from the BMPs can determine the release of hydrogen sulphur compounds, polycyclic aromatic hydrocarbons and VOCs into the atmosphere.

The presence of odour emissions in the ambient air can cause discomfort to plant employees and residents of neighbouring areas. In recent years, many complaints have been received from residents, and the authorities have been alerted to the problem of odour nuisance. In addition, some of these compounds can cause various psychosomatic symptoms such as anxiety, stress, headaches and dizziness, nausea and loss of consciousness. Odorants with a low olfactory threshold can influence the discomfort associated with the perception of unpleasant odours of different intensities and hedonic tones. Furthermore, even if unpleasant odours are not necessarily direct triggers of health effects, they may be associated with releasing other harmful compounds. While odour abatement remains at the forefront of research in this area, it has been suggested that a project can only be considered successful with community approval, a fair assessment given the time and cost sometimes required

to address community concerns. These concerns appear to be multi-dimensional. It is not only the perceived odour that determines the impact of malodour exposure on a community, but cognitive appraisal, community interests and several other factors play a role in shaping the impact of malodour. These factors may explain why intolerance to formal odours appears to be increasing. Understanding these factors may also explain why governing bodies have found it difficult to establish fair and effective regulations that meet the community's needs despite the enormous effort that has gone into creating odour parameters. European countries such as Portugal, Greece and Austria currently have no specific odour legislation, while others such as Germany only have regulations for waste management activities.

There is no national regulation in Italy. The previous Italian government made a minor amendment to the Italian National Regulation on the Environment, adding Article 272-bis, which gave the Italian regions the power to regulate odours. [87] This minor amendment was essential to regulating odours in the Italian regions. Some regions and provinces have adopted their regulations to define how odour emissions and nuisances should be managed. Some regions, such as Puglia, Lombardia, Piemonte and the province of Trento, have regional laws on odours. Lombardia has been a pioneer in Italy, publishing a regional directive specifically on odour emissions. [88] Like other European regulations, this directive is based on dynamic olfactometry and dispersion modelling. However, although this directive defines the requirements for odour impact studies using emission dispersion simulation, it doesn't set any acceptance criteria.

Today's environmental monitoring solutions are characterised by high cost and installation complexity, often requiring extensive resources, infrastructure and expertise. Odour impact is generally determined from odour concentration data, expressed in Odorimetric Units per cubic metre (O.U./m³), representing the number of dilutions required for 50% of tasters not to perceive the odour of the sample analysed. [89] However, olfactometry has some limitations, such as the high cost of laboratory analysis of air samples and the impossibility of continuous measurements. Electronic noses could be the best solution to meet the expectations of the different actors working on environmental issues regarding odour nuisance. However, their use is still limited by technological problems such as sensor drift over time and unwanted variability due to atmospheric conditions. However, advances in sensor and analysis networks and automated and remote sampling techniques have opened up a new avenue in environmental monitoring.

5.1. Case studies

The Pyxis GC system is an innovative on-field gas-chromatograph system that is carrier-gas free, permitting continuous monitoring of VOCs. It combines the Micro-Electro-Mechanical (MEMS) System of microfluidics for the selective pre-concentration and the gas-chromatographic separation with the peak quantification given by the Miniaturized Photoionization Detector (PID). It can be connected through Wi-Fi, Ethernet, or 4G. The software permits the monitoring and management on a cloud platform, so remote real-time monitoring is achievable.



Figure 3. Pyxis GC system (left) and a detail of its interior (right).

This system has allowed obtaining “fingerprints” of odorous compounds that could annoy the workers and the general population.

5.1.1. Bituminous conglomerate production activities monitoring

The PyxisGC instrument was calibrated to identify the characteristic profile of the bitumen mix; the instrument is also capable of detecting xenobiotic profiles originating from other emission sources. The bitumen mix profile has been verified in the field, placing the instrument at the bitumen discharge area inside the plant.



Figure 120 – PyxisGC system in the proximity of the bitumen mix discharge tank

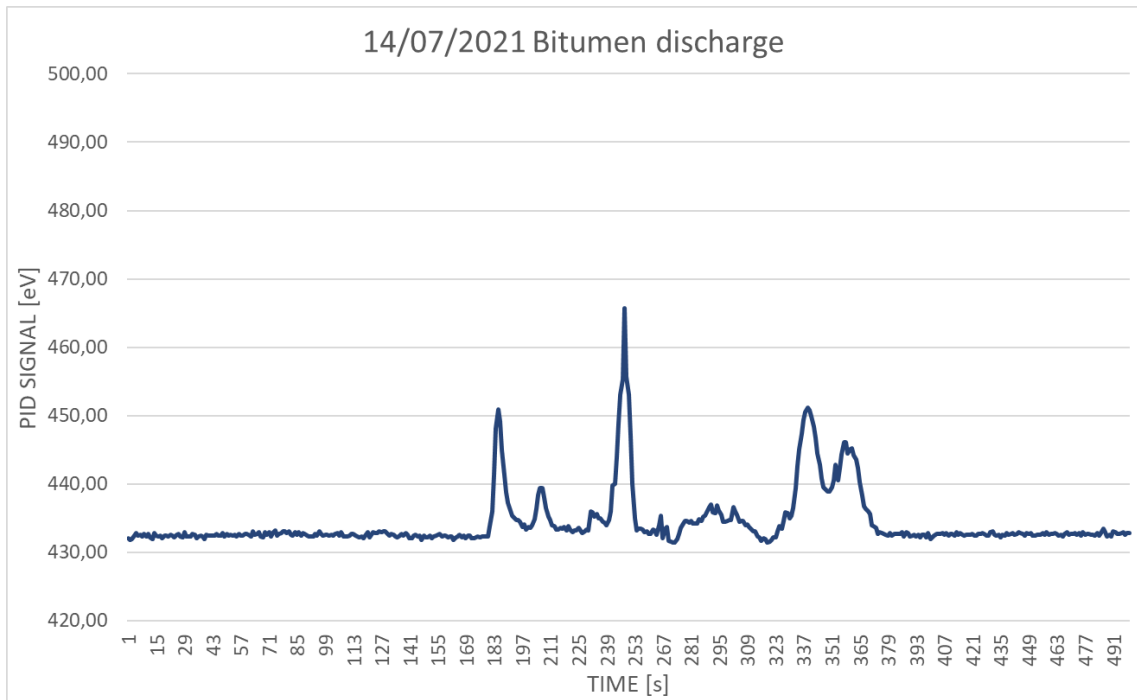


Figure 121 – Photoionization detector signal [eV] during the bitumen discharge

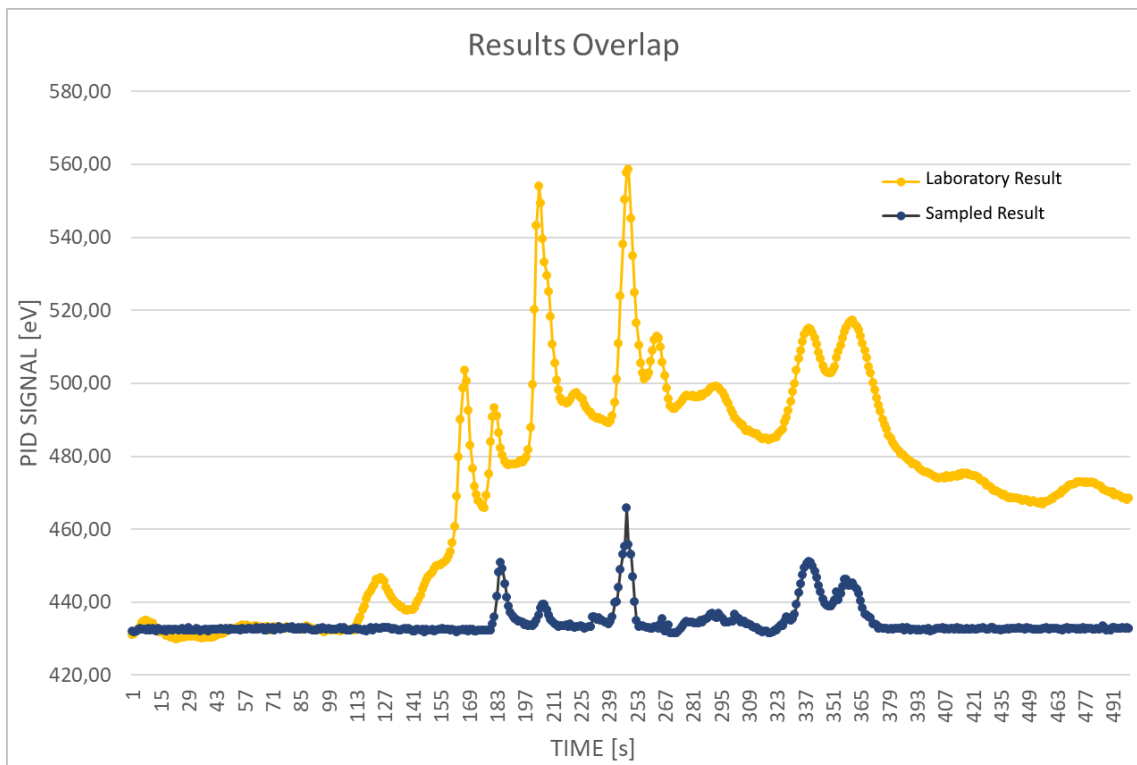


Figure 122 – Photoionization detector signal [eV] obtained in the laboratory overlapped with the one sampled during the bitumen discharge

Figure 121 shows the chromatogram resulting from sampling during bitumen loading and unloading, while Figure 122 shows the overlap between the profile sampled and that obtained in the laboratory.



Figure 123 – PyxisGC installed between the bituminous conglomerate plant and the receptors

The objective was to detect and circumscribe in real time any olfactory nuisance perceived by receptors in the area of interest, flanking the characteristic profile of the emission source responsible for the reported nuisance with the measurement of olfactometric units. Thus, the PyxisGC instrument was installed in the area adjacent to the bituminous conglomerate plant for approximately one month.

During the monitored period, during the plant's opening hours (from 06:00 to 16:00), the profile of volatile organic compounds associated with the odorous emission of the asphalt was never found.

For example, in Figure 124, the chromatograms deriving from the monitoring on an average day are reported. The peak of toluene can be easily recognised.

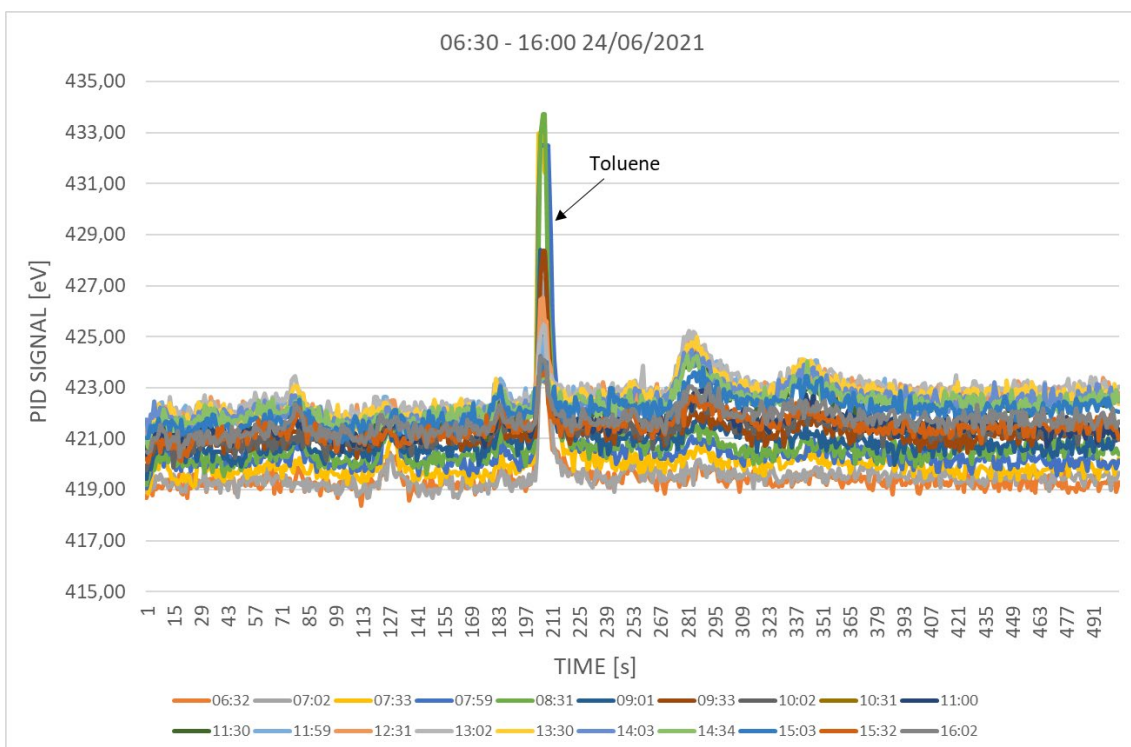


Figure 124 – Chromatograms of the 24th of June 2021

Moreover, in Figure 125, the overlap between the average signal detected in the monitored area and the average signal detected in an urban area of Florence, which is assumed as the environmental background value, is depicted.

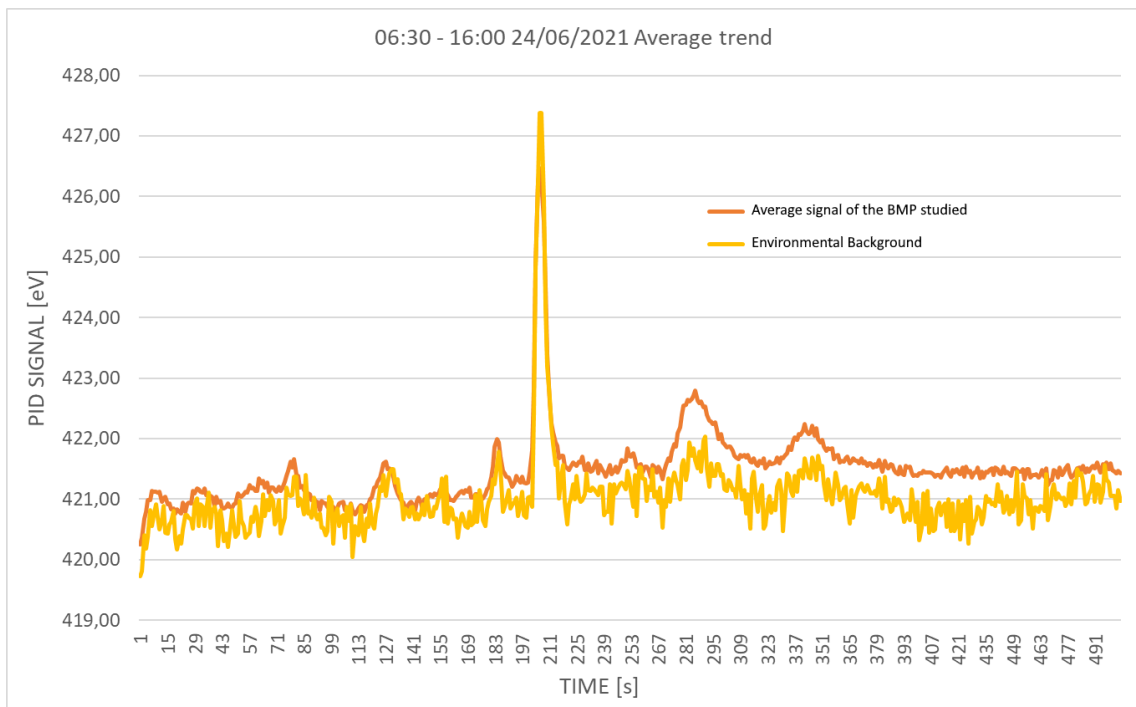


Figure 125 – Average photoionization detector signal [eV] of the monitored area (orange) and the average signal obtained in an urban area of Florence (yellow)

5.1.2. Odour nuisance within the municipality of Calenzano

Various production areas characterise the municipality of Calenzano. The main production areas in the area are the Settimello industrial zone, characterized by the presence of Buzzi-Unichem (cement plant) and Palmieri Foundries (cast iron production), the Chiosina area, considered an extension of Settimello, Fibianna, and Le Prata bordering Campi Bisenzio, where the ENI fuel depot is located. The prevailing sector in the municipality of Calenzano is metal processing and production, followed by tanning, the wood industry, and publishing. Construction, logistics, transportation services, and wholesale trade play a significant role.

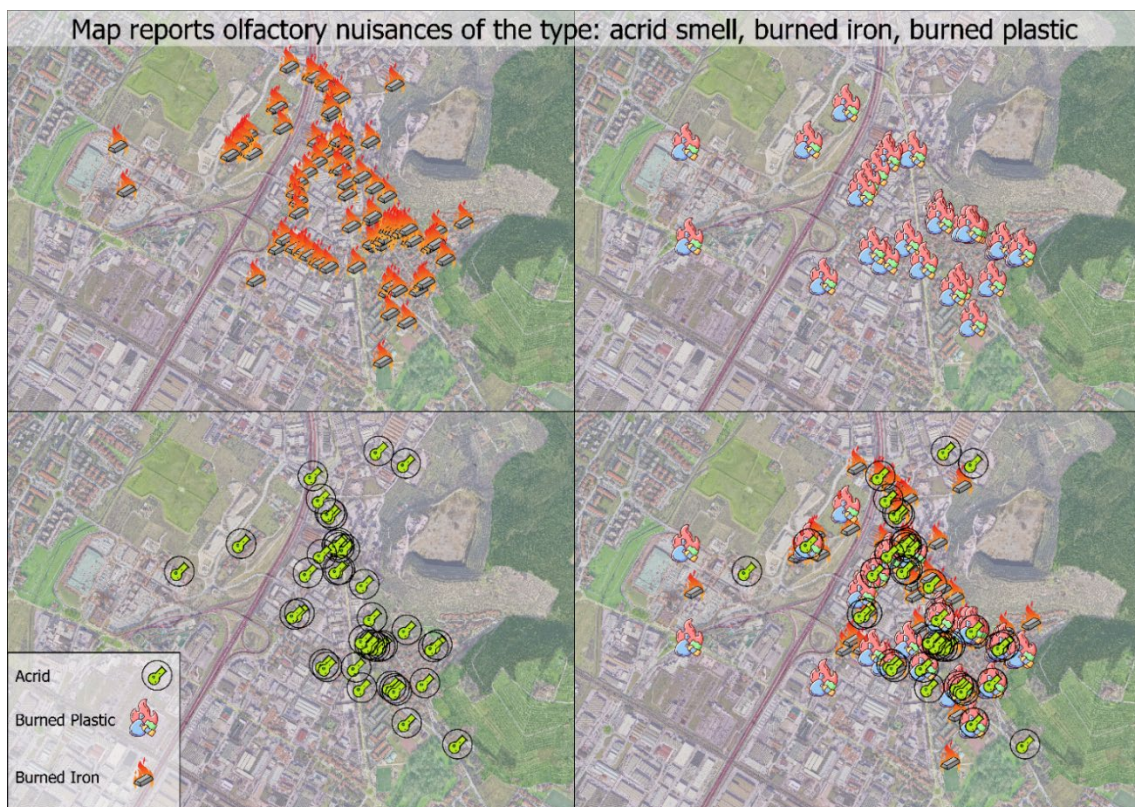


Figure 126 – Map reports of odour nuisances

In Figure 126 are highlighted the historical reports that the citizens have made over the years. Mainly, they regard olfactory nuisances of the type: the acrid smell, the burned iron, and the burned plastic.

Some citizens have been chosen to be “noses” in the monitoring: they have been endowed with passive samplers, specifically MonoTrap, introduced in section 2.3.1.1, which is a newly developed, state-of-the-art sorptive media based on the high surface area of silica monolith. It is designed to enrich flavours, aromas, and fragrances rapidly. It can be easily used for analysing volatile and semivolatile compounds for quality control, environment, and forensic applications. The passive sampler was

provided already inserted into the sampling holder inside a sealed tube. Upon perception of harassment, the device is opened and left in the uptake position for at least 8 hours. At the end of sampling, the system should be reinserted into the tube (without touching the uptake substrate by hand) and sealed. Once collected, samples are analysed in GC-MS after thermal desorption in a dedicated Multimode injection system inlet OPTIC4, shown in Figure 127 – GC-MS equipped with Multimode injection system inlet OPTIC4.



Figure 127 – GC-MS equipped with Multimode injection system inlet OPTIC4

In addition, continuous monitoring was carried out using the Pyxis GC system at Via dei Tessitori and Via Dante Alighieri between March and May 2022.

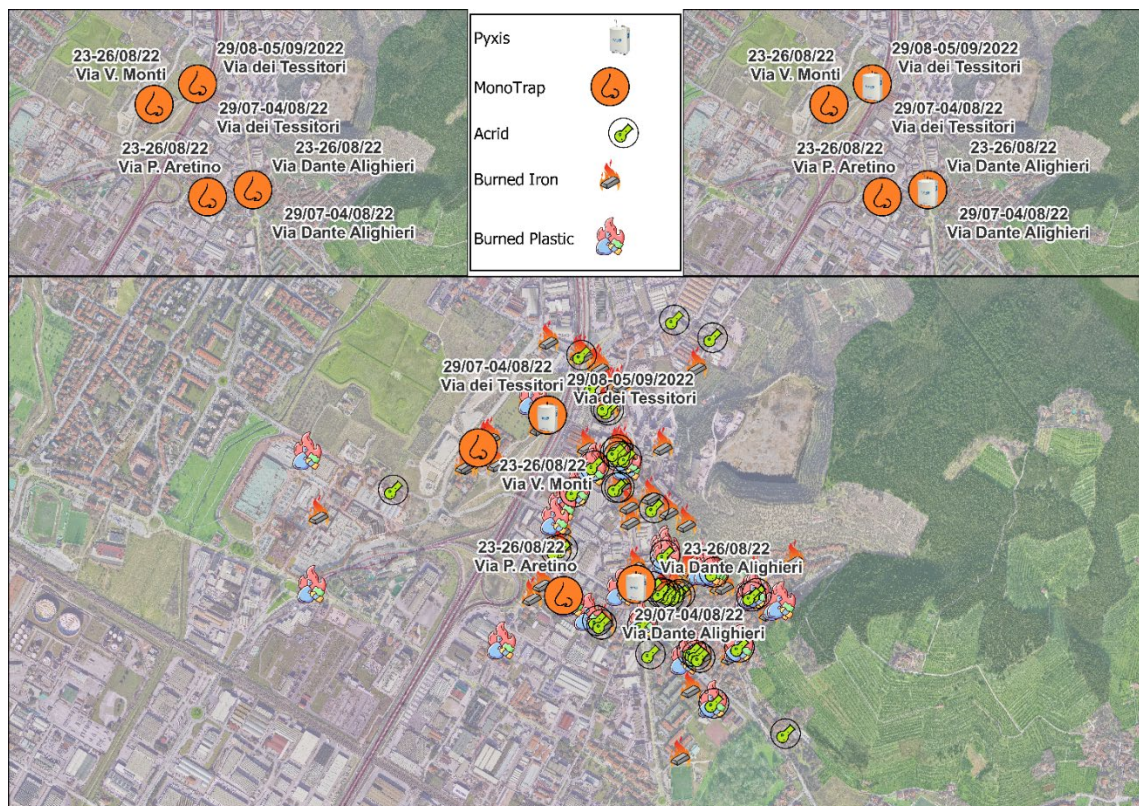


Figure 128 – Sampling location with MonoTrap samplers, the location where PyxisGC was placed for continuous monitoring, and sampling locations selected compared with pre-study reports

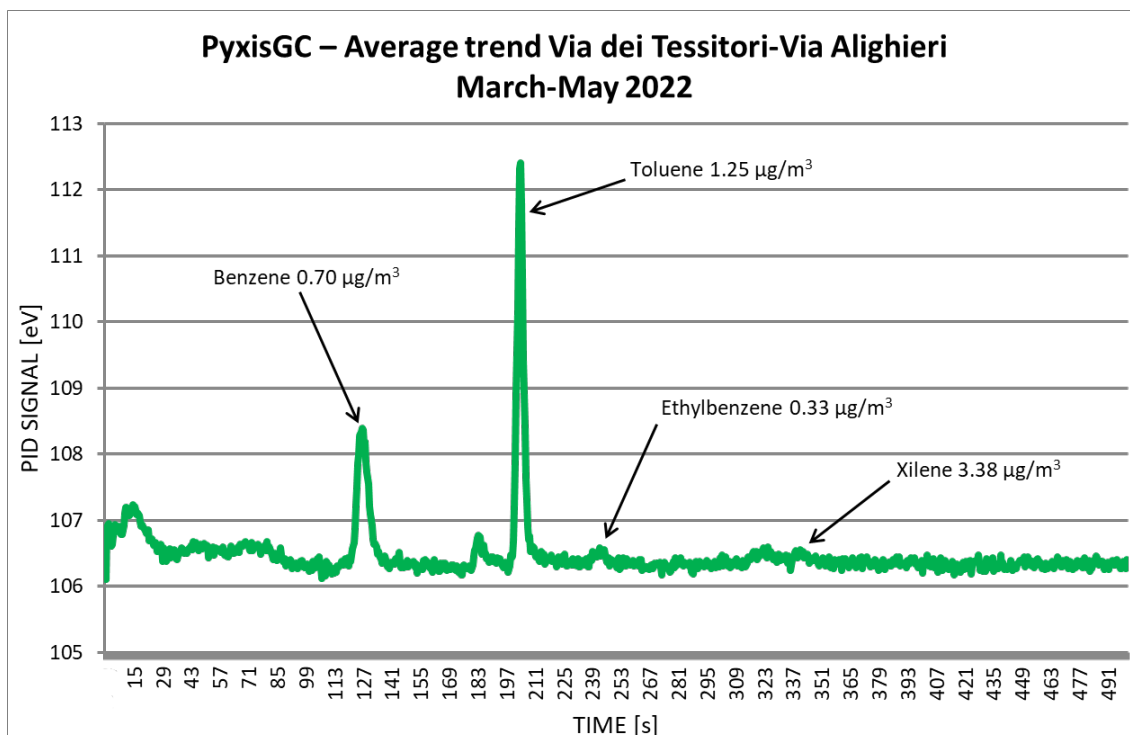


Figure 129 – Average trend observed with PyxisGC between Via dei Tessitori and Via Alighieri from March to May 2022

This system has allowed obtaining “fingerprints” of odorous compounds that could annoy the general population.

On May 4, a failure of the deodourising plant at the Palmieri Foundries was reported. The graphs show the average trend in the concentration of volatile organic compounds on May 4th and 5th. No significant signals are found; the peak in the middle of the graph is due to the ubiquitous presence of toluene (0.22-0.38 ppb).

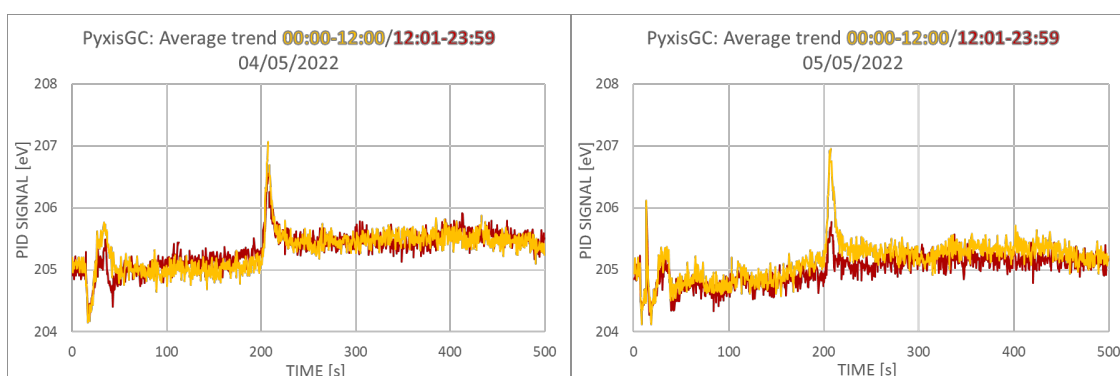


Figure 130 – Average trend observed with PyxisGC on the 4th and the 5th of May 2022

Table 11 reports the time and location of sampling with MonoTrap devices.

Table 13 – MonoTrap Sampling

MonoTrap N°	Sampling time	Location of the sampling
1	29/07-04/08/2022	Via dei Tessitori
2	29/07-04/08/2022	Via Alighieri
3	23/08-26/08/2022	Via Monti
4	23/08-26/08/2022	Via Aretino
5	23/08-26/08/2022	Via Alighieri
6	29/08-05/09/2022	Via dei Tessitori

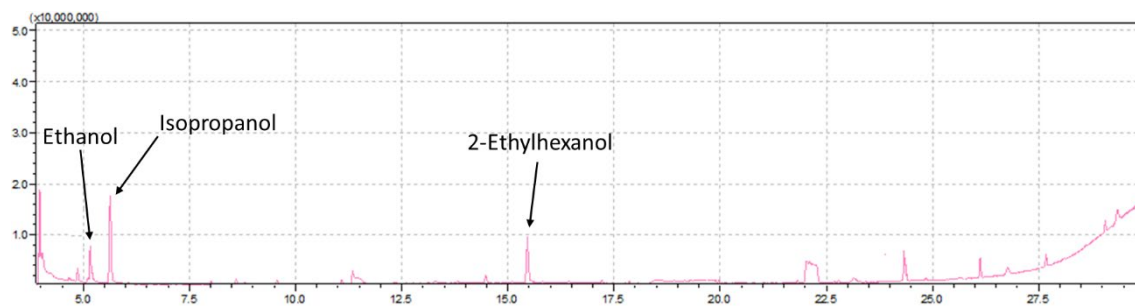


Figure 131 – Chromatograph of MonoTrap 1

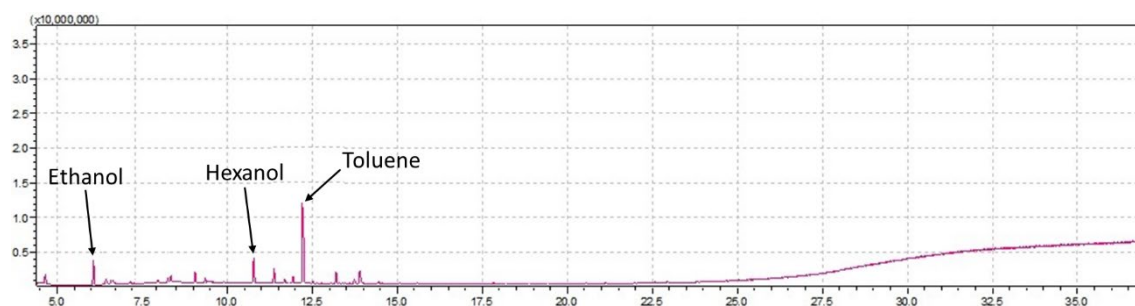


Figure 132 – Chromatograph of MonoTrap 2

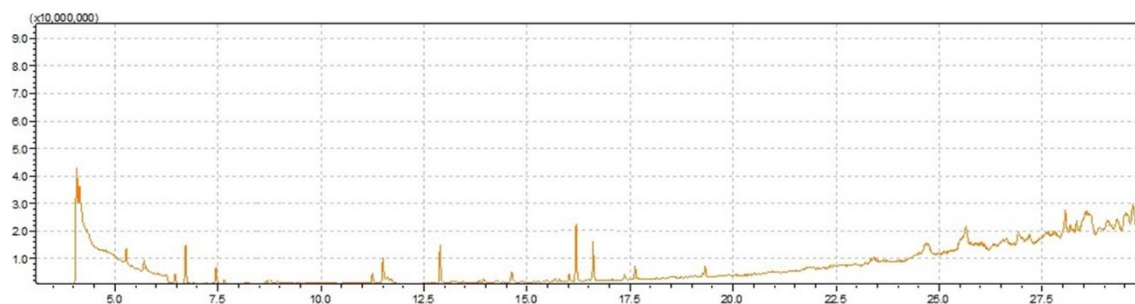


Figure 133 – Chromatograph of MonoTrap 3

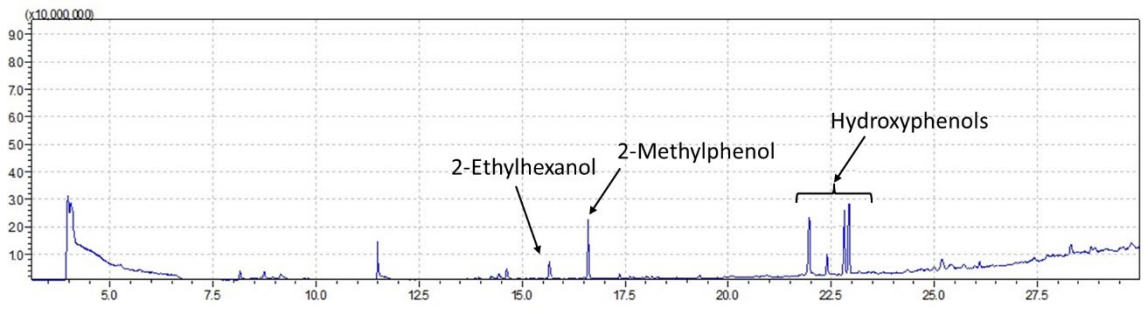


Figure 134 – Chromatogram of MonoTrap 4

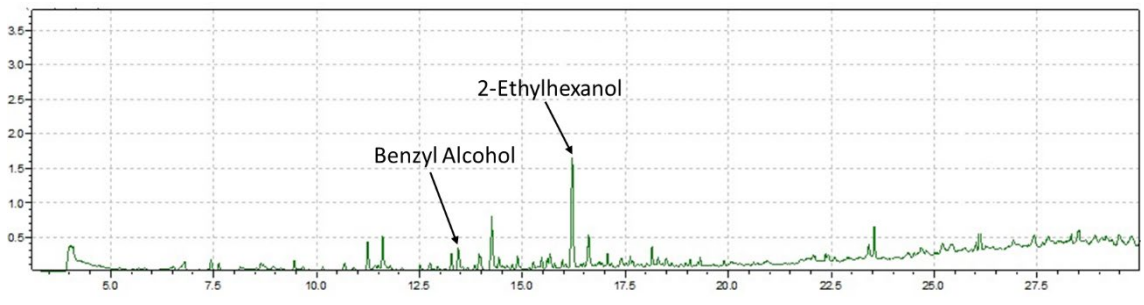


Figure 135 – Chromatogram of MonoTrap 5

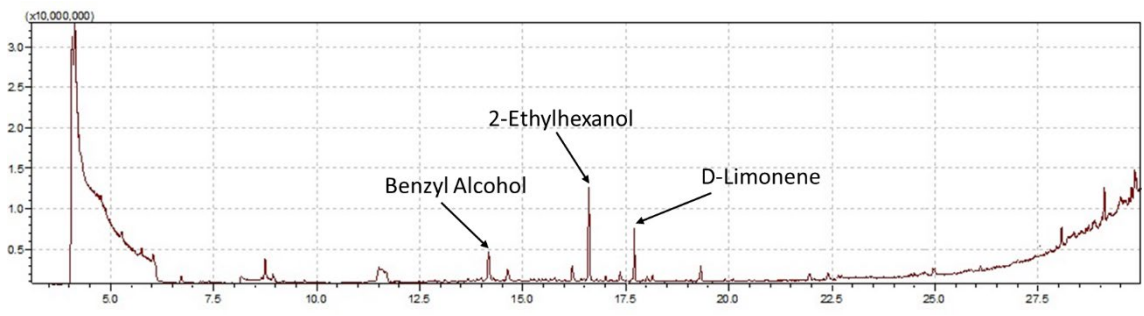


Figure 136 – Chromatogram of MonoTrap 6

Table 14 – Compounds sampled with MonoTrap

Compound	CAS Number	Odour threshold [ppm]	Odour traits
Ethanol	64-17-5	0.520	Sweetish, Fruity
Hexanol	111-27-3	0.006	Chemical, Fruity, Sweet
Isopropanol	67-63-0	26.000	Alcoholic, Pungent
Toluene	108-88-3	0.330	Sweet, Pungent
2-Ethylhexanol	104-76-7	0.0009	Plastic, Acrid
Benzyl alcohol	100-51-6	5.500	Sweet
2-Methylphenol	95-48-7	0.00028	Sweet, Acrid
Hydroxyphenols	---	---	---
D-Limonene	138-86-3	1.700	Lemon

From the analysis of samples collected from citizens, the compounds shown in Table 14 were identified by characteristic mass spectrum and comparison with analytical standards. The chromatographs of the analysed samples are reported from Figure 131 to Figure 136. These compounds can be traced to burnings, plastic materials, and odourants (e.g., limonene).

5.1.3. Odorous emissions from wastewater plant

The monitored wastewater treatment plant treats sewage up to 190,000 p.e.; on weekdays, it can treat up to 39,000 m³/day and remove up to 20,000 kg/day of COD and 1,100 kg/day of surfactants. It basically consists of equalisation, primary sedimentation, denitrification, biological oxidation, secondary sedimentation, final clariflocculation, sand filters and ozonation. The sludge line consists of gravity-thickening and mechanical dewatering with a centrifuge and filter press. The resulting sludge from the depuration process can amount to 10,000 t/y with a moisture content between 64 and 74%.

The monitoring has been conducted near the biological oxidation tanks and biofilters.

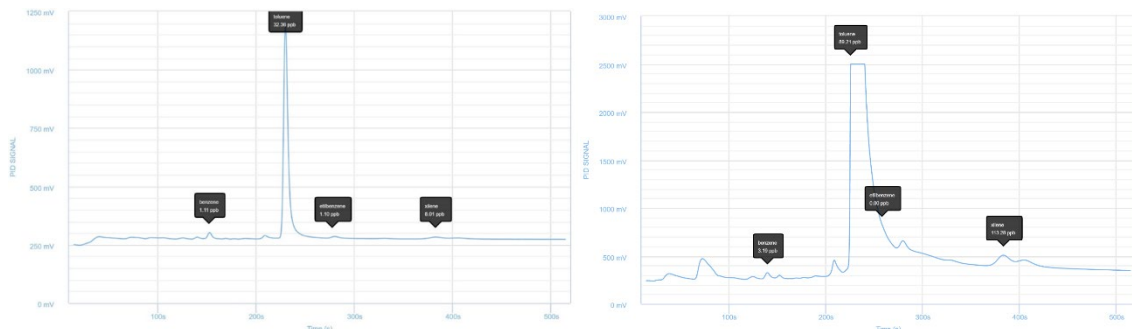


Figure 137 – An increase in the signal with peak saturation

As can be observed in Figure 137, an increase in the PID signal led to the saturation of the peak of toluene.

In addition to sampling with the PyxisGC, bags were collected and analysed in order to determine odorimetric units and correlate them with the chromatogram detected by the PyxisGC. Once this correlation is finalised, the PyxisGC will be able to continuously provide an estimate of the disturbance expressed in odorimetric units.

Table 15 – Correlation between the Chromatograms and the odorimetric units/m³ deriving from the bags

Date	Hour	O.U./m ³	Chromatogram
02/02/2023	14:15	1'750	1
02/02/2023	14:45	2'500	2
16/02/2023	09:04	-	3
16/02/2023	11:19	725	4
16/02/2023	12:45	510	5
16/02/2023	15:50	-	6
22/02/2023	09:40	1'750	-
22/02/2023	15:10	1'650	-

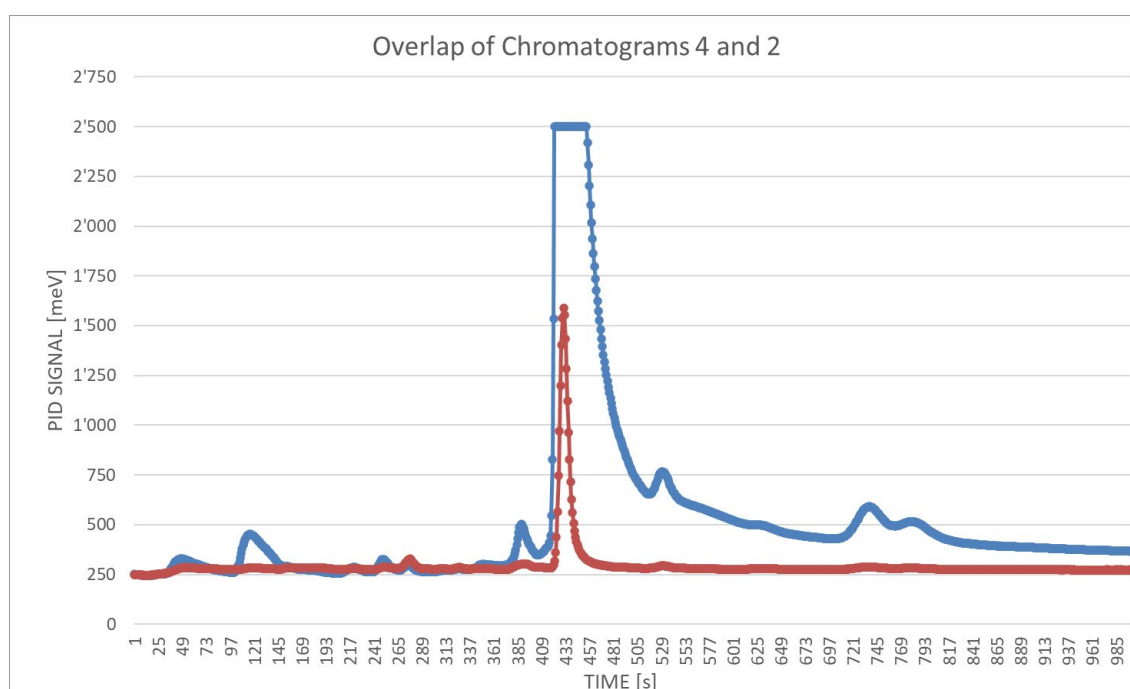


Figure 138 – Overlap of chromatogram 4 (725 O.U./m³) and chromatogram 2 (2,500 O.U./m³)

The PID Signal increases with the increase of the odorimetric units; however, the chromatographic information can be altered by the presence of a compound or a class of compounds which saturate the instrumental signal. To overcome this issue, a PyxisGC with a minor sensitivity has been proposed to understand the saturated peak better.

The workflow proposed is:

- The characterization of the background of the site.
- The monitoring and characterization of channelled emissions.
- The monitoring and characterization of diffuse emissions.
- Mathematical elaboration of chromatographic dynamics.

- Identification/classification of chromatographic dynamics of interest.
- Definition of pre-alert levels.

The characterization of the site's background will be obtained through the installation of the PyxisGC far from the emissions spots to define the level of odorimetric units not identified as odorous nuisance and to identify the chromatographic dynamic.

The monitoring and characterization of channelled emissions interest the biofilter emissions, as shown in Figure 139.

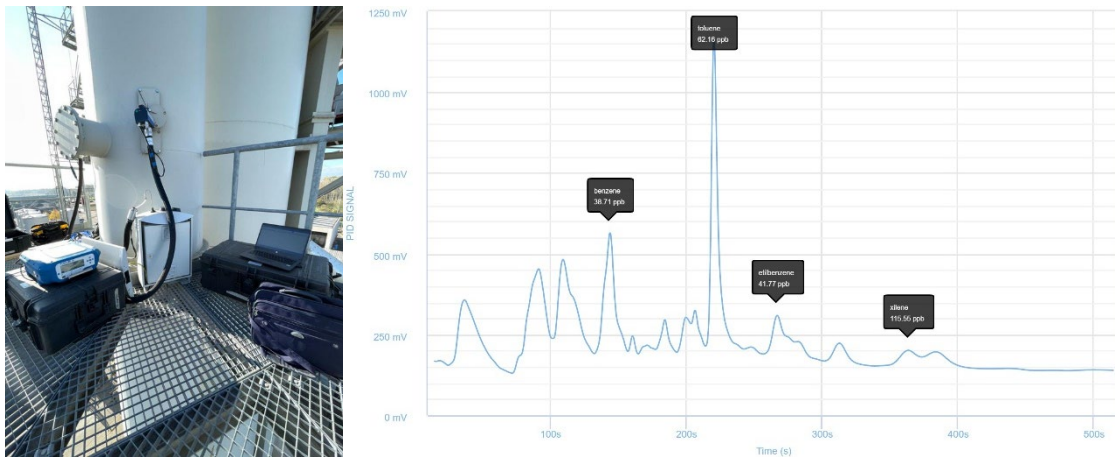


Figure 139 – Monitoring and characterization of channelled emissions

The monitoring and characterization of diffuse emissions interest the biological oxidation tanks' emissions, as shown in Figure 140.

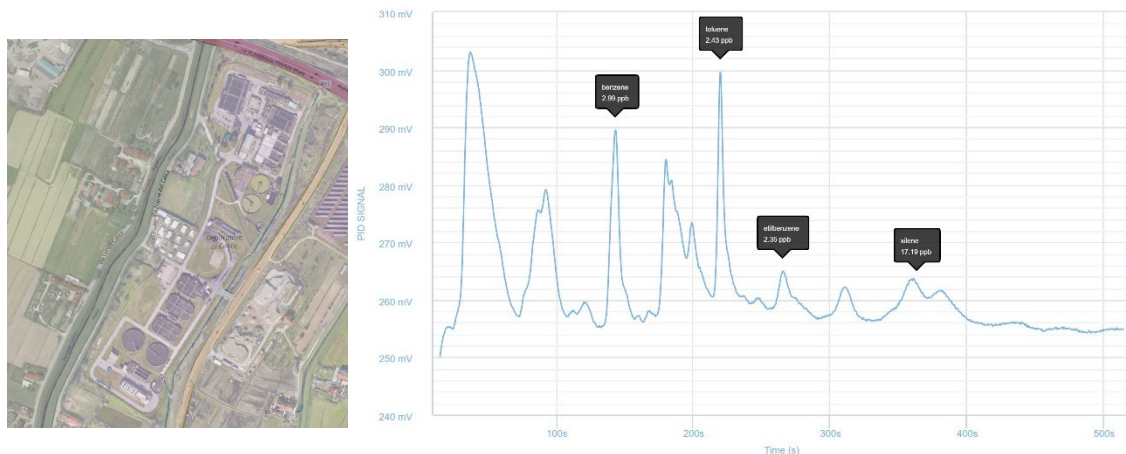


Figure 140 – Monitoring and characterization of diffuse emissions

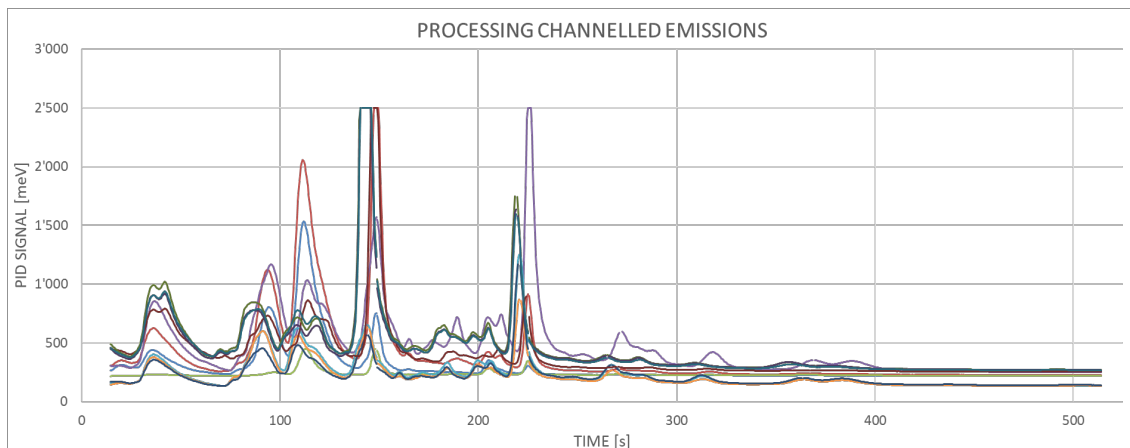


Figure 141 – Mathematical elaboration of chromatographic dynamics of channelled emissions

5.2. Emissions models

5.2.1. Emissions inventory

Emissions of pollutants into the atmosphere are at the root of some environmental problems that are now considered priorities in all national and international fora: climate change, the ozone hole in the stratosphere, an increase in tropospheric ozone, and atmospheric acidification (so-called acid rain). To prepare action plans and programmes for the remediation or conservation of ambient air, already provided for by Legislative Decree 351/1999, it is indispensable to know the sources of atmospheric emissions and their distribution over the territory employing the Emissions Inventory. The National Inventory of Atmospheric Emissions, carried out by ISPRA, is the primary tool for verifying compliance with the commitments that Italy has made at the international level on the protection of the atmospheric environment, providing central and peripheral institutions with support in understanding the problems inherent in climate change and atmospheric pollution; this support is indispensable for planning and implementing effective environmental policies. [90] Knowledge of the emission pressures on the territory is a necessary information support to develop pollution abatement strategies, identify priorities through integrated models, and verify the consequences at different levels of the policies and measures undertaken by institutional bodies to reduce emissions. The Emission Inventory is a dynamic tool constantly evolving, both in terms of improving the reliability and level of detail of the data and in terms of updating the information. In particular, the updating of the Inventory becomes opportune as a result of specific investigations in particular sectors or in the case of finding information at further levels of detail. The Inventory can be carried out according to the CORINAIR

methodology, developed by the European Environment Agency (EEA), and provides an estimate of the total annual emissions, disaggregated by emission activity at the various SNAP (Selected Nomenclature for Air Pollution) classification levels and spatially broken down. According to the SNAP classification, all anthropogenic and natural activities that can give rise to emissions into the atmosphere are broken down into eleven macro-sectors:

1. Energy production and fuel transformation.
2. Non-industrial combustion.
3. Combustion in industry.
4. Production processes.
5. Extraction and distribution of fossil fuels, geothermal energy.
6. Use of solvents and other products.
7. Road transport.
8. Other mobile sources and machinery.
9. Waste treatment and disposal.
10. Agriculture.
11. Other emission and absorption sources.

Each macro sector is subdivided into two further levels so that each activity is assigned a code that uniquely identifies it.

5.2.2. Emissions models

A pollutant released into the atmosphere at a given point in time is subjected to multiple chemical and physical phenomena, such as:

- Transport due to the action of the wind.
- Dispersion due to the effect of turbulent motions in the lower layers of the atmosphere.
- The eventual chemical transformation and deposition of the substance itself.

Due to these chemical-physical phenomena, it is possible to find the pollutant, after a more or less long time, in other points of the territory and with different concentration values. The objective of atmospheric pollutant simulation models is to assess the values assumed by the concentration of a given pollutant at all points in space and at different times.

There are many different categories of air quality models, also very different in complexity and fields of application. This implies that, before adopting and using a model, a careful analysis of the existing models in the literature must be carried out

in order to choose the most suitable one for one's needs. In general, in order to function properly, a model must have input information such as:

- The physical-chemical-mathematical or statistical schematisation of dispersion, transformation and deposition phenomena.
- The characterisation of the territory under examination (orography, land use type).
- The description of winds and atmospheric turbulence.
- The characterisation of emission sources.

The methodology for producing Emission Inventories envisages attributing the emission data to the territory on the basis of the administrative location of the source; this approximation is not always negligible because the fallout may significantly affect territories other than that of the municipality in which the emission sources are present.

Pollutant dispersion modelling using three-dimensional codes is able to spatially represent the concentrations of the various atmospheric pollutants, optimising the process of integrating information from the monitoring stations on the state of air quality with information on emission pressures from the Emission Inventories.

There are three main levels of emission processing:

1. Spatial disaggregation.
2. The chemical speciation.
3. Temporal modulation.

5.2.2.1. Spatial disaggregation

The process involves the spatialisation, on the simulation calculation grid, of emissions associated with anthropogenic or natural activities defined as areal and linear sources in the Emission Inventories. This process is made possible by intersecting the emission polygons with the simulation calculation grid: for each polygon, emissions are distributed over the cells obtained from the intersection between the grid geometry and the area of the polygon itself based on the information contained in a gridded thematic layer, obtained for example from land use data or cartographic data, specifying for each cell the percentage of area occupied by the selected feature. For example, emissions from domestic heating in a municipality are not uniformly distributed over all cells within the municipal area but only over those corresponding to the thematic layer defining the built-up areas.

Emissions from linear sources, being normally associated with a road graph, i.e. cartographic elements (road arcs) identified by segment start and end coordinates, do not require the spatialisation process described above but are simply projected onto the simulation calculation grid.

With regard to emissions from point sources identified by specific coordinates corresponding to individual chimneys, the spatialisation process is not necessary as these are treated separately from the emission model.

5.2.2.2. Time modulation

The time module of the emission modelling chain distributes the emission summation (provided by the Emission Inventories in tonnes/year) over the calendar year by dividing it hourly, taking into account the specific time profiles associated with each source type. The modulation over time of the emissions is, therefore, based on the intersection of daily (distribution over 24 hours), weekly (distribution over the week) and annual (distribution over the year) modulation profiles. In addition, the allocation of daily profiles differentiated by weekday, pre-holiday and holiday is possible. Specific modulation profiles can be provided for each emission category (e.g., for each SNAP code level: macro sector, sector or activity) and for each source.

5.2.2.3. Chemical speciation

If a code capable of simulating the main photochemical reactions occurring in the atmosphere is used in the modelling chain, the emission data must undergo further processing. As a result, we obtain, for each anthropogenic and natural activity, a breakdown of the emission summation into the various organic species according to the aggregation criterion provided by the chemical mechanism adopted (e.g. alkanes, aldehydes, ketones, aromatics, olefins, terpenes), based on specific speciation and size profiles for each emission category. The chemical model then uses the output information from the emission model to reproduce, from the various emitted chemical species (emission input) and turbulence information (meteorological input), the pollutant species' formation, dispersion and fallout processes.

5.2.2.4. Deterministic models

The classification of mathematical models for studying pollutants is reported:

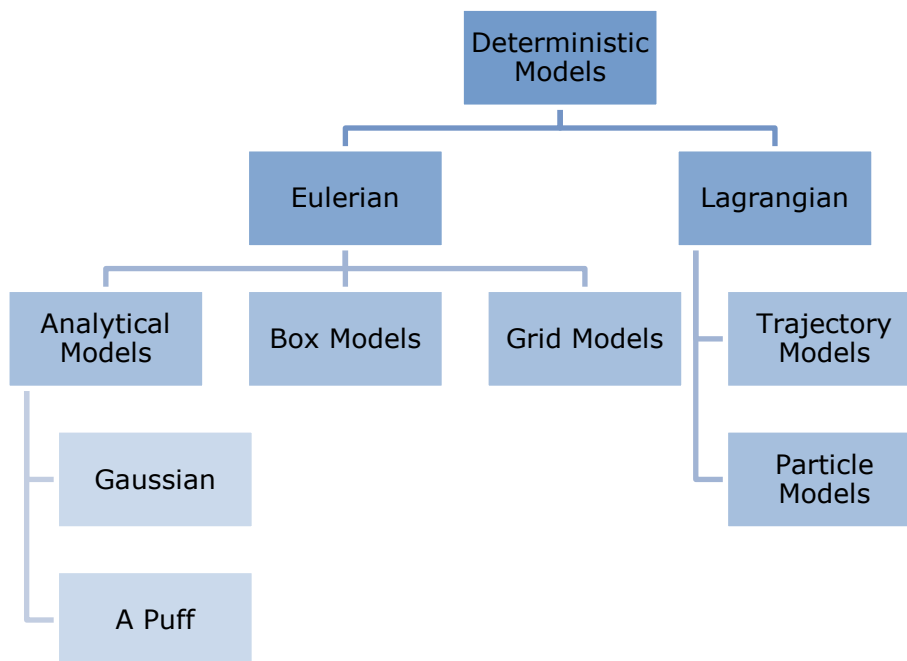


Figure 142 – Classification of mathematical models

The purpose of the models is to quantitatively reconstruct the phenomena that determine the spatio-temporal evolution of the concentration of pollutants in the air.

Eulerian models refer to a fixed coordinate system. They are, therefore, based on the integration of the differential diffusion equation derived from the mass balance applied to the infinitesimal volume as a function of specific assumptions. Depending on how the equation is solved, one can deal with:

1. Analytical Models:

- a. Gaussian: these are capable of describing the ground trend of the concentration due to a continuous point source, assuming a dispersion that follows a Gaussian-type law. These are easy-to-use models that are based on a series of simplifications, such as stationary and homogeneous meteorological conditions, horizontal wind velocity that is non-zero in the wind direction and mean zero in the plane orthogonal to it, flat terrain and the absence of chemical reactions.
 - b. A Puff: these are an extension of Gaussian models and allow the reconstruction of concentration values under non-homogeneous and non-stationary conditions. The concentration value at a point is obtained from the sum of the contributions of the concentrations of the various puffs within the domain (the dispersion follows a Gaussian-type law for each puff).
2. Box models: these divide the domain into one or more cells in which the pollutants are considered to have infinite dispersion coefficients, i.e. there is instantaneous dispersion of the pollutant. This allows the balance equation to be written so that it can be easily solved and, depending on the background concentration, wind speed, deposition rate, height of the mixing layer and other specific parameters, calculate the concentration for the individual cell.
3. Grid Models: divide the domain into three-dimensional cells within which the solution of the diffusion equation is obtained via finite differences, obtaining a concentration value for each grid point. As the number of grid nodes increases, the calculation complexity increases.

Lagrangian models refer to a mobile coordinate system integral with the displacements of the air masses whose behaviour is to be reproduced. One can have:

1. Trajectory models: the evolution of a column of air moving under the action of the average wind speed component (assumed to be horizontal and uniform with altitude) is simulated.
2. Particle models: the emission of pollutants is simulated with the generation of a number of particles emitted for each time step, and then the concentration field at each time step is reconstructed as a function of the number of particles passing through a specific volume of space.

5.2.2.5. Model applications

There are three possible scenarios:

1. Dispersion of pollutants released from linear sources, areal sources, and non-isolated point sources (microscale and local scale).
2. Dispersion of pollutants released from non-isolated, areal and linear point sources related to suburban traffic (local and mesoscale).
3. Formation and dispersion of secondary pollutants (mesoscale).

There is a partial overlap between these, but each scenario relates to one of the most frequently encountered situations: the assessment of ambient air over an urban area, even a large one (scenario 1), the assessment of the impact on ambient air of an industrial emission or road infrastructure (scenario 2), the assessment of tropospheric ozone pollution over the territory of one or more neighbouring regions (scenario 3). The indications regarding scenarios 2 and 3, taken together, provide the methodological helpful framework for the use of the models within the assessment of ambient air in a regional context, provided for by Legislative Decree 351/1999.

Dispersion of pollutants released from linear, areal, non-isolated point sources, whose hourly average concentrations and short- and long-term ground deposition are to be determined

Field of applicability:

- Microscale or local scale (varies from 500x500 m² to 10x10 km²).
- Any period: as far as the time scale is concerned, hourly averages are usually calculated. Scenario analysis is possible considering the cyclicity of emissions and the characteristics of the typical or representative day. For climatological or statistical simulations, models are fed with annual or time series of limited extent but with seasonal or periodic representativeness, composed of hourly data.
- Any site (such as urbanised territories, large industrial complexes close to manufactured areas, large connecting infrastructures, also located in complex orography or coastal areas). Flows peculiar to the water-soil or mountain-valley interface should be included in the calculation of the dynamic parameters) and source (single linear source, intersecting linear sources (series of roads between building blocks), chimneys or isolated natural or forced expulsion ventilations, elevated above ground level. Areal sources, car parks or groups of linear sources that are difficult to characterise as separate

entities may be considered. Usually, many models can treat all types of sources up to a maximum limit depending on the model).

- Non-reactive pollutants. Theoretically, all models can include reactions involving precursors. Reactions vary in number and complexity, as do the demands on the input data set. In the absence of any relationship between precursors and products, inert pollutants are considered.

The scenario considers situations of great topographical complexity where concentrations can reach high levels due to the concomitance of heavy traffic flows and poor ventilation.

Models are usually used:

- To interpret data measured at points close to the source in an urban environment.
- For urban planning and traffic management. They are also used to estimate the exposure of inhabitants and particular occupational groups to pollutants emitted by vehicle traffic.
- For environmental impact assessments or the design of smokestacks themselves and to define the quantitative and temporal characteristics of the emission. In large industrial complexes, microscale simulation can be used to design emergency plans and prevent personnel's chronic exposure (design of vent orientation).

Screening models

These are simple models designed to provide immediate answers with very little essential input data; they are based on empirical relationships derived from field experience or simulations using more complex models. These models calculate hourly concentrations or process percentiles under adverse weather conditions and for one type of source at a time. The model's response is immediate, and the application is very economical, but the objective of the calculation is limited to checking the proximity or otherwise of concentrations to the limits; only in the case of non-proximity can further investigations be avoided. The necessary input data are emission and wind speed data. In some cases, roughness length choices (predefined classes) are required.

Models of higher complexity

Classical or modified Gaussian models to represent complex orography or distortions induced by the presence of buildings, plume and box models or compositions of the previous solutions.

These are analytical models of the Gaussian family with different levels of complexity, dependent on the meteorological parameterisation and the type of function used to describe the influence of obstacles. The presence of the obstacle is not resolved explicitly but is considered through a function that corrects the shape of the distribution. Traditional or new-generation Gaussian models, i.e., those with a more sophisticated treatment of turbulence, can be prepared to incorporate meteorological input based on aggregated statistical meteorological data processing. Short-term models can be run to simulate the elementary interval and then iterated to cover the time interval of interest.

Dispersion of pollutants released from point sources, including isolated, areal, and linear in relation to suburban traffic

Field of applicability:

- Local and mesoscale (from a few kilometres, typically 5x5 km² for small releases, up to 100x100 km² for large sources).
- Any period: critical cases related to short-duration episodes, such as accidental releases or tailbacks and blocked traffic, are considered, as well as typical day analysis up to climatological type simulation related to the estimation of seasonal and annual averages.
- Any site: industrial areas and major roadways are present at sites of varying complexity; flows peculiar to the water-soil or upstream-valley interface should be included in the calculation of dynamic parameters.
- Any source: single or multiple point sources (smokestacks), single linear sources or simplified graphs (major arterial roads in a given domain); areal sources such as landfills or extended industrial complexes with many emission points of no significant magnitude to be treated separately may also be considered.
- Non-reactive pollutants: only primary pollutants with low reactivity or with transformation processes not relevant to the calculation domain and their residence time are considered. However, dry and wet deposition phenomena and first-order transformations, i.e. with decay expressed by a time constant, can be treated.

The scenario considers very common situations with a great variety of case histories: from the assessment of the fallout on the ground of pollutants emitted from high chimneys tens of kilometres away to the assessment of air quality in the vicinity of a motorway or a landfill site; from the study of critical episodes lasting only a few minutes to the definition of annual average concentrations; the calculation domains on which the assessments are to be made may be flat or of great topographical complexity, and the meteorological - diffusive characteristics may be simple or complex. The current availability of models for these case histories is high and not very differentiated regarding spatial or temporal scales or types of site and sources: when choosing which models to use, the degree of accuracy that one wants or can achieve must be considered. A hierarchy of models allowing more realistic simulations of the dispersion of pollutants in the atmosphere will be presented next, but in choosing one model or another, it will be necessary to assess the available resources in terms of available data (in particular meteorological measurements and land characteristics), computing power, time available for the study, targets to be reached, and the preparation of available personnel. The models on this sheet are used to assess and interpret data measured by monitoring networks in the region of impact of the sources to estimate the exposure of people or ecosystems to pollutants emitted into the atmosphere by the various sources; they are also usable and indispensable in EIA (Environmental Impact Assessment) studies for new industrial sites or civil infrastructures.

Analytical stationary plume, Gaussian and non-Gaussian models

These are simple models where the concentration calculation is solved by a single analytical formula into which meteorological and emission data are fed, and due to their practicality, they have been and are still widely used. These models are suitable for simulating homogeneous situations in space and stationary in time. There are traditional formulations (Gaussian models), in which the turbulent dispersion is parameterised with empirical coefficients derived from experimental campaigns (Pasquill - Gifford or Briggs curves), and more advanced ones (hybrid models), in which the dispersion is parameterised directly as a function of meteorological data that provide information on the thermal and mechanical structure of the lower layers of the atmosphere. It is not advisable to use these models for single event simulations as their simplification of the dispersive phenomenon makes results on single hourly averages and on single points of the calculation domain unrealistic, while the use of statistical type (seasonal/yearly averages) is more correct.

These codes can be used in two versions:

1. Long-term, involving the use of Joint Frequency Functions (JFF) - frequency tables (seasonal, annual or multi-year) calculated on the statistics of wind speed, wind direction and atmospheric stability conditions.
2. Short term, if time series of meteorological data (wind and stability) are available for at least one full year with hourly or tri-hourly resolution.

The first modality should only be considered a qualitative assessment with some drawbacks: the calculation of percentiles is problematic, and sources with time-varying emissions (typically plants operating at full load during the day and reduced load at night or daily modulation of traffic flow) cannot be considered correctly. The most critical conditions for using these models are calm winds and orographically complex terrain. However, in principle, introducing several corrective measures allows them to be used in all conditions. These models can be used as an initial screening to assess the significance of a source's impact, for simulations of low-emission sources and when little meteorological data is available. By using these models with conservative options, one can assess whether to switch to the use of other more realistic and complex models if critical conditions are predicted.

Non-stationary puff or segment models

These models are an improvement on the stationary models because, in addition to considering a Gaussian formulation for dispersion, they can vary the direction of transport in space and time. In these models, each emitted plume follows the path indicated by a single trajectory in the three-dimensional wind field that describes the motion of its centroid. They can be considered valid as long as a single trajectory adequately represents the transport of pollutants. Under highly inhomogeneous conditions, this approximation significantly reduces the accuracy of the final results. A trajectory representing the movement of the centroid of a puff does not adequately represent pollutant cloud transport because wind intensity and direction generally vary with altitude. In more complex conditions, such as breeze situations, a single trajectory is insufficient to correctly reproduce what is happening in the atmosphere.

Lagrangian and Eulerian 3D models

Lagrangian particle models and Eulerian grid models are the most advanced tools for the simulation of dispersion in the atmosphere: the former simulates the dispersion of emitted pollutants with computational particles moving in the three-dimensional wind and turbulence field, while the latter numerically solves the diffusion equation of the emitted pollutant in the same three-dimensional domain subdivided into grids even of variable size. They can fully account for all available meteorological measurements and their spatial and temporal variations; the limitations are currently in the incomplete knowledge of turbulence mechanisms and the excessive calculation time required for the most complex simulations. Full year-long simulations are costly, so these models should be used mainly to assess the situations that are assumed to be the most critical. However, it is possible to reconstruct seasonal average trends, even with limited calculation means, by simulating a few dozen statistically significant days over the year (divided equally between the different seasons). Then, seasonal and annual average concentration maps can be derived by weighing the different meteorological situations according to their frequency. Particle models are preferable at the local scale because of the greater detail near the source since grid models immediately dilute the source term on the volume of a cell, which, for computational requirements, cannot be too small. Furthermore, in the case of several sources, in order to attribute the weight each source has in the determination of air concentrations (source-receptor matrices), the simulations must be repeated in order to calculate the contribution of each source; in the case of particle models, on the other hand, the particles can be coloured differently according to the different sources and pollutants and the different contributions can be calculated in a single simulation. On the other hand, the use of grid models is indispensable for simulations in which chemical reactions come into play (see scenario 3). Finally, the use of three-dimensional models, Lagrangian or Eulerian, is practically indispensable in the case of mesoscale simulations, as the atmospheric circulation at the synoptic scale and its spatial and temporal variations must be taken into account.

Formation and dispersion of secondary pollutants

This scenario is dominated by secondary pollutants and is characterised by a lower spatial variability of pollutant concentration than urban scenarios and a marked diurnal and seasonal cycle.

Field of applicability:

- Mesoscale (50x50 km² to 500x500 km² as horizontal extent and vertical extent depending on the variation of the surface atmospheric layer, typically 1-2 km).
- Short period, as, for example, the atmospheric processes of photochemical pollution take place over time intervals of 1 to 3-4 days.
- Any site and source capable of emitting the precursors involved in photochemical pollution (might be point, linear, areal and biogenic, i.e. emissions from vegetation and soil).
- Reactive pollutants, such as nitrogen oxides and volatile organic compounds.

Modelling applications must consider two possible time dimensions, depending on their objective:

1. Short-to-medium term analysis (from one hour to one week): analysis of single pollution episodes applied to evaluate photochemical pollution reduction strategies.
2. Long-term analysis (seasonal and annual): to assess pollution, i.e., exceeding reference levels set by regulations.

6. Conclusion and future trends

This work collects the results of the research activity on the automatization and remote control of the procedures necessary for monitoring the workplace exploited at the Occupational and Environmental Hygiene and Toxicology Laboratory of the University of Florence during the years 2020-2023. The research activity carried out during the Ph.D. period is mainly related to the sampling procedures and devices, which can also comprise other phases such as purification and enrichment of the sample, the monitoring and the reduction of exposure to formaldehyde, with all the aspects connected to this objective and the presentation of two case studies, the monitoring and the reduction of exposure to airborne particulate matter and nanoparticles, with the presentation of four case studies, the monitoring of odour nuisances, with the presentation of three case studies. Regarding the research methodology, a preliminary literature research study was conducted, followed by the choice and testing of monitoring instruments and devices, which involved a significant experimental activity in real occupational scenarios. Such on-field monitoring has allowed us to identify practical issues connected to the selected instruments and devices that would not have arisen without a practical confrontation with the occupational environments.

The role of METs has gained significance in various analytical fields due to their adherence to Green Analytical Chemistry (GAC) requirements. METs are progressively evolving, given the vast potential applications they offer. This growing interest in METs has stimulated a rapid expansion of solutions to carry out miniaturised and automated sample preparation. Chapter 2 illustrates that the novel methods can concomitantly execute the analytical system's sample collection, extraction, concentration, and sample introduction. The replacement of traditional analytical techniques with miniaturised solutions in recent years is significant and, as previously stated, fully aligned with GAC's requirements, focused on a smart blend of cost-effective and eco-friendly methodologies. In addition to various miniaturised techniques, green solvents and enhancers for enhancing sample preparation efficiency (such as high temperature and/or pressure, microwave and UV radiation, and ultrasound energy) are incorporated into new analytical solutions as highly recommended. Likewise, the implementation of greener practices and complete automation in analytical processes has exponentially increased, leading to a surge in the usage of miniaturised techniques. This increase in usage has resulted in reduced solvent use, faster sample preparation, lower costs and analysis errors, enhanced traceability, and complete instrument automation. [10] While most chromatography labs already use autosamplers, this sophisticated technology allows for automation

beyond mere injection. A range of tools is available on the market, including barcode readers, automatic liner and syringe changers, decappers, heaters, stirrers, shaking and/or filtration modules, solvent additions, and Local Area Network (LAN) connections, which enhance usability and effectiveness. [11]

Various aspects of formaldehyde monitoring have been studied and presented in this work. It is essential to highlight how the available techniques for monitoring and assessing formaldehyde exposure allow the working environment to be monitored around the clock. As the two case studies have shown, monitoring has been successfully carried out over long periods without requiring daily visits to the APL observed. In addition, the results show that a continuous monitoring device, if well positioned and set up, can be used to assess personal exposure, as shown in Table 3. Monitoring devices, which can be operated automatically and remotely, have entirely changed the possibilities for evaluating exposure and studying the effects of working environments and procedures on exposure. Thanks to the achievements of these instruments, exposure can be reduced by introducing new techniques, updating equipment that is obsolete or no longer suitable for conditions or workloads, and establishing standardised operating procedures aimed at reducing contamination and accidental exposure.

As demonstrated in the case studies of airborne particulate matter and nanoparticle exposure assessment, the MiniWRAS instrument enables the gathering of data on the parameters outlined in the UNI EN 16966:2019 standard, including number ($\#/cm^3$), surface area ($\mu m^2/cm^3$), mass ($\mu g/m^3$), or volume ($\mu m^3/m^3$). Moreover, the tool yields data on Lung Deposited Surface Area, a key metric in conveying the harmful effects of airborne particles. If, in this instance, the baseline value can be determined, MiniWRAS supplies all the necessary information for utilizing the methodology provided by ISO/TS 12901-2:2014 (ISO 2014). Furthermore, this device can be used remotely without needing an electric connection, making it a thorough and appropriate instrument for continuously evaluating nanoparticle exposure.

Last but not least, the assessment of odorous nuisances is developing with various sampling devices, some of which have already been presented in section 2.3, and instruments that allow the recognition of specific fingerprints and the continuous monitoring on-field. According to the current state of the art, the assessment of odour nuisance should be complemented by modelling, taking into account meteorological conditions and orography; this could allow the study of the diffusion of the nuisance and, therefore, of the activities necessary to reduce it.

References

- [1] United Nations, "Take Action for the Sustainable Development Goals," [Online]. Available: <https://www.un.org/sustainabledevelopment/sustainable-development-goals/>. [Accessed 24 June 2023].
- [2] International Labour Organization, "ILOSTAT explorer SDG indicator 8.8.1 - Non-fatal occupational injuries per 100'000 workers-Annual," [Online]. Available: https://www.ilo.org/shinyapps/bulkexplorer34/?lang=en&id=SDG_N881_SEX_MIG_RT_A. [Accessed 24 June 2023].
- [3] International Labour Organization, "ILOSTAT explorer SDG indicator 8.8.1 - Fatal occupational injuries per 100'000 workers-Annual," [Online]. Available: https://www.ilo.org/shinyapps/bulkexplorer34/?lang=en&id=SDG_N881_SEX_MIG_RT_A. [Accessed 24 June 2023].
- [4] B. O. Alli, *Fundamental principles of occupational health and safety* Second edition, vol. 15, Geneva: International Labour Organization, 2008.
- [5] J. LaDou and R. Harrison, *CURRENT Diagnosis & Treatment Occupational and Environmental Medicine*, 5th Edition, McGraw Hill, 2014.
- [6] K. Ball, *Electronic Monitoring and Surveillance in the Workplace. Literature review and policy recommendations*, Luxembourg: Publications Office of the European Union, 2021.
- [7] N. Klepeis, W. Nelson, W. Ott, J. Robinson, A. Tsang, P. Switzer, J. Behar, S. Hern and W. Engelmann, "The National Human Activity Pattern Survey (NHAPS): a resource for assessing exposure to environmental pollutants," *Journal of Exposure Science & Environmental Epidemiology*, vol. 11, no. 3, pp. 231-252, 2001.
- [8] N. Good, A. Mölter, C. Ackerson, A. Bachand, T. Carpenter, M. Clark, K. Fedak, A. Kayne, K. Koehler, B. Moore, C. L'Orange, C. Quinn, V. Ugave, A. Stuart, J. Peel and J. Volckens, "The Fort Collins Commuter Study: Impact of route type and transport mode on personal exposure to multiple air pollutants," *Journal of*

exposure science & environmental epidemiology, vol. 26, no. 4, pp. 397-404, 2016.

- [9] M. Glasgow, C. Rudra, E. Yoo, M. Demirbas, J. Merriman, P. Nayak, C. Crabtree-Ide, A. Szpiro, A. Rudra, J. Wactawski-Wende and L. Mu, "Using smartphones to collect time-activity data for long-term personal-level air pollution exposure assessment," *Journal of exposure science & environmental epidemiology*, vol. 26, no. 4, pp. 356-364, 2016.
- [10] S. Dugheri, N. Mucci, A. Bonari, G. Marrubini, G. Cappelli, D. Ubiali, M. Campagna, M. Montalti and G. Arcangeli, "Solid phase microextraction techniques used for gas chromatography: a review," *Acta Chromatographica*, vol. 32, no. 1, pp. 1-9, 2020.
- [11] S. Dugheri, N. Mucci, A. Bonari, G. Marrubini, G. Cappelli, D. Ubiali, M. Campagna, M. Montalti and G. Arcangeli, "Liquid phase microextraction techniques combined with chromatography analysis: a review," *Acta Chromatographica*, vol. 32, no. 2, pp. 69-79, 2020.
- [12] S. Ma and S. K. Chowdhury, Eds., *Identification and Quantification of Drugs, Metabolites, Drug Metabolizing Enzymes, and Transporters: Concepts, Methods and Translational Sciences*, Elsevier, 2020.
- [13] M. C. Hennion, "Solid-phase extraction: method development, sorbents, and coupling with liquid chromatography," *Journal of chromatography A*, vol. 856, no. 1-2, pp. 3-54, 1999.
- [14] H. L. Lord, W. Zhan and J. Pawliszyn, "Fundamentals and applications of needle trap devices: a critical review," *Analytica chimica acta*, vol. 677, no. 1, pp. 3-18, 2010.
- [15] J. Pawliszyn, Ed., *Handbook of solid phase microextraction*, Elsevier, 2011.
- [16] S. Dugheri, G. Marrubini, N. Mucci, G. Cappelli, A. Bonari, I. Pompilio, L. Trevisani and G. Arcangeli, "A review of micro-solid-phase extraction techniques and devices applied in sample pretreatment coupled with chromatographic analysis," *Acta Chromatographica*, vol. 33, no. 2, pp. 99-111, 2021.

- [17] S. Dugheri, N. Mucci, G. Cappelli, L. Trevisani, A. Bonari, E. Bucaletti, D. Squillaci and G. Arcangeli, "Advanced solid-phase microextraction techniques and related automation: a review of commercially available technologies," *Journal of Analytical Methods in Chemistry*, 2022.
- [18] A. Speltini, A. Scalabrini, F. Maraschi, M. Sturini and A. Profumo, "Newest applications of molecularly imprinted polymers for extraction of contaminants from environmental and food matrices: A review," *Analytica Chimica Acta*, vol. 974, pp. 1-26, 2017.
- [19] S. Dugheri, A. Bonari, I. Pompilio, M. Colpo, N. Mucci, M. Montalti and G. Arcangeli, "Development of an innovative gas chromatography-mass spectrometry method for assessment of formaldehyde in the workplace atmosphere," *Acta Chromatographica*, vol. 29, no. 4, pp. 511-514, 2017.
- [20] S. Dugheri, A. Bonari, I. Pompilio, M. Colpo, N. Mucci and G. Arcangeli, "An integrated air monitoring approach for assessment of formaldehyde in the workplace," *Safety and health at work*, vol. 9, no. 4, pp. 479-485, 2018.
- [21] C. L. Arthur and J. Pawliszyn, "Solid phase microextraction with thermal desorption using fused silica optical fibers," *Analytical chemistry*, vol. 62, no. 19, pp. 2145-2148, 1990.
- [22] C. Poole, Z. Mester, M. Miró, S. Pedersen-Bjergaard and J. Pawliszyn, "Glossary of terms used in extraction (IUPAC Recommendations 2016)," *Pure and Applied Chemistry*, vol. 88, no. 5, pp. 517-558, 2016.
- [23] V. Jalili, A. Barkhordari and A. Ghiasvand, "A comprehensive look at solid-phase microextraction technique: A review of reviews," *Microchemical Journal*, vol. 152, p. 104319, 2020.
- [24] M. A. Jochmann, X. Yuan, B. Schilling and T. C. Schmidt, "In-tube extraction for enrichment of volatile organic hydrocarbons from aqueous samples," *Journal of Chromatography A*, vol. 1179, no. 2, pp. 96-105, 2008.
- [25] C. Nerín, J. Salafranca, M. Aznar and R. Batlle, "Critical review on recent developments in solventless techniques for extraction of analytes," *Analytical and bioanalytical chemistry*, vol. 393, pp. 809-833, 2009.

- [26] E. Boyacı, Á. Rodríguez-Lafuente, K. Gorynski, F. Mirnaghi, É. A. Souza-Silva, D. Hein and J. Pawliszyn, "Sample preparation with solid phase microextraction and exhaustive extraction approaches: Comparison for challenging cases," *Analytica chimica acta*, vol. 873, pp. 14-30, 2015.
- [27] M. Piergiovanni, F. Gosetti, P. Rocío-Bautista and V. Termopoli, "Aroma determination in alcoholic beverages: Green MS-based sample preparation approaches," *Mass Spectrometry Reviews*, p. e21802, 2022.
- [28] A. Grafit, D. Muller, S. Kimchi and Y. Y. Avissar, "Development of a Solid-phase microextraction (SPME) Fiber protector and its application in flammable liquid residues analysis," *Forensic science international*, vol. 292, pp. 138-147, 2018.
- [29] K. C. D. P. Roux, É. F. Jasinski, J. Merib, M. L. Sartorelli and E. Carasek, "Application of a robust solid-phase microextraction fiber consisting of NiTi wires coated with polypyrrole for the determination of haloanisoles in water and wine," *Analytical Methods*, vol. 8, no. 27, pp. 5503-5510, 2016.
- [30] F. Michel, R. E. Shirey, Y. Chen, L. Sidisky and É. A. Souza-Silva, "Advantages of PDMS-overcoated adsorbent based SPME fiber for extraction in complex samples," in *Proceedings of the ExTech Conference*, Guangzhou, China, 2015.
- [31] A. Helin, T. Rönkkö, J. Parshintsev, K. Hartonen, B. Schilling, T. Läubli and M. L. Riekkola, "Solid phase microextraction Arrow for the sampling of volatile amines in wastewater and atmosphere," *Journal of Chromatography A*, vol. 1426, pp. 56-63, 2015.
- [32] E. Baltussen, P. Sandra, F. David and C. Cramers, "Stir bar sorptive extraction (SBSE), a novel extraction technique for aqueous samples: theory and principles," *Journal of Microcolumn Separations*, vol. 11, no. 10, pp. 737-747, 1999.
- [33] O. Zuloaga, N. Etxebarria, B. González-Gaya, M. Olivares, A. Prieto and A. Usobiaga, "Stir-bar sorptive extraction," in *Solid-Phase Extraction*, Elsevier, 2020, pp. 493-530.
- [34] G. A. Gómez-Ríos, M. Tascon, N. Reyes-Garcés, E. Boyacı, J. Poole and J. Pawliszyn, "Quantitative analysis of biofluid spots by coated blade spray mass

- spectrometry, a new approach to rapid screening," *Scientific Reports*, vol. 7, no. 1, p. 16104, 2017.
- [35] R. V. Emmons, R. Tajali and E. Gionfriddo, "Development, optimization and applications of thin film solid phase microextraction (TF-SPME) devices for thermal desorption: A comprehensive review," *Separations*, vol. 6, no. 3, p. 39, 2019.
- [36] R. T. Marsili and C. R. Laskonis, "Evaluation of sequential-SBSE and TF-SPME extraction techniques prior to GC-TOFMS for the analysis of flavor volatiles in beer," *Journal of the American Society of Brewing Chemists*, vol. 77, no. 2, pp. 113-118, 2019.
- [37] Y. Huang, C. S. M. Liew, S. X. L. Goh, R. M. V. Goh, K. H. Ee, A. Pua, S. Q. Liu, B. Lassabliere and B. Yu, "Enhanced extraction using a combination of stir bar sorptive extraction and thin film-solid phase microextraction," *Journal of Chromatography A*, vol. 1633, p. 461617, 2020.
- [38] M. Mieth, S. Kischkel, J. K. Schubert, D. Hein and W. Miekisch, "Multibed needle trap devices for on site sampling and preconcentration of volatile breath biomarkers," *Analytical chemistry*, vol. 81, no. 14, pp. 5851-5857, 2009.
- [39] S. Maleki, P. Hashemi, F. Rasolzadeh, S. Maleki and A. R. Ghiasvand, "A needle trap device packed with nanoporous silica sorbents for separation and gas chromatographic determination of polycyclic aromatic hydrocarbons in contaminated soils," *Journal of chromatographic science*, vol. 56, no. 9, pp. 771-778, 2018.
- [40] P. Porto-Figueira, J. Pereira, W. Miekisch and J. S. Câmara, "Exploring the potential of NTME/GC-MS, in the establishment of urinary volatome profiles. Lung cancer patients as case study," *Scientific Reports*, vol. 8, no. 1, p. 13113, 2018.
- [41] M. Iwai, F. Kondo, T. Suzuki, T. Ogawa and H. Seno, "Quantification of ethanol in whole blood by extraction using NeedlEx® and gas chromatography/mass spectrometry," *Medical Mass Spectrometry*, vol. 3, no. 1, pp. 30-34, 2019.
- [42] P. Fuchsmann, M. T. Stern, P. Bischoff, R. Badertscher, K. Breme and B. Walther, "Development and performance evaluation of a novel dynamic headspace vacuum transfer "In Trap" extraction method for volatile compounds and

comparison with headspace solid-phase microextraction and headspace in-tube extraction," *Journal of Chromatography A*, vol. 1601, pp. 60-70, 2019.

- [43] P. Fuchsmann, F. Wahl, P. Bischoff and M. T. STERN, "DYNAMIC HEADSPACE VACUUM TRANSFER " IN TRAP " EXTRACTION METHOD AND APPARATUS". United States Patent US 2022/0018740 A1, 20 Gennaio 2022.
- [44] M. J. Trujillo-Rodríguez, A. J. L. S. J. Dunham, V. L. Noad and D. B. Cardin, "Vacuum-assisted sorbent extraction: An analytical methodology for the determination of ultraviolet filters in environmental samples," *Talanta*, vol. 208, p. 120390, 2020.
- [45] H. H. Jeleń, A. Gaca and M. Marcinkowska, "Use of sorbent-based vacuum extraction for determination of volatile phenols in beer," *Food Analytical Methods*, vol. 11, pp. 3089-3094, 2018.
- [46] G. Cohen, N. Kreutzer, K. Mowat, A. A. Hassan and B. Dvorak, "Compliance with hand sanitizer quality during the SARS-CoV-2 pandemic: Assessing the impurities in an ethanol plant," *Journal of Environmental Management*, vol. 297, p. 113329, 2021.
- [47] P. Porto-Figueira, J. A. Figueira, J. A. Pereira and J. S. Câmara, "A fast and innovative microextraction technique, μ SPEed, followed by ultrahigh performance liquid chromatography for the analysis of phenolic compounds in teas," *Journal of Chromatography A*, vol. 1424, pp. 1-9, 2015.
- [48] M. Locatelli, A. Tartaglia, S. Piccolantonio, L. A. Di Iorio, E. Sperandio, H. I. Ulusoy, K. G. Furton and A. Kabir, "Innovative configurations of sample preparation techniques applied in bioanalytical chemistry: a review," *Current Analytical Chemistry*, vol. 15, no. 7, pp. 731-744, 2019.
- [49] W. Li, W. Jian and Y. Fu, *Sample preparation in LC-MS bioanalysis*, Hoboken, NJ, USA,: John Wiley & Sons, 2019.
- [50] H. Fleischer, D. Baumann, S. Joshi, X. Chu, T. Roddelkopf, M. Klos and K. Thurow, "Analytical measurements and efficient process generation using a dual-arm robot equipped with electronic pipettes," *Energies*, vol. 11, no. 10, p. 2567, 2018.

- [51] G. J. Van Berkel and V. Kertesz, "An open port sampling interface for liquid introduction atmospheric pressure ionization mass spectrometry," *Rapid Communications in Mass Spectrometry*, vol. 29, no. 19, pp. 1749-1756, 2015.
- [52] N. T. Looby, M. Tascon, V. R. Acquaro, N. Reyes-Garcés, T. Vasiljevic, G. A. Gomez-Rios, M. Wasowicz and J. Pawliszyn, "Solid phase microextraction coupled to mass spectrometry via a microfluidic open interface for rapid therapeutic drug monitoring," *Analyst*, vol. 144, no. 12, pp. 3721-3728, 2019.
- [53] A. Klimek-Turek, A. Chomicki, E. Fornal, A. Pradiuch, M. Hys and T. H. Dzido, "Solvent front position extraction with semi-automatic device as a powerful sample preparation procedure to quantitation of tryptophan in human plasma," *Scientific Reports*, vol. 10, no. 1, p. 15063, 2020.
- [54] A. Sorribes-Soriano, S. Sánchez-Martínez, R. Arráez-González, F. A. Esteve-Turrillas and S. Armenta, "Methylone determination in oral fluid using microextraction by packed sorbent coupled to ion mobility spectrometry," *Microchemical Journal*, vol. 153, p. 104504, 2020.
- [55] T. E. Lockwood, M. Talebi, A. Minett, S. Mills, P. A. Doble and D. P. Bishop, "Micro solid-phase extraction for the analysis of per-and polyfluoroalkyl substances in environmental waters," *Journal of Chromatography A*, vol. 1604, p. 460495, 2019.
- [56] T. Salthammer, "Formaldehyde sources, formaldehyde concentrations and air exchange rates in European housings," *Building and environment*, vol. 150, pp. 219-232, 2019.
- [57] B. Li, Z. Cheng, R. Yao, H. Wang, W. Yu, Z. Bu, J. Xiong, T. Zhang, E. Essah, Z. Luo, M. Shahrestani and H. Kipen, "An investigation of formaldehyde concentration in residences and the development of a model for the prediction of its emission rates," *Building and environment*, vol. 147, pp. 540-550, 2019.
- [58] Agency for Toxic Substances and Disease Registry (ATSDR), "Toxicological Profile for Formaldehyde," USA.gov, 12 Maggio 2015. [Online]. Available: <https://wwwn.cdc.gov/TSP/ToxProfiles/ToxProfiles.aspx?id=220&tid=39>. [Accessed 22 August 2023].
- [59] S. Dugheri, D. Massi, N. Mucci, G. Marrubini, G. Cappelli, A. Speltini, C. Bonferoni and G. Arcangeli, "Exposure to airborne formaldehyde: Sampling and

analytical methods—A review,” *Trends in Environmental Analytical Chemistry*, vol. 29, p. e00116, 2021.

- [60] Occupational Safety and Health Administration (OSHA), “Alphabetic Index of Sampling and Analytical Methods - F,” [Online]. Available: <https://www.osha.gov/chemicaldata/methods?letter=F>. [Accessed 26 August 2023].
- [61] P. H. Dixneuf and J. F. Soulé, *Organometallics for green catalysis* (Vol. 63), Gewerbestrasse, Switzerland: Springer, 2019.
- [62] M. M. Sampson, D. M. Chambers, D. Y. Pazo, F. Moliere, B. C. Blount and C. H. Watson, “Simultaneous analysis of 22 volatile organic compounds in cigarette smoke using gas sampling bags for high-throughput solid-phase microextraction,” *Analytical chemistry*, vol. 86, no. 14, pp. 7088-7095, 2014.
- [63] L. Viallon, E. Flores, F. Idrees, P. Moussay, R. I. Wielgosz, D. Kim, Y. D. Kim, S. Lee, S. Persijn and N. Aoki, “CCQM-K90, formaldehyde in nitrogen, 2 $\mu\text{mol mol}^{-1}$ Final report,” *Metrologia*, vol. 54, no. 1A, p. 08029, 2017.
- [64] N. Mucci, S. Dugheri, V. Rapisarda, M. Campagna, G. Garzaro, A. Farioli, G. Cappelli and G. Arcangeli, “Occupational exposure to airborne formaldehyde in hospital: setting an automatic sampling system, comparing different monitoring methods and applying them to assess exposure,” *La Medicina del lavoro*, vol. 110, no. 6, p. 446, 2019.
- [65] G. D. Nielsen, S. T. Larsen and P. Wolkoff, “Re-evaluation of the WHO (2010) formaldehyde indoor air quality guideline for cancer risk assessment,” *Archives of toxicology*, vol. 91, pp. 35-61, 2017.
- [66] H. Reingruber and L. B. Pontel, “Formaldehyde metabolism and its impact on human health,” *Current opinion in toxicology*, vol. 9, pp. 28-34, 2018.
- [67] S. Dugheri, D. Massi, N. Mucci, N. Berti, G. Cappelli and G. Arcangeli, “Formalin safety in anatomic pathology workflow and integrated air monitoring systems for the formaldehyde occupational exposure assessment,” *International Journal of Occupational Medicine and Environmental Health*, vol. 34, no. 3, pp. 319-338, 2020.

- [68] L. Vimercati, A. Carrus, T. Martino, I. Galise, V. Minunni, F. Caputo, A. Dell'Erba and G. Assennato, "Formaldehyde exposure and irritative effects on medical examiners, pathologic anatomy post-graduate students and technicians," *Iranian journal of public health*, vol. 39, no. 4, p. 26, 2010.
- [69] E. G. Lee, R. Magrm, M. Kusti, M. L. Kashon, S. Guffey, M. M. Costas, C. J. Boykin and M. Harper, "Comparison between active (pumped) and passive (diffusive) sampling methods for formaldehyde in pathology and histology laboratories," *Journal of occupational and environmental hygiene*, vol. 14, no. 1, pp. 31-39, 2017.
- [70] S. Dugheri, D. Massi, N. Mucci, N. Berti, G. Cappelli and G. Arcangeli, "How improvements in monitoring and safety practices lowered airborne formaldehyde concentrations at an Italian university hospital: a summary of 20 years of experience," *Arhiv za higijenu rada i toksikologiju*, vol. 71, no. 3, pp. 178-188, 2020.
- [71] J. C. Soo, E. G. Lee, R. F. LeBouf, M. L. Kashon, W. Chisholm and M. Harper, "Evaluation of a portable gas chromatograph with photoionization detector under variations of VOC concentration, temperature, and relative humidity," *Journal of occupational and environmental hygiene*, vol. 15, no. 4, pp. 351-360, 2018.
- [72] J. J. Scherer, J. B. Paul, J. Thiebaud and S. So, "MIRA: A New, Ultrasensitive, Middle Infrared Laser-Based "Lab in a Lunchbox","" *Optics and Photonics for Sensing the Environment*, pp. ETu2A-1, 2019.
- [73] S. Dugheri, G. Cappelli, L. Isolani, L. Trevisani, D. Squillaci, E. Bucaletti, J. Ceccarelli, S. Pettinari, G. Amagliani, N. Fanfani, N. Mucci and G. Arcangeli, "Strategy to monitor and evaluate the impact of airborne formaldehyde in anatomical pathology laboratory. Part I: occupational exposure and cancer risk assessment," Submitted.
- [74] S. Dugheri, N. Mucci, G. Cappelli, A. Bonari, G. Garzaro, G. Marrubini, G. Bartolucci, M. Campagna and G. Arcangeli, "Monitoring of air-dispersed formaldehyde and carbonyl compounds as vapors and adsorbed on particulate matter by denuder-filter sampling and gas chromatographic analysis," *International Journal of Environmental Research and Public Health*, vol. 16, no. 11, p. 1969, 2019.

- [75] K. Koehler, N. Good, A. Wilson, A. Mölter, B. F. Moore, T. Carpenter, J. L. Peel and J. Volckens, "The Fort Collins commuter study: Variability in personal exposure to air pollutants by microenvironment," *Indoor air*, vol. 29, no. 2, pp. 231-241, 2019.
- [76] X. Yu, A. L. Stuart, Y. Liu, C. E. Ivey, A. G. Russell, H. Kan, L. R. F. Henneman, S. E. Sarnat, S. Hasan, A. Sadmani, X. Yang and H. Yu, "On the accuracy and potential of Google Maps location history data to characterize individual mobility for air pollution health studies," *Environmental pollution*, vol. 252, pp. 924-930, 2019.
- [77] M. Ogawa, I. Kabe, Y. Terauchi and S. Tanaka, "A strategy for the reduction of formaldehyde concentration in a hospital pathology laboratory," *Journal of occupational health*, vol. 61, no. 1, pp. 135-142, 2019.
- [78] X. C. Jin, R. M. Ballentine, W. P. Gardner, M. S. Melvin, Y. B. Pithawalla, K. A. Wagner, K. C. Avery and M. Sharifi, "Determination of Formaldehyde Yields in E-Cigarette Aerosols: An Evaluation of the Efficiency of the DNPH Derivatization Method," *Separations*, vol. 8, no. 9, p. 151, 2021.
- [79] W. Yuniati, T. Amelia, S. Ibrahim and S. Damayanti, "Analytical method development for determining formaldehyde in cream cosmetics using hyphenated gas chromatography," *ACS omega*, vol. 6, no. 42, pp. 28403-28409, 2021.
- [80] W. Hoeflinger and T. Laminger, "PM_{2.5} or respirable dust measurement and their use for assessment of dust separators," *Journal of the Taiwan Institute of Chemical Engineers*, vol. 94, pp. 53-61, 2019.
- [81] J. S. Brown, T. Gordon, O. Price and B. Asgharian, "Thoracic and respirable particle definitions for human health risk assessment," *Particle and fibre toxicology*, vol. 10, pp. 1-12, 2013.
- [82] Istituto Nazionale per l'Assicurazione contro gli Infortuni sul Lavoro (INAIL), "Le polveri inerti," 11 07 2022. [Online]. Available: <https://www.inail.it/cs/Satellite?c=Page&cid=2443085355717&d=68&pagina me=Internet%2FPage%2FpaginaFoglia%2Flayout>. [Accessed 04 12 2023].
- [83] L. Salo, T. Rönkkö, S. Saarikoski, K. Teinilä, J. Kuula, J. Alanen, A. Arffman, H. Timonen and J. Keskinen, "Concentrations and size distributions of particle

lung-deposited surface area (LDSA) in an underground mine," *Aerosol and Air Quality Research*, vol. 21, no. 8, p. 200660, 2021.

- [84] H. Rieder, A. Dillhöfer, M. Spies, J. Bamberg and T. Hess, "Online monitoring of additive manufacturing processes using ultrasound," in *Proceedings of the 11th European Conference on Non-destructive testing*, 2014.
- [85] IFA, "Criteria for Assessment of the Effectiveness of Protective Measures," [Online]. Available: <https://www.dguv.de/ifa/fachinfos/nanopartikel-am-arbeitsplatz/beurteilung-von-schutzmassnahmen/index-2.jsp>. [Accessed 10 Novembre 2021].
- [86] M. Seipenbusch, A. Binder and G. Kasper, "Temporal evolution of nanoparticle aerosols in workplace exposure," *Annals of occupational hygiene*, vol. 52, no. 8, pp. 707-706, 2008.
- [87] Ministero dell'Ambiente e della Sicurezza Energetica, "Indirizzi per l'applicazione dell'articolo 272-bis del D.Lgs 152/2006 in materia di emissioni odorigene di impianti e attività," Governo Italiano, 28 June 2023. [Online]. Available: <https://www.mase.gov.it/pagina/indirizzi-lapplicazione-dellarticolo-272-bis-del-dlgs-1522006-materia-di-emissioni-odorigene>. [Accessed 10 September 2023].
- [88] Assolombarda, "Dgr 15 febbraio 2012, n. 3018 Linee Guida caratterizzazione emissioni gassose da attività a forte impatto odorigeno," 15 February 2012. [Online]. Available: <https://www.assolombarda.it/servizi/ambiente/documenti/dgr-15-febbraio-2012-n.-3018-linee-guida-caratterizzazione-emissioni-gassose-da-attivita-a-forte-impatto-odorigeno/view>. [Accessed 10 September 2023].
- [89] European Committee for Standardization, *EN 13725:2022 Stationary source emissions - Determination of odour concentration by dynamic olfactometry and odour emission rate*, 2022.
- [90] ISPRA Istituto Superiore per la Protezione e la Ricerca Ambientale, "Emissioni - Inventari Locali," [Online]. Available: <https://emissioni.sina.isprambiente.it/inventari-locali/>. [Accessed 20 September 2023].

- [91] M. Pacenti, S. Dugheri, P. Traldi, F. Degli Esposti, N. Perchiazzi, E. Franchi, M. Calamante, I. Kikic, P. Alessi, A. Bonacchi, E. Salvadori, G. Arcangeli and V. Cupelli, "New automated and high-throughput quantitative analysis of urinary ketones by multifiber exchange-solid phase microextraction coupled to fast gas chromatography/negative chemical-electron ionization/mass spectrometry," *Journal of Analytical Methods in Chemistry*, vol. 2010, 2010.
- [92] E. Jääskeläinen, S. Vesterinen, J. Parshintsev, P. Johansson, M. L. Riekkola and J. Björkroth, "Production of buttery-odor compounds and transcriptome response in *Leuconostoc gelidum* subsp. *gasicomitatum* LMG18811T during growth on various carbon sources," *Applied and Environmental Microbiology*, vol. 81, no. 6, pp. 1902-1908, 2015.
- [93] M. Fabjanowicz, K. Kalinowska, J. Namieśnik and J. Płotka-Wasyłka, "Evaluation of green sample preparation techniques for organic compounds," *Current Green Chemistry*, vol. 5, no. 3, pp. 168-176, 2018.
- [94] E. Omena, A. L. Oenning, J. Merib, P. Richter, M. Rosero-Moreano and E. Carasek, "A green and simple sample preparation method to determine pesticides in rice using a combination of SPME and rotating disk sorption devices," *Analytica Chimica Acta*, vol. 1069, pp. 57-65, 2019.
- [95] R. W. Brown, J. P. Mayser, C. Widdowson, D. R. Chadwick and D. L. Jones, "Dependence of thermal desorption method for profiling volatile organic compound (VOC) emissions from soil," *Soil Biology and Biochemistry*, vol. 160, p. 108313, 2021.